Molecular mechanisms of early-life stress in 5-Htt deficient mice:

Gene x environment interactions and epigenetic programming

Molekulare Mechanismen von Entwicklungsstress bei 5-Htt defizienten Mäusen:

Gen x Umwelt Interaktionen und epigenetische Programmierung

Doctoral thesis for a doctoral degree
at the Graduate School of Life Sciences,
Julius-Maximilians-Universität Würzburg

Submitted by
Sissi Jakob
from Groß-Umstadt, Germany

Würzburg, 2012

Submitted on: ....

Members of the Promotionskomitee:

Chairperson: Prof. Dr. Utz Fischer

Primary Supervisor: Prof. Dr. Klaus-Peter Lesch

Supervisor (Second): Prof. Dr. Thomas Dandekar

Supervisor (Third): Dr. Cornelius Gross

Supervisor (Fourth): Dr. Daniel van den Hove

Date of Public Defence: ....

Date of receipt of Certificates: ....

Table of Contents

Preface

Understanding the molecular mechanisms underlying vulnerability and resilience to emotional disorders like depression and anxiety disorders is of great interest for psychiatrists, psychologists, neurobiologists and patients, as it helps to identify new routes to diagnose and treatment. For this purpose, mouse models of depression and anxiety have been generated. This thesis describes three different animal models that address the emerging concept of early-life programming and related gene x environment interactions. Some of the animals in my thesis were heterozygous for the serotonin transporter (5-Htt+/-) gene, a gene that is associated with depression and anxiety traits in humans and in all of the three animal models, mice were exposed to early-life stress. The main work of my thesis was to study the behavior of and to perform gene expression and DNA methylation screenings in prenatally stressed (PS) 5-Htt+/- female mice and wild-type control animals (see 3. Results).

Stress during development, especially when it comes along with a genetic predisposition, can have longlasting consequences including psychopathology in adulthood. At the basis of these gene x environment interactions lie epigenetic mechanisms, that pre- and posttranscriptionally alter mRNA production - sometimes in a stable fashion -, therefore programming the organism for later life. As the aim of my thesis was to study the molecular mechanisms that determine the outcome of early-life stress programming to be either negative (vulnerable offspring) or positive (resilient offspring), I looked at one candidate gene, the brain-derived neurotrophic factor (Bdnf), which is known for its prominent role in neuronal and synaptic plasticity and related cognitive and affective functions. I investigated the DNA methylation pattern (one epigenetic modification) of various *Bdnf* promoters in the hippocampus and cortex of PS and control mice by the help of EpiTYPER MALDI-TOF mass spectrometry and pyrosequencing (see appendix 5.2). Further, I applied bisulfite sequencing to study differences in the methylation pattern of *ADP-ribosylation factor guanine nucleotide-exchange factor (Arfgef) 1* between mice exposed to low and mice experienced high levels of maternal care (see appendix 5.3).

In particular, I thank Prof. Dr. K.-P. Lesch and Dr. DLA van den Hove for discussion and valuable comments on this work. Further, my thanks go to the DFG SFB TRR 58 and to EC 6th framework programme NewMood, who funded this project.

Sissi Jakob

Summary

Early-life stress has been shown to influence the development of the brain and to increase the risk for psychiatric disorders later in life. Furthermore, variation in the human serotonin transporter (5-HTT, SLC6A4) gene is suggested to exert a modulating effect on the association between early-life stress and the risk for depression. At the basis of these gene x environment (G x E) interactions, epigenetic mechanisms, such as DNA-methylation, seem to represent the primary biological processes mediating early-life programming for stress susceptibility or resilience, respectively. The exact molecular mechanisms however remain to be elucidated, though.

In the present study, we used two different stress paradigms to assess the molecular mechanisms mediating the relationship between early-life stress and disorders of emotion regulation later in life. First, a 5-Htt x prenatal stress (PS) paradigm was applied to investigate whether the effects of PS are dependent on the 5-Htt genotype. For this purpose, the effects of PS on cognition and anxiety- / depression-related behavior were examined using a maternal restraint stress paradigm of PS in C57BL/6 wild-type (WT) and heterozygous 5-Htt deficient (5-Htt+/-) mice. Additionally, in female offspring, a genome-wide hippocampal gene expression and DNA methylation profiling was performed using the Affymetrix GeneChip® Mouse Genome 430 2.0 Array and the AffymetrixGeneChip® Mouse Promoter 1.0R Array. Some of the resulting candidate genes were validated by quantitative real-time PCR. Further, the gene expression of these genes was measured in other brain regions of the PS animals as well as in the hippocampus of offspring of another, 5-Htt x perinatal stress (PeS) paradigm, in which pregnant and lactating females were stressed by an olfactory cue indicating infanticide. To assess resilience to PS and PeS, correlation studies between gene expression and behaviour were performed based on an initial performance-based LIMMA analysis of the gene expression microarray.

5-Htt+/- offspring of the PS paradigm showed enhanced memory performance and signs of reduced anxiety as compared to WT offspring. In contrast, exposure of 5-Htt+/- mice to PS was associated with increased depression-like behavior, an effect that tended to be more pronounced in female offspring. Further, 5-Htt genotype, PS and their interaction differentially affected the expression and DNA methylation of numerous genes and related pathways within the female hippocampus. Specifically, MAPK and neurotrophin signaling were regulated by both the 5-Htt+/- genotype and PS exposure, whereas cytokine and Wnt signaling were affected in a 5-Htt genotype x PS manner, indicating a gene x environment interaction at the molecular level. The candidate genes of the expression array could be validated and their expression patterns were partly consistent in the prefrontal cortex and striatum. Furthermore, the genotype effect of XIAP associated factor 1 (Xaf1) was also detected in the mice of the PeS paradigm. Concerning resilience, we found that the expression of growth hormone (Gh), prolactin (Prl) and fos-induced growth factor (Figf) were downregulated in WTPS mice that performed well in the forced swim test (FST). At the same time, the results indicated that Gh and Prl expression correlated positively with adrenal weight, whereas Figf expression correlated positively with basal corticosteron concentration, indicating an intricate relationship between depression-like behavior, hippocampal gene expression and the hypothalamo-pituitary-adrenal (HPA) axis activity. Correlation studies in the PeS animals revealed a link between Gh / Prl expression and anxiety-like behavior. In conclusion, our data suggest that although the 5-Htt+/- genotype shows clear adaptive capacity, 5-Htt+/- mice, particularly females, appear to be more vulnerable to developmental stress exposure when compared to WT offspring. Moreover, hippocampal gene expression and DNA methylation profiles suggest that distinct epigenetic mechanisms at the molecular level mediate the behavioral effects of the 5-Htt genotype, PS exposure, and their interaction. Further, resilience to early-life stress might be conferred by genes whose expression is linked to HPA axis function.

Zusammenfassung

Zahlreiche Studien haben gezeigt, dass Stress während der Entwicklung die Gehirnentwicklung beinflusst und das Risiko an psychischen Störungen zu erkranken erhöht. Weiterhin wird vermutet, dass eine Variation im humanen Serotonintransportergen (5-HTT, SLC6A4) einen modulierenden Einfluss auf die Assoziation zwischen Entwicklungsstress und dem Risiko für Depression ausübt. Als Basis dieser Gene x Umwelt (GxE)-Interaktion scheinen epigenetische Mechanismen, wie DNA-Methylierung, die biologischen Prozesse darzustellen, die die Programmierung von Stressanfälligkeit oder Resilienz vermitteln. Die exakten molekularen Mechanismen sind jedoch noch unbekannt.

In dieser Studie wurden zwei verschiedene Stressparadigma verwendet um die molekularen Mechanismen zu klären, die Stress während der Entwicklung und emotionalen Störungen später im Leben zu Grunde liegen. Zuerst wurde ein 5-Htt x pränatales Stress (PS)-Paradigma verwendet um zu untersuchen, ob die Effekte von pränatalem Stress abhängig von dem 5-Htt Genotypen sind. Aus diesem Grund wurden die Effekte von PS auf Kognition, Angst- und Depressions-ähnliches Verhalten untersucht indem ein "maternal restraint stress"-Paradigma in C57BL/6-Wildtyp (WT) und heterozygoten 5-Htt defizienten (5-Htt+/-) Mäusen angewandt wurde. Zusätzlich wurde mit Hilfe des Affymetrix GeneChip® Mouse Genome 430 2.0 Arrays und des AffymetrixGeneChip® Mouse Promoter 1.0R Arrays bei den weiblichen Nachkommen ein Genexpressions- und DNA-Methylierungsprofil erstellt. Einige der daraus resultierenden Kandidatengene wurden mit quantitativer real-time PCR (qRT-PCR) validiert. Weiterhin wurde die Genexpression von diesen Genen auch in anderen Gehirnregionen der PS-Mäuse und im Hippocampus von Nachkommen aus einem perinatalem (PeS) Paradigma gemessen. In dem PeS-Paradigma wurden schwangere und stillende Weibchen durch einen olfaktorischen Stimulus, der Infantizid anzeigt, gestresst und die Nachkommen (WT und 5-Htt+/-) untersucht. Um PS- und PeS-Resilienz zu messen wurden Korrelationsstudien durchgeführt. Zuvor wurde eine LIMMA-Analyse, die auf dem Verhalten von den Mäusen im Forced swim-Test (FST) beruht, gerechnet.

Im Vergleich zu WT Nachkommen zeigten 5-Htt+/- Nachkommen des PS-Paradigmas verbesserte Gedächtnisleistung und Zeichen von reduzierter Angst. Im Gegensatz dazu war PS-Exposition von 5-Htt+/- Mäusen mit erhöhtem Depressions-ähnlichem Verhalten assoziiert, ein Effekt, der tendenziell eher in den weiblichen Nachkommen auffiel. Weiterhin beeinflussten der 5-Htt-Genotyp, PS und die Interaktion von beiden die Genexpression und DNA-Methylierung zahlreicher Gene und damit

verbundene Signalwege im weiblichen Hippocampus. Der MAPK- und Neurotrophin-Signalweg wurden zum Beispiel durch den 5-Htt-Genotyp und PS-Exposition reguliert, wohingegen der Zytokin- und Wnt-Signalweg in einer 5-Htt x PS Art beeinflusst wurden, was Gen x Umwelt-Interaktionen auf der molekularen Ebene andeutet. Die Kandidatengene konnten zumeist validiert werden und waren zum Teil auch im präfrontalen Kortex sowie im Striatum differentiell exprimiert. Weiterhin konnte der Genotypeffekt von XIAP associated factor 1 (Xaf1) in den Mäusen des PeS-Paradigmas nachgewiesen werden. Bezüglich der Resilienz konnten wir eine Herunterregulierung der Expression des Wachstumshormons (Gh), Prolaktins (Prl) und des fos-induzierten Wachstumsfaktors (Figf) in den WTPS-Mäusen detektieren, die eine gute Leistung im FST gezeigt haben. Gleichzeitig korrelierten die Gh- und Prl-Expression positiv mit dem Gewicht der Nebennieren, wohingegen die Figf-Expression mit dem basalen Kortikosteron-Konzentration positiv korrelierte, was eine komplizierte Beziehung zwischen Depressions-ähnlichem Verhalten, hippocampaler Genexpression und der Hypothalamus-Hypophysen-Nebennieren (HPA)-Achsenaktivität andeutet. Korrelationsstudien über die PeS-Tiere deckten einen Link zwischen der Gh- und Prl-Expression und Angst-ähnlichem Verhalten auf. Schließlich lassen unsere Daten den Schluss zu, dass, auch wenn der 5-Htt-Genotyp eine klare adaptive Kapazität aufweist, die 5-Htt+/- Mäuse, insbesondere die Weibchen im Vergleich zu den WT-Mäusen eine erhöhte Vulnerabilität für Entwicklungsstress zu zeigen scheinen. Weiterhin könnten die hippocampale Genexpressions- und DNA-Methylierungsprofile darauf schließen lassen, dass epigenetische Mechanismen auf der molekularen Ebene die Verhaltenseffekte des 5-Htt Genotyps, PS-Exposition und ihrer Interaktion vermitteln. Darüber hinaus könnte Resilienz zu Entwicklungsstress durch Gene reguliert werden, die mit der HPA-Achsen-Funktion assoziiert sind.

1. Introduction

1. Introduction

Goethe´s Faust seemed to be very depressed as he tried to kill himself with a poison (Faust I, V732-737).

„Hier ist ein Saft, der eilig trunken macht.

Mit brauner Flut erfüllt er deine Höhle.

Den ich bereite, den ich wähle,

Der letzte Trunk sei nun, mit ganzer Seele,

Als festlich hoher Gruß, dem Morgen zugebracht!

(Er setzt die Schale an den Mund)"

"Here is a juice, one's quickly drunk with it.

With its brown flood it fills thy ample bowl.

This I prepared, I choose this, high upborne;

Be this my last drink now, with all my soul,

A festal, lofty greeting pledged to morn!

(He puts the goblet to his lips.)"

Emotional disorders like depression can lead, in their severe forms, to suicide. According to the World Health Organisation (WHO) "depression is a common mental disorder that presents with depressed mood, loss of interest or pleasure, feelings of guilt or low self-worth, disturbed sleep or appetite, low energy, and poor concentration". These symptoms can become chronic or cyclic and can hinder individuals in their daily life and responsibilities. Depression is a major reason for disability worldwide and has a lifetime prevalence of 16.6% (Kessler *et al.* 2005). Similarly, anxiety disorders can also have a strong emotional component. For example, being emotionally blunted, flat or numb or fear of loosing control or getting a heart attack. Anxiety disorders have a lifetime prevalence of 28.8% and the average age of onset is 11 years (Kessler *et al.* 2005). Although several lines of evidence suggest an important role for serotonin (5-hydroxytryptamine, 5-HT) in the pathophysiology of depression and anxiety disorders, the exact underlying molecular mechanisms still remain to be elucidated.

Twin studies proposed that genetic factors may contribute to mood disorders like depression and anxiety (Sullivan *et al.* 2000). In this context, the serotonergic system, as a target for several antidepressants (see chapter 1.1), might play a pivotal role (Lesch and Heils 2000). A polymorphism in the 5-HT transporter (5HTT, SLC6A4) gene has been shown to be linked to depression- and anxiety-related personality traits (Lesch *et al.* 1996). To further study the underlying mechanisms of 5-HTT-related emotional vulnerability, 5-Htt deficient mice have been generated to model the human allelic variation in 5-HTT function (Bengel *et al.* 1998). Generally, these mice display elevated depressive- and anxiety-like behavior, altered stress coping abilities, and memory deficits like a disability in extinction recall (Holmes *et al.* 2002; Holmes *et al.* 2003; Carroll *et al.* 2007; Wellman *et al.* 2007; Heiming *et al.* 2009; Bartolomucci *et al.* 2010; Jansen *et al.* 2010).

As discussed in chapter 1.2, in addition to genetic vulnerability, a stressful early life environment, in particular during pregnancy, may also contribute to the development of psychopathology. For example, physical or emotional stress during gestation has been shown to influence the development of the fetal brain, thereby increasing the risk for neuropsychiatric disorders in adulthood, particularly disorders of emotion regulation such as depression (see review by Weinstock 2008). Likewise, prenatal stress (PS) exposure in rodents, particularly when exposure occurs during the last phase of pregnancy, is associated with a dysregulated hypothalamo–pituitary–adrenal (HPA) axis, concomitant with an increase in learning and memory deficits, as well as increased anxiety and depression-like behavior in adulthood (Pallares *et al.* 2007; Zuena *et al.* 2008; van den Hove *et al.* 2010; see also reviews by Weinstock 2001; Huizink *et al.* 2004). Nevertheless, the biological mechanisms by which PS exposure renders subjects susceptible to the development of neuropsychiatric disorders are as yet not fully understood.

By now, it has become increasingly clear that neither genetic nor environmental factors alone can account for the development of emotional disorders (see chapter 1.3). As such, variation in the 5-HTT gene was proposed to exert a modulating effect on the association between adverse experiences and the risk for anxiety disorders and depression (Collier *et al.* 1996; Lesch *et al.* 1996). Caspi and his colleagues (2003) tested maltreated children on depressive behavior in adulthood. They found that only the short (s) variant of the 5-HTT gene-linked polymorphic region (5-HTTLPR) generated the depressive outcome of early life maltreatment.

The present study aimed to examine the effects of early-life stress on cognition, anxiety- and depression-like behavior using a maternal restraint stress paradigm of PS in C57BL/6 wild-type (WT) and 5-Htt+/- mice. More knowledge on the molecular basis of such a G x E interaction might help to identify novel targets for the diagnosis and treatment of disorders of cognition and emotion regulation. For that purpose, we performed a genome-wide expression and methylation profiling on the hippocampus - a brain region participating in learning and memory as well as in emotion regulation (Fanselow and Dong 2010)- derived from the female offspring, which showed most pronounced behavioral changes mediated by variation in 5-Htt genotype, PS, and their interaction.

1.1 Genetic variation of the serotonin transporter

Serotonin was first discovered by Vittoria Esparmer in the enterochromaffine cells of the gut in the early 1930ths. More than 10 years later, it was also found in the blood serum displaying vasoconstrictive features, for which it was called serotonin (“serum” and “tonus”) from then on. In 1967, Coppen and colleagues for the first time discussed a decreased activity of serotonergic neurons in view of the pathogenesis of affective disorders (Coppen 1967; Coppen *et al.* 1967). In the same year, Schildkraut and Kety proposed the monoamine hypothesis of depression (Schildkraut and Kety 1967). 30 years later again, Lesch and colleagues identified an association between variation in 5-HTT genotype and anxiety-related traits comprising the personality dimension of “neuroticism” (Lesch *et al.* 1996).

1.1.1 Localization and impact of the serotonergic system

Neuronal 5-HT is located in the brain stem, especially in the pons and medulla oblongata. There, the serotonergic neurons form single groups of cells, which are described as the raphe-nuclei (B1-B9, see Fig.1-1). From there, two main complexes project into various areas of the brain and spinal cord: Neurons of the caudal raphe-complex (medulla oblongata and caudal pons; B1-4) descend to the motoric and autonomic system in the spinal cord. They activate motoric anterior horn cells and inhibit the dorsal horn of the spinal cord, which mediates nociception. Secondly, serotonergic groups of the rostral raphe-complex (mesencephalon and rostral pons; B5-B9) project mainly to the diencephalon and the forebrain. There, the serotonergic fibers innervate various brain regions including the (prefrontal) cortex, striatum, hippocampus and amygdala, thereby contributing to the regulation of mood, cognition, sleep-wake cycle, thermoregulation, and eating and sexual behavior.

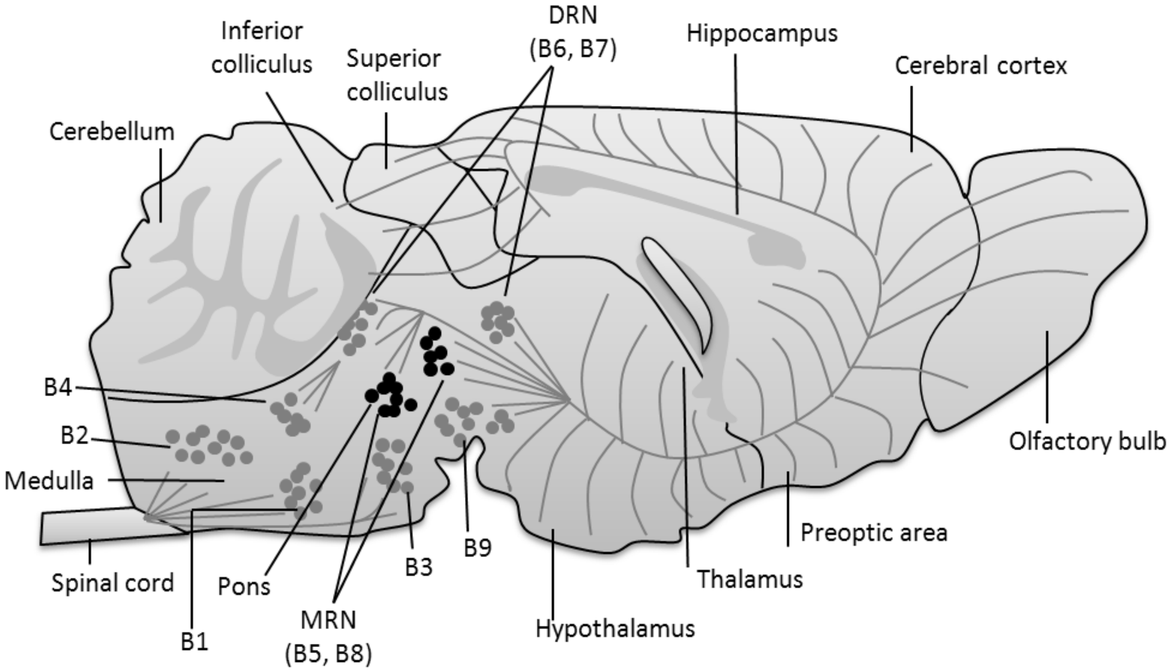

Figure 1-1. The murine central serotonergic system (Modified from Murphy and Lesch 2008). CNS 5-HT neuron cell-body groups in the nine raphe nuclei, B1–B9. The more caudal nuclei (B1–B3) in the medulla send axons to the spinal cord and the periphery. The more rostral raphe nuclei contain the principal dorsal raphe groups (B6 and B7; shown in grey) and the median raphe groups (B5 and B8; shown in black), which project to different brain areas.

1.1.2 Synthesis and metabolism of 5-HT

5-HT, as an indolamine, belongs to the monoamine neurotransmitters like the catecholamines adrenaline, noradrenaline and dopamine. Monoamines have an aminogroup and therefore closely resemble the amino acids from which they are produced. The synthesis of 5-HT occurs mainly in the soma, but to a lesser extent also in the dendrites and axons, in two distinct steps. In the first, rate-limiting step, the essential amino acid tryptophan (TP) is hydroxylated to 5-hydroxytryptophan (5-HTP). This reaction is catalysed by tryptophan hydroxylase (TPH). To date, two isoforms of TPH (TPH1 and TPH2) have been identified. Whereas TPH1 is expressed in the periphery and pineal gland, TPH2 is specific to the brain (Gutknecht *et al.* 2009). In the faster, second step of 5-HT synthesis, the carboxyl group of 5-HTP is removed by the aromatic L-aminoacid decarboxylase (AAAD) in order to yield 5-HT. AAAD is a soluble, ubiquitary enzyme, which is not specific for the decarboxylation of 5-HTP, but also contributes to the biosynthesis of the catecholamines. Decarboxylated monoamine transmitters like 5-HT are not able to cross the blood-brain barrier. If a deficiency of transmitters is assumed, like in the 5-HT-deficiency hypothesis of depression, the 5-HT production can be enforced by increasing the availability of their amino acid precursors (L-tryptophan and L-5-HTP), which are able to pass the blood-brain barrier.

To guarantee a regulated release of transmitters, 5-HT is stored in intracellular vesicles (see Fig. 1-2). Neuronal 5-HT-containing vesicles are located in the cell body, along the axon and at the synapse. Upon stimulation by an action potential there is an influx of Ca^{2+} which activates the vesicles to move towards the presynaptic membrane where they merge with the membrane and release 5-HT into the synaptic cleft.

5-HT conveys its manifold physiological and pathophysiological effects through the activation of receptors, which are bound to the pre- and postsynaptic membrane (5-HT_1 – 5-HT_7). The presynaptic autoreceptors 5-HT_{1A}, 5-HT_{1B} and 5-HT_{1D} are responsible for negative feedback. In various depressive and anxiety disorders, a decreased 5-HT_{1A} receptor binding and 5-HT_{1A} density has been observed in different brain regions like the frontal cortex, hippocampus (where 5-HT_{1A} is situated at the postsynapse) and the raphe nuclei (Sargent *et al.* 2000; Lundberg *et al.* 2007).

The 5-HTT removes 5-HT out of the synaptic cleft back into the presynaptic neuron. Part of the 5-HT is transported back into the presynaptic cell and is packed into vesicles again, whereas the rest is degraded by the monoamine oxidase A (MAO-A) to 5-hydroxyindole-3-acetaldehyde (5-HIAL). Subsequently, in the second step 5-hydroxyindolacetic acid (5-HIAA) is formed upon oxidation by aldehyde dehydrogenase.

1.1.3 Serotonin transporter

The 5-HTT is located in the presynaptic membrane and is a monoamine transporter. It terminates serotonergic neurotransmission by actively transporting 5-HT back into the presynaptic neuron, thereby regulating the extracellular concentration of 5-HT and contributing to the maintenance of homeostasis (Torres *et al.* 2003). The 5-HTT is a target of several antidepressants like the selective 5-HT reuptake inhibitors (SSRIs, e.g. fluoxetine), tricyclic antidepressants (TCAs) and illicit drugs like cocaine and 3,4-methylenedioxymethamphetamine (MDMA or “ecstasy”), which underlines the monoamine hypothesis of depression (Torres *et al.* 2003). In the brain, the 5-HTT is found exclusively in the raphe-complex and along the axons of serotonergic neurons (Chen *et al.* 1992; Blakely *et al.* 1994). The gene for the human 5-HTT is located at 17q.12.2, consists of 14 exons, is 35 kb long and has various 5' flanking regions and non-coding regulatory sequences (Lesch *et al.* 1994; Bengel *et al.* 1997). The transcriptional activity of the 5-HTT gene is regulated by a polymorphic repetitive element [5-HTT gene-linked polymorphic region (5-HTTLPR)] in the 5' untranslated region (Lesch *et al.* 1996), together with other allelic variations (Kilic *et al.* 2003; Prasad *et al.* 2005; Sutcliffe *et al.* 2005; Hu *et al.* 2006). The long (l) and s-alleles of the 5-HTTLPR are associated with high versus low 5-HTT protein expression, respectively. The rate of 5-HT reuptake is two times higher in cells which are homozygous for the l-variant when compared to cells which have one or two s-variants (Lesch *et al.* 1996). On average, the lower expressing s-allele carriers seem to be more at risk for anxiety, depressive and obsessive-compulsive disorders than l-allele carriers (Collier *et al.* 1996; Lesch *et al.* 1996; Hu *et al.* 2006). Besides some other deficits concerning emotionality, s-allele carriers excel in some cognitive functions, e.g. they show higher cognitive flexibility (for review see Homberg and Lesch 2011; Homberg 2012).

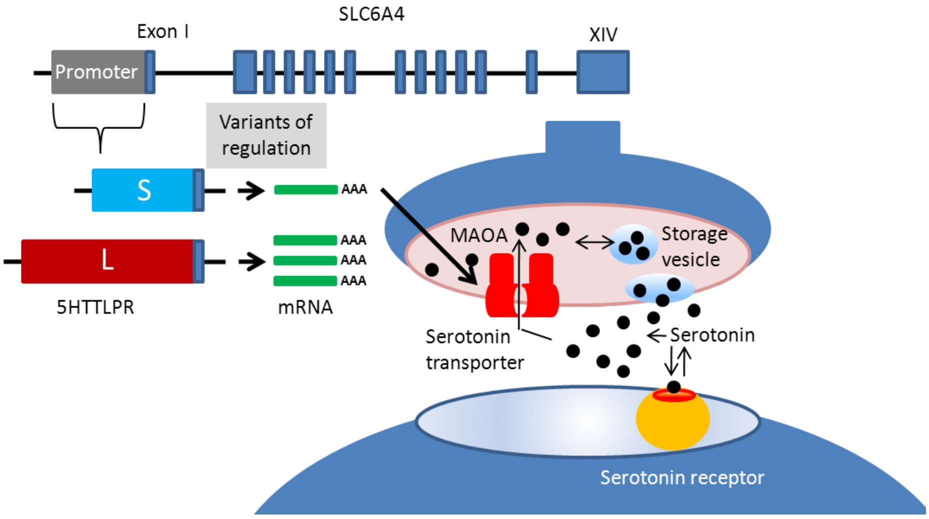

Figure 1-2. The serotonin transporter (5-HTT) and the associated 5-HT neurotransmission. Allelic variation of 5-HTT function in anxiety-related personality disorders, depression and other disorders of emotion regulation. The short (S) 5-HTTLPR variant (blue) of the 5-HTT gene (SLC6A4) produces significantly less 5-HTT mRNA and protein, as indicated by the green lines, than the long (L) variant (red), which results in higher levels of 5-HT in the synaptic cleft. The short variant is linked with anxiety-related personality traits such as neuroticism, which are risk factors for affective spectrum disorders. MAOA, monoamine oxidase A; (Modified from Canli and Lesch 2007)

To study the biological function of the 5-HTT in detail, an animal model with a targeted disruption (knockout; KO; -/-) of the 5-Htt was generated (Bengel *et al.* 1998). In 5-Htt-/- mice, the second exon of the 5-Htt gene has been eliminated by homologous recombination and therefore these mice express a truncated, non-functional 5-Htt protein. Thus, 5-HT cannot be taken up by the transporter which has been shown to lead to a 7-13 fold increase of the extracellular concentration of 5-HT in the prefrontal cortex (PFC), striatum, caudate putamen and nucleus accumbens (Mathews *et al.* 2004; Shen *et al.* 2004). On the other hand, the extracellular 5-HT concentration in the hippocampus, frontal cortex and the striatum is decreased (Bengel *et al.* 1998), which may be caused by an altered 5-HT metabolism and/or compensatory alterations in 5-HT receptor levels. In the dorsal raphe nucleus (DRN), there is a decrease of 5-HT_{1a} receptor-density and response, while in the substantia nigra similar effects were observed for 5-HT_{1b} (Fabre *et al.* 2000). The reduction of $5HT_{1a}$ receptors is more pronounced in females (Li *et al.* 2000). Another compensatory mechanism in 5-Htt deficient mice might be the upregulation of a polyspecific organic cation transporter, OCT3, which transports 5-HT, albeit with low affinity, back into the cell (Schmitt *et al.* 2003). Moreover, Nietzer *et al*. revealed that 5-Htt-/- mice differ from controls when it comes to dendritic length, spine density and complexity of pyramidal neurons in the infralimbic cortex, and in the basolateral and lateral nucleus of the amygdala (Nietzer *et al.* 2011).

5-Htt-/- mice are more anxious than their WT littermates as measured in the light dark test and open field (Heiming *et al.* 2009). Furthermore 5-Htt-/- mice are less aggressive as tested in the resident-intruder test (Holmes *et al.* 2002) and in another social interaction test (Lewejohann *et al.* 2010). 5-Htt+/- mice, which show intermediate levels of 5-Htt, display no changes in daily behavior in regard of locomotion, socio-positive and aggressive behavior, compared to WT mice, whereas 5-Htt-/- show a decrease in locomotion and an elevation in socio-positive behavior (Lewejohann *et al.* 2010). Overall, it seems as the 5-HTT mediates the effects of stress. In this context, an interaction between stress and the serotonergic system has been proposed (Andrews and Matthews 2004).

As some of these changes observed in 5-Htt deficient mice resemble the human phenotype of s-allele carriers, the 5-Htt deficient mouse model has been recognized as a valuable animal model for investigating the molecular mechanisms of emotion dysregulation.

1.2 Prenatal Stress

Stress is the major environmental factor known to increase the susceptibility for emotional disorders. Depending on the stage of the development, stress is known to exert a different impact on individuals. In general, the following rule applies: the earlier the stress is experienced, the more persistent the effects on the organism (Lupien *et al.* 2009). Pregnancy, for example, is a critical phase during which the programming of the HPA axis is extremely vulnerable to developmental stress exposure (Liu *et al.* 2001).

The idea that the maternal environment may be reflected in the child is not new. Leonardo Da Vinci wrote in his *Quaderni*: “The things desired by the mother are often found impressed on the child that the mother carries at the time of the desire… one and the same soul governs the two bodies, and the same body nourished both.” According to the “developmental origins of disease concept” (Gillman 2005), the increased risk for endocrine, metabolic and emotional diseases in adulthood may in part be dependent on variations of the early environment. In turn, the “predictive adaptive response” hypothesis (Gluckman and Hanson 2004) proposes that, for an optimal survival, the developing child tries to anticipate the environmental conditions with which it is confronted later on and adapts its physiology accordingly. Recently, epigenetic mechanisms like DNA methylation have been shown to represent a molecular memory by which environmental adversity can program the DNA to change an individual’s physiology and behavior throughout the lifespan (Tsankova *et al.* 2007).

As such, emotional or physical stress experienced by the mother during pregnancy may affect the developing fetus and might result in physical or mental disorders in the offspring´s later life. Although the long period between the adverse event and the onset of the disease makes it hard to estimate the exact number of people which are affected by PS, several retrospective studies document an increased incidence of pathological behavior in children exposed to maternal stress *in utero*. Stressful situations with longterm detrimental effects include familial and marital conflicts (Stott 1973), death of the husband (Huttunen and Niskanen 1978), threat related to wartime (Meijer 1985), an intense earthquake (Watson *et al.* 1999), and job loss (Schneiderman *et al.* 2005). Furthermore, depression and anxiety disorders during pregnancy represent stressful states as well. Importantly, women in their childbearing years are at an increased risk to develop these disorders (Kessler *et al.* 2005). Recent studies revealed that 10% of pregnant women suffer from depression and 18% show at least some symptoms (Heron *et al.* 2004; Marcus 2009), while anxiety affects approximately 13% of pregnant mothers (Heron *et al.* 2004).

Prenatal maternal stress has been associated with attention-deficit/hyperactivity disorder (Clements 1992), Gilles de la Tourette’s syndrome (Pasamanick and Kawi 1956), schizophrenia, autism, reduced cognitive ability, anxiety and depression (Stott 1973; Huttunen and Niskanen 1978; Meijer 1985; Ward 1991; van Os and Selten 1998; Watson *et al.* 1999; DiPietro 2006; Talge *et al.* 2007). In view of the mechanisms that underlie the relationship between PS exposure and adult psychopathology in humans, PS has been linked with an elevated incidence of congenital malformations (Hansen *et al.* 2000), lower birth weight, smaller head circumference (corrected for birth weight) and preterm delivery (Stein *et al.* 1987; Pagel *et al.* 1990; Hedegaard *et al.* 1993; Wadhwa *et al.* 1993; Lou *et al.* 1994; Copper *et al.* 1996; Hedegaard *et al.* 1996; Ruiz *et al.* 2002; Rondo *et al.* 2003; Torche 2011; Coussons-Read *et al.* 2012).

In animals, antenatal stress has been linked to a reduced birth weight and a greater risk to become ill or die before weaning (Cabrera *et al.* 1999). Moreover, PS is associated with hyperglycaemia and glucose intolerance (Lesage *et al.* 2004), an altered immune response (Coe and Lubach 2005), a disturbed HPA axis (see e.g. review by Weinstock 2005), deficits in learning and memory (Hayashi *et al.* 1998; Gue *et al.* 2004), elevated anxiety levels (Griffin *et al.* 2003; Dickerson *et al.* 2005; Estanislau and Morato 2005; Van den Hove *et al.* 2006; Heiming *et al.* 2009; Laloux *et al.* 2012) and increased depression–related behavior in later life (Secoli and Teixeira 1998; Morley-Fletcher *et al.* 2003; Morley-Fletcher *et al.* 2003; van den Hove *et al.* 2011).

The route by which PS regulates the development of the fetus and newborn is not entirely clear. In general, it has been proposed that PS results in a permanent hypersensitization of the brain to following stressful situations (Weinstock 1997; Weinstock 2005). Most of the studies placed reprogramming of the HPA axis into the spotlight as its regulation and response to stress is disturbed in offspring exposed to PS. Therefore, their reaction to adverse life events might be inappropriate. Next to changes in the HPA axis, a decreased nutrient and oxygen supply as a result of a (stress-dependent) reduced blood transfer through the placenta have been described (see review by Huizink *et al.* 2004).

1.2.1 HPA axis

The body aims to maintain a complex equilibrium (homeostasis), which is constantly disturbed by stressors (Habib *et al.* 2001). It is very important that an organism is able to react properly to these disruptions and adapts itself to its environment (McEwen 1999), a process which is also called allostasis (McEwen 2003). In mediating these adaptive responses, the HPA axis plays a major role.

In response to stress, higher brain regions like the hippocampus, the cortex and the amygdala activate two important stress systems (see Figure 1-3). Firstly, the very fast acting sympathetic-adrenal-medullary axis is activated, which has the catecholamines adrenalin and noradrenaline as its effectors. Secondly, HPA axis activation results in a release of corticotrophin releasing hormone (CRH) into the hypophyseal portal vessel by the hypothalamic paraventricular nucleus (PVN). CRH, together with the antidiuretic hormone arginine vasopressine (AVP) that is also released by the PVN, stimulate the production and release of adrenocorticotrophic hormone (ACTH) from the anterior pituitary gland into the circulation (Whitnall 1989). From there, ACTH reaches the adrenal cortex. Along this road, CRH and ACTH control the production and secretion of glucocorticoids, i.e. cortisol in humans and nonhuman primates and corticosterone in rodents, from the adrenal cortex. Furthermore, CRH activates noradrenergic neurons in the locus coeruleus, which in turn may activate the hypophysial adrenal axis and therefore may stimulate the sympathetic nervous system (Valentino *et al.* 1983; Rassnick *et al.* 1994). Finally, the glucocorticoids and catecholamines lead to an elevation of hepatic glucose synthesis and secretion, as well as an elevation of cardiovascular muscle tone (Sapolsky and Meaney 1986; Herman *et al.* 1996) in order to meet the threatening situation. On the other hand, reproduction, growth and certain components of the immune system are inactivated (Munck *et al.* 1984; Sapolsky *et al.* 1986; Herman *et al.* 1996). In the short run, these adaptations in response to stress are generally positive. However, if the stress systems are overactive for too long this can lead to damage or a so called "wear and tear on the body and brain (allostatic load)", which in turn may lead to psychopathology (for review see McEwen 2003).

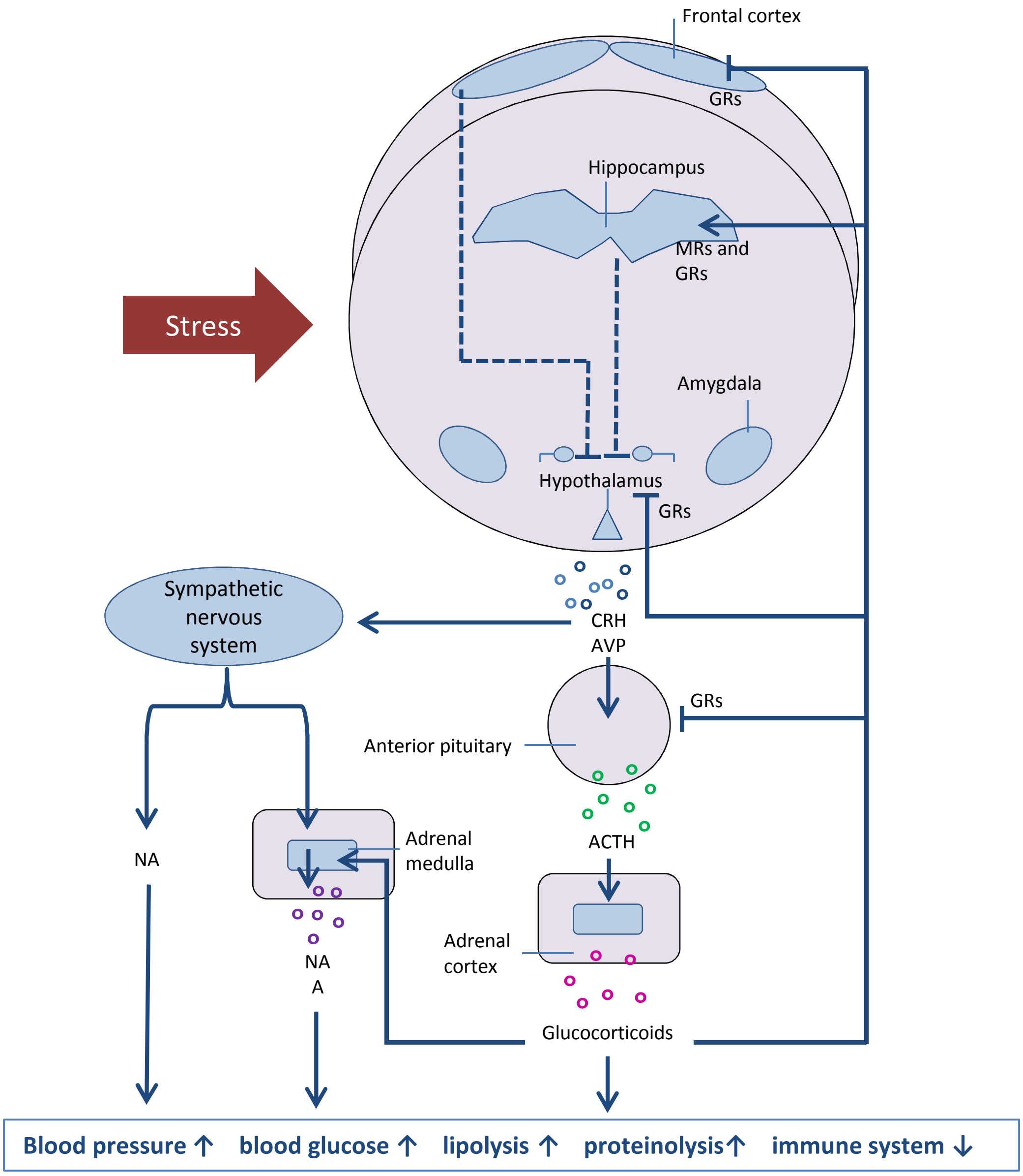

Figure 1-3 The two most important stress axes: the sympathico-adrenal-medullary axis and the hypothalamo-pituitary-adrenal (HPA) axis (modified from Lupien *et al.* 2009); After stress is perceived by higher brain regions, the sympathetic-adrenal-medullary axis and the HPA axis are activated. As a very fast response the sympathetic nervous system releases noradrenaline (NA) in the brain and activates the adrenal medulla to release NA and adrenaline (A). In addition, the slower but more perpetuate response from the HPA axes is initiated. The hypothalamus releases corticotrophin releasing hormone (CRH) and vasopressin (AVP). Subsequently, ACTH is secreted from the anterior pituitary to activate the release of glucocorticoids from the adrenal cortex. NA, A and glucocorticoids activate physiological responses and decrease immune system responses. As a negative feedback, glucocorticoids stimulate the glucocorticoid receptors (GR) at several levels, which, in turn inhibit the further production of glucocorticoids and therefore normalize the HPA axis.

For a proper regulation of the HPA axis, a negative feedback mechanism exists, which acts at several levels, namely at the hippocampus, hypothalamic PVN, and the pituitary gland. The feedback system is mediated by the two corticosteroid receptors, i.e. the mineralocorticoid receptor (MR, type 1) and the glucocorticoid receptor (GR type 2) (Reul and de Kloet 1985). It is suggested that the high affinity-MR mainly acts at basal stress levels whereas the low-affinity GR acts when the organisms is stressed (De Kloet *et al.* 1998). An impaired negative feedback could stem from stress-induced damage to the hippocampus (McEwen 1999), or from a downregulation of GR in the PVN, pituitary gland and hippocampus (Prickaerts 2005).

1.2.2 Implication of the HPA axis activity in pregnancy

HPA axis regulation of pregnant women deviates slightly from non-pregnant women. Pregnant women have an ever increasing rate of plasma CRH concentration because the placenta releases CRH gradually into the maternal and fetal compartments across gestation (Petraglia *et al.* 1996; Weinstock 2005). In contrast to the brain, CRH release from the placenta is not inhibited but activated by cortisol in a positive feed-forward mechanism (Robinson *et al.* 1988; Majzoub and Karalis 1999). Thus, gestation can be considered as a situation of smooth and perpetuated hypercortisolism (McLean and Smith 1999). Importantly, the placenta acts like a barrier to secure the future child from pathologically high levels of CRH. It does so by means of binding and inactivating CRH through the CRH binding protein (CRH-BP). Towards the end of pregnancy the concentration of CRH-BP decreases thereby elevating free maternal CRH-BP (Perkins *et al.* 1995), which might initiate parturition (for review see Grammatopoulos 2008). Further, another protective mechanism concerning maternal cortisol/corticosterone exists. The placenta expresses the enzyme 11-β-hydroxysteroid dehydrogenase type 2 (11-β-HSD-2), which changes cortisol/corticosterone into bio-inactive 11-keto forms, i.e., cortisone and 11-dehydrocorticosterone (White *et al.* 1997). Despite its buffering capacity, there is still a linear relation between maternal and fetal cortisol levels (Gitau *et al.* 1998), which might be an issue in stressful situations (see below).

1.2.3 Reprogramming of the HPA axis by maternal stress exposure

Although the reactivity of pregnant mothers to acute stress seems to be mitigated, they display clear physiological reactions to stress, the extend of which differs between individuals (de Weerth and Buitelaar 2005). Generally, high levels of stress lead to increased CRH and ACTH levels in pregnant women (Wadhwa *et al.* 1996; Weinstock 2005) indicating that the suppressive mechanisms of HPA-feedback, which usually protect the organism from abnormal high levels of free CRH, may be impaired by prolonged stress. Though glucocorticoids are vital for developmental organizational processes they have become major candidates when it comes to an impaired programming of the fetal HPA axis. For example, 10-year-old children of mothers with gestational anxiety showed a significant correlation between the degree of maternal anxiety and waking levels of plasma cortisol (O'Connor *et al.* 2005). In rat studies, antenatal stress leads to an increase of corticosterone levels in the mother and the fetus (Dauprat *et al.* 1984; Cadet *et al.* 1986). Furthermore maternal brain GR receptors may decline in sensitivity and number after chronic or repeated stress during pregnancy, which is supposed to lead to a dysfunction in maternal HPA axis regulation (see above). Of note, mothers that are determined to deliver preterm have higher CRH concentrations at mid-gestation than mothers that deliver at term (McLean *et al.* 1995). Abnormally high concentrations of maternal hormones can in turn reach the fetus and influence its development. Possibly, a hyperactive HPA axis of the mother may lead to fetal growth retardation, preterm delivery, and disturbed HPA axis function in the offspring (Weinstock 2001; Huizink *et al.* 2004; Weinstock 2005).

As already stated above, the future child is normally protected from high concentrations of CRH and glucocorticoids by factors like CRH-BP and 11-β-HSD-2. These protective mechanisms, however, might fail when they have to cope with high levels of stress-induced CRH and glucocorticoids. Furthermore, next to variability in placental 11-β-HSD-2 (Welberg *et al.* 2000) activity, PS has been shown to decrease placental 11-β-HSD-2, which might be another mechanism in fetal HPA axis programming (O'Donnell *et al.* 2012). In line with this, low 11-β-HSD-2 activity is linked with disturbed fetal growth (Benediktsson *et al.* 1997).

1.3 Gene x environment interactions

Emotional disorders may result from a complex interaction between an individual's genetic make-up and environmental factors. The hypothesis of gene x environment (G x E) interaction is based on the assumption that subtle genetic differences lead to different susceptibilities to environmental cues. This might be an explanation why some people are at a greater risk to develop a depression or an anxiety disorder after an environmental insult.

Research on G x E interactions in psychiatry has started with epidemiological studies using twins (e.g. (Cantor-Graae *et al.* 1994)). Although studies like these suggest that psychiatric diseases and normal behavior depend upon both environmental and genetic variation, they are not able to explore the underlying molecular mechanisms (Caspi and Moffitt 2006). The first study that suggested that genotype moderates the outcome of an adverse environmental event was published in 2002 (Bennett *et al.* 2002). One year later, Caspi and his group reported an interaction between the 5-HTT polymorphism and childhood maltreatment on depressive outcome (Caspi *et al.* 2003). They revealed that early-life stress (between age 3 and 11) could predict adult depression (between age 21 and 26) but only in s-allele carriers and not in ll-carriers. Many other studies have tried to replicate this G x E interaction by the use of different populations and different study designs (Caspi *et al.* 2010), but this interaction could not be replicated in all investigations and some meta-analysis in fact described a negative effect (Munafo *et al.* 2008; Munafo *et al.* 2009; Risch *et al.* 2009). There are several reasons for these discrepancies, for example the fact that timing and type of stress (Karg *et al.* 2011) or the definition of the outcome variable may be different. Uher and colleagues (2011) reported that s-allele carriers exposed to early-life stress displayed an increased risk for (persistent) depression diagnosed at at least two time points, but not for single-episode depression. Further, differences in genetic backgrounds could contribute to the discrepancies as many other polymorphisms may also form the basis for this G x E interaction. For example, polymorphisms in the CRH receptor 1 (CRHR1) gene (Bradley *et al.* 2008), the GR gene (Bet *et al.* 2009), the hsp co-chaperone of the GR (FKBP5) gene (Luijk *et al.* 2010; Roy *et al.* 2010), the 5-HT$_{3A}$ receptor and brain derived neurotrophic factor (BDNF) genes (Gatt *et al.* 2010), the dopamine D2 gene (Hayden *et al.* 2010) and the oxytocin receptor gene (Thompson *et al.* 2011) have been suggested to interact with early-life stress to predict depression.

Moreover, besides depression, the 5-HTTLPR x early-life stress interaction may also predict other stress-related traits. By the use of functional magnetic resonance imaging (fMRI), several studies revealed that different brain regions of s-allele carriers display altered neural activity and connectivity in response to emotional stimuli (Hariri *et al.* 2002; Canli *et al.* 2005; Heinz *et al.* 2005; Pezawas *et al.* 2005; Canli *et al.* 2006; Canli *et al.* 2008). For example, children that carry the s-allele display increased excitability in various brain regions while watching sad movies compared to l-allele carriers (Fortier *et al.* 2010).

Rhesus macaques posses a repeat length variation (rh-5-HTTLPR) which is in structure and function orthologous to the human 5-HTTLPR (Lesch *et al.* 1997). That makes them attractive to study 5-HTT x early adversity interactions. Champoux and colleagues (2002) separated infants (sl and ll) from their mothers at day 1-3 after birth and reared them in a nursery facility. Infants carrying the s-allele displayed decreased orientation, lower attentional capabilities and a heightened affective response compared to ll-carriers. This increased behavioral stress-reactivity of the sl-infants was more pronounced in the maternal separation group than in the mother-reared group. Further, the endocrine response to stress was assessed in female and male rhesus infants, that were reared maternally or only in peer groups. ACTH and cortisol plasma levels were measured several times during the first 6 month of age at baseline and after a 30 min separation from the mother or peer group. Male infants with the s-variant of the rh5HTTLPR had higher ACTH levels when compared to monkeys homozygous for the l-variant. ACTH levels increased during separation and s-allele carriers that were reared among peers displayed higher ACTH levels during separation than the ll-monkeys. In addition, cortisol levels increased during separation and infants of the peer-only group showed diminished cortisol levels. Interestingly, especially female monkeys with the s-allele had lower cortisol levels in response to stress and increased ACTH responses to stress, but only in those females with a history of adversity. These sex differences may explain why women are more prone to stress and have a higher incidence of stress-related disorders (Barr *et al.* 2004). Overall, these findings resemble human studies, confirming that impaired function of the 5-HTT influences the HPA axis and that the effect of the rh5HTTLPR on hormonal responses to stress is moderated by adverse early life events in a sex dependent manner (O'Hara *et al.* 2007; Mannie *et al.* 2009; Wust *et al.* 2009).

Carroll and colleagues (2007) were the first who studied the interaction of early-life stress and the 5-HTT gene in mice. From postnatal day 7 on over a period of one week, mouse pups received three mild footshocks (150 s) per day. In adulthood, anxiety and depression-related behaviors were assessed using the elevated plus-maze, light/dark test, open field and FST. This type of stress was not able to alter the enhanced anxiety- and depression-like phenotype of the 5-Htt deficient mice. In another study, pregnant and lactating female mice, which were heterozygous for the 5-Htt, were exposed to an unfamiliar male bedding (Heiming *et al.* 2009). This olfactory cue was considered to be dangerous for the mothers as it indicates infanticide by the unfamiliar male. The offspring of mothers who lived in a threatening environment displayed elevated anxiety-like and diminished exploration behavior compared to controls. These effects were more pronounced in 5-Htt-/- mice. Another study examined the interaction of the 5-HTT gene and maternal neglect during the first weeks of life (Carola *et al.* 2008). Offspring suffering from low maternal care displayed deficient gamma-aminobutyric acid-A (GABA-A) receptor binding in the amygdala. Further, 5-Htt+/- mice were more anxious, showed more signs of depression-like behavior and diminished 5-HT turnover in the hippocampus and striatum compared to controls. Interestingly, Bdnf mRNA concentrations in the hippocampus were only increased in 5-Htt+/- mice suffering from low maternal care. This may indicate that Bdnf is a common neuronal substrate of the 5-Htt x maternal neglect interaction.

Together with the findings in rhesus macaques it is tempting to speculate that the 5-HTT plays a pivotal role in modifying the long-term behavioral effects of the early life environment and that the underlying molecular mechanisms of this GxE interaction identified in animal models are important in the developmental programming of adult psychopathology (for review see Lesch 2011).

1.4 Resilience

Resilience is the ability to cope with stressful situations and not to succumb to adversity. Thus, resilient individuals show only few symptoms of psychiatric diseases like depression and anxiety disorders when compared to susceptible subjects. There are several psychosocial factors which allow resilient people to bounce back after stressful situations. For example, active coping strategies like problem solving and planning increase well-being. Also physical exercise can be considered as an active coping mechanism as it may lead to e.g. improved mood and dampened responses to stress (Southwick *et al.* 2005). Further, resilience requires optimism and high positive emotionality including humor, hope, joy, contentment, pride and love (Tugade and Fredrickson 2004; Ong *et al.* 2006). Such an attitude promotes adaptive coping, openness to social support (Ong *et al.* 2006), cognitive flexibility, exploration and a broadened focus of attention (Fredrickson 2001). Resilient individuals are characterized to have a sense of purpose in life, a moral compass, spirituality and the ability to find meaning in the midst of adverse events.

The underlying physiological, neurobiological and molecular mechanisms of resilience have just begun to be elucidated as the focus so far has been more on the negative effects of stress (i.e. vulnerability to psychopathology). For example, resilient individuals are thought to activate the stress response very fast but also terminate it efficiently. Therefore, a proper function of negative feedback of the HPA axis is needed, including optimal function and balance between MR and GR (Charney 2004; de Kloet *et al.* 2005; de Kloet *et al.* 2007). Further, dehydroepiandrosterone (DHEA; also secreted in response to stress) sulphate/cortisol levels might indicate an individual´s buffering capacity to stress. For example, soldiers who had higher DHEA levels during acute stress (rigorous survival training) displayed lower dissociative symptoms and performed better in the military when compared to their companions (Morgan *et al.* 2004). Also male veterans with posttraumatic stress disorder (PTSD) display higher DHEA when symptoms improve (Yehuda *et al.* 2006). In this context neuropeptide Y (NPY) seems to play an important role as well. NPY shows anxiolytic-like effects and is supposed to increase cognition during stress exposure. Furthermore, it has opposing effects as compared to CRH when it comes to anxiety. Thus, resilient behavior might include a balanced NPY/CRH level during stress exposure (Sajdyk *et al.* 2004). An indication for that might be that soldiers with higher NPY levels performed better in the survival training (Morgan *et al.* 2000) and veterans without PTSD display higher plasma NPY levels as compared to those with PTSD (Yehuda *et al.* 2006).

Again, animal models help to provide insights into the underlying molecular mechanisms. Although not all psychological characteristics can be assessed in animals, they display traits which can be referred to as vulnerable or resilient responses to stress. For example, active coping or fight-or-flight responses like attempts to escape or aggression are considered as resilient. On the other hand, freezing and submission are passive reactions to stress reflecting a more vulnerable phenotype (Korte *et al.* 2005). A well-known mouse model for resilience is e.g. the social defeat stress paradigm. Krishnan and colleagues stressed C57BL/6 mice by introducing them into an area of a more aggressive CD1 mouse for 10 consecutive days (Krishnan *et al.* 2007). During 10 min of interaction with the aggressor the C57BL/6 mice were attacked and showed subordinate posturing. When tested on day 11, resilient mice displayed less social avoidance measured by the time spent in the interaction zone while a social target is present versus the time spent in the interaction zone without such a target. Interestingly, the group of Vialou found later, that ΔFosB is needed to show resilient behavior to social avoidance (Vialou *et al.* 2010). Furthermore, Schmidt and colleagues exposed mice to an unstable hierarchical situation during adolescence and the young adult period (Schmidt *et al.* 2010). Five weeks after the end of the stress exposure, basal morning corticosterone was measured. In comparison to vulnerable mice, resilient animals recovered faster from the stress (lower corticosterone levels). Further, they found that vulnerable subjects showed a higher number of AMPA receptor availability. Next to this, Shishkina and colleagues tested whether rats are resilient to the development of depression-like behavior in the FST. 40% of the animals showed resilience and had increased anti-apoptotic B cell lymphoma like X (Bcl-xl) to pro-apoptotic Bcl2-associated X (Bax) ratios in the hippocampus (Shishkina *et al.* 2010). Moreover, the work from Meaney and colleagues demonstrated that a positive environment can foster resilience. Offspring that experienced high licking-and-grooming and arched-back nursing displayed decreased anxiety and cared more about their own pups. Further, they showed dampened corticosterone responses to stress (for review see

(Meaney and Szyf 2005)). Another study used rough-and-tumble play, which elicits hedonic ultrasonic vocalizations (USVs) in rats, as a positive social environment (Burgdorf *et al.* 2010). They observed that this positive interaction was associated with an increase in insulin like-growth factor I (IgfI).

As indicated above, susceptible and resilient responses to stress can be very different in genetically identical rodents within a highly controlled environment. This makes it tempting to speculate that, genetic and environmental influences as well as their interactions are based on epigenetic mechanisms when it comes to variability in behavior.

1.5 DNA methylation and epigenetic programming

Epigenetic mechanisms represent heritable changes in gene expression caused by mechanisms other than variation in the underlying DNA sequence. These mechanisms are thought to play a crucial role in the interplay of genetic and environmental factors in determining a subject's phenotype. Many of those structural adaptations, which all act in concert to regulate gene transcription, have now been identified (e.g. DNA methylation, histone modifications and non-coding RNAs). Generally, gene transcription can occur if the chromatin (i.e. the combination of DNA, histones and other proteins associated with the DNA) is in an active, open state (euchromatin). An inactive, closed state (heterochromatin) does not allow gene transcription and results in gene silencing (for review see Tsankova *et al.* 2007).

DNA methylation is one of the best studied epigenetic modifications. The DNA is methylated at cytosine (C) residues (5-methylcytosine; 5mC) by DNA methyltransferases (Dnmt) (Yoder *et al.* 1997). Although not exclusively, DNA methylation takes place at loci where a C is followed by a guanine (G), i.e. so called CpG dinucleotides (Suzuki and Bird 2008; Lister *et al.* 2009). The frequency of CpG dinucleotides is unexpectedly low in mammalian genomes. This is due to the evolutionary loss of CpGs by *de novo* methylation of CpGs followed by spontaneous deamination of the C which transforms into a thymine (T) (Zemojtel *et al.* 2011). When a DNA sequence of at least 300 bp has a C+G content greater than 0.55, it is called a CpG island (Aerts *et al.* 2004). Generally, CpG islands are unmethylated and are associated with 75% of human genes (Ioshikhes and Zhang 2000). Recent studies showed that only approximately 50% of the CpG islands mark promoters of 5' regions of protein-encoding genes, whereas the other CpG islands are found in gene bodies (in the transcribed regions), sometimes in promoter sequences of regulatory RNAs and in regions of unknown function (Illingworth *et al.* 2008). Usually, methylation of the promoter region leads to gene silencing (see Fig. 1-4) (Jaenisch and Bird 2003), whereas recent studies have shown that gene-body methylation results in an increase of gene expression (Hellman and Chess 2007; Backdahl *et al.* 2009). These effects are brought about by the recruitment of methyl-CpG-binding proteins (MBD such as MeCP2), histone modifying enzymes (e.g. histone deacetylases; HDAC) and microRNAs (see Fig. 1-4), which mediate chromatin remodeling and associated alterations in gene expression.

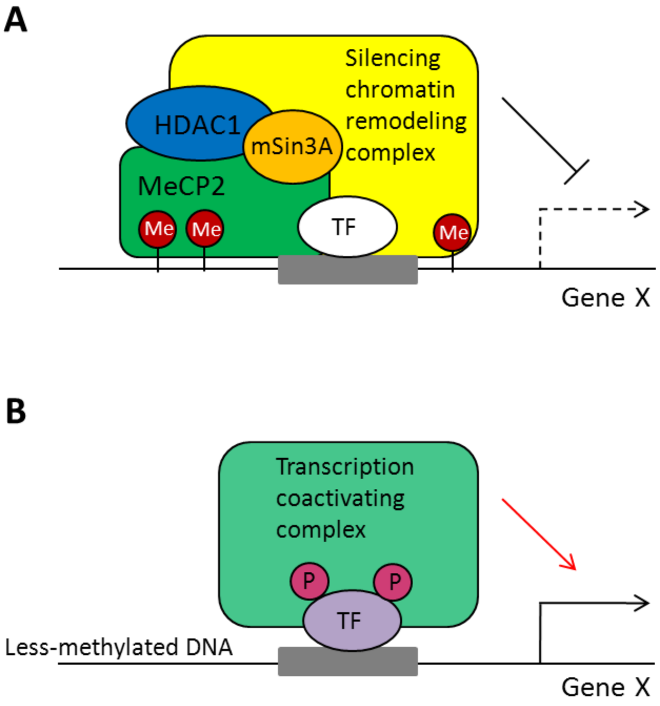

Figure 1-4. DNA methylation-mediated regulation of gene transcription A) DNA methylation is suggested to recruit methyl-CpG binding proteins (MBD) such as MeCP2, which in turn recruits histone deacetylases (HDACs) by the corepressor mSin3A to form a complex that mediates inactive chromatin remodelling. As such, transcription factors may not bind leading to gene silencing. B) When the DNA is less methylated, MeCP2 dissociates, so that transcription factors can bind and gene transcription is possible. (Modified from Martinowich *et al.* 2003)

Recently, several studies demonstrated that DNA methylation is negatively correlated with expression. For example, increased hippocampal GR expression in rats, which were exposed to high levels of maternal care, is associated with a reduced DNA methylation within the GR exon 1_7 promoter in the hippocampus, as well as elevated histone acetylation (Weaver *et al.* 2004). By these epigenetic modifications, the binding of the transcriptional activator nerve growth factor 1 (NGF1A) to the GR promoter is eased (Weaver *et al.* 2007), which might be a plausible mechanism for the epigenetic programming of gene function by a caring mother early in life (Dudley *et al.* 2011). Interestingly, hippocampal GR mRNA was decreased and promoter DNA methylation was increased in suicide victims with a history of childhood abuse (McGowan *et al.* 2009). Although this is an indirect correlation, one can speculate that the epigenetic modifications involved in mediating stress vulnerability in rodents can be translated to humans. Another study shows that the elevated stress sensitivity of mice, that were maternally separated, is associated with increased expression of AVP in the hypothalamus and decreased levels of DNA methylation at particular CpG dinucleotides within an AVP enhancer region that is important for the binding of MeCP2 (Murgatroyd *et al.* 2009). Next to maternal care, also PS exposure seems to have an effect on epigenetic programming. For example, Mueller and Bale (2008) stressed pregnant mice during the first week of pregnancy and found elevated DNA methylation at GR and CRH promoter regions in the hippocampus of male offspring. However, less is known about the molecular mechanisms of early-life stress in 5-Htt+/- mice.

2. Materials and methods

2. Materials and Methods

This series of experiments consisted of two different mouse studies. In the first, 5-Htt x PS study, WT and 5-Htt+/- deficient mice were exposed to prenatal restraint stress in order to assess the behavioral effects of PS exposure in male and female offspring. Brains of these animals were used to screen for associated gene expression and DNA methylation changes. In a second study, brain material derived from another, 5Htt x *perinatal* stress (PeS) paradigm was used to screen for expression changes in candidate genes derived from the PS study.

2.1 Prenatal stress exposure

2.1.1 Animals and ethics

Animal handling and behavioral studies were performed in collaboration with Daniel van den Hove and his colleagues from the Maastricht University. This study was approved by the Animal Ethics Board of Maastricht University, The Netherlands (Permit number: OE 2007-109). All efforts were made to minimize suffering.

For breeding, acclimatized female 5-Htt+/- and male 5-Htt+/- deficient mice ([B6.129(Cg)-Slc6a4tm1Kpl/J] (Bengel *et al.* 1998)) were utilized. The mice were housed in individual cages. The temperature was controlled (21±1°C) and a 12 h light/12 h dark cycle (lights on from 7.00 h) was set. Standard rodent chow and water was available *ad libitum*. Pregnancy was determined by observation of vaginal plugs (embryonic day 0 – E0). Prenatal maternal stress (n=15) was performed daily during the last part of pregnancy (E13–E17). The dams were restraint in transparent 250 ml glass cylinders filled up to a height of 5 mm with water, whilst being exposed to bright light, 3 times daily (between 8.00 and 10.00 h, 12.00 and 14.00 h and 16.00 and 18.00 h), for 45 min per session (adapted from (Behan *et al.* 2011)). Control pregnant females (n = 14) were left undisturbed in their home cages and maternal weight was measured at E0, E12 and E17. To protect the litters for cannibalism, they were left undisturbed for 5 days after birth (P5). Only litters of 5 or more pups were included in the present study. Genotyping was performed by using polymerase chain reaction (PCR). DNA-fragments of either 225 bp refer to 5-Htt+/+, 272 bp to 5-Htt-/- or both to 5-Htt+/- mice. Offspring were individually housed in ventilated cages (TouchSLIMLine, Techniplast, Italy) after weaning (P25) under a reversed day-night cycle (12 h light/12 h dark cycle; lights on from 19.00 h). Pup mortality was monitored from P5 onwards. No more than two male and/or two female pups per litter were used to prevent litter effects (Chapman and Stern 1979). Behavioral experiments were started when the offspring reached the age of 2 months (P60) (n=10-14/group). First, memory abilities were measured using the object recognition task (ORT). Next, anxiety- and depression-like behavior were assesed using the elevated zero maze (EZM) and forced swim task (FST), respectively. Tests were always performed in the dark phase (between 9.00 and 17.00 h for the ORT and between 9.00 and 13.00 h for the other tasks). Males and females were tested in all experiments separately. One week after behavioral tests, stress-induced plasma corticosterone (CORT) secretion was examined. One week later, the mice were sacrificed and brains removed. In addition, the adrenals were removed and weighted. Brains and blood samples were immediately placed on dry ice and stored at -80°C for future experiments.

2.1.2 Behavioral and physiological assessments

The behavioral studies were performed in collaboration with Daniel van den Hove and his colleagues at the Maastricht University.

Object recognition task (ORT)

Object recognition memory with mice was performed as described elsewhere (Sik *et al.* 2003). The apparatus consisted of a circular arena, 43 cm in diameter. The test was performed with a constant illumination of approximately 20 lux. Two objects were placed symmetrically 5 cm away from the wall. Four objects were used: (1) a cone made of brass (maximal diameter 6 cm and total height 3.8 cm), (2) a transparent glass bottle (diameter 2.7 cm, height 8.5 cm) filled with sand, (3) a metal cube (2.5 cm× 5 cm× 7.5 cm) with two holes (diameter 1.5 cm), and (4) an aluminium cube with a tapering top (4.5 cm × 4.5 cm × 8.5 cm). Each object was available in triplicate. In the first week, the animals were handled daily and were allowed to explore the arena, twice for 5 min each day, without any objects. Next, the mice were assessed until they showed a good discrimination performance. A testing session comprised of two trials. The duration of each trial was 5 min. During the first trial (T1) the apparatus contained two identical objects. A mouse was always placed in the apparatus facing the wall at the middle of the front (transparent) segment. After the first exploration period, the mouse was put back in its home cage. Subsequently, after a predetermined delay interval (2, 3 or 4 h), the mouse was put back in the apparatus for the second trial (T2). However, now there were two dissimilar objects, a familiar one and a new one. The times spent exploring each object during T1 and T2 were recorded manually using a personal computer. Exploration was defined as follows: directing the nose to the object at a distance of no more than 2 cm and/or touching the object with the nose. Sitting on the object was not considered as exploratory behavior. In order to avoid the presence of olfactory cues the objects were always thoroughly cleaned with 70% ethanol before each trial. All combinations and locations of objects were used in a balanced manner to reduce potential biases due to preferences for particular locations or objects. Each delay interval was tested once in each animal. At least a two-day period was in between any delay test sessions with a particular animal. The testing order was determined randomly. The relative discrimination index (RDI) ([time spent on new object in the second trial T2 - time spent on familiar object in T2]/total exploration time during T2) was determined for all mice.

Elevated zero maze (EZM)

The EZM is a task to measure anxiety-like behavior (Shepherd *et al.* 1994). The test was conducted on a maze constructed of black plastic, transparent for infrared light. The circular runway was 50 cm in diameter, with a pathway width of 5 cm placed 10 cm above floor level. The maze was equally separated in 2 opposite open and 2 opposite closed parts enclosed by 50 cm high side walls. To prevent falls, a 5 mm high rim lined the open parts. A mouse was placed into the middle of one of the open parts, facing the outside of the maze. The mouse was allowed to explore the arena for a 5 min period. The distance travelled and % of time spent in the open parts of the maze was determined under low light conditions (20 lux) by use of an infrared video tracking system (Ethovision Pro, Noldus, Wageningen, The Netherlands; van Donkelaar *et al.* 2010). In order to avoid the presence of olfactory cues the arena was always thoroughly cleaned with 70% ethanol before each trial.

FST

The FST is commonly utilized to score behavioral despair in rodents (Borsini and Meli 1988; van Donkelaar *et al.* 2010). Animals were individually placed in a transparent perspex cylinder (40 cm tall; 19 cm in diameter; filled to a height of 15 cm with water of 31°C; (van Donkelaar *et al.* 2010)). Distance moved, as an indicator of mobility of the mice was measured in a 5 min session using a computerized system (Ethovision Pro, Noldus, The Netherlands).

CORT response

When the offspring used in the behavioral testing reached an age of 3 months (P90) a blood sample was taken from the saphenous vein (basal CORT level). Subsequently, these mice were subjected to 20 min of restraint stress by a procedure identical to the PS procedure applied to the dams. Immediately following restraint stress, a second blood sample was taken (stress-induced CORT level). The mice were then returned to their home-cage for a 40 min recovery period, after which a third and final blood sample was taken ('recovery' CORT level). Blood collection, sample preparation and determination of plasma CORT levels were done as described in detail previously (Van den Hove *et al.* 2006). All blood samples were taken between 10:30 -13:00 h.

2.1.3 Expression study

RNA isolation and microarray

For this purpose, the left half of the hippocampus of females and males was used. The tissue was homogenized using 500 µl PegGOLD RNAPure (Peglab, Erlangen, Germany) and metal beads for 3 min at 20Hz in a Tissue Lyser (Qiagen, Hilden, Germany)). Subsequently, 100 µl chloroform was added and samples were centrifuged for 5 min at 4° C and 12.000 x g. The water phase was then mixed with 250 µl ethanol and from that point on the protocol of the RNeasy Mini kit (Qiagen, Hilden, Germany) was followed. RNA-quality was checked by the use of Experion (Bio-Rad, Munich, Germany). Afterwards, the RNA of female samples was pooled according to performance in the FST, creating 3 pools per group. Prior to hybridization, RNA integrity and comparability were tested by a BioAnalyzer (Agilent Technologies, Palo Alto, CA). RNA integrity numbers (RIN) of all RNAs was between 8.3 and 8.6. cDNA synthesis, labelling and the actual microarray analysis were performed by the Interdisciplinary Centre for Clinical Research (IZKF) at the University of Wuerzburg. Generation of double-stranded cDNA, preparation and labelling of cRNA, hybridization to GeneChip® Mouse Genome 430 2.0 Arrays (Affymetrix, Santa Clara, CA) and washing were performed according to the standard Affymetrix protocol. The arrays were scanned using a GeneChip® Scanner 3000 (Affymetrix Santa Clara, CA). Data analysis was performed using different R packages from the Bioconductor project (www.bioconductor.org). Probe sets were summarized using the PLIER algorithm. Resulting signal intensities (signal intensity from a specific probeset is referred to as the expression of the associated gene from here onwards) were normalized by variance stabilization normalization (VSN) (Huber *et al.* 2002). Quality and comparability of all data sets were tested by density plot, RNA degradation plot and correspondence analysis. All data is MIAME compliant and the raw data has been deposited in the Gene Expression Omnibus (GEO) (accession number: GSE26025).

Enriched pathway analysis

The Database for Annotation, Visualization and Integrated Discovery (DAVID) 2007 Functional Annotation Clustering was utilized to search the database of the Kyoto Encyclopedia of Genes and Genomes (KEGG) (Dennis *et al.* 2003; Huang da *et al.* 2009) in order to identify significantly over-represented pathways in the subset of differentially expressed genes. More specifically, the latter is a curated pathway database comprising biological signaling pathways that are based on current knowledge of molecular interactions involved in various cellular processes. Settings used were: Count (2); EASE (0.1); P<0.05.

Quantitative real-time PCR

The validity of the microarray results was subsequently tested via quantitative real-time PCR (qRT-PCR) using the Bio-Rad CFX384 Real-Time PCR Detection System (in technical triplicates). For validation we selected 8 genes which showed a fold change (FC) > 1.5 (or 2.5) in the microarray (see below). The same RNA as for the microarray was utilized for cDNA synthesis which was performed by the use of the iScript™ kit (Bio-Rad, Munich, Germany) according to the manufacturer´s instructions. Mean efficiencies were calculated by LinReg (Ruijter *et al.* 2009). Reference genes for normalization were selected from the microarray and tested for stability using geNorm (Vandesompele *et al.* 2002). For normalization *CCCTC-binding factor (Ctcf), guanosine diphosphate (GDP) dissociation inhibitor 2 (Gdi2)* and *gap junction protein, alpha 1 (Gja1)* genes were used. Relative expression data were calculated with the normalization factors obtained from geNorm and the mean efficiencies from LinReg.

2.1.4 DNA methylation study

Methylated DNA immunoprecipitation followed by tiling array

For this study, the right part of the hippocampus of 16 5-Htt+/- and 14 WT female mice was utilized. Genomic DNA was extracted from the tissue using phenol/chloroform/isoamyl alcohol extraction. 300 µl 0.5%-SDS extraction buffer were added to the frozen tissue. The tissue was subsequently homogenized at 4°C in the Tissue Lyser (Qiagen, Hilden, Germany) using a metallic bead (30 sec – 1 min, 25 Hz, 4°C). After adding 200 µl 0.5% SDS extraction buffer and 50 µl proteinase K with a concentration of either 10 or 20 mg/µl , samples were incubated at 55°C over night/or 3 h. Following this, samples were incubated with 50 µl RNAse A with a concentration of 10mg/µl for 1 h at 37°C and then mixed with 700 µl of phenol/chloroform/isoamyl alcohol mixture (25:24:1). Phases were separated using MaXtract high density tubes (Qiagen, Hilden, Germany) by centrifuging the samples at 14000 rpm for 5 min at RT. The aqueous phase was then mixed with 700 µl phenol isoamyl alcohol (24:1) and phases were again separated by centrifuging the samples in MaXtract high density tubes as described above. DNA was precipitated with 50 µl sodium acetate and 1000 µl cold absolute ethanol (incubation 10 min at -20°C, centrifugation 20 min at 4°C, 14 000 rpm). The resulting pellet was washed with 500 µl cold 80%-ethanol using the same conditions as for the precipitation, dried at RT for 5 to 30 min and resuspended in 50 µl 1xTE. DNAs of single animals were then pooled, creating 3 pools per group. To gain fragments of 300 +/- 200 bp size, DNA was sheared by the BiorupterTM UCD-200 (Diagenode, Liège, Belgium). Conditions were 20 KHz, 30 sec ON alternated by 30 sec OFF, for 3 x 5 min at low power. Efficiency of the shearing was controlled with the Bioanalyzer 2100 (Agilent, Santa Clara, USA). Methyl DNA immunoprecipitation (MeDIP, Diagenode, Liège, Belgium) was performed as described in the Diagenode manual. IP samples were performed in duplicate, input sample once. 1000 ng of DNA were used for each IP and 100 ng for the input. DNA was then purified using IPure (Diagenode, Liège, Belgium) according to the manufacturer's manual and the resulting IP DNA samples belonging together were pooled. Pooled IP DNA and input DNA was then amplified using two-step Whole Genome Amplification (GenomePlex Kit, Sigma, St. Louis, USA). Amplification, labeling, hybridization, and the actual tiling analysis were performed by the Interdisciplinary Centre for Clinical Research (IZKF) at the University of Wuerzburg. 7.5 µg DNA from the second amplification round were fragmented and labeled using the GeneChip 10K Xba Assay kit (Affymetrix, Santa Clara, USA). The size of the obtained biotinylated cDNA fragments was controlled with the Bioanalyzer (Agilent, Santa Clara, USA) and was in between 25 and 250 bp (peak at 100 bp). Hybridization to GeneChip ® Mouse Promoter 1.0R Arrays and washing using the GeneChip® Expression Wash, Stain and Scan Kit (Affymetrix, Santa Clara, USA) were performed as described in the Affymetrix manuals. Arrays were scanned with the GeneChip® Scanner 3000 (Affymetrix, Santa Clara, USA). The promoter tiling array used in this study is comprised of over 4.6 million 25-mer probes tiled to interrogate over 28,000 mouse promoter regions. Each promoter region covers approximately 6 kb upstream through 2.5 kb downstream of 5' transcription start sites. The probes are tiled at an average resolution of 35 bp, leaving a gap of approximately 10 bp between probes.

Affymetrix quality metrics and visual inspection of overall microarray signals confirmed high-quality readout from the hybridized samples. Genomic locations of microarray probes were adjusted to the *Mus musculus* NCBI assembly version 37.1 (MMv37 thereafter). Probe signals from corresponding MeDIP and input samples were subjected to within-sample pairwise loess normalization and calculation of MeDIP-input signal $\log_2$ ratios (SLRs). Quantiles normalization was employed to ensure a common signal distribution between samples. To decrease the noise in the experiment readout, a sliding-window approach was applied to determine SLR medians in successive genomic regions of 300 bp width. The SLRs were then found to be free from biases introduced by varying probe GC content and particular probe sequence compositions (data not shown), thus confirming successful data normalization. A correspondence analysis further confirmed the absence of extreme outliers in samples and/or SLRs.

2.1.5 Statistical analyses

Percentage of maternal weight increase over the last week of gestation was compared using a one-way ANOVA (condition). EZM and FST data were explored by three-way ANOVAs (genotype x condition x sex). Data on the ORT were analyzed using a repeated measures ANOVA, as well as by a separate analysis at the distinct time-points. Furthermore, for the ORT the RDI from every group was compared to an RDI of 0 (no discrimination) as described previously (Sik *et al.* 2003). CORT data were ln-transformed prior to ANOVA and were analyzed using a repeated measures ANOVA, as well as by a separate analysis at the distinct time-points. Overall interaction effects were examined in more detail using Least Significant Difference (LSD) tests. In the absence of an interaction, main effects of genotype and condition were analyzed by an additional stratified analysis – i.e. stratified per genotype and sex in case of a condition effect, in order to test whether overall effects were specific to, or more pronounced in, a particular genotype or sex. This was expected, since the 5-HTT genotype is known to have specific effects on various behavioral phenotypes and may selectively affect the interaction with stressful life events (see e.g. Homberg and Lesch 2011), whereas, in addition, PS is known for its sex-specific effects on offspring outcome (e.g. Behan *et al.* 2011). The failure to detect significant interactions using the three-way ANOVA approach may be explained by the relative conservative nature of F-tests in general, in combination with the intricate logistical experimental design (with its associated breeding restrictions), resulting in a relative lack of statistical power. Perinatal and post-weaning mortality were examined using a one-sided Fisher´s exact test.

Statistical analysis to choose differentially expressed genes was performed using the Linear Models for Microarray Analysis (LIMMA) package (Smyth and Speed 2003; Smyth *et al.* 2005). LIMMA is a library for the analysis of gene expression microarray data, especially concerning the use of linear models for analyzing designed experiments and the assessment of differential gene expression profiles. As an output a table of the top-ranked genes from the linear model fit including a gene list, ratio on the log2 scale, average gene intensities, moderated t-statistic, adjusted P-value (false discovery rate) and log odds were created. By using LIMMA we calculated the following differences:

between 5-Htt+/- (HET) and WT mice [(HETPS+HETC)-(WTPS+WTC)] (G effect), between PS and control (C) animals [(WTPS+HETPS)-(WTC+HETC)] (E effect) and the interaction of G and E [(HETPS-HETC)-(WTPS-WTC)] (G x E effects). Genes were identified as differentially expressed if they showed a nominal P-value less than 0.01. There was no "cut off" for the linear FC concerning the microarray data (FC of 1 indicates no change, while a FC of 2 equals a double amount of cRNA).

Results of the gene expression microarray were validated by means of qRT-PCR. For the G and E effects we considered only genes with a FC > 1.5 to achieve reliable validation. We further restricted the selection by only choosing genes with an annotation grade (see affymetrix.com) of A or B into account. For an exact validation, we used only those genes for which we were able to amplify the same sequence as recognized by the microarray. These criteria encouraged us to pick *FBJ osteosarcoma oncogene* (*Fos*) and *paired-like homeobox 2a* (*Phox2a*) out of the 15 genes altered >1.5 fold by PS. Of the 29 genes altered >1.5 fold by the 5-Htt+/- genotype we selected *XIAP associated factor 1* (*Xaf1*), *zinc finger*, *ZZ-type with EF hand domain 1* (*Zzef1*), *protein phosphatase 1, regulatory (inhibitor*) *subunit 1B* (*Ppp1r1b*), *Kv channel-interacting protein 2* (*Kcnip2*) and *myelin basic protein* (*Mbp*). In addition, we validated the G x E effect of the *thyrotropin releasing hormone receptor* (*Trhr*), as the expression of this gene between WTC and WTPS differed 2.5 fold. Gene expression data using qRT-PCR were analyzed by two-way ANOVA (genotype x condition) for males and females separately because we wanted to validate the microarray which was performed only with females. The level of statistical significance was assumed to exist at P<0.05 in all tests. Except for microarray data analysis, all statistical analyses were performed using the SPSS 20.0 software package.

In each sample of the DNA methylation array, genomic regions enriched by the MeDIP procedure were detected by the CMARRT algorithm (Kuan *et al.* 2008). Briefly, this does not apply a fixed threshold to all SLRs, but rather tests for increased signal content correcting for the signal autocorrelation in considered genomic regions, resulting in higher sensitivity and specificity of the detected enriched regions. For CMARRT modeling, the typical fragment length after DNA sonication was assumed to be 300 bp; enriched regions were required to cover at least five consecutive array probes and to display an enrichment statistic with a false discovery rate (FDR) less than 0.05. Of all detected regions, only those were consistently retained in the analysis that were found within each analysis group. With the present (=1) and absent (=0) calls for MeDIP enrichment, effect directions were determined as previously described (van den Hove *et al.* 2011). Briefly, genotype (G) effect directions (d) were calculated by G_d = ((HETC + HETPS) – (WTC + WTPS)) * 0.5, environment (E) effect directions by $E_d = ((WTPS + HETPS) - (WTC + HETC)) * 0.5$ and interaction (GxE) effect directions by $GxE_d = ((HETPS - HETC) - (WTPS - WTC)) * 0.5$.

Preprocessing and analysis of Affymetrix tiling arrays were performed with R v2.15 along with the Bioconductor package Starr (Zacher *et al.* 2010). The package ChIPpeakAnno (Zhu *et al.* 2010) was used for annotation of enriched regions.

2.2 Perinatal stress exposure

2.2.1 Animals

The brains of animals used for this study were obtained from Dr. Rebecca Heiming and Prof. Dr. Norbert Sachser at the University of Münster. Animals, general housing conditions, olfactory stimulation of the mothers and the effects on the offspring are described in detail previously (Heiming *et al.* 2009). Briefly, pregnant and lactating 5-Htt+/- and WT mice (for this study the null mutant 5-Htt-/- mice were omitted) were treated with neutral bedding or bedding that stemmed from the cages of unfamiliar adult males. The mothers were treated every 2-3 days in the morning, starting at experimental day 8. The dams received five treatments during the gestational period and two to five treatments during lactation. We analyzed brains of the following number of offspring: 6 male control WT mice, 9 female control WT mice, 9 male control 5-Htt+/- mice, 9 female control 5-Htt+/- mice, 9 male WT mice with PeS, 8 female WT mice with PeS, 10 male 5-Htt+/- mice with PeS and 6 female 5-Htt+/- mice with PeS.

2.2.2 Statistical analysis

qRT-PCR data were analyzed by two-way ANOVA for females and males separately to match the analyses for the PS exposure.

2.3 Resilience to stress exposure

For the microarrays, statistical analysis to select differentially expressed genes was performed using the LIMMA package (Smyth and Speed 2003; Smyth *et al.* 2005). As an output a table of the top-ranked genes from the linear model fit including a gene list, ratio on the log2 scale, average gene intensities, moderated t-statistic, adjusted P-value (false discovery rate) and log odds were created. By using LIMMA we calculated the changes in expression between all animals of the HETC group and the good or poor performers in the FST of the HETPS group as a representative comparison identifying specific molecular changes in resilient and vulnerable HETPS offspring, respectively. Further, we compared all WTC animals with the good or poor performers of the WTPS group in order to identify molecular mechanisms specific to resilient and vulnerable WTPS offspring, respectively (see Figure 2-1). Genes were identified as differentially expressed if they showed a nominal P-value of less than 0.01.

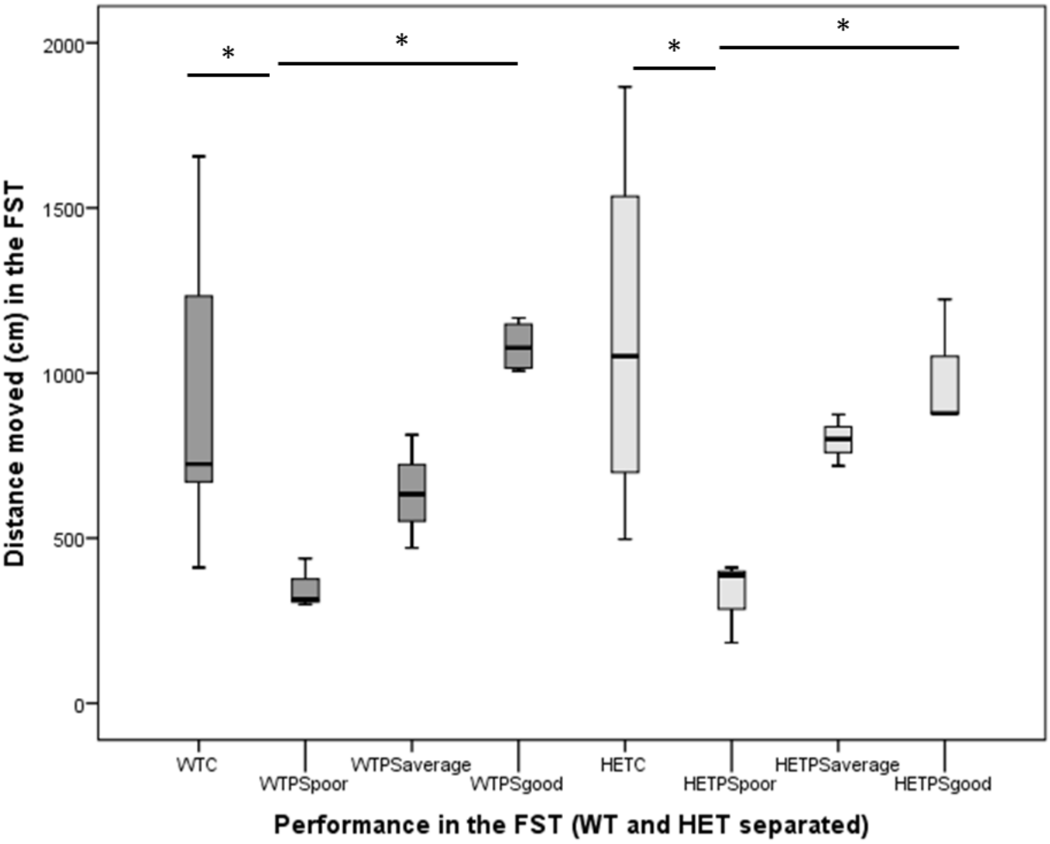

Figure 2-1. Performance in the forced swim test (FST). Wild-type (WT) and heterozygous (HET) prenatally stressed (PS) animals that performed poorly in the FST differ significantly from the respective controls (C). Further, poor and good performers of the respective group differ significantly (Mann-Whitney-U test without Bonferroni correction; n=3-10). * $p<0.05$

There was no “cut off” for the linear FC concerning the microarray data. From the microarray we picked following genes and performed qRT-PCR as explained above: *Growth hormone (Gh), prolactin (Prl), c-fos induced growth factor (Figf), synaptotagmin V (Syt 5)* and *calcium/calmodulin-dependent protein kinase II alpha (Camk2a)*. These genes were selected, because they showed a FC > 1.5 in WTPS or HETPS good performers. *Galanin receptor 3 (Galr3)* was chosen as the gene expression data obtained from the microarray correlated strongly with those of *Gh* and *Prl* (data not shown).

Additionally, we selected *protein kinase, cAMP dependent regulatory, type II beta (Prkar2b)*, because it was the only gene which was upregulated in the good performers and downregulated in the bad performers of the HETPS group. In general, we only picked genes which had an annotation grade (see affymetrix.com) of at least A or B and the ability to amplify the same sequence as recognized by the microarray.

Performance-oriented LIMMA analysis on the mRNA expression microarray data was followed by subsequent Spearman correlation analysis linking the individual mRNA expression data as obtained by qRT-PCR to behavioral performance as well as to neuroendocrinological measures. More specifically, the performance-based LIMMA analysis offers the opportunity to identify molecular mechanisms specific to either vulnerability or resilience to PS. The level of statistical significance was assumed to exist at $P<0.05$ in all tests. Except for microarray data analysis, all statistical analyzes were performed using the SPSS 20.0 software package.

3. Results

3. Results

3.1 Behavior

Dam weights during gestation and litter sizes

Increase of dam weight during pregnancy is depicted in Table 3-1. No differences in weight increase during the first two weeks of gestation between stressed versus unstressed dams were observed. Over the last week of pregnancy stressed dams gained significantly less weight when compared to control animals ($F_{1,25}$=25.024; P<0.001). Further, no differences were found in the litter sizes of stressed and control dams.

Table 3-1. Dam weight during pregnancy and litter size.

Condition	% Weight increase (E0-E12)	% Weight increase (E12-E17)	Litter size
C	33.78 ± 2.41	30.04 ± 1.16	7.08 ± 0.72
PS	33.44 ± 2.13	17.52 ± 1.94***	7.25 ± 0.66

During the last part of pregnancy (E12-E17), stressed (PS) dams gained significantly less weight compared to control (C) animals (***P<0.001). Data represent means ± S.E.M. N=12-15 litters/condition

Pre- and postweaning mortality

Preweaning mortality did not differ between the various groups (data not shown). A significantly higher postweaning mortality (P=0.04) was observed in PS offspring (7 out of 51 [13.7%] in PS animals vs. 1 out of 44 [2.3%] in controls; data not shown). Genotype had no effect on postweaning mortality.

Offspring cognition, anxiety, and depression-like behavior

Memory performance in the ORT is depicted in Table 3-2. Interval duration and recognition scores were negatively correlated ($F_{6,58}$=21.993; P<0.001). Further, an interval x genotype ($F_{6,58}$=24.851; P=0.027) and a condition x sex interaction ($F_{7,58}$=4.273; P=0.043) were observed, the latter of which indicated that PS particularly impaired memory performance in female offspring. When looking at the individual intervals, at the 2-hour interval, all animals were able to distinguish the old from the new object. Further, a significant condition x sex interaction was seen ($F_{7,60}$=6.518; P=0.013). Specifically, PS was associated with impaired memory performance in female offspring as post-hoc analysis showed a significant decrease in memory performance in PS versus control females (P=0.049). At the 3-hour interval, among males, only WT controls were able to remember the old object. Further, all 5-Htt+/- groups still displayed intact memory performance. In line with this, a significant overall effect of genotype was observed at this interval ($F_{7,62}$=4.501; P=0.038), with 5-Htt+/- mice showing improved memory function as compared to WT animals. At the 4-hour interval, all groups displayed impaired memory performance. Of note, no differences in exploration times between groups were observed at any interval.

Table 3-2. Memory performance as assessed in the Object Recognition Test (ORT).

Group			2h	3h	4h	Exploration Time (sec)
WT	**M**	**C**	**0.286 ± 0.092**	**0.296 ± 0.066**	0.081 ± 0.074	18.16 ± 0.84
		PS	**0.452 ± 0.080**	0.195 ± 0.103	0.148 ± 0.066	17.83 ± 0.73
	F	**C**	**0.358 ± 0.078**	0.096 ± 0.065	0.225 ± 0.086	18.37 ± 0.83
		PS	**0.319 ± 0.082**	0.116 ± 0.102	-0.132 ± 0.123	17.98 ± 0.95
5Htt +/-	**M**	**C**	**0.355 ± 0.067**	**0.248 ± 0.070**	0.054 ± 0.085	18.58 ± 0.67
		PS	**0.436 ± 0.075**	**0.393 ± 0.056**	-0.014 ± 0.066	17.91 ± 0.74
	F	**C**	**0.509 ± 0.087**	**0.281 ± 0.062**	0.001 ± 0.099	18.13 ± 1.40
		PS	**0.217 ± 0.071**	**0.266 ± 0.098**	0.056 ± 0.093	17.66 ± 0.76

Bold data indicate intact memory performance, i.e., when animals were able to distinguish the old from the new object. At the 2-hour interval, a significant condition × sex interaction was observed (P=0.013). At the 3-hour interval, a significant overall effect of 5-Htt genotype was observed (P=0.038). See results section for more details. Data in the first three columns represent mean relative discrimination index (RDI) ± S.E.M. The last column shows the average exploration times (the average time (seconds) spent exploring each object during T1 and T2, averaged over the 3 intervals), which did not differ between groups. Abbreviations: WT, wild-type; M, males; F, females; C, control offspring; PS, prenatally stressed offspring. N=7-10 mice/group.

In Figure 3-1, the effects of PS on anxiety-like behavior in the EZM are shown. Time spent in the open arms of the EZM was significantly enhanced in 5-Htt+/- versus WT animals ($F_{7,64}$=4.466; P=0.038), indicating lower levels of anxiety in 5-Htt+/- offspring. In addition, females spent less time in the open arms of the EZM ($F_{7,64}$=20.091; P<0.001), indicating higher levels of anxiety in this sex. Distance covered within the EZM was decreased by PS ($F_{7,64}$=10.314; P=0.002). When stratifying the analysis per genotype, the observed PS effect was only significant in WT, but not in 5-Htt+/- offspring ($F_{3,29}$=8.343; P=0.007, versus $F_{3,30}$=2.493; P=0.123, respectively). Similarly, when stratifying for sex, the PS effect was only significant for males and not for females ($F_{3,34}$=7.199; P=0.011, versus $F_{3,30}$=3.527; P=0.070, respectively).

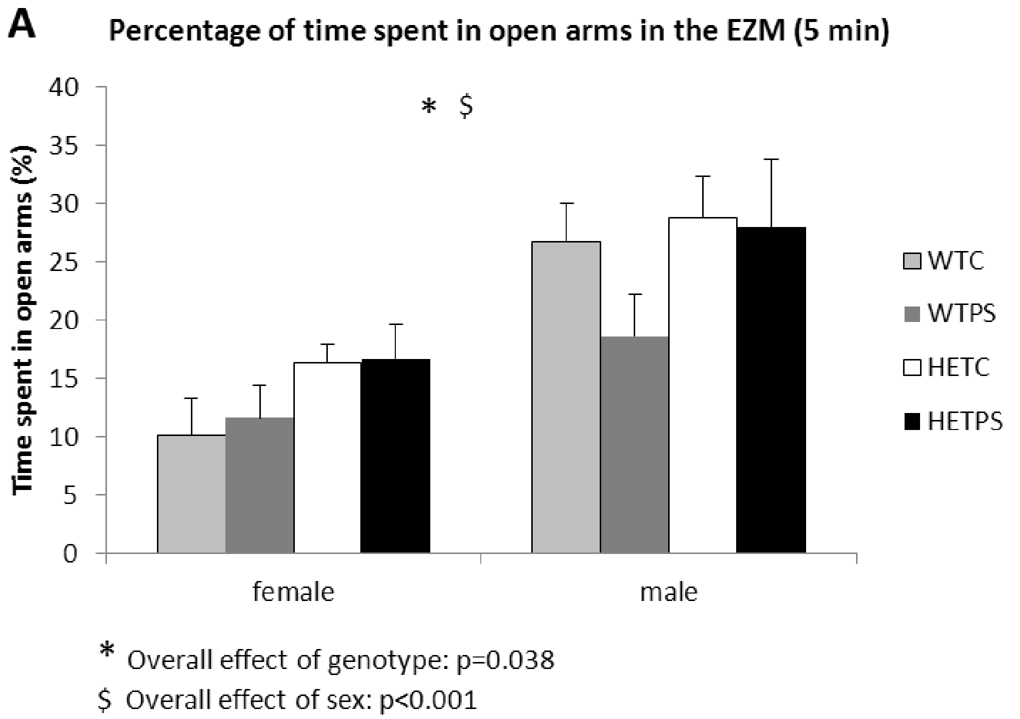

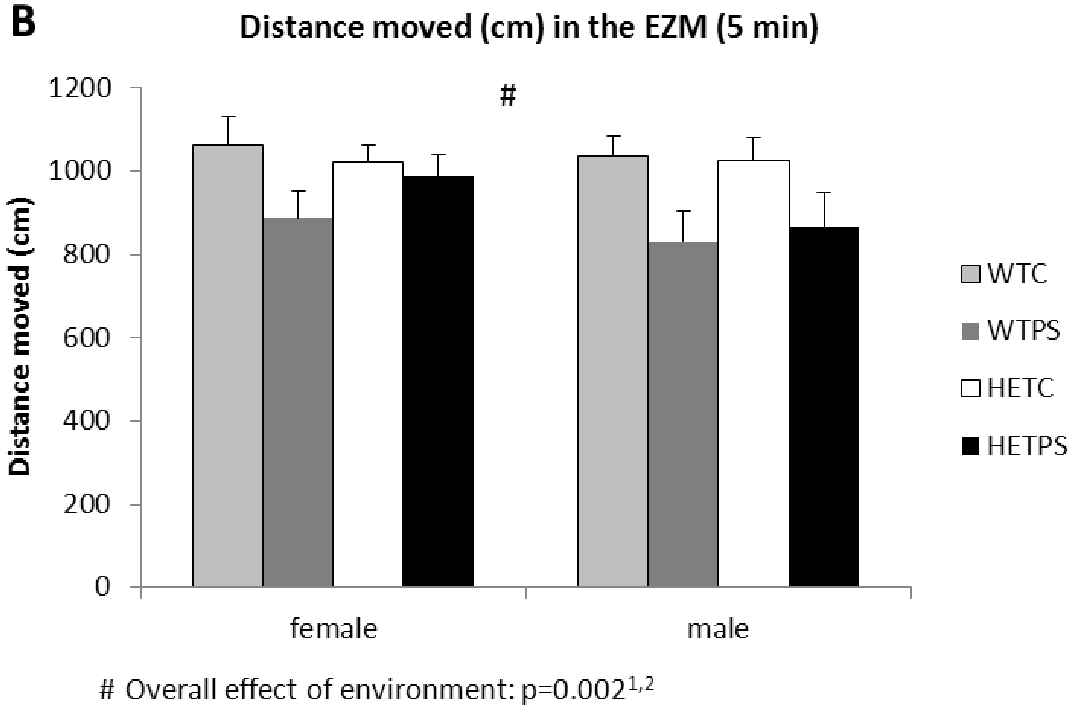

Figure 3-1. Performance in the Elevated Zero Maze (EZM). A) Time spent in the open arms of the EZM was significantly elevated in 5-Htt+/- versus wild-type (WT) animals (P=0.038). In addition, females (F) spent less time in the open arms of the EZM when compared to male (M) offspring (P<0.001). B) Distance covered within the EZM was decreased by prenatal stress (PS; P=0.002). Data represent mean + S.E.M. Abbreviation: C, control offspring. N=7-10 mice/group. [1]Only significant in WT offspring when stratified for genotype; [2]Only significant in male offspring when stratified for sex (see results section for more details).

Depression-like behavior in the FST is shown in Figure 3-2. Overall, a significant effect of condition was observed, indicating that PS animals exhibit more depression-like behavior ($F_{7,67}$=4.544; P=0.037). When stratifying the FST analysis per genotype, the observed PS effect was only significant in 5-Htt+/-, but not in WT offspring ($F_{3,36}$=6.869; P=0.013, versus $F_{3,31}$=0.395; P=0.534, respectively). Similarly, when stratifying for sex, the PS effect was only significant for females ($F_{3,35}$=0.980; P=0.329 versus $F_{3,32}$=5.494; P=0.025, for males and females, respectively). Of note, these observations also propose that the effect in the FST was independent from the lower mobility as observed in the EZM, the latter of which was primarily seen in WT male offspring (Figure 3-1B).

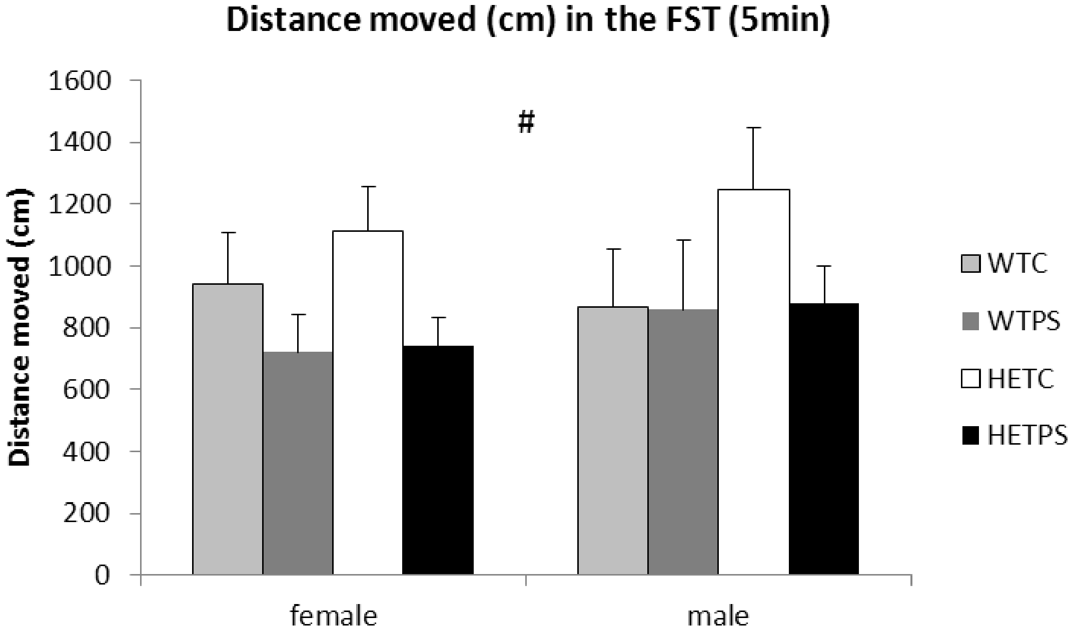

Overall effect of environment: p=0.037[1,2]

Figure 3-2. Performance in the Forced Swim Test (FST). Distance swum in the FST (5-minute period) was significantly decreased in prenatally stressed (PS) versus control (C) animals (P=0.037). Data represent mean + S.E.M. Abbreviation: WT, wild-type. N=7-10 mice/group. [1]Only significant in 5-Htt+/- offspring when stratified for genotype; [2]Only significant in female offspring when stratified for sex (see results section for more details).

Stress-induced plasma corticosterone (CORT) secretion

Data on stress-induced plasma CORT secretion of the offspring are depicted in Figure 3-3. Overall, a significant effect of time was observed ($F_{6,63}$=263.413; P<0.001). Furthermore, a time x genotype interaction was seen ($F_{6,63}$=3.594; P=0.030). In addition, over all 3 time points, significant effects of genotype and sex ($F_{7,64}$=4.000; P=0.050 and $F_{7,64}$=92.908; P<0.001, respectively) were observed, indicating lower CORT levels in 5-Htt+/- versus WT mice and higher levels in female versus male offspring, respectively. When looking at the individual time points, female offspring had higher CORT levels when compared to male offspring at all time points (overall sex effect; F>37.187; P<0.001 in all cases). Further, at baseline, an overall genotype effect ($F_{7,65}$=6.476; P=0.013) was seen, indicating that basal CORT levels were lower in 5-Htt+/- as compared to WT mice, an effect that tended to be more profound in male offspring (when stratified for sex; $F_{3,33}$=6.678; P=0.014, versus $F_{3,32}$=1.444; P=0.238, in males versus females; see Figure 3).

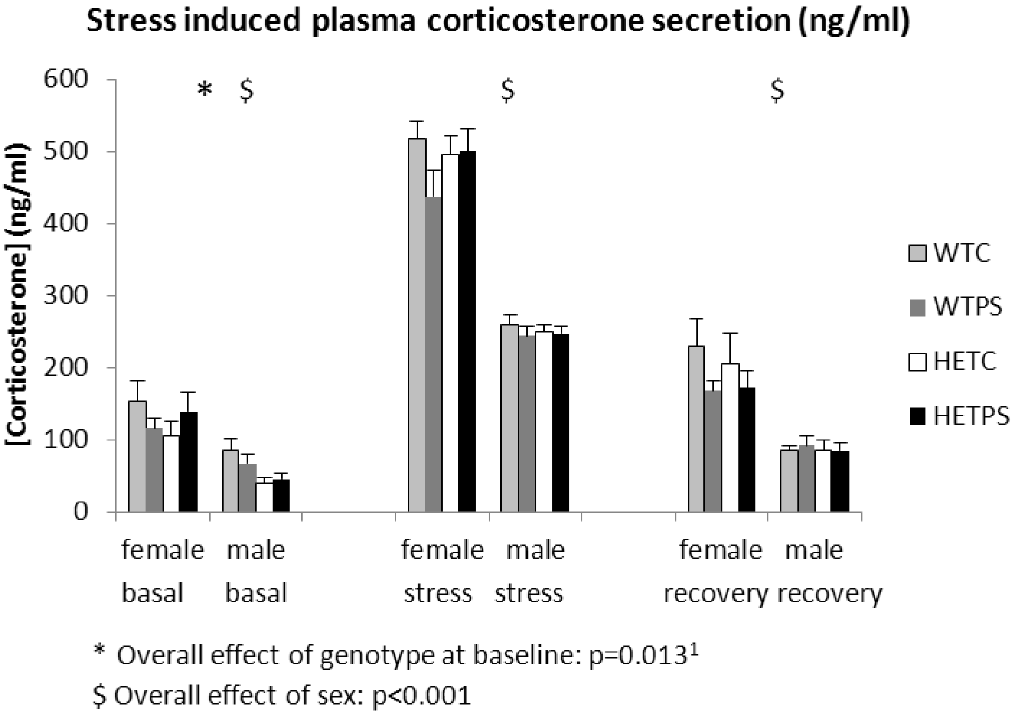

Figure 3-3. Stress-induced plasma corticosterone (CORT) secretion. At all time points, female (F) offspring had higher CORT levels when compared to male (M) offspring (overall sex effect; P<0.001 in all cases). At baseline, a significant genotype effect was observed (P=0.013). Abbreviations: WT, wild-type; C, control offspring. Data represent mean + S.E.M. N=7-10 mice/group. [1]Only significant in male offspring when stratified for sex (see results section for more details).

Adrenal weight

Adrenal weight was higher in female versus male offspring ($F_{7,56}$=166.817; P<0.001; Figure 3-4). In addition, overall, adrenal weight was heavier in 5-Htt+/- offspring when compared to WT animals ($F_{7,56}$=5.524; P=0.022), an effect that seemed to be particularly present in females ($F_{3,30}$=5.902; P=0.021, versus $F_{3,26}$=0.517; P=0.478, for females and males, respectively; see Figure 3-4 for more details).

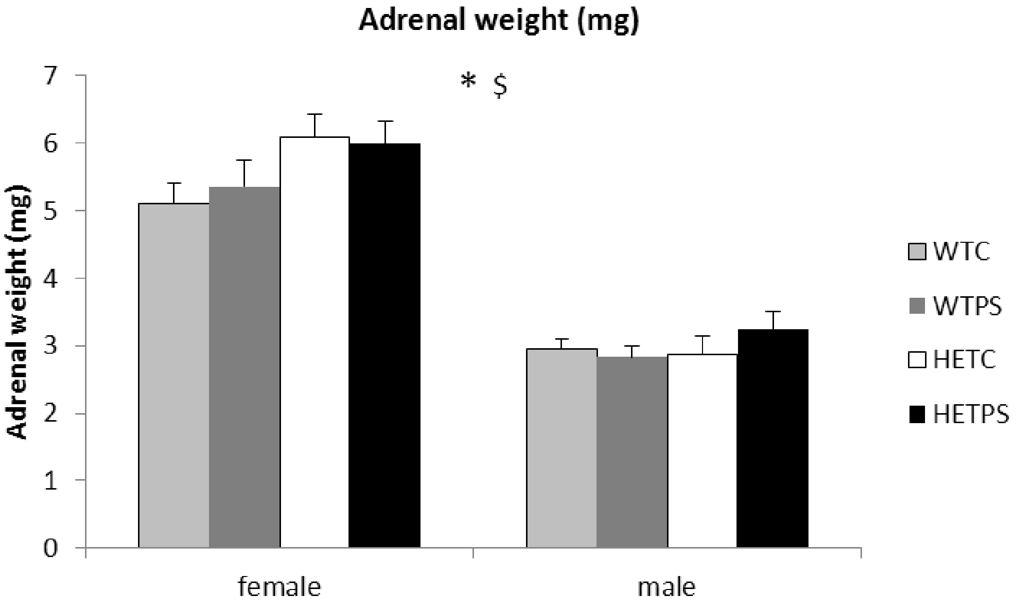

* Overall effect of genotype: p=0.022[1]
$ Overall effect of sex: p<0.001

Figure 3-4. Adrenal weight. Adrenal weight was higher in female (F) versus male (M) offspring (P<0.001). Adrenal weight was elevated in 5-Htt+/- offspring when compared to wild-type (WT) animals (P=0.022). Data represent mean + S.E.M. Abbreviations: C, control offspring; PS, prenatally stressed offspring. N=7-10 mice/group. [1]Only significant in female offspring when stratified for sex (see results section for more details).

3.2 Gene expression study

3.2.1 Gene expression microarray

To further study the molecular mechanisms underlying the behavioral observations in female offspring – which showed most pronounced behavioral changes mediated by variation in 5-Htt genotype, PS, and their interaction –, we conducted a microarray-based expression profiling on the female hippocampus, a brain region participating in learning and memory as well as in emotion regulation (Fanselow and Dong 2010). For microarray analysis we focused on three different comparisons. We measured the changes between 5-Htt+/- and WT mice (G effect), in the differences between PS and control mice (E effect), and, moreover, in the interaction between G and E (G x E effects), i.e. indicating those genes of which the effect of PS exposure is depended upon the 5-Htt genotype. In brief, the 5-Htt+/- genotype and PS exposure changed the expression of 773 and 960 genes, respectively (Figure 3-5; also see Supplemental material 5.1.1 and 5.1.2 for a complete overview of all genes significantly affected by G and E, respectively). Furthermore, 651 genes were affected in a G x E manner (Supplemental material 5.1.3; also see Figure 3-5). In addition, G and E showed overlap in the expression of 110 genes. Of those, 22 genes were upregulated, and 77 were downregulated by both. 11 genes were affected by G and E in an opposite direction (see Figure 3-5) whereas the expression of 3 genes was altered by G, E and in a G x E manner. To functionally categorize the differentially expressed genes we performed a pathway analysis using DAVID. We found 10 KEGG pathways affected by G, 9 by E and 10 by G x E (Table 3-3).

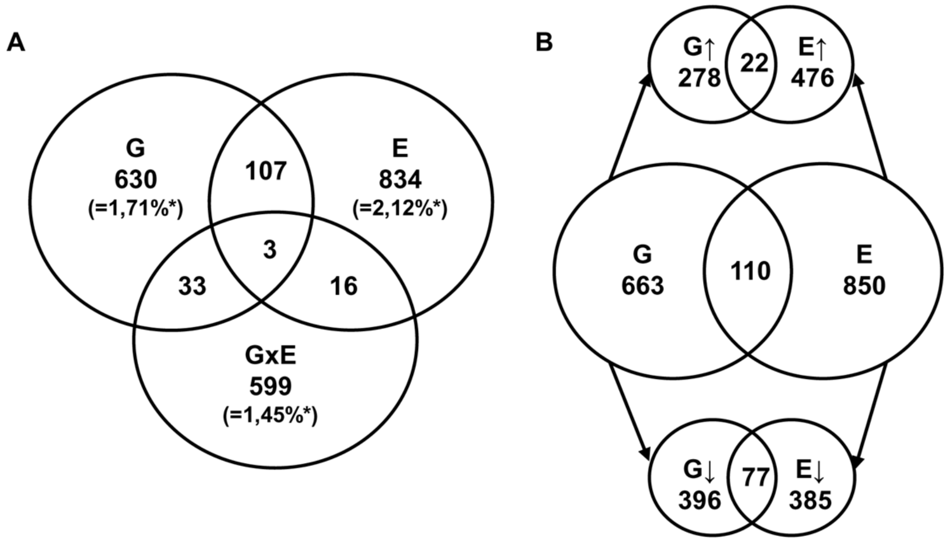

Figure 3-5. Gene expression analysis. A) Venn diagram illustrating the number of genes altered by the genotype (G; i.e. 5-Htt+/- versus wild type, 773 genes), the environment (E; i.e. prenatal stress versus control, 960 genes), both (110 genes), or in an interactive manner (G x E; i.e. indicating those genes of which the effect of the environment depends upon the genotype, 651 genes). B) Venn diagram illustrating the number of genes regulated by G, E or both, including the corresponding direction in which the 5-Htt+/- genotype and PS regulated their expression. Eleven genes were regulated in an opposite direction by G and E (not shown); *Percentage of probesets examined. (van den Hove *et al.* 2011)

Table 3-3. Significant KEGG pathways

FACTOR	DAVID ID	NAME	# GENES	P-VALUE
Genotype (G)	mmu04010	MAPK signaling pathway	26	1.79E-10
	mmu05200	Pathways in cancer	20	0.011
	mmu05412	Arrhythmogenic right ventricular cardiomyopathy	8	0.012
	mmu04810	Regulation of actin cytoskeleton	15	0.013
	mmu05410	Hypertrophic cardiomyopathy (HCM)	8	0.021
	mmu04722	Neurotrophin signaling pathway	10	0.029
	mmu05218	Melanoma	7	0.030
	mmu05414	Dilated cardiomyopathy	8	0.033
	mmu04114	Oocyte meiosis	9	0.037
	mmu04142	Lysosome	9	0.044
Environment (E)	mmu04010	MAPK signaling pathway	24	5.24E-11

	mmu04510	Focal adhesion	18	0.003
	mmu04012	ErbB signaling pathway	10	0.009
	mmu04722	Neurotrophin signaling pathway	12	0.018
	mmu04150	mTOR signaling pathway	7	0.023
	mmu00052	Galactose metabolism	5	0.024
	mmu05219	Bladder cancer	6	0.028
	mmu04520	Adherens junction	8	0.037
	mmu04114	Oocyte meiosis	10	0.047
G x E	mmu04060	Cytokine-cytokine receptor interaction	12	0.009
	mmu04310	Wnt signaling pathway	9	0.009
	mmu04672	Intestinal immune network for IgA production	5	0.022
	mmu04640	Hematopoietic cell lineage	6	0.023
	mmu05310	Asthma	4	0.027
	mmu05330	Allograft rejection	5	0.028
	mmu04012	ErbB signaling pathway	6	0.029
	mmu04514	Cell adhesion molecules (CAM)	8	0.033
	mmu04510	Focal adhesion	9	0.043
	mmu04360	Axon guidance	7	0.045

Significant KEGG pathways affected by genotype (G; i.e. 5-Htt+/- versus wild type), the environment (E; i.e. prenatal stress versus control) or in an interactive manner (GxE; i.e. indicating those genes of which the effect of the environment depends upon the genotype). Acquired using DAVID analysis.

Gene expression changes accompanying variations in 5-Htt genotype

Of the 773 genes affected by the 5-Htt+/- genotype, 300 genes were upregulated and 473 downregulated (Figure 3-5; also see supplemental material 5.1.1 for a complete overview of all genes regulated by 5-Htt genotype). Amongst others, DAVID analysis revealed the mitogen-activated protein kinase (MAPK) signaling pathway and neurotrophin signaling as significantly overrepresented pathways affected by G (see Table 3-3 for a complete overview of the functionally enriched pathways). In the MAPK signaling pathway, 73% of the 26 genes were downregulated, such as *fibroblast growth factor 1 (Fgf1), calcium channel voltage dependent, L type, alpha 1D subunit (Cacna1d)* and *mitogen-activated protein kinase 8 interacting protein 3* (*Mapk8ip3*; see Table 3-4A for an overview of all genes affected in the MAPK signaling pathway). In the neurotrophin signaling pathway, 10 genes were significantly affected, among which was the *neurotrophic tyrosine kinase, receptor type 2 (Ntrk2*; also known as *TrkB receptor*) and *transformation related protein 53 (Trp53*; see Table 3-4B for a complete overview). Interestingly, the MAPK and neurotrophin signaling KEGG pathway partially overlap. One gene, namely the *v-crk sarcoma virus CT10 oncogene homolog (avian; Crk)*, was affected in both KEGG pathways. Of note, the expression of the *solute carrier family 6, member 4* (*Slc6a4*, encoding for the 5-Htt) was upregulated in 5Htt +/- mice 10.6 fold indicating an upregulation of the allele leading to a truncated protein (see Ravary *et al.* 2001).

Table 3-4. Genes regulated by the 5-Htt+/- genotype

A. MAPK signaling pathway

EFFECT	AFFY ID	DAVID GENENAME	ENTREZ SYMBOL	# (%) GENES	FC	P-VALUE
up	1432647_at	*epidermal growth factor receptor*	*Egfr*		1.2	0.007
	1444344_at	*fibroblast growth factor 10*	*Fgf10*		1.2	0.007
	1460296_a	*fibroblast growth factor 22*	*Fgf22*		1.2	0.005
	1421473_at	*interleukin 1 alpha*	*Il1a*		1.1	0.005
	1452383_at	*ribosomal protein S6 kinase polypeptide 3*	*Rps6ka3*		1.2	0.009
	1449901_a	*mitogen-activated protein kinase kinase kinase 6*	*Map3k6*		1.2	0.007
	1460176_at	*v-crk sarcoma virus CT10 oncogene homolog (avian)*	*Crk*	**7 (27%)**	1.3	4.68E-04
down	1438031_at	*RAS, guanyl releasing protein 3*	*Rasgrp3*		1.2	0.003
	1421297_a	*calcium channel, voltage-dependent, L type, alpha 1C*	*Cacna1c*		1.1	0.008
	1428051_a	*calcium channel, voltage-dependent, L type, alpha 1D*	*Cacna1d*		1.2	0.004
	1425812_a	*calcium channel, voltage-dependent, N type, alpha 1B*	*Cacna1b*		1.3	0.004
	1450520_at	*calcium channel, voltage-dependent, gamma subunit 3*	*Cacng3*		1.3	0.001
	1450869_at	*fibroblast growth factor 1*	*Fgf1*		1.1	0.004
	1418498_at	*fibroblast growth factor 13*	*Fgf13*		1.3	0.009
	1425911_a	*fibroblast growth factor receptor 1*	*Fgfr1*		1.3	0.003
	1427776_a	*fibroblast growth factor receptor 4*	*Fgfr4*		1.2	0.003
	1426677_at	*filamin, alpha*	*Flna*		1.1	0.009
	1450097_s_	*guanine nucleotide binding protein, alpha 12*	*Gna12*		1.2	0.002
	1417885_at	*microtubule-associated protein tau*	*Mapt*		1.2	0.001
	1425679_a	*mitogen-activated protein kinase 8 interacting protein 1*	*MAPK8ip*		1.1	0.008
	1416437_a	*mitogen-activated protein kinase 8 interacting protein 3*	*MAPK8ip*		1.3	0.003
	1421446_at	*protein kinase C, gamma*	*Prkcc*		1.3	6.73E-04
	1424287_at	*protein kinase, X-linked*	*Prkx*		1.3	0.004
	1450368_a	*protein phosphatase 3, regulatory subunit B, alpha*	*Ppp3r1*		1.3	0.007
	1427739_a	*transformation related protein 53*	*Trp53*		1.2	0.010
	1420837_at	*neurotrophic tyrosine kinase, receptor, type 2*	*Ntrk2*	**19**	1.5	2.93E-04
Total				**26**		

B. Neurotrophin signaling pathway

EFFECT	AFFY ID	DAVID GENENAME	ENTREZ SYMBOL	# (%) GENES	FC	P-VALUE
up	1437122_at	*predicted gene 3655; B-cell leukemia/lymphoma 2*	*Bcl2*		1.16	0.008
	1454378_at	*predicted gene, EG546165; predicted gene 2423; hypothetical protein LOC674211; tyrosine 3-monooxygenase/tryptophan 5-monooxygenase activation protein, theta polypeptide*	*Ywhaq*		1.78	0.008
	1452383_at	*ribosomal protein S6 kinase polypeptide 3*	*Rps6ka3*		1.21	0.009
	1439005_x_at	*tyrosine 3-monooxygenase/tryptophan 5-monooxygenase activation protein, zeta polypeptide; predicted gene 4202*	*Ywhaz**		1.26	0.009

	1460176_at	*v-crk sarcoma virus CT10 oncogene homolog (avian)*	*Crk*	**5 (45%)**	1.39	4.68E-04
down	1448668_a_at	*interleukin-1 receptor-associated kinase 1*	*Irak1*		1.20	0.005
	1420837_at	*neurotrophic tyrosine kinase, receptor, type 2*	*Ntrk2*		1.57	2.93E-04
	1425070_at	*neurotrophic tyrosine kinase, receptor, type 3; similar to neurotrophic tyrosine kinase, receptor, type 3*	*Ntrk3*		1.23	0.008
	1427739_a_at	*transformation related protein 53*	*Trp53*		1.28	0.010
	1452325_at	*transformation related protein 73*	*Trp73*		1.21	0.008
	1448218_s_at	*tyrosine 3-monooxygenase/tryptophan 5-monooxygenase activation protein, zeta polypeptid; predicted gene 4202*	*Ywhaz**	**6 (55%)**	1.24	0.004
Total				**11**		

Differentially expressed genes within the mitogen-activated protein kinase (MAPK) signaling (A) and neurotrophin signaling (B) pathways (5-Htt+/- versus wild type). Abbreviation: FC, fold change. * Probesets recognize different transcripts.

Gene expression changes induced by PS exposure

The expression of 960 genes was altered by PS exposure, of which 462 were upregulated and 498 downregulated (Figure 3-5; also see supplemental material 5.1.2 for a complete overview of all genes regulated by PS exposure). Moreover, 9 KEGG pathways with significant P-values were detected by DAVID analysis (see Table 3-3). As the 5Htt +/- genotype, PS affected the MAPK and the neurotrophin signaling pathway (Table 3-5; see Table 3-3 for a complete overview of the functionally enriched pathways). The *calcium channel, voltage-dependent, gamma subunit 3 (Cacng3)* and *protein kinase C, gamma (PrKcc)* are examples of genes negatively influenced by both G and E.

Table 3-5. Genes regulated by prenatal stress

A. MAPK signaling pathway

EFFECT	AFFY ID	DAVID GENENAME	ENTREZ SYMBOL	# (%) GENES	FC	P-VALUE
up	1444199_at	*ELK4, member of ETS oncogene family*	*Elk4*		1.16	0.007
	1423100_at	*FBJ osteosarcoma oncogene*	*Fos*		1.76	0.001
	1417409_at	*Jun oncogene*	*Jun*		1.22	0.005
	1438992_x_at	*activating transcription factor 4*	*Atf4*		1.30	1.16E-04
	1447511_at	*calcium channel, voltage-dependent, N type, alpha 1B subunit*	*Cacna1b*		1.28	0.006
	1420287_at	*calcium channel, voltage-dependent, P/Q type, alpha 1A subunit*	*Cacna1a*		1.32	7.17E-04
	1449773_s_at	*growth arrest and DNA-damage-inducible 45 beta*	*Gadd45b*		1.19	0.003
	1452318_a_at	*heat shock protein 1B*	*Hspa1b*		1.35	0.001
	1448950_at	*interleukin 1 receptor, type I*	*Il1r1*		1.20	0.006

	1443540_at	*mitogen-activated protein kinase kinase kinase 1*	*Map3k1*		1.24	0.009
	1438908_at	*mitogen-activated protein kinase kinase kinase 12*	*Map3k12*		1.19	0.003
	1447667_x_at	*mitogen-activated protein kinase kinase kinase 4*	*Map3k4*		1.14	0.010
	1456467_s_at	*nemo like kinase*	*Nlk*		1.15	0.007
	1421416_at	*predicted gene 14378; similar to transforming growth factor, beta receptor III (betaglycan, 300kDa); mitogen-activated protein kinase kinase 7*	*Map2k7*	**14 (58%)**	1.18	0.004
down	1447941_x_at	*Braf transforming gene*	*Braf*		1.21	0.006
	1450520_at	*calcium channel, voltage-dependent, gamma subunit 3*	*Cacng3*		1.34	3.88E-04
	1424932_at	*epidermal growth factor receptor*	*Egfr*		1.13	0.007
	1425911_a_at	*fibroblast growth factor receptor 1*	*Fgfr1*		1.27	0.006
	1426677_at	*filamin, alpha*	*Flna*		1.19	0.001
	1453712_a_at	*mitogen-activated protein kinase kinase 5*	*Map2k5*		1.22	0.010
	1455441_at	*mitogen-activated protein kinase kinase kinase 7; predicted gene 8188*	*Map3k7*		1.23	0.005
	1421446_at	*protein kinase C, gamma*	*Prkcc*		1.31	0.001
	1451943_a_at	*protein phosphatase 1A, magnesium dependent, alpha isoform*	*Ppm1a*		1.18	0.006
	1429759_at	*ribosomal protein S6 kinase polypeptide 6*	*Rps6ka6*	**10 (42%)**	1.31	1.48E-04
Total				**24**		

B. Neurotrophin signaling pathway

EFFECT	**AFFY ID**	**DAVID GENENAME**	**ENTREZ SYMBOL**	**# (%) GENES**	**FC**	**P-VALUE**
up	1417409_at	*Jun oncogene*	*Jun*		1.21	0.005
	1438992_x_at	*activating transcription factor 4*	*Atf4*		1.29	1.16E-04
	1443540_at	*mitogen-activated protein kinase kinase*	*Map3k1*		1.24	0.009
	1425514_at	*phosphatidylinositol 3-kinase, regulatory subunit, polypeptide 1 (p85 alpha)*	*Pik3r1*		1.18	0.005
	1421416_at	*predicted gene 14378; similar to transforming growth factor, beta receptor III (betaglycan, 300kDa); mitogen-activated protein kinase kinase 7*	*Map2k7*		1.18	0.004
	1454378_at	*predicted gene, EG546165; predicted gene*	*Ywhaq*		1.79	0.004
	1439005_x_at	*tyrosine 3-monooxygenase/tryptophan 5-monooxygenase activation protein, zeta polypeptide*	*Ywhaz*		1.36	5.72E-04
	1436981_a_at	*tyrosine 3-monooxygenase/tryptophan 5-monooxygenase activation protein, zeta polypeptide*	*Ywhaz*	**8 (62%)**	1.28	0.005
down	1447941_x_at	*Braf transforming gene*	*Braf*		1.21	0.006

	1455869_at	*calcium/calmodulin-dependent protein kinase II, beta*	*Camk2b*		1.77	9.13E-04
	1453712_a_at	*mitogen-activated protein kinase kinase 5*	*Map2k5*		1.22	0.010
	1429759_at	*ribosomal protein S6 kinase polypeptide 6*	*Rps6ka6*		1.31	1.48E-04
	1438839_a_at	*tyrosine 3-monooxygenase/tryptophan 5-monooxygenase activation protein, epsilon polypeptide*	*Ywhae*	**5 (38%)**	1.19	0.008
Total				**13**		

Differentially expressed genes within the mitogen-activated protein kinase (MAPK) signaling (A) and neurotrophin signaling (B) pathways (PS versus control). Abbreviation: FC, fold change.

Gene expression profiles indicating a gene x environment interaction

At the G × E level, 651 genes displayed a significant expression pattern (Figure 3-5; see Supplemental material 5.1.3 for a complete overview of all genes regulated in a G x E fashion). DAVID pathway analysis revealed that G x E significantly enriched 10 pathways (Table 3-3). The most significantly enriched biological process was cytokine-cytokine receptor interactions (Table 3-6; see Table 3-3 for a complete overview of the functionally enriched pathways). Examples of genes affected within this pathway are *interleukin 4 (Il4), interleukin 12a (Il12a)* and *tumor necrosis factor receptor superfamily, member 1a (Tnfrsf1a)*. Another pathway significantly influenced in a G x E manner was the Wnt signaling pathway amongst which the *RAS-related C3 botulinum substrate 2 (Rac2), Rho-associated coiled-coil containing protein kinase 1 (Rock1), calcium/calmodulin-dependent protein kinase II, delta (Camk2d)* and *presenilin 1(Psen1)* were differentially expressed.

Table 3-6. Genes regulated in a gene x environment manner

A. Cytokine-cytokine receptor interactions

AFFY ID	DAVID GENENAME	ENTREZ SYMBOL	P-VALUE
1437382_at	*activin receptor IIA*	*Acvr2a*	0.004
1421188_at	*chemokine (C-C motif) receptor 2*	*Ccr2*	0.003
1421843_at	*interleukin 1 receptor accessory protein*	*Il1rap*	0.005
1425454_a_at	*interleukin 12a*	*Il12a*	0.004
1422397_a_at	*interleukin 15 receptor, alpha chain*	*Il15ra*	0.008
1449864_at	*interleukin 4*	*Il4*	0.009
1415855_at	*kit ligand*	*Kitl*	0.006
1450272_at	*tumor necrosis factor (ligand) superfamily, member 8*	*Tnfsf8*	0.009
1430259_at	*tumor necrosis factor receptor superfamily, member 11a*	*Tnfrsf11a*	0.003

1427600_at	*tumor necrosis factor receptor superfamily, member 19*	*Tnfrsf19*	0.005
1417291_at	*tumor necrosis factor receptor superfamily, member 1a*	*Tnfrsf1a*	0.006
1448951_at	*tumor necrosis factor receptor superfamily, member 1b*	*Tnfrsf1b*	0.007

B. Wnt signaling pathway

AFFY ID	DAVID GENENAME	ENTREZ SYMBOL	P-VALUE
1417620_at	*RAS-related C3 botulinum substrate 2*	*Rac2*	4.86E-04
1441162_at	*Rho-associated coiled-coil containing protein kinase 1*	*Rock1*	0.007
1422659_at	*calcium/calmodulin-dependent protein kinase II, delta*	*Camk2d*	0.009
1449730_s_at	*frizzled homolog 3 (Drosophila)*	*Fzd3*	0.007
1458002_at	*mitogen-activated protein kinase 10*	*Mapk10*	0.002
1434275_at	*naked cuticle 2 homolog (Drosophila)*	*Nkd2*	0.007
1425549_at	*presenilin 1*	*Psen1*	0.005
1443270_at	*prickle-like 2 (Drosophila)*	*Prickle2*	0.005

Differentially expressed genes within the cytokine-cytokine receptor interactions (A) and Wnt signaling (B) pathways involving genes regulated in a genotype (G) x environment (E) manner, i.e. indicating those genes of which the effect of the (prenatal) environment depends upon the 5-Htt genotype).

3.2.2 Validation of the expression microarray

Using qRT-PCR we tried to confirm the microarray data. Of the 8 genes, 6 were replicated in terms of the overall G, E or G x E effects, such as *Fos* ($F_{3,32}=7.076$; P=0.012), *Mbp* (G effect: $F_{3,32}=9.421$; P=0.004; E effect: $F_{3,32}=12.152$; P=0.001; G x E effect: $F_{3,32}=4.897$; P=0.034), *Ppp1r1b* ($F_{3,32}=9.055$; P=0.005*)*, *Trhr* (E effect: $F_{3,32}=5.087$; P=0.031; G x E effect: $F_{3,32}=15.599$; P<0.001), *Xaf1* ($F_{3,32}=102.615$; P<0.001) and *Zzef1* ($F_{3,32}=14.128$; P=0.001). We could not replicate the overall effect of 5-Htt genotype for *Kcnip2* (G effect: $F_{3,32}=2.048$; P=0.162; G x E effect: $F_{3,32}=5.612$; P=0.024) and the overall effect of PS for *Phox2a* ($F_{3,30}=2.871$; P=0.101) (see table 3-7 for more details).

Table 3-7. Genes validated by qRT-PCR

Gene	WTFC	WTFPS	5-Htt+/- FC	5-Htt+/- FPS	Main effect(s) Microarray	Main effect(s) qRT-PCR
Fos	100 ± 22.2	123.9 ± 10.5	94.3 ± 14.0	137.7 ± 15.6	E (↑)	E (↑)
Kcnip2	100 ± 5.3	97.6 ± 6.8	86.1 ± 5.4	101.0 ± 3.8	G (↓)	G x E
Mbp	100 ± 4.7	127.4 ± 7.7	95.9 ± 4.9	102.0 ± 5.8	G (↓)	G (↓), E (↑), G x E
Phox2a	100 ± 20.0	98.6 ± 9.2	77.4 ± 11.6	118.6 ± 19.7	E (↑)	-

Ppp1r1b	100 ± 14.3	118.4 ± 13.6	89.1 ± 8.2	83.6 ± 2.9	G (↓)	G (↓)
Trhr	100 ± 20.4	51.2 ± 20.8	74.9 ± 9.5	88.2 ± 8.3	G x E	E (↓), G x E
Xaf1	100 ± 14.3	478.0 ± 117.9	2582.7 ± 8.3	2599.3 ± 9.4	G (↑)	G (↑)
Zzef1	100 ± 3.5	102.7 ± 3.7	86.6 ± 5.2	91.3 ± 6.1	G (↓)	G (↓)

Genes validated by qRT-PCR. Values indicate average expression as percentage of wild type female control offspring. Data represent mean ± S.E.M. Abbreviations: WT, wild type; F, females; C, control offspring; PS, prenatally stressed offspring.

Furthermore, of these 8 genes differentially expressed within the female hippocampus, we examined the expression patterns in both the cortex and striatum of the PS males and females, as well as in the hippocampus of the animals of the 5-Htt x PeS paradigm. Of the 8 genes, the observed effects of 5 were also detected in other brain regions or the other sex of the PS model, such as *Fos* ($_{F3,32}$=9.399; P=0.004), *Mbp* ($_{F3,34}$=3.218; P=0.082), *Trhr* ($_{F3,32}$=3.807; P=0.06; different direction), *Xaf1* (male HIP: $F_{3,35}$=112.041; P<0.01; female PFC: $F_{3,32}$=230.247; P<0.01; male PFC: $F_{3,34}$=163.184; P<0.01; female Str: $F_{3,32}$=78.742; P<0.01) and *Zzef1* ($F_{3,32}$=6.054; P=0.019). Next to this, in the hippocampus of the PeS mice, *Xaf1* was differentially expressed between 5-Htt+/- and WT offspring (female: $F_{3,28}$=2750.193; P<0.01; male: $F_{3,30}$=155.341; P<0.01).

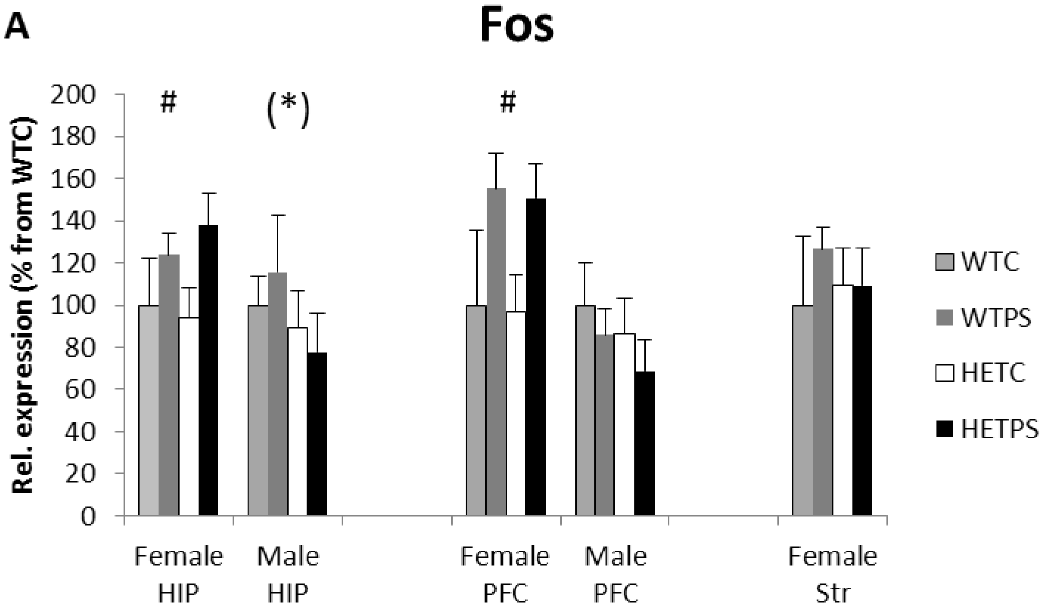

(*) Overall effect of genotype: p=0.084

\# Overall effect of environment: p=0.012 (HIP), p<0.01 (PFC)

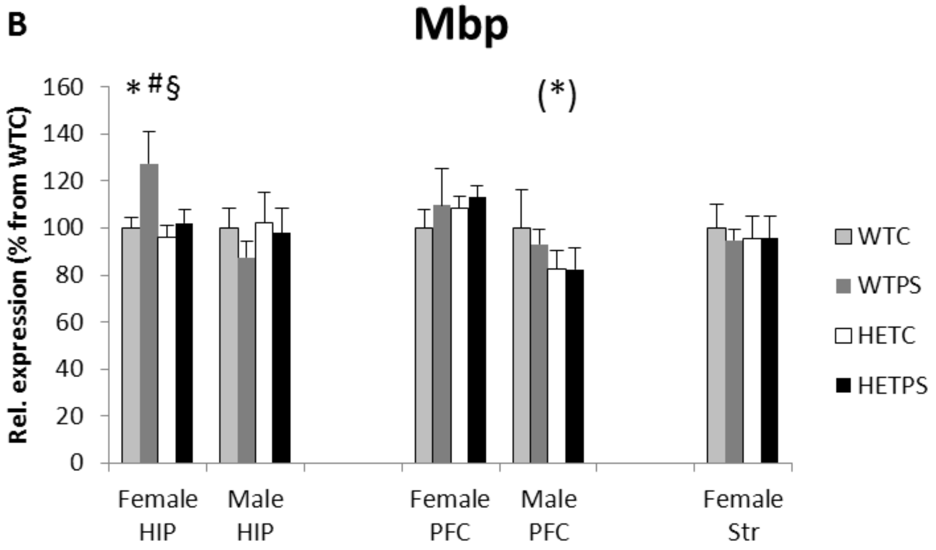

* Overall effect of genotype: p<0.01

(*) Overall effect of genotype: p=0.082

\# Overall effect of environment: p<0.01

§ Overall effect of gene x environment: p=0.034

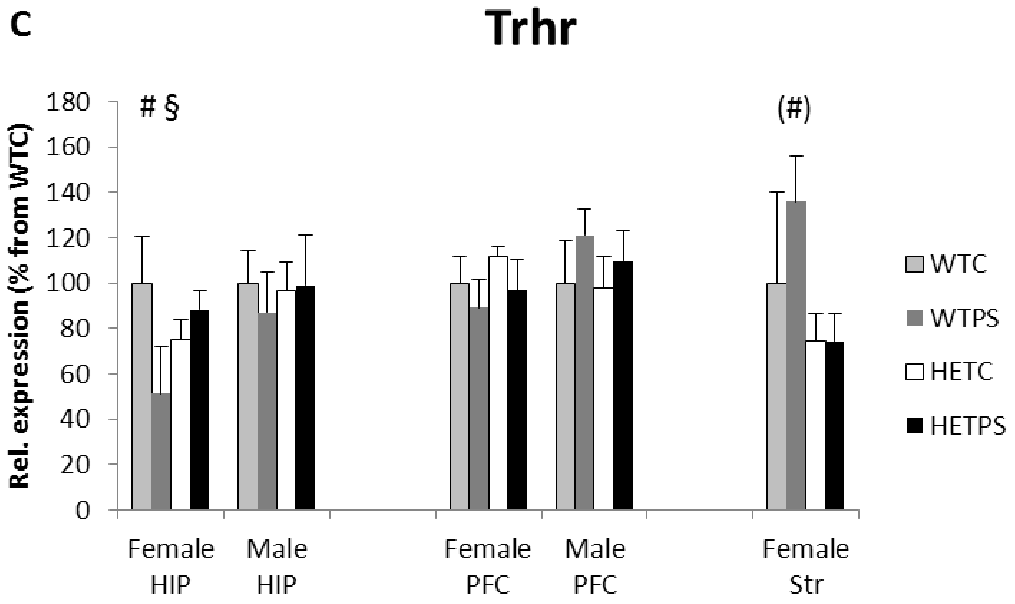

\# Overall effect of environment: p=0.031

(#) Overall effect of environment: p=0.06

§ Overall effect of gene x environment: p<0.01

D

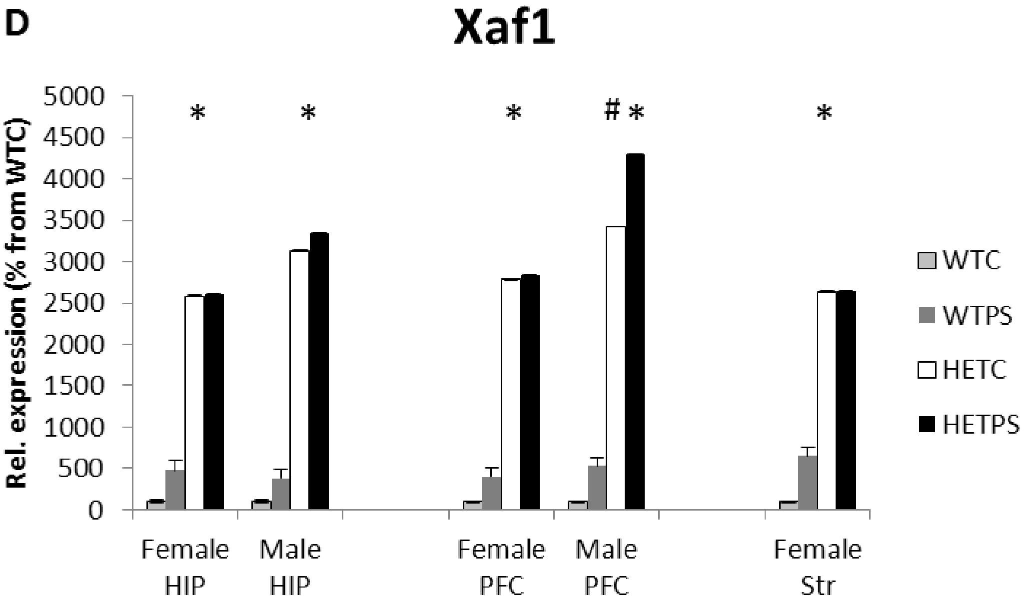

* Overall effect of genotype: p<0.01

\# Overall effect of environment: p=0.026

E

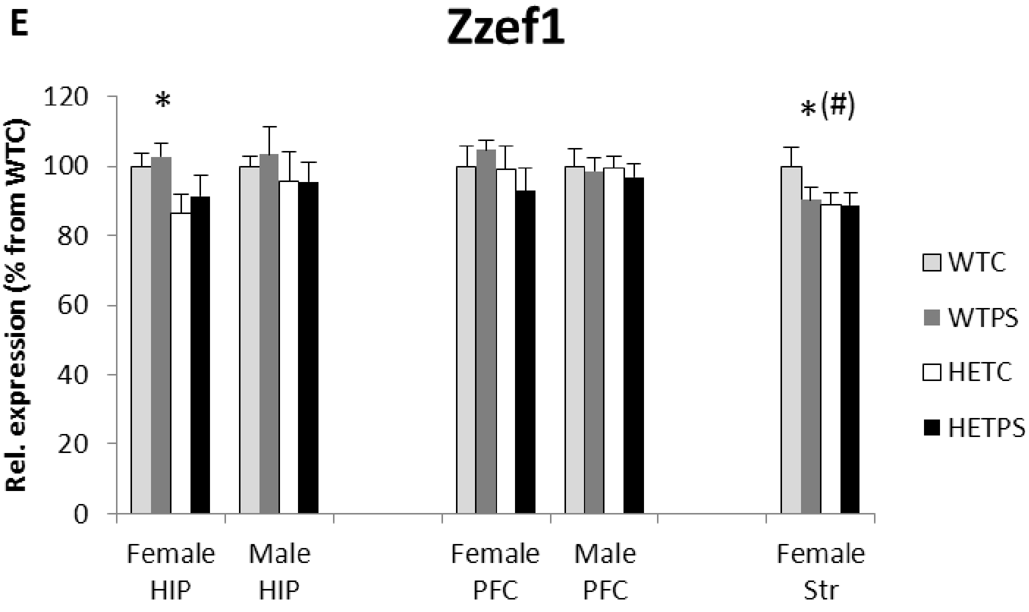

* Overall effect of genotype: p<0.01 (HIP), p=0.019 (Str)

(#) Overall effect of environment: p=0.061

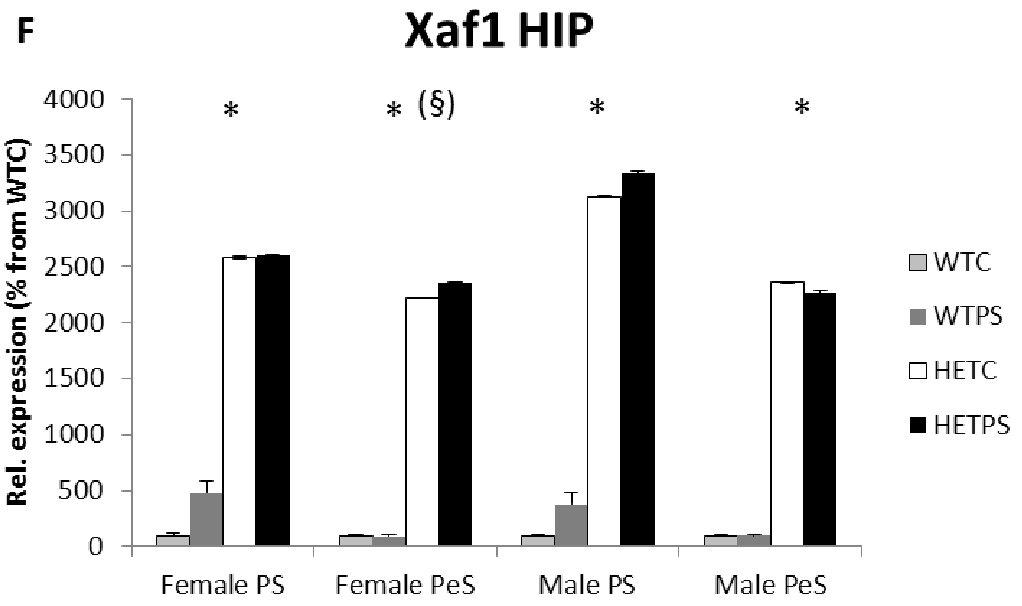
Xaf1 HIP

* Overall effect of genotype:p<0.01(PS, PeS)
(§) Overall effect of gene x environment: p=0.096

Figure 3-6. Validation of gene expression differences in distinct brain regions of male and female prenatal (PS; A-E) and perinatal (PeS; F) animals. Abbreviations: WT, wild-type; C, control offspring.; HET, 5-Htt+/- offspring. Data represent mean + S.E.M. N=7-10 mice/group. ( ): 0.05<p<0.1 (tendency)

3.3 DNA methylation study

3.3.1 DNA methylation microarray

To further investigate the molecular mechanisms underlying the behavior of the female offspring and to see which genes may be regulated by DNA methylation we conducted a microarray-based methylation profiling on the female hippocampus. As in the gene expression profiling, we concentrated on three different comparisons. We measured the changes between 5-Htt+/- genotype and WT mice (G effect), as well as the differences between PS and control mice (E effect), and the interaction of G and E (GxE effects). In brief, the 5-Htt+/- genotype and PS exposure altered the methylation of 279 and 400 genes, respectively (Figure 3-7; see also Supplements 5.1.4 and 5.1.5 for a complete overview of all genes significantly affected by G and E, respectively). Further, 268 genes were affected in a GxE manner (see Supplements 5.1.6 and Figure 3-7). In addition, G and E showed overlap in the methylation of 10 differentially methylated regions (DMRs; one gene can be composed of several regions which can be differentially regulated). Of those, 6 DMRs were upregulated and one – *titin (Ttn)* - downregulated by both. Moreover, the methylation of 3 DMRs – *Ttn, phospholipase A2, group IIA (Pla2g2a) and Pla2g V (Pla2g5)* - was affected in a G, E and GxE manner.

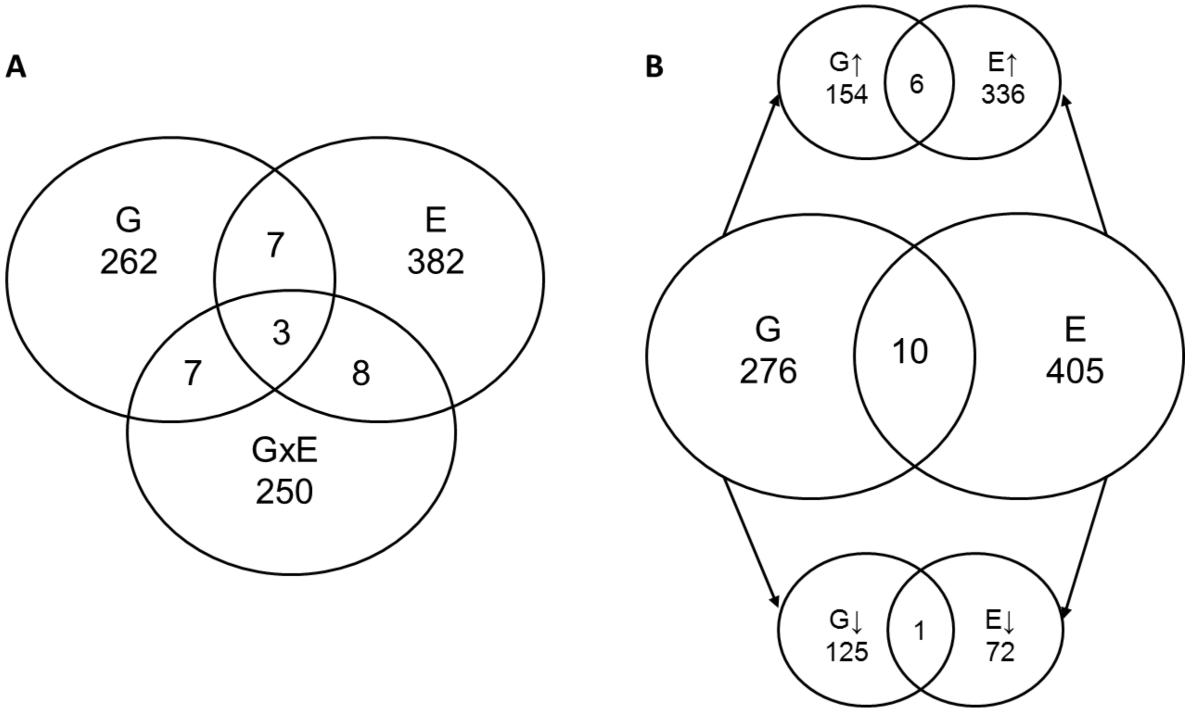

Figure 3-7. Methylation - number of altered genes. A) Number of differentially methylated genes regulated by either the 5-Htt+/- genotype (G), the environment (E) or in a GxE fashion. B) Number of differentially methylated regions (DMRs) which are either up or downregulated.

Additionally, 28 (G), 37 (E) and 24 (GxE) genes showed an overlap between methylation and gene expression (see Figure 3-8). One gene - *Pla2g5* - was affected by both, G and GxE, whereas around half of those genes showed classical methylation, indicating upregulated methylation and downregulated expression or vice versa (see Table 3-8).

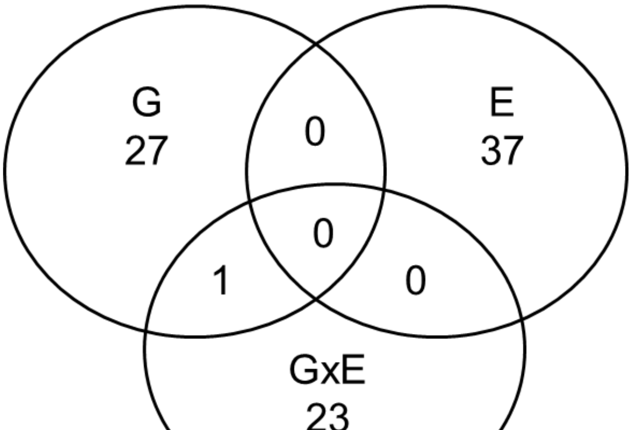

Figure 3-8. Overlap of differentially methylated and expressed genes. Number of genes that were differentially methylated and differentially expressed by the 5-Htt+/- genotype (G), the environment (E) or GxE interaction.

Tab. 3-8 A. Genes affected by gene expression and methylation through 5-Htt genotype

#	SYMBOL	GENENAME	Effect exp	Effect meth	FC exp
1	0610040J01Rik	RIKEN cDNA 0610040J01 gene	-	-	1.12
2	Akap6	A kinase (PRKA) anchor protein 6	+	-	1.14
3	Bbx	bobby sox homolog (Drosophila)	+	+	1.26
4	BC030307	cDNA sequence BC030307	+	+	1.15
5	Bcl2l11	BCL2-like 11 (apoptosis facilitator)	-	+	1.11
6	Bmpr1b	bone morphogenetic protein receptor, type 1B	-	+	1.19
7	C030046E11Rik	RIKEN cDNA C030046E11 gene	+	-	1.14
8	Cybrd1	cytochrome b reductase 1	+	-	1.13
9	Dhx32	DEAH (Asp-Glu-Ala-His) box polypeptide 32	-	-	1.19
10	E2f3	E2F transcription factor 3	+	-	1.14
11	Fabp6	fatty acid binding protein 6, ileal (gastrotropin)	-	+	1.27
12	Fank1	fibronectin type 3 and ankyrin repeat domains 1	-	-	1.17
13	Fgfr4	fibroblast growth factor receptor 4	-	+	1.26
14	Kcnj5	potassium inwardly-rectifying channel, subfamily J, member 5	+	+	1.18
15	Kif13a	kinesin family member 13A	-	-	1.12
16	Krt23	keratin 23	-	-	1.21
17	Ldlrad3	low density lipoprotein receptor class A domain containing 3	-	+	1.12
18	Lgr5	leucine rich repeat containing G protein coupled receptor 5	+	+	1.13
19	Mllt6	myeloid/lymphoid or mixed-lineage leukemia (trithorax homolog, Drosophila); translocated to, 6	-	-	1.23
20	Mttp	microsomal triglyceride transfer protein	+	+	1.25
21	Nr5a1	nuclear receptor subfamily 5, group A, member 1	-	-	1.17
22	Pdlim4	PDZ and LIM domain 4	-	+	1.21
23	Pla2g5	phospholipase A2, group V	-	+	1.60
24	Smad7	MAD homolog 7 (Drosophila)	-	+	1.12
25	Spsb1	splA/ryanodine receptor domain and SOCS box containing 1	-	+	1.19
26	Tcea3	transcription elongation factor A (SII), 3	-	-	1.30
27	Tmem100	transmembrane protein 100	+	-	1.22
28	Ttn	titin	+	-	1.21

Tab. 3-8 B. Genes affected by gene expression and methylation through PS exposure

#	SYMBOL	GENENAME	Effect exp	Effect meth	FC exp
1	Akap13	A kinase (PRKA) anchor protein 13	-	+	1.10
2	BC051628	cDNA sequence BC051628	+	-	1.12
3	Bcl10	B-cell leukemia/lymphoma 10	+	-	1.18
4	Cdc73	cell division cycle 73, Paf1/RNA polymerase II complex component, homolog (S. cerevisiae)	+	-	1.15
5	Chaf1b	chromatin assembly factor 1, subunit B (p60)	+	+	1.24
6	Cldn18	claudin 18	+	+	1.19
7	Clstn2	calsyntenin 2	-	+	1.19
8	Ddx46	DEAD (Asp-Glu-Ala-Asp) box polypeptide 46	-	+	1.16
9	Dna2	DNA replication helicase 2 homolog (yeast)	+	+	1.25
10	Fjx1	four jointed box 1 (Drosophila)	-	+	1.20
11	Gja1	gap junction protein, alpha 1	-	+	1.42
12	Kat2a	K(lysine) acetyltransferase 2A	-	+	1.15

13	Kcnh3	potassium voltage-gated channel, subfamily H (eag-related), member 3	-	+	1.11
14	Kdm6b	KDM1 lysine (K)-specific demethylase 6B	+	+	1.14
15	Map3k1	mitogen-activated protein kinase kinase kinase 1	+	+	1.24
16	Mast4	microtubule associated serine/threonine kinase family member 4	+	-	1.14
17	Mcm3	minichromosome maintenance deficient 3 (S. cerevisiae)	+	+	1.18
18	Mettl7a1	methyltransferase like 7A1	+	+	1.13
19	Msi1	Musashi homolog 1(Drosophila)	+	+	1.24
20	Nos1	nitric oxide synthase 1, neuronal	-	+	1.20
21	Nr2c1	nuclear receptor subfamily 2, group C, member 1	-	+	1.19
22	Pnlip	pancreatic lipase	+	+	1.25
23	Prkab1	protein kinase, AMP-activated, beta 1 non-catalytic subunit	-	+	1.13
24	Prok2	prokineticin 2	+	+	1.15
25	Prss23	protease, serine, 23	-	-	1.17
26	Ptpn21	protein tyrosine phosphatase, non-receptor type 21	+	+	1.15
27	Rad9b	RAD9 homolog B (S. cerevisiae)	-	+	1.18
28	Ropn1l	ropporin 1-like	-	+	1.15
29	Slc30a1	solute carrier family 30 (zinc transporter), member 1	-	+	1.15
30	Sox6	SRY-box containing gene 6	+	-	1.14
31	Stt3b	STT3, subunit of the oligosaccharyltransferase complex, homolog B (S. cerevisiae)	+	+	1.22
32	Tex2	testis expressed gene 2	+	+	1.16
33	Tlr12	toll-like receptor 12	-	+	1.10
34	Tmtc2	transmembrane and tetratricopeptide repeat containing 2	+	-	1.14
35	Xpo7	exportin 7	+	+	1.15
36	Xpot	exportin, tRNA (nuclear export receptor for tRNAs)	+	+	1.14
37	Zfp64	zinc finger protein 64	+	+	1.21

Tab.3-8 C. Genes affected by gene expression and methylation in a gene x environment fashion

#	SYMBOL	GENENAME
1	2010001K21Rik	RIKEN cDNA 2010001K21 gene
2	5430421N21Rik	RIKEN cDNA 5430421N21 gene
3	Ank3	ankyrin 3, epithelial
4	Atp10b	ATPase, class V, type 10B
5	Cabin1	calcineurin binding protein 1
6	Cage1	cancer antigen 1
7	Chrna9	cholinergic receptor, nicotinic, alpha polypeptide 9
8	Clpb	ClpB caseinolytic peptidase B homolog (E. coli)
9	Dppa3	developmental pluripotency-associated 3
10	F10	coagulation factor X
11	Fam135a	family with sequence similarity 135, member A
12	Fam170a	family with sequence similarity 170, member A
13	Foxj1	forkhead box J1
14	Glra1	glycine receptor, alpha 1 subunit
15	Heatr1	HEAT repeat containing 1
16	Mbp	myelin basic protein
17	Parp14	poly (ADP-ribose) polymerase family, member 14
18	Pcdhb5	protocadherin beta 5

19	Pim1	proviral integration site 1
20	Pla2g5	phospholipase A2, group V
21	Psd3	pleckstrin and Sec7 domain containing 3
22	Tcof1	Treacher Collins Franceschetti syndrome 1, homolog
23	Uevld	UEV and lactate/malate dehyrogenase domains
24	Wdr66	WD repeat domain 66

Affected genes by gene expression and methylation through the 5-Htt genotype, PS exposure and gene x environment interactions. Abbreviations: exp, expression; FC, Fold change; meth, methylation

3.4 Resilience to stress exposure

3.4.1 Prenatal stress exposure

All of the 7 selected resilience genes from the microarray (see Supplement 5.1.7 and 5.1.8) showed several correlations with distinct behaviors in the PS group (see Tab. 3-9). For example, in female WTPS mice, *Figf* correlated with basal corticosterone (CORTb) concentration (r=-0.767; P= 0.016). Further, *Galr3* showed a significant negative correlation with stressed CORT levels in female 5-Htt+/-PS mice (CORTs; r=-0.713; P=0.021). As depicted in Figure 3-10 C and D, *Gh* (r=-0.714; p= 0.071) and *Prl* (r=-0.714; p= 0.071) tended to correlate positively with adrenal weights.

Table 3-9. Correlation of resilience genes with behavior

Gene	Female		Male	
	Spearman Correlation		Spearman Correlation	
	WTPS (n=7-9)	HETPS (n=9-10)	WTPS (n=8-9)	HETPS (n=6-9)
Gh	FST: P=0.099; r=-0.583 Adr: P=0.071; r=0.714	EZMdm: P=0.099; r=0.583	EZMdm: P=0.099; r=-0.583	
Prl	FST: P=0.058; r=-0.65 Adr: P=0.071; r=0.714	EZMdm: P=0.099; r=0.583	EZMoA: P=0.088; r=-0.6	Adr: P=0.024; r=-0.870
Camk2a			CORTb: P=0.016; r=-0.767	
Figf	EZMdm: P=0.067; r=-0.633 CORTb: P=0.016; r=-0.767		EZMoA: P=0.067; r=0.633 CORTr: P<0.01; r=-0.933	CORTb: P=0.067; r=0.633 AdrBW: P= 0.02; r=0.75
Galr3	EZMdm: P=0.088; r=-0.6	CORTs: P=0.021, r=-0.713	CORTb: P=0.067; r=-0.633 Adr: P<0.01; r=-0.838	
Syt5	EZMdm: P=0.088; r=-0.6		CORTb: P=0.088; r=-0.6 CORTr: P=0.025; r=-0.733 Adr: P<0.01; r=-0.922	
Prkar2b		CORTr: P=0.056; r=0.62	CORTb: P=0.025; r=-0.733	

Correlations of resilience genes with behavior. Abbreviations: Adr, Adrenal weight; AdrBW; Adr corrected for body weight; CORTln, logarithm of the corticosterone concentration (B, basal; R, recovery; S, stress); EZMdm, distance moved in the elevated zero maze; EZMoA, time spent in open arms of the elevated zero maze; FST, forced swim test

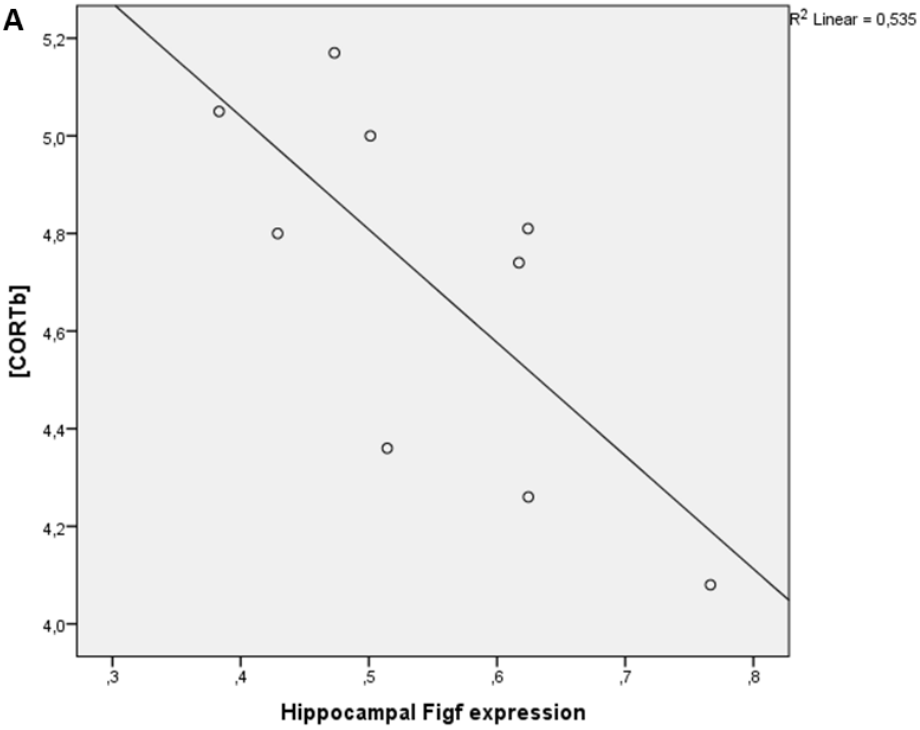

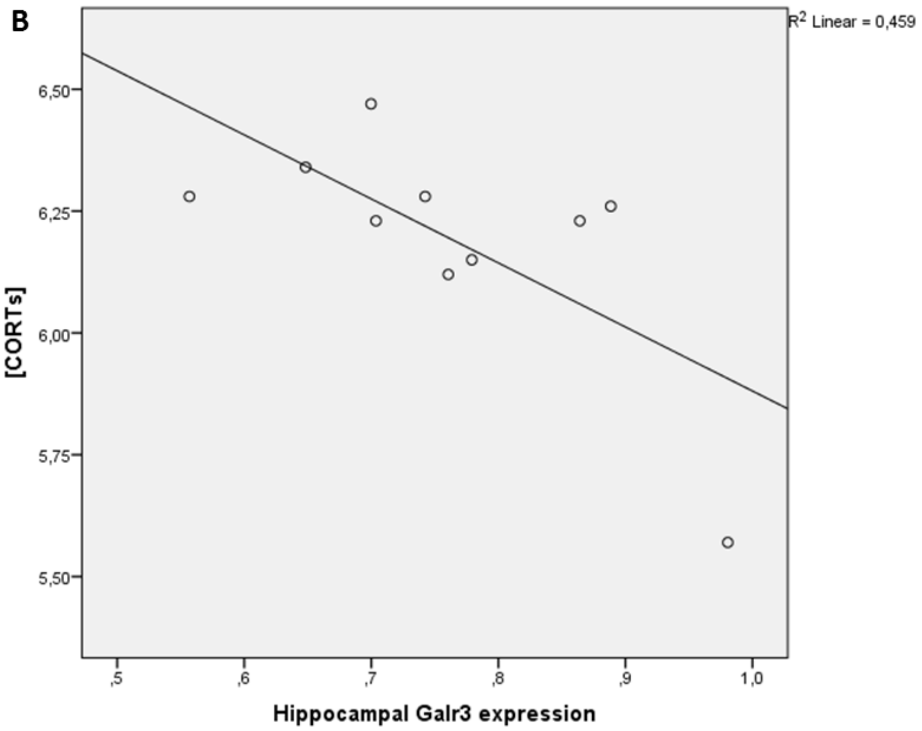
B
R^2 Linear = 0,459
[CORTs]
6,50
6,25
6,00
5,75
5,50
,5
,6
,7
,8
,9
1,0
Hippocampal Galr3 expression

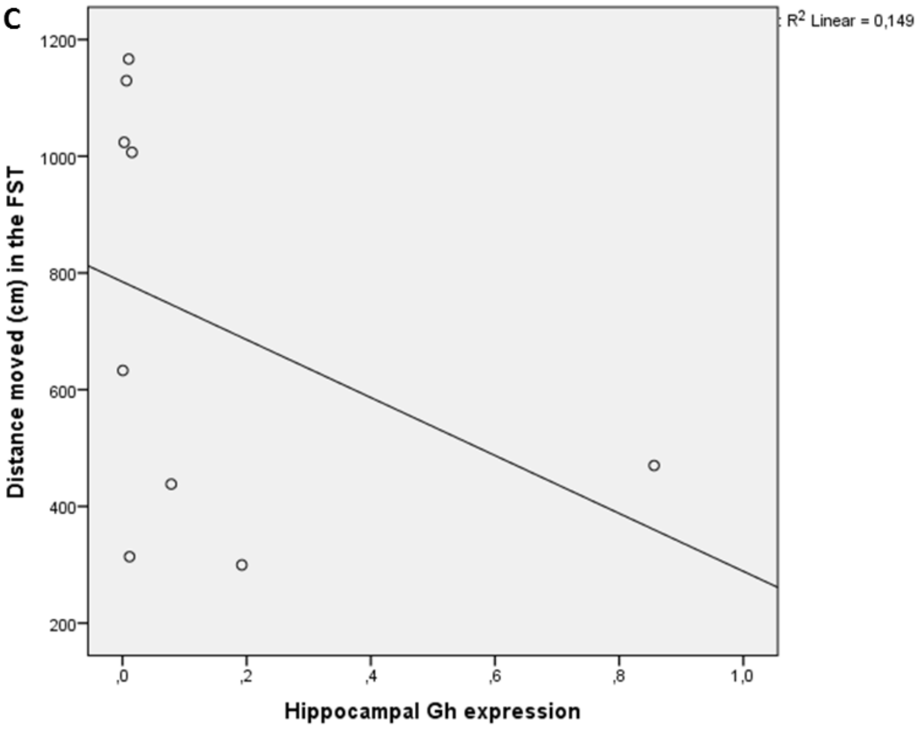
C
R^2 Linear = 0,149
Distance moved (cm) in the FST
1200
1000
800
600
400
200
,0
,2
,4
,6
,8
1,0
Hippocampal Gh expression

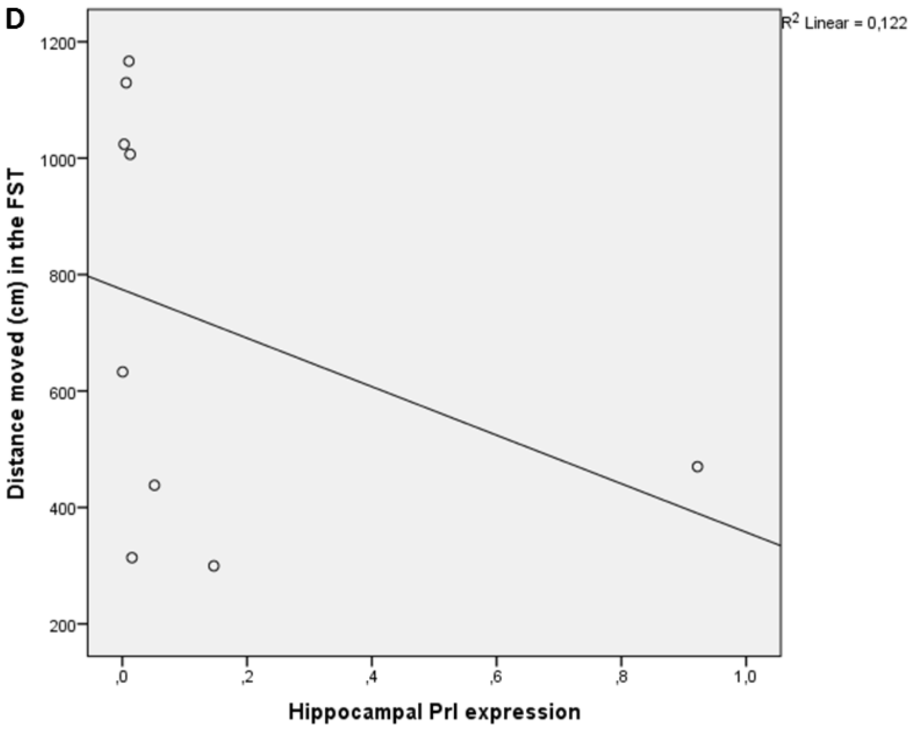

Figure 3-9 A-D. Scatterplot of correlation of resilience genes with behavior in the prenatal stress paradigm. A) *Fos-induced growth factor (Figf)* correlated negatively with basal corticosteron levels (CORTb). B) *Galanin receptor 3 (Galr3)* is negatively correlated with CORT stress (CORTs) concentrations. C.) *Growth hormone (Gh)* tended to correlate posetively with adrenal weights as did *prolactin (Prl*; D)

3.4.2 Perinatal stress exposure

We tested, whether *Gh* and *Prl* also correlated with behavior in the 5-Htt x PeS paradigm. Accordingly, *Gh* expression tended to show a negative correlation with the percentage of time spent on the open arms of the elevated plus maze (EPM; r=-0.69, P=0.058) in WTPeS animals. Further, *Prl* correlated positively with the percentage of time spent in the open arms of the EPM (r=0.812, P=0.05; see Figure 3-11) in the HETPeS group.

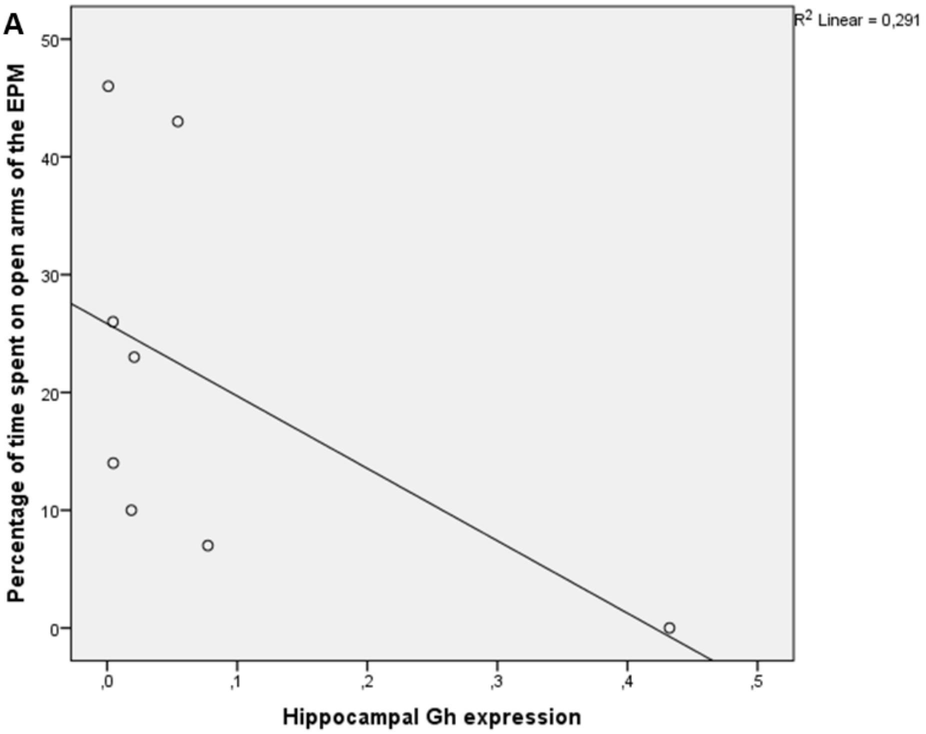

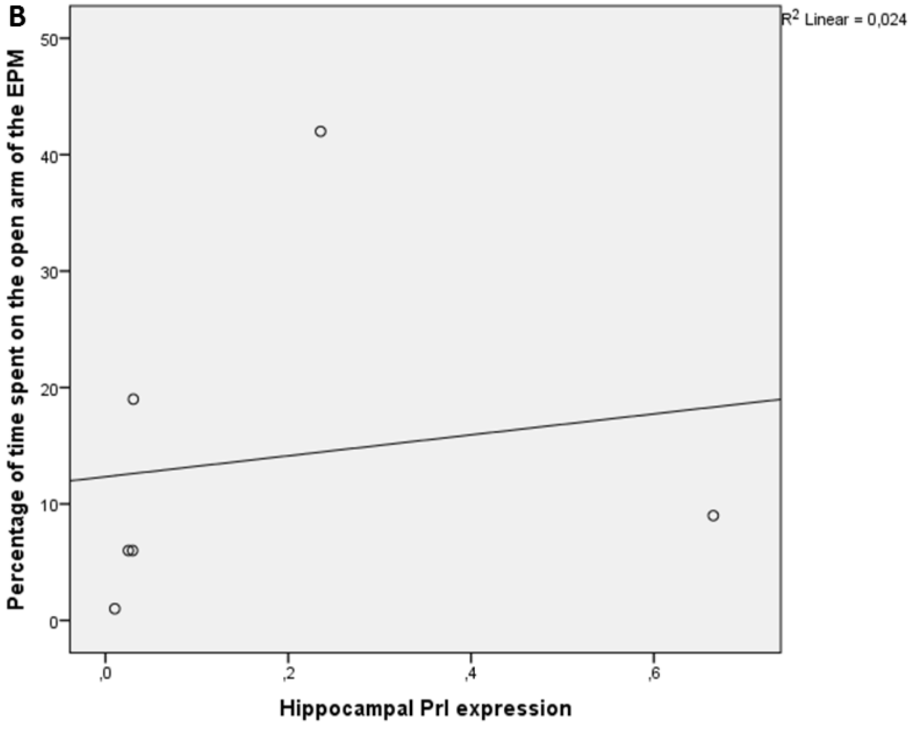

Figure 3-11 A-B. Scatterplot of correlation of resilience genes with behavior in the perinatal stress paradigm. A) Growth hormone (Gh) expression tended to correlate negatively with the percentage of time spent on open arms of the eleveated plus maze (EPM). Spearman correlation, $0.05<P<0.1$ B) Prolactin (Prl) displayed a significant, positive correlation with the percentage of time spent on open arms of the EPM. Spearman correlation, $P<0.05$

4. Discussion

4. Discussion

The present study demonstrates that exposure of 5-Htt+/- mice to prenatal maternal stress is associated with increased depression-like behavior, an effect that appeared to be more profound in female offspring. Conversely, adult 5-Htt+/- mice displayed increased memory performance as well as signs of reduced anxiety in comparison to WT offspring. Further, female 5-Htt genotype, PS and their interaction were associated with distinct hippocampal gene expression and DNA methylation profiles, the implications of which are discussed in more detail below. In addition, this study indicated an intricate relationship between PS/PeS exposure, emotional behavior and the HPA axis.

Combined behavioral effects of offspring 5-Htt genotype and PS

This is the first study measuring the effects of developmental stress exposure on adult cognition, anxiety and depression-like behavior as well as HPA axis responsivity in both male and female 5-Htt+/- offspring. While, 5-Htt+/- mice showed improved memory performance in the ORT when compared to WT offspring, PS exposure appeared to impair object memory performance in the same task. Further, rather unexpectedly, 5-Htt+/- mice seemed to be less anxious in comparison to WT mice, as indicated by an increased time spent in the open arms of the EZM. While PS exposure did not affect this particular type of anxiety-like behavior, it did reduce exploratory behavior in the same task. This was indicated by a reduced distance moved, primarily in WT offspring. In addition, exposure to the FST was linked to an enhanced depression-like behavior in PS mice, an effect which seemed to be particularly pronounced in 5-Htt+/- female offspring. Furthermore, 5-Htt+/- mice showed reduced basal CORT levels when compared to WT offspring.

While, the 5-Htt+/- genotype showed beneficial effects in the ORT, PS exposure appeared to impair object memory performance, which is in line with previous observations (Behan *et al.* 2011). The 'protective' genotype effect is in contrast with a previous study by Olivier and coworkers (Olivier *et al.* 2008), which demonstrated that 5-Htt+/- rats have impaired object memory when using longer intervals in the ORT. There is limited information about the role of the human 5-HTT genotype in learning and memory. In line with our data, Roiser and colleagues (Roiser *et al.* 2007) found that individuals homozygous for the 5HTTLPR s-allele show improved memory and attention in comparison to ll-carriers. Recently, it has been proposed that the beneficial cognitive effects of the s-allele may explain why genetic variation resulting in low 5-HTT function has been maintained throughout evolution (Homberg and Lesch 2011). The exact role of the 5-HTT in cognition remains to be elucidated, though. For example, it would be interesting to study the effects of 5-Htt genotype variation in spatial, hippocampus-dependent memory processing, by e.g. employing a spatial variant of the ORT, i.e., the object location test (OLT; see (Vanmierlo *et al.* 2011)).

Observations in the EZM revealed a significant genotype effect indicating that 5-Htt+/- mice were less anxious when compared to WT mice. A recent study by Heiming and colleagues (Heiming *et al.* 2009), which measured exposure of 5-Htt+/- females to olfactory cues of unfamiliar adult males during pregnancy and lactation did not detect any differences in anxiety between 5-Htt+/- and WT offspring. Another recent investigation by Jones and coworkers (Jones *et al.* 2010) indicated that offspring of both 5-Htt+/- and WT dams, which were stressed during pregnancy showed signs of reduced anxiety as compared to control offspring. Next to this, maternal stress exposure enhanced anxiety-like behavior in offspring from WT mothers only. Another study by Carola *et al.* (Carola *et al.* 2008) revealed clear signs of evidence for enhanced anxiety in male 5-Htt+/- mice when exposed to low levels of maternal care during early life. The observed discrepancy between the various investigations might be based on different study designs. First, diverse breeding schemes were employed. Second, maternal and/or paternal genotype varied. Third, there were different experimentally induced variations in the pre- and postnatal environment. Forth, the age differed at which the behavioral testing was performed. For example, in the study by Heiming and coworkers (Heiming *et al.* 2009), 5-Htt+/- dams were exposed to stress perinatally. Jones and colleagues (Jones *et al.* 2010), applied a different breeding design and utilized a chronic variable stress paradigm, starting from gestational day 6 and lasting until parturition. Further, offspring genotype was not taken into account in that study, which makes accurate comparison of the data difficult. In the study by Carola et al. (Carola *et al.* 2008), reciprocal inter-crossing between C57BL/6J and BALB/cByJ was applied, in order to measure the effect of variations in maternal care. Both strains carried different alleles of Tph2, thereby introducing additional genetic variation to the study design. In fact, the Tph2 genotype significantly affected the behavioral outcome, indicating a G x G x E effect. In addition, only WT mothers were utilized for breeding in that study. All in all, when it comes to adult anxiety-like behavior, exposure of 5-Htt+/- mice to developmental stress may have various, differential, complex programming effects, the nature of which is dependent on numerous factors.

Of interest, especially male 5-Htt+/- mice seemed to have lower basal CORT levels in comparison to WT offspring. At the same time, female 5-Htt+/- mice seemed to have larger adrenals compared to WT mice. Thus, one might speculate that the 5-Htt+/- genotype is linked with a sex-dependent change in the set-point of the HPA axis, which, in turn, may be related to the different susceptibility of both sexes when it comes to e.g. developmental stress exposure. In this context, Wuest and colleagues demonstrated that male ss-allele carriers displayed the lowest cortisol awakening response (an indirect measurement of the basal cortisol secretion) when compared to sl- and ll-carriers, whereas female ss-carriers showed the highest (Wust *et al.* 2009). Whether the diminished basal CORT levels in 5-Htt+/- offspring contribute to the reduced levels of anxiety as seen in the EZM in 5-Htt+/- mice remains to be elucidated.

Adaptive capacity of variations in the 5-Htt genotype

All in all, the increased memory performance and decreased anxiety as seen in 5-Htt+/- mice underscore the adaptive capacity of this specific genetic variation (Homberg and Lesch 2011; Homberg 2012). In fact, when looking more closely at the FST data, control 5-Htt+/- offspring even appeared to show lower levels of depression-like behavior in comparison to WT mice. At the same time, only 5-Htt+/- mice exposed to PS showed enhanced levels of depression-like behavior. Taken together, these findings echo the perception that the classical deficit-oriented association of the 5-HTTLPR variants may be too simple. In effect, our current data propose that variation in the 5-Htt genotype acts in concert with variations in the prenatal environment, thereby determining (i.e. programming), in a sex-specific manner, whether a response to an acute environmental challenge in adulthood (e.g. cognitive and/or emotional) will turn out to be positive or negative.

Overall, the current data indicate that although the 5-Htt+/- genotype shows clear adaptive capacity, while it appears to enhance the susceptibility to developmental stress exposure, predominantly in female offspring.

Hippocampal gene expression profiles

Microarray analysis indicated various effects of female 5-Htt genotype, PS, and their interaction on hippocampal gene expression profiles, which may partly explain the distinct behavioral phenotypes observed among the different experimental groups. Below, the role of several relevant genes and biological pathways are discussed in more detail.

MAPK signaling

DAVID analysis indicated an overall negative effect of the 5-Htt+/- genotype and a neutral to positive effect of PS on the MAPK signaling pathway within the female hippocampus. MAPK signaling plays an important role in embryogenesis, cell differentiation, cell proliferation and cell death (Asaoka and Nishina 2010; Keshet and Seger 2010). Aberrant MAPK signaling has been implicated in the development and course of several psychiatric disorders (Pearson *et al.* 2001; Li *et al.* 2009). The MAPK pathway comprises three major signaling cascades, i.e. the extracellular signal-regulated kinases 1 and 2 (ERK 1/2) cascade, the c-Jun N-terminal kinases (JNK) cascade and the p38 pathway, all of which are regulated in a complex, interactive manner. Downstream signaling is mediated via a kinase phosphorylation cascade culminating in the activation of transcription factors and the expression of specific genes.

When scrutinizing the impact of the 5-Htt+/- genotype and PS exposure, we found that PS, but not the 5-Htt+/- genotype, exerts a strong positive effect on the JNK cascade, whereas the p38 cascade remains nearly unaffected. A similar effect was demonstrated by Liu *et al*. (Liu *et al.* 2004) and Meller *et al*. (Meller *et al.* 2003) after acute stress in both the mouse and rat hippocampus. We found three JNK-activating genes, the *interleukin 1 receptor, type 1 (Il1r1), mitogen-activated protein kinase kinase kinase 12 (Map3k12)* and *mitogen-activated protein kinase kinase 7 (Map2k7)* and one Jnk-substrate, *jun oncogene (Jun*, also known as *c-Jun*) being up-regulated by PS. Furthermore, both the 5Htt+/- genotype and PS exert an overall negative effect on the ERK1/2 cascade. Genes which were down-regulated by both factors are e.g. the *calcium channel, voltage-dependent, gamma subunit 3 (Cacng3), protein kinase C (Prkcc)* and the *fibroblast growth factor receptor 1 (Fgfr1)*. In addition, the 5Htt+/- genotype decreased the expression of *Fgf1*, the major ligand of *Fgfr1*. Interestingly, a dysfunction in FGF signaling has been proposed to play an important role in the etiology of mood disorders (Turner *et al.* 2006), which is underlined by the finding that patients with major depression disorder (MDD) show an increased *FGFR1* expression in various hippocampal subregions (Gaughran *et al.* 2006). Next to this, the expression of *Fos*, a transcription factor, which represents a critical downstream target of the ERK pathway, was increased after PS exposure (an effect which was validated by qRT-PCR).

Neurotrophin signaling pathway

The neurotrophin family consists of BDNF, nerve growth factor (NGF), neurotrophin 3 (NT-3), and neurotrophin 4 (NT-4), which bind to the tyrosine kinase (Trk) receptor family (including TrkA, TrkB and TrkC) as well as to the p75 neurotrophin receptor ($p75^{NTR}$). This leads to the activation of different downstream signaling cascades which modulate neuronal and synaptic plasticity. Thus, the neurotrophin signaling pathway is implicated in the etiology and therapy of depression ("neurotrophin hypothesis of depression";(Duman *et al.* 2000; Jacobs *et al.* 2000)). We demonstrated that the 5-Htt+/- genotype and PS exposure significantly affect neurotrophin signaling indicating that both genetic and environmental factors contribute to dynamic neuronal and synaptic plasticity in the hippocampus. More specifically, TrkB signaling was targeted by both the 5Htt+/- genotype and PS. For example, *Ntrk2 (TrkB)* receptor expression itself was diminished in 5-Htt+/- offspring. Besides its essential role in promoting long-term potentiation, hippocampal TrkB signaling is critical in cell survival (Lu *et al.* 2005; see below). The TrkB receptor is activated by Bdnf and controls three different major pathways, the P13 kinase cascade, the PLC-γ1 cascade and the ERK1/2 MAPK cascade (Reichardt 2006). The last one was primarily influenced by both 5-Htt+/- and PS. This cascade targets Creb1 whose nuclear activation is an important component of a general switch that converts short-term into long-term plasticity (Barco *et al.* 2002). Before inducing Creb1-dependent transcription, its transcriptional repressor Creb2 (or activating transcription factor 4; Atf4) has to be released. Consequently, it could be suggested that the observed decline in *Ntrk2* expression in 5-Htt+/- animals, in combination with the increase in *Creb2* expression, induced by PS exposure, contributed to impaired Bdnf signaling and related neuronal and synaptic plasticity, thereby eliciting depression-like behavior (Taliaz *et al.* 2010).

While both 5-Htt+/- genotype and PS appear to impair TrkB signaling in a similar manner, G and E seem to affect $p75^{NTR}$ signaling in an opposite way. The majority of genes influenced by the 5-Htt+/- genotype showed decreased expression patterns, among which are the *transformation-related protein 73 (Trp73), transformation-related protein 53 (Trp53), tyrosine 3-monooxygenase / tryptophan 5-monooxygenase activation protein, zeta polypeptide (Ywhaz),* and the *interleukin-1 receptor-associated kinase 1 (Irak1)*. On the other hand, the vast majority of genes affected by PS in this pathway displayed enhanced expression patterns, among which the *mitogen-activated protein kinase kinase kinase 1 (Map3k1)*, *mitogen-activated protein kinase kinase 7 (Map2k7)* and *c-Jun* could be found. Activation of the $P75^{NTR}$ pathway is proposed to play a prodepressive role (Martinowich *et al.* 2007). In more detail the activation of the $P75^{NTR}$ pathway has been linked to an elevation in long term depression (LTD) (Woo *et al.* 2005). Emerging evidence supports the idea that LTD may play a role in regulating stress- and depression-like behavior. For example, several studies reported a correlation between (behavioral) stress and the induction of LTD in adult rats (Xu *et al.* 1997; Holderbach *et al.* 2007). Moreover, treatment with antidepressants could reverse chronic mild stress–induced LTD (Holderbach *et al.* 2007). All in all, hypothetically, dysfunctional neurotrophin signaling, might mediate, at least in part, the altered depression-like behavior observed in PS 5-Htt+/- mice.

Cytokine-Cytokine receptor interaction

Although the 5-Htt+/- genotype and PS exposure often act on distinct specific molecular targets, there is extensive degree of overlap when considering the biological signaling pathways they affect *independently* from each other. When it comes to hippocampal gene expression profiles that indicate a G x E interaction, i.e. those genes of which the regulatory impact of PS is *dependent* upon the 5-Htt genotype, a different pattern is observed. In this respect, our data propose that cytokine-cytokine receptor interactions play a vital role when a dysfunctional 5-HT system and stress interact. This notion is supported by the study of Fredericks *et al.* (Fredericks *et al.* 2010) who found that healthy women homozygous for the s-allele of the 5-HTTLPR have enhanced pro-inflammatory cytokine levels and a higher IL-6/IL-10 ratio both at baseline and during stress, when compared to ll-individuals. Interestingly, the risk for developing a clinically relevant depression after cytokine therapy is elevated in people who carry the s-allele (Lotrich *et al.* 2009). Further, the pro-inflammatory cytokine level of patients suffering from major depression is higher in comparison to non-depressed individuals (Tsao *et al.* 2006; Capuron *et al.* 2008; Cizza *et al.* 2008; Dantzer *et al.* 2008). However, treatment with selective serotonin reuptake inhibitors (SSRIs) is able to reduce this enhancement (Kenis and Maes 2002; Dantzer *et al.* 2008). In addition, after experimental or therapeutic administration of pro-inflammatory cytokines, humans with originally no signs of depression, show depressive symptoms (Capuron *et al.* 2000; Reichenberg *et al.* 2001; Miller *et al.* 2009; Raison *et al.* 2009). For example, about half of all patients treated for a long period with interferon get depressed, and this state of mood can be meliorated by SSRI treatment (Capuron *et al.* 2002). Interestingly, it has been proposed that interferon-induced immune activation on depression may be explained in part by alterations in neurotrophin signaling capacity, reflected by decreases in serum BDNF following interferon treatment (Kenis *et al.* 2011). In the present study neurotrophin signaling was affected by both G and E. In this context, it has been suggested that pro-inflammatory cytokines like interferon-γ (INF-γ) and tumour necrosis factor α (TNFα) reduce the availability of tryptophan, the precursor for 5-HT, by inducing indoleamine-2,3-dioxygenase (IDO) (Robinson *et al.* 2005; Schiepers *et al.* 2005; Leonard and Myint 2009). In addition, the expression of several members of the Tnf and Tnf receptor superfamily, such as *Tnfsf8, Tnfrsf11a, Tnfrsf1a, Tnfrsf1b*, was regulated in a G x E manner. Further evidence for a molecular interaction between 5-HT and cytokines is given by the observation that mice lacking the interleukin-15 receptor (Il15ra), the expression of which was also affected within our model in a G x E manner, showed increased depression-like behavior, whereas fluoxetine was able to reduce it. These Il15ra knockout mice displayed decreased hippocampal expression of 5-Ht_{1A} receptor, increased hippocampal expression of 5-Ht_{2C}, and region-specific alterations of 5Htt immunoreactivity (Wu *et al.* 2011). Furthermore, the lack of Il15ra resulted in decreased anxiety in these mice (Wu *et al.* 2010), which indicates a comparable behavioral phenotype as observed in the present study. All in all, it may be hypothesized that, when challenged by e.g. developmental stress exposure, a dysfunctional 5-HT system could lead to a disturbed cytokine balance thereby increasing the vulnerability to stress, eventually resulting in psychiatric conditions.

Wnt signaling pathway

Next to cytokine-cytokine receptor interactions, also Wnt signaling was significantly influenced in a G x E manner. Wnt proteins are required for basic developmental processes and act via at least 3 different Wnt pathways: the canonical pathway, the planar cell polarity (PCP) pathway and the Wnt/Ca^{2+} pathway (Staal *et al.* 2008). All 3 cascades are initiated via Wnt binding to frizzled (Fzd). Interestingly, the mRNA expression of *frizzled homolog 3 (Fzd3)* was altered in the present study in a G x E fashion, indicating that all three abovementioned cascades are affected in our model. Furthermore, our microarray analysis revealed 4 other affected genes in the PCP signaling pathway, among which were *Rac2* and *Rock1*. With respect to this pathway, binding to Fzd3 results in the activation of the small GTPases RhoA and Rac1, which activate the stress kinase Jnk (Jun N-terminal kinase) and Rock, which eventually induces remodelling of the cytoskeleton and associated changes in cell adhesion and motility. The canonical Wnt pathway and especially 2 of its key players, glycogen synthase kinase 3beta (GSK-3beta) and beta-catenin, have been highly implicated in the etiology of psychiatric disorders such as depression, schizophrenia and bipolar disorder (Emamian *et al.* 2004; Gould *et al.* 2004; Gould *et al.* 2008; Wada 2009). Moreover, diminished Gsk-3beta and enhanced beta-catenin levels in the mouse brain have been associated with a better performance in the FST (Gould *et al.* 2008). Although these two key players were not directly affected in terms of gene expression within our 5-Htt x PS model, the mRNA expression of *presenilin1 (psen1)*, whose protein product is known to bind and stabilize beta-catenin (Chen and Schubert 2002), was regulated in a G x E fashion.

Xaf1, Mbp and Trhr

qRT-PCR validation revealed significant genotype effects for e.g. *Xaf1, Mbp* and *Trhr*. Xaf1 plays an important role in programmed cell death by inhibiting the anti-apoptotic functions of the X-linked inhibitor of apoptosis (XIAP) and of other members of the family of inhibitors of apoptosis (IAP), like survivin (Arora *et al.* 2007). Xiap has trophic effects on hippocampal neurons by enhancing *Bdnf* and *TrkB* activity (Kairisalo *et al.* 2009). Thus, the observed elevation in *Xaf1* and the decline in *TrkB* expression (see above) in adult 5-Htt+/- mice suggest a decreased resistance to apoptosis in these animals. Previous investigations by Ravary *et al.* (Ravary *et al.* 2001) and Persico *et al.* (Persico *et al.* 2003) demonstrated no signs of elevated neuronal apoptosis in 5-Htt+/- versus WT mice. Whether additional environmental stress exposure influences the levels of apoptosis in 5-Htt+/- animals remains to be elucidated. Next to *Xaf1*, the effects of e.g. *Mbp* and *Trhr* were also validated by qRT-PCR. Mbp is involved in myelinisation of the central nervous system and has recently been linked to schizophrenia (Martins-de-Souza *et al.* 2010). Trhr plays a role in the hormone system and neuromodulation. Interestingly, mice with a deficiency for the *Trhr1* show an anxiety- and depression-like behavior (Zeng *et al.* 2007). Evidently, the implications of the present findings await further research.

DNA methylation

Microarray analysis indicated that several genes that were differentially expressed were also differentially methylated. Below, the role of several relevant genes, which were both differentially expressed and methylated, is discussed in more detail.

The gene expression and DNA methylation screenings showed that the expression of Mbp is dependent on the interaction of 5-Htt+/- genotype and PS exposure, the regulation of which may be mediated by Mbp promoter methylation. Approximately 40% of the myelin in the CNS is composed of Mbp. In the rat brain, myelin formation is initiated at postnatal day 14 and is active during the next 7 days, leading to an accumulation of myelin in all brain areas. During the following month, myelinisation is decreased (Akiyama *et al.* 2002). Interestingly, early weaning, which is accompanied by an increased anxiety-like behaviour in adulthood (Kikusui *et al.* 2004), resulted in an increase of Mbp expression in the third week and a decline in the fifth week when compared to normally weaned mice, proposing that early maternal deprivation induces precocious myelin formation (Kikusui *et al.* 2007). In humans, cortical postmortem tissue of bipolar and major depressive disorder patients showed a reduction in myelin (Ongur *et al.* 1998), indicating that Mbp might also play a role in affective disorders as it obviously does in schizophrenia (Hakak *et al.* 2001; Hof *et al.* 2003; Martins-de-Souza *et al.* 2010). Further, corticosterone metabolites led to a decrease in Mbp in oligodendrocytes (Melcangi *et al.* 1997). An independent study by our group in the hippocampus of C57BL/6 mice revealed a decreased Mbp protein level in WT female offspring when compared to 5-Htt+/- mice, which supprts the notion that Mbp plays an important role when it comes to developmental stress exposure (Föcking 2012, in preparation).

Our microarrays revealed that the expression of *bone morphogenetic protein receptor type 1B (Bmpr1b)* and *MAD homolog 7 (Drosophila; Smad7)* was downregulated, whereas the methylation was upregulated in 5-Htt+/- mice when compared to WT mice. BMPs belong to the TGFß superfamily and are secretory growth factors. They promote astrogliagenesis *in vivo* and *in vitro* (Gross *et al.* 1996; Bonaguidi *et al.* 2005) and neurogenesis in the cortex (Li *et al.* 1998; Mabie *et al.* 1999), whereas neurogegesis is inhibited by BMP2 and -4 in the embryonic and adult striatum (Gross *et al.* 1996; Lim *et al.* 2000). Inhibition of BMP signalling by HDACs or the downstream cytoplasmic factor Smad7 leads to increased neurogenesis (on the expense of astrogliagenesis) in the ganglionic eminence, whereas this has opposite effects in the embryonic cortex (Shaked *et al.* 2008). Evidently, BMPs play a major role in the switch from neurogenesis to astrogliagenesis in late gestation. Interestingly, mice that were constitutively deficient for *Bmpr1b* and conditionally deficient for *Bmpr1a*, the dentate gyrus was markedly diminished in size when compared to control mice and the stem cell niche that generates new neurons in the adult hippocampus was reduced. Furthermore, these double mutant mice responded less to fear- and anxiety-provoking stimuli (Caronia *et al.* 2010). Whether the reduced expression of *Bmpr1b* in 5-Htt+/- deficient mice leads to a decreased anxiety remaines to be clarified. Next to this, the expression of *potassium inwardly-rectifying channel, subfamily J, member 5 (Kcnj5*, also known as *Girk4*) appeared to be upregulated in the 5-Htt+/- mice. Kcnj5 could be inhibited by several antidepressants (Kobayashi *et al.* 2011). The methylation, was upregulated as well which crashes with the classical notion that an increased methylation leads to a decrease in expression. Recently, it was suggested that the classical point of view is oversimplified (for review see Suzuki and Bird 2008).

Our microarrays indicated that the expression and the methylation of *prokineticin 2 (Prok2)* was upregulated in PS animals. Prok2 belongs to a pair of cysteine-rich secretory proteins and has recently been suggested to be a central output molecule of the suprachiasmatic nucleus (SCN) (Cheng *et al.* 2002; Cheng *et al.* 2005), the pacemaker that drives circadian rhythms (Moore 1997). Interestingly, a disruptive circadian rhythm is linked to several mood disorders including depression (McClung 2007; Turek 2007). For instance, mice that are deficient for Prok2 showed decreased anxiety-like and depression-like behaviors (Li *et al.* 2009), which suggests that the observed increase of Prok2 as seen in our study might play an important role in conveying depression-like behavior in the PS mice. Further, the microarrays revealed an upregulated methylation and a downregulated expression of *nitric oxide synthase 1, neuronal (Nos1)* in PS compared to control mice. Nos1 has been shown to be an important neurotransmitter in the nervous system. It is involved in the regulation of various cognitive and emotional processes involved in depression and anxiety (Wiley *et al.* 1995; Harkin *et al.* 1999). Selective inhibitors of Nos1 have antidepressant- and anxiolytic-like effects (Volke *et al.* 2003), Nos1 knockout mice however, did not show any differences in depression-like behaviour compared to WT mice (Wultsch *et al.* 2007). Merely, these knockout mice showed reduced anxiety-like behavior (Wultsch *et al.* 2007). Wether the reduced expression of Nos1 in the PS mice mediates the observed depression-like effects needs to be further investigated.

Vulnerability and resilience to PS

Performance-oriented LIMMA analysis on the mRNA expression microarray data followed by subsequent Spearman correlation analysis linking the individual mRNA expression data as obtained by qRT-PCR to behavioral performance as well as to neuroendocrinological measures revealed various significant correlations pinpointing specific molecular substrates that may, at least in part, explain the behavioral response to PS. More specifically, the performance-based LIMMA analysis offers the opportunity to identify molecular mechanisms specific to either vulnerabilty or resilience to PS. Accordingly, amongst PS WT animals, we observed a negative correlation between *Figf* expression and basal plasma CORT levels. Similarly, among PS 5-Htt+/- mice, *Galr3* expression was negatively correlated with stress-induced plasma CORT levels. Furthermore, in WT animals, *Gh* and *Prl* expression tended to correlate positively with adrenal weights.

Figf belongs to the family of vascular endothelial growth factors (Vegf) and is also known as Vegf-D. Within the vascular system, Figf plays a major role in the regulation of lymphangiogenesis (Joukov *et al.* 1996; Achen *et al.* 1998; Kranich *et al.* 2009). As other members of the Vegf family are well studied in the brain, our knowledge about Figf and its function in the brain is poor. Here, we demonstrate that *Figf* is expressed within the hippocampus, the extent of which is correlated with basal corticosterone levels. A study of Kranich and colleagues has already shown that *figf* was expressed in different brain cells (Kranich *et al.* 2009), among which e.g. microglial, schwannoma and glial precursor cells (GPCs), whereas the expression of its receptor Vegfr-3 was restricted to GPCs. This suggests an autocrine and paracrine function of Figf in the brain. Next to this, Figf was able to increase cell proliferation and the migration of GPC. Overall, the authors hypothesized that figf might play an important role in neurogenesis, possibly after ischemic insults or during brain development. In the present study, *figf* showed a negative correlation to basal CORT levels. This is consistent with a study of Yano and colleagues who demonstrated that (synthetic) glucocorticoids decrease Vegf production directly via the GR (Yano *et al.* 2006). Interrestingly, in the view of the notion that those animals showing the lowest basal CORT levels in response to stress exposure could be regarded as resilient (Schmidt *et al.* 2010) our data suggest that an elevated hippocampal *figf* expression might play an important role in mediating the central aspects of resilience in this respect.

Galr3 is one of the three receptor subtypes of galanin (Galr1-3). Galr3 mRNA is localized in distinct brain regions such as locus coeruleus, DRN, caudate putamen, hypothalamus, pituitary, spinal cord, but also in the pancreas, liver, kidney, stomach and adrenal gland suggesting that Gal3 might play an important role in emotion, feeding, pituitary hormone release, nociception and metabolism (Mennicken *et al.* 2002). Its localization in the brain might indicate that Galr3 in particular mediates especially the mood-related function of galanin. Galanin itself is a neuropeptide and is involved in the modulation of acetylcholine release and associated memory functions, and, as such, has been shown to be implicated in Alzheimer’s disease (Crawley 1996; McDonald and Crawley 1997). In addition, galanin is known to influence the serotonergic, noradrenergic and dopaminergic system and has therefore been suggested to be implicated in the regulation of e.g. feeding behavior (Leibowitz 1995), pain (Kask *et al.* 1997) and affective states (Bing *et al.* 1993; Fuxe *et al.* 1998; Weiss *et al.* 1998; Moller *et al.* 1999; Khoshbouei *et al.* 2002; Lu *et al.* 2005). When galanin is injected into the DRN it decreases extracellular 5-HT output in the hippocampus which can be partly reversed by a Galr3 antagonist. This antagonist has anxiolytic- and antidepressant-like effects and identifies Galr3 to take part in the inhibitory effect of galanin in anxious and depressive states (Swanson *et al.* 2005). Furthermore, when galanin is injected into the paraventricular nucleus of the hypothalamus, it inhibits corticosterone release (Tempel and Leibowitz 1990), whereas peripheral administration shows no effect (Dunning and Taborsky 1988), indicating that this inhibition is mediated centrally. In line with this observed negative interaction, the present data show that increasing *Galr3* levels are linked to lower stressed plasma CORT levels, thereby possibly conferring resilience to PS exposure.

The present study revealed that hippocampal *Gh* expression was markedly downregulated in animals that performed well in the FST, and that *Gh* expression tended to correlate positively to adrenal weight. Gh is a 19-21 kDa cytokine polypeptide and is primarily expressed in the anterior pituitary, where it mediates longitudinal growth in the postnatal period (Kopchick and Andry 2000). Recently, evidence for an endogenous hippocampal *Gh* expression emerged (Donahue *et al.* 2002; Sun *et al.* 2005). In the hippocampus, it possibly induces long term potentiation via Creb-1 and may be involved in synaptic plasticity (Zearfoss *et al.* 2008), which might explain its role in memory formation (van Dam and Aleman 2004; Sonntag *et al.* 2005). Further, an acute stressor was able to increase Gh production in the hippocampus, possibly indicating a higher degree of learning (Donahue *et al.* 2002; Donahue *et al.* 2006). On the other hand, Gh decelerates extinction in rats (Schneider-Rivas *et al.* 2007), possibly indicating that the resilient animals do not learn the stressful stimulus or forget it faster and therefore display less depression-like behavior compared to the poorly performing mice. Interestingly, in Gh-deficient rats, Gh prevents adrenal weight growth, which is normally seen in early experimental diabetes (Kunjara *et al.* 2012). Along similar lines, insulin-like growth factor, the downstream effector of Gh, increases adrenal growth (Jackson *et al.* 1991). If, and if so, how hippocampal *Gh* expression regulates adrenal functions and therefore may confer resilience remains to be investigated.

The present study revealed that hippocampal *Prl* expression is markedly downregulated in animals who performed well in the FST, whereas its expression tended to correlate positively to adrenal weight. Prl is a polypeptide hormone secreted by the anterior pituitary which might act directly on the adrenal gland. For example, it stimulates steroidogenesis synergisticly with ACTH (Ogle and Kitay 1979). Several studies delineated that Prl stimulates aldosterone-producing adenomas and adrenocortical carcinoma (Carroll *et al.* 1982; Bole-Feysot *et al.* 1998). Interestingly, hyperprolactinemia in rodents resulted in an absolute and relative enhancement of adrenal weight (Fang *et al.* 1974; Bartke *et al.* 1984; Phelps *et al.* 1987; Silva *et al.* 2004). When looking at the perinatal stress paradigm, Prl significantly correlated with the percentage of time spent on open arms of the EPM in a positive manner indicating an increased *Prl* expression in anxiety-resilient animals. Prl has recently been suggested to act as a neuropeptide and its receptors can be found in the brain, including the hippocampus (Clapp *et al.* 1994; Ben-Jonathan *et al.* 1996; Pi and Grattan 1998). Interestingly, the Prl receptors in the brain convey anxiolysis (Torner *et al.* 2001), which makes it tempting to speculate that the higher Prl level in unsusceptible compared to susceptible mice confers an anxiety-resilient state.

Study limitations

It should be noted that the present study has several limitations. For example, animals were housed individually from weaning onwards in order to prevent the establishment of a hierarchy. Although the cages were in close proximity to each other (enabling visual contact between neighbouring mice) and the home cage was enriched with paper tissues and a cardboard tube, the isolated housing conditions could represent an additional stressor to the animals. Further, it is likely that the behavioral testing paradigms exhibited an independent effect on hippocampal gene expression profiles. Although behavioral task exposure was identical for all groups, one cannot exclude that the animals' response to it was different among groups. Thus, behavioral testing may have left a permanent imprint on hippocampal gene expression patterns in a genotype- and/or condition-dependent manner. Evidently, investigating behavior and its underlying biological mechanisms in the same set of animals enables the possibility of linking both features in a more direct way. Similarly, prior behavioral testing may have had an influence on the basal and stress-induced CORT levels. Nevertheless, an acute effect can be excluded, since the animals were left undisturbed for a week in between behavioral test sessions and blood sampling. Another remarkable notion is the fact that PS was associated with a higher degree of mortality in the offspring. Although a similar effect has been reported previously (e.g. Patin *et al.* 2002), in the present study this effect was observed immediately after weaning, when the offspring were moved to IVC cages. Personal observations suggest that the affected mice were too small and weak to drink enough water out of the IVC sipper tubes. In light of previous work from our group, which has shown a direct correlation between low birth weight –as a consequence of restricted fetal growth associated with PS exposure– and, amongst others, adult depression-like behavior (van den Hove *et al.* 2010), the consequent loss of these mice in the behavioral comparison later in life may have even weakened some of the observed behavioral effects of PS. Concerning the expression array, the information on the array (from 2002) and the current information about the genes did not match in all cases leading to false or non-annotated genes. Furthermore, we did not control for the estrous cycle in the female animals. As Gh and Prl are regulated by estrogens (Donahue *et al.* 2006; Nogami *et al.* 2007) we cannot rule out that a different state in the estrous cycle can confer resilience or vulnerability. This might also explain the high variations in the *Gh* results (data not shown).

Conclusion

Taken together, the present data suggest that the 5-Htt+/- genotype is associated with improved object memory function as well as signs of reduced anxiety. In contrast, exposure of 5-Htt+/- mice to

PS was associated with increased depression-like behavior, an effect that tended to be more pronounced in female offspring. Furthermore, 5-Htt genotype, PS and their interaction differentially affected the expression of numerous genes and related pathways within the female hippocampus. Whereas MAPK and neurotrophin signaling were regulated by both the 5-Htt+/- genotype and PS exposure, cytokine and Wnt signaling were affected in a 5-Htt genotype x PS manner, indicating a G x E interaction at the molecular level. Thus, the present study indicates that the long-term stress- and depression-related behavioral effects of PS in C57BL/6 mice are partly dependent on the 5-Htt genotype. Moreover, our gene expression and DNA methylation findings provide evidence for a molecular basis of such a G x E interaction, which eventually might help to identify novel targets for the diagnostic assessment and treatment of disorders of emotion regulation.

Outlook

As the current study design was not primarily designed to study the concept of resilience, one may come up with a modified resilience-based study design with more animals to increase power. To investigate our candidate genes, an overexpression of the candidates in the hippocampus can be performed. Further, we may perform fluorescence or magnetic activated cell sorting (FACS or MACS) to analyze specifically neuronal cells.

Nevertheless, the investigated genes are promising candidates and need to be further examined to acquire more knowledge about the neurobiological basis of emotional disorders. This knowledge is essential for understanding the molecular mechanisms underlying the emergence of these disorders and for the development of new treatment strategies.

5. Appendix

5. Appendix

5.1 Gene lists

5.1.1 Gene expression affected by the genotype (5-Htt+/- versus wild-type)

ID: Affymetrix ID; EFFECT: direction of effect; “+”: gene expression upregulated in 5-Htt+/- versus wild-type mice; “-“: downregulated in 5-Htt+/- versus wild type mice; FC: fold-change in mRNA expression. Genes have been ordered alphabetically by symbol.

#	ID	SYMBOL	GENENAME	EFFECT	FC	P-Value
1	1432532_at	0610025J13Rik	RIKEN cDNA 0610025J13 gene	+	1.3	0.0001
2	1431884_at	1110019B22Rik	RIKEN cDNA 1110019B22 gene	+	1.2	0.0078
3	1439363_at	1200014J11Rik	RIKEN cDNA 1200014J11 gene	-	1.6	0.0000
4	1451082_at	1300018I05Rik	RIKEN cDNA 1300018I05 gene	-	1.2	0.0037
5	1429091_at	1600002K03Rik	RIKEN cDNA 1600002K03 gene	+	1.2	0.0081
6	1429324_at	1700012A16Rik	RIKEN cDNA 1700012A16 gene	+	1.2	0.0097
7	1432983_at	1700026H06Rik	RIKEN cDNA 1700026H06 gene	+	1.2	0.0089
8	1430513_at	1700055N04Rik	RIKEN cDNA 1700055N04 gene	+	1.4	0.0024
9	1429198_at	1810030O07Rik	RIKEN cDNA 1810030O07 gene	-	1.3	0.0043
10	1441251_a_at	2010001A14Rik	RIKEN cDNA 2010001A14 gene	+	1.3	0.0008
11	1439561_at	2010012O05Rik	RIKEN cDNA 2010012O05 gene	-	1.2	0.0039
12	1460478_at	2200002J24Rik	RIKEN cDNA 2200002J24 gene	+	1.2	0.0049
13	1437145_s_at	2310002J15Rik	RIKEN cDNA 2310002J15 gene	+	1.3	0.0095
14	1429844_at	2310043J07Rik	RIKEN cDNA 2310043J07 gene	+	1.2	0.0075
15	1427922_at	2310061C15Rik	RIKEN cDNA 2310061C15 gene	+	1.2	0.0062
16	1432650_at	2510019K15Rik	RIKEN cDNA 2510019K15 gene	+	1.2	0.0086
17	1451078_at	2510039O18Rik	RIKEN cDNA 2510039O18 gene	-	1.2	0.0026
18	1431679_at	2510042H12Rik	RIKEN cDNA 2510042H12 gene	+	1.4	0.0046
19	1430876_at	2610312I10Rik	RIKEN cDNA 2610312I10 gene	+	1.9	0.0039
20	1424984_at	2700078E11Rik	RIKEN cDNA 2700078E11 gene	-	1.3	0.0045
21	1430178_at	2810408A11Rik	RIKEN cDNA 2810408A11 gene	+	1.4	0.0023
22	1433387_at	2900022M07Rik	RIKEN cDNA 2900022M07 gene	+	1.4	0.0011
23	1432861_at	2900046F13Rik	RIKEN cDNA 2900046F13 gene	+	1.3	0.0033
24	1432995_at	2900057E15Rik	RIKEN cDNA 2900057E15 gene	+	1.3	0.0099
25	1432797_at	2900060N12Rik	RIKEN cDNA 2900060N12 gene	+	1.3	0.0036
26	1458869_at	2900076A13Rik	RIKEN cDNA 2900076A13 gene	+	1.2	0.0057
27	1430162_at	3830417A13Rik	RIKEN cDNA 3830417A13 gene	-	1.2	0.0077
28	1454439_at	4833419G08Rik	RIKEN cDNA 4833419G08 gene	+	1.2	0.0055
29	1419636_at	4833420G17Rik	RIKEN cDNA 4833420G17 gene	-	1.2	0.0063
30	1419635_at	4833420G17Rik	RIKEN cDNA 4833420G17 gene	-	1.3	0.0072
31	1459879_at	4921513D23Rik	RIKEN cDNA 4921513D23 gene	+	1.2	0.0056
32	1430732_at	4921525D07Rik	RIKEN cDNA 4921525D07 gene	+	1.3	0.0096
33	1432123_at	4930455H04Rik	RIKEN cDNA 4930455H04 gene	-	1.2	0.0033
34	1453549_at	4930500G05Rik	RIKEN cDNA 4930500G05 gene	+	1.3	0.0042
35	1439133_at	4930524O07Rik	RIKEN cDNA 4930524O07 gene	+	1.4	0.0014
36	1432364_at	4930556N13Rik	RIKEN cDNA 4930556N13 gene	+	1.2	0.0061
37	1418870_at	4930579J09Rik	RIKEN cDNA 4930579J09 gene	-	1.4	0.0032
38	1433056_at	4931407J08Rik	RIKEN cDNA 4931407J08 gene	+	1.2	0.0097
39	1432882_at	4932431P20Rik	RIKEN cDNA 4932431P20 gene	+	1.5	0.0032
40	1453652_at	4933400F21Rik	RIKEN cDNA 4933400F21 gene	+	1.3	0.0039
41	1454539_at	4933417G07Rik	RIKEN cDNA 4933417G07 gene	+	1.3	0.0002
42	1453894_at	4933434C23Rik	RIKEN cDNA 4933434C23 gene	+	1.2	0.0037
43	1452696_a_at	4933439C10Rik	RIKEN cDNA 4933439C10 gene	-	1.2	0.0080
44	1431521_at	5033428B15Rik	RIKEN cDNA 5033428B15 gene	-	1.3	0.0025
45	1428220_at	5730419I09Rik	RIKEN cDNA 5730419I09 gene	+	1.2	0.0079
46	1432696_at	5830431M20Rik	RIKEN cDNA 5830431M20 gene	+	1.2	0.0085
47	1432625_at	5830487K18Rik	RIKEN cDNA 5830487K18 gene	+	1.4	0.0016
48	1440849_at	6330417G04Rik	RIKEN cDNA 6330417G04 gene	+	1.2	0.0066
49	1441725_at	6530402F18Rik	RIKEN cDNA 6530402F18 gene	+	1.3	0.0013
50	1429731_at	6530403G13Rik	RIKEN cDNA 6530403G13 gene	-	1.2	0.0091
51	1423071_x_at	6720475J19Rik	RIKEN cDNA 6720475J19 gene	+	1.3	0.0009
52	1429620_at	8430406I07Rik	RIKEN cDNA 8430406I07 gene	+	1.3	0.0080
53	1430438_at	8430439j12rik	RIKEN cDNA 8430439J12 gene	+	1.3	0.0034
54	1453638_at	9030420J04Rik	RIKEN cDNA 9030420J04 gene	+	1.2	0.0055
55	1430103_at	9030607L20Rik	RIKEN cDNA 9030607L20 gene	+	1.2	0.0009
56	1454361_at	9230106L01Rik	RIKEN cDNA 9230106L01 gene	+	1.2	0.0057
57	1457671_at	9330120H11Rik	RIKEN cDNA 9330120H11 gene	+	1.2	0.0071
58	1454588_at	9430006E15Rik	RIKEN cDNA 9430006E15 gene	+	1.4	0.0089
59	1457161_at	9530029O12Rik	RIKEN cDNA 9530029O12 gene	+	1.3	0.0012
60	1433289_at	9530078B04Rik	RIKEN cDNA 9530078B04 gene	+	1.3	0.0008
61	1440884_s_at	A530047J11Rik	RIKEN cDNA A530047J11 gene	+	1.3	0.0046

#	ID	SYMBOL	GENENAME	EFFECT	FC	P-Value
62	1440413_at	A830006F12Rik	RIKEN cDNA A830006F12 gene	+	1.4	0.0091
63	1445721_at	A830021M18	hypothetical protein A830021M18	+	1.3	0.0036
64	1442844_at	A830052D11Rik	RIKEN cDNA A830052D11 gene	+	1.2	0.0033
65	1419797_at	AA672641	expressed sequence AA672641	+	1.2	0.0093
66	1430394_a_at	Abcb9	ATP-binding cassette, sub-family B (MDR/TAP), member 9	-	1.3	0.0039
67	1421212_at	Abcc6	ATP-binding cassette, sub-family C (CFTR/MRP), member 6	-	1.3	0.0036
68	1450141_at	Abcg3	ATP-binding cassette, sub-family G (WHITE), member 3	+	1.3	0.0007
69	1447548_at	Abhd5	abhydrolase domain containing 5	-	1.3	0.0027
70	1422635_at	Ache	acetylcholinesterase	-	1.3	0.0004
71	1418677_at	Actn3	actinin alpha 3	+	1.2	0.0036
72	1419173_at	Acy1	aminoacylase 1	-	1.3	0.0040
73	1450801_at	Adam21	a disintegrin and metallopeptidase domain 21	+	1.2	0.0075
74	1424798_a_at	Adam5	a disintegrin and metallopeptidase domain 5	+	1.2	0.0069
75	1427139_at	Adamts10	a disintegrin-like and metallopeptidase (reprolysin type) with thrombospondin type 1 motif, 10	-	1.3	0.0025
76	1446666_at	Adamts12	a disintegrin-like and metallopeptidase (reprolysin type) with thrombospondin type 1 motif, 12	-	1.2	0.0096
77	1455965_at	Adamts4	a disintegrin-like and metallopeptidase (reprolysin type) with thrombospondin type 1 motif, 4	-	1.2	0.0063
78	1420953_at	Add1	adducin 1 (alpha)	-	1.2	0.0061
79	1420954_a_at	Add1	adducin 1 (alpha)	-	1.3	0.0064
80	1416225_at	Adh1	alcohol dehydrogenase 1 (class I)	-	1.4	0.0006
81	1446675_at	Adk	adenosine kinase	+	1.3	0.0027
82	1443847_x_at	Aff2	AF4/FMR2 family, member 2	+	1.2	0.0047
83	1422116_at	Aff2	AF4/FMR2 family, member 2	-	1.2	0.0085
84	1431722_a_at	Afmid	arylformamidase	+	1.3	0.0009
85	1420428_at	Ager	advanced glycosylation end product-specific receptor	+	1.2	0.0047
86	1421024_at	Agpat1	1-acylglycerol-3-phosphate O-acyltransferase 1 (lysophosphatidic acid acyltransferase, alpha)	-	1.3	0.0033
87	1445647_at	AI447881	expressed sequence AI447881	+	1.2	0.0051
88	1438270_at	AI846148	expressed sequence AI846148	-	1.3	0.0045
89	1443565_at	AI849538	expressed sequence AI849538	+	1.2	0.0097
90	1418279_a_at	Akap1	A kinase (PRKA) anchor protein 1	-	1.2	0.0092
91	1452684_at	Akt1s1	AKT1 substrate 1 (proline-rich)	-	1.2	0.0056
92	1425376_at	Alox8	arachidonate 8-lipoxygenase	-	1.3	0.0024
93	1449417_at	Ambn	ameloblastin	-	1.2	0.0066
94	1431121_at	Amotl1	angiomotin-like 1	-	1.2	0.0043
95	1453307_a_at	Anapc5	anaphase-promoting complex subunit 5	-	1.4	0.0003
96	1450085_at	Angptl2	angiopoietin-like 2	-	1.2	0.0043
97	1437895_at	Ano8	anoctamin 8	-	1.2	0.0047
98	1429246_a_at	Anxa6	annexin A6	-	1.3	0.0083
99	1415818_at	Anxa6	annexin A6	-	1.3	0.0009
100	1452490_a_at	Ap2a2	adaptor protein complex AP-2, alpha 2 subunit	-	1.4	0.0007
101	1418383_at	Apcdd1	adenomatosis polyposis coli down-regulated 1	-	1.3	0.0081
102	1416134_at	Aplp1	amyloid beta (A4) precursor-like protein 1	-	1.5	0.0034
103	1421889_a_at	Aplp2	amyloid beta (A4) precursor-like protein 2	-	1.2	0.0015
104	1417561_at	Apoc1	apolipoprotein C-I	-	1.3	0.0058
105	1446580_at	Apool	apolipoprotein O-like	+	1.2	0.0061
106	1419833_s_at	Arap3	ArfGAP with RhoGAP domain, ankyrin repeat and PH domain 3	-	1.2	0.0088
107	1423743_at	Arcn1	archain 1	-	1.3	0.0003
108	1438661_a_at	Arf2	ADP-ribosylation factor 2	-	1.4	0.0019
109	1457219_at	Arhgef18	rho/rac guanine nucleotide exchange factor (GEF) 18	-	1.4	0.0032
110	1429859_a_at	Arl2bp	ADP-ribosylation factor-like 2 binding protein	-	1.2	0.0083
111	1451131_at	Arl6ip1	ADP-ribosylation factor-like 6 interacting protein 1	-	1.2	0.0092
112	1429816_at	Armc3	armadillo repeat containing 3	-	1.2	0.0084
113	1427002_s_at	Arsg	arylsulfatase G	-	1.3	0.0044
114	1427759_a_at	Art5	ADP-ribosyltransferase 5	+	1.3	0.0030
115	1424225_at	Asb8	ankyrin repeat and SOCS box-containing 8	-	1.3	0.0062
116	1460703_at	Ascc1	activating signal cointegrator 1 complex subunit 1	-	1.3	0.0059
117	1418292_at	Asna1	arsA arsenite transporter, ATP-binding, homolog 1 (bacterial)	-	1.4	0.0033
118	1420036_at	Ate1	arginyltransferase 1	+	1.3	0.0026
119	1416794_at	Atl2	atlastin GTPase 2	-	1.3	0.0017
120	1427481_a_at	Atp1a3	ATPase, Na+/K+ transporting, alpha 3 polypeptide	-	1.3	0.0088
121	1459924_at	Atp6v0a1	ATPase, H+ transporting, lysosomal V0 subunit A1	+	1.3	0.0051
122	1416769_s_at	Atp6v0b	ATPase, H+ transporting, lysosomal V0 subunit B	-	1.4	0.0077
123	1444355_at	Atp8a1	ATPase, aminophospholipid transporter (APLT), class I, type 8A, member 1	+	1.3	0.0046
124	1421166_at	Atrn	attractin	+	1.2	0.0071
125	1425656_a_at	Baiap2	brain-specific angiogenesis inhibitor 1-associated protein 2	-	1.3	0.0008
126	1440645_at	BB114814	expressed sequence BB114814	+	1.3	0.0073
127	1427513_at	BC024137	cDNA sequence BC024137	+	1.3	0.0019
128	1437122_at	Bcl2	B-cell leukemia/lymphoma 2	+	1.2	0.0077
129	1456006_at	Bcl2l11	BCL2-like 11 (apoptosis facilitator)	+	1.4	0.0049
130	1425532_a_at	Bin1	bridging integrator 1	-	1.2	0.0093
131	1451870_a_at	Brd4	bromodomain containing 4	-	1.3	0.0013

#	ID	SYMBOL	GENENAME	EFFECT	FC	P-Value
132	1456616_a_at	Bsg	basigin	-	1.4	0.0010
133	1444666_at	Bxdc1	brix domain containing 1	+	1.5	0.0000
134	1451085_at	C030006K11Rik	RIKEN cDNA C030006K11 gene	-	1.3	0.0095
135	1433932_x_at	C030046I01Rik	RIKEN cDNA C030046I01 gene	-	1.2	0.0039
136	1433931_at	C030046I01Rik	RIKEN cDNA C030046I01 gene	-	1.3	0.0043
137	1422772_at	C1galt1	core 1 synthase, glycoprotein-N-acetylgalactosamine 3-beta-galactosyltransferase, 1	+	1.3	0.0017
138	1449401_at	C1qc	complement component 1, q subcomponent, C chain	-	1.2	0.0070
139	1449308_at	C6	complement component 6	-	1.2	0.0084
140	1419969_at	C77370	expressed sequence C77370	+	1.3	0.0047
141	1442540_at	C77609	expressed sequence C77609	+	1.3	0.0065
142	1441401_at	C79329	expressed sequence C79329	+	1.6	0.0003
143	1421255_a_at	Cabp1	calcium binding protein 1	-	1.3	0.0045
144	1425963_at	Cabp7	calcium binding protein 7	-	1.3	0.0065
145	1425812_a_at	Cacna1b	calcium channel, voltage-dependent, N type, alpha 1B subunit	-	1.4	0.0043
146	1421297_a_at	Cacna1c	calcium channel, voltage-dependent, L type, alpha 1C subunit	-	1.2	0.0083
147	1428051_a_at	Cacna1d	calcium channel, voltage-dependent, L type, alpha 1D subunit	-	1.2	0.0035
148	1450520_at	Cacng3	calcium channel, voltage-dependent, gamma subunit 3	-	1.3	0.0014
149	1453455_at	Camta1	calmodulin binding transcription activator 1	+	1.2	0.0085
150	1417462_at	Cap1	CAP, adenylate cyclase-associated protein 1 (yeast)	-	1.2	0.0029
151	1456848_at	Ccdc123	coiled-coil domain containing 123	-	1.2	0.0077
152	1457628_at	Ccdc53	coiled-coil domain containing 53	+	1.4	0.0071
153	1430670_at	Ccdc91	coiled-coil domain containing 91	+	1.3	0.0047
154	1418459_at	Ccdc91	coiled-coil domain containing 91	-	1.2	0.0034
155	1444323_at	Ccnd3	cyclin D3	+	1.2	0.0091
156	1415907_at	Ccnd3	cyclin D3	-	1.2	0.0060
157	1433741_at	Cd38	CD38 antigen	-	1.2	0.0085
158	1443976_at	Cdk5rap2	CDK5 regulatory subunit associated protein 2	-	1.3	0.0031
159	1419497_at	Cdkn1b	cyclin-dependent kinase inhibitor 1B	-	1.4	0.0003
160	1454891_at	Cds2	CDP-diacylglycerol synthase (phosphatidate cytidylyltransferase) 2	-	1.2	0.0087
161	1434533_x_at	Ceacam11	carcinoembryonic antigen-related cell adhesion molecule 11	-	1.2	0.0063
162	1418982_at	Cebpa	CCAAT/enhancer binding protein (C/EBP), alpha	-	1.2	0.0088
163	1427844_a_at	Cebpb	CCAAT/enhancer binding protein (C/EBP), beta	-	1.2	0.0039
164	1452242_at	Cep55	centrosomal protein 55	-	1.2	0.0072
165	1448052_at	Cgnl1	cingulin-like 1	-	1.2	0.0083
166	1451295_a_at	Chd4	chromodomain helicase DNA binding protein 4	-	1.2	0.0096
167	1425450_at	Chi3l4	chitinase 3-like 4	+	1.4	0.0044
168	1453844_at	Chit1	chitinase 1 (chitotriosidase)	+	1.3	0.0082
169	1456722_at	Chrdl1	chordin-like 1	+	1.2	0.0057
170	1426866_at	Chst14	carbohydrate (N-acetylgalactosamine 4-0) sulfotransferase 14	+	1.2	0.0030
171	1448140_at	Ciapin1	cytokine induced apoptosis inhibitor 1	-	1.2	0.0037
172	1450014_at	Cldn1	claudin 1	+	1.2	0.0036
173	1416003_at	Cldn11	claudin 11	-	1.3	0.0088
174	1429574_at	Clic3	chloride intracellular channel 3	-	1.3	0.0006
175	1431098_at	Clip1	CAP-GLY domain containing linker protein 1	-	1.2	0.0089
176	1425321_a_at	Clmn	calmin	-	1.2	0.0039
177	1416883_at	Clptm1	cleft lip and palate associated transmembrane protein 1	-	1.3	0.0012
178	1430519_a_at	Cnot7	CCR4-NOT transcription complex, subunit 7	-	1.4	0.0006
179	1449296_a_at	Cnp	2',3'-cyclic nucleotide 3' phosphodiesterase	-	1.3	0.0033
180	1435166_at	Cntn2	contactin 2	-	1.3	0.0034
181	1420384_at	Col4a3bp	collagen, type IV, alpha 3 (Goodpasture antigen) binding protein	+	1.2	0.0081
182	1417752_at	Coro1c	coronin, actin binding protein 1C	-	1.2	0.0017
183	1417747_at	Cplx1	complexin 1	-	1.3	0.0015
184	1436383_at	Cplx2	complexin 2	-	1.2	0.0057
185	1460176_at	Crk	v-crk sarcoma virus CT10 oncogene homolog (avian)	+	1.4	0.0005
186	1422577_at	Cs	citrate synthase	-	1.2	0.0059
187	1425810_a_at	Csrp1	cysteine and glycine-rich protein 1	-	1.4	0.0013
188	1416274_at	Ctns	cystinosis, nephropathic	-	1.6	0.0000
189	1422680_at	Ctr9	Ctr9, Paf1/RNA polymerase II complex component, homolog (S. cerevisiae)	-	1.2	0.0014
190	1448732_at	Ctsb	cathepsin B	-	1.4	0.0023
191	1419728_at	Cxcl5	chemokine (C-X-C motif) ligand 5	-	1.3	0.0008
192	1422186_s_at	Cyb5r3	cytochrome b5 reductase 3	-	1.2	0.0065
193	1425329_a_at	Cyb5r3	cytochrome b5 reductase 3	-	1.2	0.0064
194	1422185_a_at	Cyb5r3	cytochrome b5 reductase 3	-	1.3	0.0007
195	1457271_at	Cym	chymosin	+	1.4	0.0021
196	1448997_at	Cyth1	cytohesin 1	-	1.3	0.0024
197	1446958_at	D13Ertd150e	DNA segment, Chr 13, ERATO Doi 150, expressed	+	1.3	0.0044
198	1446564_at	D18Ertd169e	DNA segment, Chr 18, ERATO Doi 169, expressed	+	1.3	0.0081
199	1452343_at	D18Ertd653e	DNA segment, Chr 18, ERATO Doi 653, expressed	-	1.3	0.0057
200	1443458_at	D630033O11Rik	RIKEN cDNA D630033O11 gene	+	1.3	0.0026
201	1442409_at	D9Wsu90e	DNA segment, Chr 9, Wayne State University 90,	+	1.2	0.0097

#	ID	SYMBOL	GENENAME	EFFECT	FC	P-Value
			expressed			
202	1423872_a_at	Dag1	dystroglycan 1	-	1.2	0.0073
203	1423446_at	Dapk3	death-associated protein kinase 3	-	1.2	0.0073
204	1455079_at	Dcun1d4	DCN1, defective in cullin neddylation 1, domain containing 4 (S. cerevisiae)	+	1.2	0.0079
205	1423495_at	Decr2	2-4-dienoyl-Coenzyme A reductase 2, peroxisomal	-	1.3	0.0004
206	1422677_at	Dgat2	diacylglycerol O-acyltransferase 2	-	1.3	0.0002
207	1416821_at	Dgcr14	DiGeorge syndrome critical region gene 14	-	1.3	0.0029
208	1438765_at	Dhx33	DEAH (Asp-Glu-Ala-His) box polypeptide 33	-	1.3	0.0008
209	1431258_at	Dido1	death inducer-obliterator 1	+	1.4	0.0034
210	1418937_at	Dio2	deiodinase, iodothyronine, type II	+	1.2	0.0053
211	1426081_a_at	Dio2	deiodinase, iodothyronine, type II	+	1.2	0.0049
212	1420335_at	Dmc1	DMC1 dosage suppressor of mck1 homolog, meiosis-specific homologous recombination (yeast)	+	1.3	0.0003
213	1420182_x_at	Dmrt3	doublesex and mab-3 related transcription factor 3	-	1.2	0.0091
214	1427252_at	Dmrtb1	DMRT-like family B with proline-rich C-terminal, 1	-	1.2	0.0096
215	1436296_x_at	Dnaic2	dynein, axonemal, intermediate chain 2	-	1.3	0.0077
216	1420629_a_at	Dnaja3	DnaJ (Hsp40) homolog, subfamily A, member 3	-	1.2	0.0007
217	1418592_at	Dnaja4	DnaJ (Hsp40) homolog, subfamily A, member 4	-	1.2	0.0055
218	1420165_s_at	Dnajc17	DnaJ (Hsp40) homolog, subfamily C, member 17	-	1.3	0.0053
219	1431215_at	Dnajc6	DnaJ (Hsp40) homolog, subfamily C, member 6	-	1.3	0.0099
220	1427754_a_at	Dnm1	dynamin 1	-	1.3	0.0058
221	1451676_at	Drap1	Dr1 associated protein 1 (negative cofactor 2 alpha)	-	1.2	0.0080
222	1422830_s_at	Drd4	dopamine receptor 4	-	1.4	0.0011
223	1417207_at	Dvl2	dishevelled 2, dsh homolog (Drosophila)	-	1.2	0.0088
224	1441924_x_at	Edn3	endothelin 3	+	2.1	0.0012
225	1416964_at	Eefsec	eukaryotic elongation factor, selenocysteine-tRNA-specific	-	1.2	0.0091
226	1448507_at	Efhd1	EF hand domain containing 1	-	1.2	0.0053
227	1444606_at	Efna2	ephrin A2	-	1.2	0.0081
228	1432647_at	Egfr	epidermal growth factor receptor	+	1.3	0.0065
229	1435054_at	Eme1	essential meiotic endonuclease 1 homolog 1 (S. pombe)	+	1.2	0.0090
230	1426541_a_at	Endod1	endonuclease domain containing 1	-	1.3	0.0095
231	1425353_at	Enpp3	ectonucleotide pyrophosphatase/phosphodiesterase 3	+	1.2	0.0026
232	1425199_a_at	Epb4.1l5	erythrocyte protein band 4.1-like 5	-	1.3	0.0004
233	1421815_at	Epdr1	ependymin related protein 1 (zebrafish)	-	1.3	0.0070
234	1422438_at	Ephx1	epoxide hydrolase 1, microsomal	-	1.3	0.0057
235	1432235_at	Epsti1	epithelial stromal interaction 1 (breast)	+	1.3	0.0076
236	1420602_a_at	Esx1	extraembryonic, spermatogenesis, homeobox 1	-	1.2	0.0034
237	1433515_s_at	Etnk1	ethanolamine kinase 1	-	1.4	0.0036
238	1423587_a_at	Exosc10	exosome component 10	-	1.2	0.0016
239	1426960_a_at	Fa2h	fatty acid 2-hydroxylase	-	1.3	0.0021
240	1450682_at	Fabp6	fatty acid binding protein 6, ileal (gastrotropin)	-	1.3	0.0016
241	1441123_at	Fam120c	family with sequence similarity 120, member C	+	1.2	0.0058
242	1421595_at	Fam184b	family with sequence similarity 184, member B	+	1.2	0.0026
243	1421070_at	Fam48a	family with sequence similarity 48, member A	-	1.3	0.0087
244	1456163_at	Fam72a	family with sequence similarity 72, member A	+	1.2	0.0092
245	1433657_at	Fam78a	family with sequence similarity 78, member A	+	1.2	0.0067
246	1418856_a_at	Fanca	Fanconi anemia, complementation group A	+	1.2	0.0085
247	1446226_at	Fancb	Fanconi anemia, complementation group B	-	1.3	0.0063
248	1424197_s_at	Fance	Fanconi anemia, complementation group E	-	1.2	0.0059
249	1460635_at	Fastk	Fas-activated serine/threonine kinase	-	1.2	0.0072
250	1460208_at	Fbn1	fibrillin 1	-	1.2	0.0034
251	1448420_a_at	Fbxl12	F-box and leucine-rich repeat protein 12	-	1.2	0.0099
252	1451543_at	Fbxo21	F-box protein 21	-	1.3	0.0018
253	1421543_at	Fbxo4	F-box protein 4	+	1.2	0.0062
254	1450869_at	Fgf1	fibroblast growth factor 1	-	1.2	0.0039
255	1418498_at	Fgf13	fibroblast growth factor 13	-	1.4	0.0091
256	1460296_a_at	Fgf22	fibroblast growth factor 22	+	1.3	0.0049
257	1425911_a_at	Fgfr1	fibroblast growth factor receptor 1	-	1.3	0.0028
258	1427776_a_at	Fgfr4	fibroblast growth factor receptor 4	-	1.3	0.0032
259	1416113_at	Fkbp8	FK506 binding protein 8	-	1.4	0.0014
260	1437536_at	Fkrp	fukutin related protein	-	1.2	0.0087
261	1426677_at	Flna	filamin, alpha	-	1.1	0.0093
262	1417544_a_at	Flot2	flotillin 2	-	1.2	0.0089
263	1451752_at	Foxk1	forkhead box K1	+	1.3	0.0056
264	1420765_a_at	Foxp3	forkhead box P3	+	1.4	0.0019
265	1427617_at	Fut10	fucosyltransferase 10	+	1.4	0.0002
266	1419451_at	Fzr1	fizzy/cell division cycle 20 related 1 (Drosophila)	-	1.2	0.0047
267	1446657_at	Galnt6	UDP-N-acetyl-alpha-D-galactosamine:polypeptide N-acetylgalactosaminyltransferase 6	-	1.2	0.0040
268	1445685_at	Gas7	growth arrest specific 7	+	1.3	0.0018
269	1451197_s_at	Gatad2a	GATA zinc finger domain containing 2A	-	1.2	0.0031
270	1437756_at	Gimap9	GTPase, IMAP family member 9	+	1.3	0.0018
271	1454082_a_at	Giyd2	GIY-YIG domain containing 2	-	1.2	0.0096
272	1448767_s_at	Gjb1	gap junction protein, beta 1	-	1.4	0.0032
273	1422179_at	Gjb4	gap junction protein, beta 4	-	1.2	0.0070
274	1436210_at	Gk5	glycerol kinase 5 (putative)	+	1.2	0.0042
275	1428421_a_at	Glod4	glyoxalase domain containing 4	-	1.2	0.0035

#	ID	SYMBOL	GENENAME	EFFECT	FC	P-Value
276	1440361_at	Gm12371	predicted gene 12371	+	1.4	0.0039
277	1457933_at	Gm1964	predicted gene 1964	+	1.2	0.0022
278	1416188_at	Gm2a	GM2 ganglioside activator protein	-	1.4	0.0022
279	1446741_at	Gm5463	predicted gene 5463	+	1.2	0.0065
280	1437004_at	Gm6021	predicted gene 6021	+	1.2	0.0093
281	1443268_at	Gm765	predicted gene 765	+	1.2	0.0068
282	1443995_at	Gm9	predicted gene 9	+	1.2	0.0039
283	1450097_s_at	Gna12	guanine nucleotide binding protein, alpha 12	-	1.3	0.0015
284	1419449_a_at	Gnai2	guanine nucleotide binding protein (G protein), alpha inhibiting 2	-	1.3	0.0044
285	1460460_a_at	Gorasp2	golgi reassembly stacking protein 2	-	1.4	0.0026
286	1416215_at	Gosr1	golgi SNAP receptor complex member 1	-	1.2	0.0043
287	1430238_at	Got1l1	glutamic-oxaloacetic transaminase 1-like 1	-	1.2	0.0039
288	1417716_at	Got2	glutamate oxaloacetate transaminase 2, mitochondrial	-	1.2	0.0071
289	1460123_at	Gpr1	G protein-coupled receptor 1	+	1.2	0.0031
290	1455828_at	Gprin1	G protein-regulated inducer of neurite outgrowth 1	+	1.4	0.0088
291	1424137_at	Gprin1	G protein-regulated inducer of neurite outgrowth 1	-	1.3	0.0029
292	1430834_at	Gprin3	GPRIN family member 3	+	1.2	0.0091
293	1417796_at	Gps2	G protein pathway suppressor 2	-	1.2	0.0022
294	1418492_at	Grem2	gremlin 2 homolog, cysteine knot superfamily (Xenopus laevis)	+	1.2	0.0073
295	1418784_at	Grik5	glutamate receptor, ionotropic, kainate 5 (gamma 2)	-	1.3	0.0061
296	1450202_at	Grin1	glutamate receptor, ionotropic, NMDA1 (zeta 1)	-	1.3	0.0032
297	1453709_at	Grit	Rho GTPase-activating protein	+	1.2	0.0036
298	1419072_at	Gstm7	glutathione S-transferase, mu 7	-	1.2	0.0094
299	1443213_at	Gtdc1	glycosyltransferase-like domain containing 1	+	1.3	0.0068
300	1460279_a_at	Gtf2i	general transcription factor II I	-	1.3	0.0022
301	1420625_at	Gtf3c6	general transcription factor IIIC, polypeptide 6, alpha	-	1.3	0.0010
302	1453771_at	Gulp1	GULP, engulfment adaptor PTB domain containing 1	-	1.3	0.0029
303	1452544_x_at	H2-D1	histocompatibility 2, D region locus 1	-	1.4	0.0000
304	1430869_a_at	Habp4	hyaluronic acid binding protein 4	-	1.3	0.0037
305	1447566_at	Hdac4	histone deacetylase 4	-	1.2	0.0024
306	1454713_s_at	Hdc	histidine decarboxylase	-	1.3	0.0012
307	1425983_x_at	Hipk2	homeodomain interacting protein kinase 2	-	1.2	0.0078
308	1416101_a_at	Hist1h1c	histone cluster 1, H1c	-	1.2	0.0042
309	1450608_at	Hist1h1t	histone cluster 1, H1t	-	1.2	0.0060
310	1420901_a_at	Hk1	hexokinase 1	-	1.3	0.0071
311	1416184_s_at	Hmga1	high mobility group AT-hook 1	-	1.2	0.0045
312	1421234_at	Hnf1a	HNF1 homeobox A	+	1.4	0.0013
313	1442816_at	Hs3st3b1	heparan sulfate (glucosamine) 3-O-sulfotransferase 3B1	+	1.2	0.0039
314	1425786_a_at	Hsf4	heat shock transcription factor 4	-	1.2	0.0054
315	1440575_at	Hspa4	heat shock protein 4	+	1.3	0.0015
316	1427216_at	Ifnz	interferon zeta	+	1.2	0.0086
317	1421991_a_at	Igfbp4	insulin-like growth factor binding protein 4	-	1.2	0.0043
318	1423756_s_at	Igfbp4	insulin-like growth factor binding protein 4	-	1.2	0.0082
319	1423757_x_at	Igfbp4	insulin-like growth factor binding protein 4	-	1.2	0.0066
320	1421992_a_at	Igfbp4	insulin-like growth factor binding protein 4	-	1.2	0.0060
321	1425625_at	Il13ra1	interleukin 13 receptor, alpha 1	+	1.2	0.0023
322	1420904_at	Il17ra	interleukin 17 receptor A	+	1.2	0.0018
323	1419671_a_at	Il17rc	interleukin 17 receptor C	-	1.3	0.0040
324	1421473_at	Il1a	interleukin 1 alpha	+	1.2	0.0046
325	1423017_a_at	Il1rn	interleukin 1 receptor antagonist	+	1.3	0.0086
326	1429533_at	Immt	inner membrane protein, mitochondrial	-	1.3	0.0055
327	1418657_at	Ino80b	INO80 complex subunit B	-	1.4	0.0054
328	1438446_x_at	Inpp5k	inositol polyphosphate 5-phosphatase K	-	1.1	0.0079
329	1448668_a_at	Irak1	interleukin-1 receptor-associated kinase 1	-	1.2	0.0053
330	1423238_at	Itgb1bp2	integrin beta 1 binding protein 2	+	1.2	0.0064
331	1420665_at	Itgb3bp	integrin beta 3 binding protein (beta3-endonexin)	+	1.2	0.0071
332	1427387_a_at	Itgb4	integrin beta 4	-	1.2	0.0024
333	1430597_at	Jakmip1	janus kinase and microtubule interacting protein 1	-	1.3	0.0086
334	1419288_at	Jam2	junction adhesion molecule 2	-	1.3	0.0095
335	1449046_a_at	Josd2	Josephin domain containing 2	-	1.2	0.0079
336	1426873_s_at	Jup	junction plakoglobin	-	1.3	0.0081
337	1425885_a_at	Kcnab2	potassium voltage-gated channel, shaker-related subfamily, beta member 2	-	1.3	0.0006
338	1425870_a_at	Kcnip2	Kv channel-interacting protein 2	-	1.6	0.0006
339	1450185_a_at	Kcnj15	potassium inwardly-rectifying channel, subfamily J, member 15	+	1.3	0.0085
340	1455896_a_at	Kcnk1	potassium channel, subfamily K, member 1	-	1.2	0.0044
341	1450747_at	Keap1	kelch-like ECH-associated protein 1	-	1.2	0.0015
342	1449057_at	Kel	Kell blood group	+	1.2	0.0068
343	1450108_at	Kif1a	kinesin family member 1A	-	1.3	0.0019
344	1450692_at	Kif4	kinesin family member 4	+	1.2	0.0072
345	1448541_at	Klc1	kinesin light chain 1	-	1.5	0.0048
346	1451739_at	Klf5	Kruppel-like factor 5	+	1.3	0.0096
347	1436952_at	Klf9	Kruppel-like factor 9	-	1.4	0.0057
348	1448164_at	Klhdc3	kelch domain containing 3	-	1.2	0.0078
349	1420770_at	Klk1b24	kallikrein 1-related peptidase b24	+	1.4	0.0035
350	1425888_at	Klra17	killer cell lectin-like receptor, subfamily A, member 17	+	1.3	0.0019

#	ID	SYMBOL	GENENAME	EFFECT	FC	P-Value
351	1426136_x_at	Klra21	killer cell lectin-like receptor subfamily A, member 21	+	1.4	0.0009
352	1418213_at	Krt23	keratin 23	-	1.2	0.0029
353	1450540_x_at	Krtap5-1	keratin associated protein 5-1	+	1.3	0.0014
354	1450114_at	Ksr1	kinase suppressor of ras 1	-	1.3	0.0085
355	1427009_at	Lama5	laminin, alpha 5	-	1.2	0.0059
356	1416343_a_at	Lamp2	lysosomal-associated membrane protein 2	-	1.4	0.0098
357	1423955_a_at	Lass2	LAG1 homolog, ceramide synthase 2	-	1.2	0.0055
358	1419317_x_at	Lce3c	late cornified envelope 3C	+	1.2	0.0075
359	1435152_at	Leng8	leukocyte receptor cluster (LRC) member 8	-	1.3	0.0053
360	1421217_a_at	Lgals9	lectin, galactose binding, soluble 9	-	1.4	0.0001
361	1440968_at	Lgtn	ligatin	-	1.2	0.0036
362	1418231_at	Lims1	LIM and senescent cell antigen-like domains 1	-	1.3	0.0028
363	1449262_s_at	Lin7c	lin-7 homolog C (C. elegans)	-	1.2	0.0087
364	1443984_at	Lin9	lin-9 homolog (C. elegans)	+	1.2	0.0076
365	1427998_at	Lsm12	LSM12 homolog (S. cerevisiae)	-	1.2	0.0076
366	1453304_s_at	Ly6e	lymphocyte antigen 6 complex, locus E	-	1.3	0.0010
367	1431607_at	Lypla1	lysophospholipase 1	+	1.3	0.0025
368	1443058_at	Macrod2	MACRO domain containing 2	-	1.2	0.0061
369	1460219_at	Mag	myelin-associated glycoprotein	-	1.3	0.0043
370	1449901_a_at	Map3k6	mitogen-activated protein kinase kinase kinase 6	+	1.2	0.0073
371	1425679_a_at	Mapk8ip1	mitogen-activated protein kinase 8 interacting protein 1	-	1.2	0.0081
372	1416437_a_at	Mapk8ip3	mitogen-activated protein kinase 8 interacting protein 3	-	1.3	0.0032
373	1427079_at	Mapre3	microtubule-associated protein, RP/EB family, member 3	-	1.3	0.0024
374	1417885_at	Mapt	microtubule-associated protein tau	-	1.3	0.0013
375	1455346_at	Masp1	mannan-binding lectin serine peptidase 1	-	1.4	0.0003
376	1454591_at	Mast4	microtubule associated serine/threonine kinase family member 4	+	1.3	0.0029
377	1451176_at	Mavs	mitochondrial antiviral signaling protein	-	1.3	0.0006
378	1449490_at	Mbd4	methyl-CpG binding domain protein 4	+	1.3	0.0006
379	1451961_a_at	Mbp	myelin basic protein	-	1.5	0.0013
380	1416357_a_at	Mcam	melanoma cell adhesion molecule	-	1.2	0.0023
381	1448374_at	Med28	mediator of RNA polymerase II transcription, subunit 28 homolog (yeast)	-	1.2	0.0026
382	1426837_at	Metap1	methionyl aminopeptidase 1	-	1.3	0.0034
383	1416358_at	Mfsd10	major facilitator superfamily domain containing 10	-	1.2	0.0085
384	1431285_at	Mgrn1	mahogunin, ring finger 1	-	1.3	0.0018
385	1452592_at	Mgst2	microsomal glutathione S-transferase 2	+	1.5	0.0004
386	1451685_at	Mllt6	myeloid/lymphoid or mixed-lineage leukemia (trithorax homolog, Drosophila); translocated to, 6	-	1.2	0.0047
387	1421010_at	Mobp	myelin-associated oligodendrocytic basic protein	-	1.2	0.0088
388	1450088_a_at	Mobp	myelin-associated oligodendrocytic basic protein	-	1.3	0.0054
389	1448768_at	Mog	myelin oligodendrocyte glycoprotein	-	1.3	0.0084
390	1440915_at	Mphosph9	M-phase phosphoprotein 9	-	1.2	0.0055
391	1430771_a_at	Msh5	mutS homolog 5 (E. coli)	+	1.3	0.0090
392	1429894_a_at	Mtap7	microtubule-associated protein 7	-	1.2	0.0067
393	1421835_at	Mtap7	microtubule-associated protein 7	-	1.3	0.0023
394	1421879_at	Mtmr1	myotubularin related protein 1	-	1.2	0.0079
395	1419399_at	Mttp	microsomal triglyceride transfer protein	+	1.2	0.0007
396	1436501_at	Mtus1	mitochondrial tumor suppressor 1	-	1.3	0.0088
397	1427938_at	Mycbp	c-myc binding protein	-	1.2	0.0047
398	1442858_at	Mycbp2	MYC binding protein 2	+	1.2	0.0080
399	1427520_a_at	Myh1	myosin, heavy polypeptide 1, skeletal muscle, adult	+	1.2	0.0083
400	1428509_at	Myo1e	myosin IE	-	1.4	0.0049
401	1418420_at	Myod1	myogenic differentiation 1	+	1.2	0.0048
402	1446189_at	Myst4	MYST histone acetyltransferase monocytic leukemia 4	+	1.5	0.0023
403	1435269_at	N6amt2	N-6 adenine-specific DNA methyltransferase 2 (putative)	-	1.2	0.0043
404	1454378_at	NA	NA	+	1.8	0.0078
405	1441066_at	NA	NA	+	1.7	0.0028
406	1445617_at	NA	NA	+	1.6	0.0000
407	1449727_x_at	NA	NA	+	1.5	0.0029
408	1446567_at	NA	NA	+	1.5	0.0032
409	1430477_s_at	NA	NA	+	1.5	0.0005
410	1446880_at	NA	NA	+	1.4	0.0017
411	1419915_at	NA	NA	+	1.4	0.0050
412	1417711_at	NA	NA	+	1.4	0.0093
413	1442857_at	NA	NA	+	1.4	0.0052
414	1447226_at	NA	NA	+	1.4	0.0097
415	1449790_at	NA	NA	+	1.4	0.0029
416	1442880_at	NA	NA	+	1.4	0.0069
417	1459297_at	NA	NA	+	1.4	0.0066
418	1443090_at	NA	NA	+	1.4	0.0001
419	1432840_at	NA	NA	+	1.3	0.0019
420	1444622_at	NA	NA	+	1.3	0.0044
421	1440606_at	NA	NA	+	1.3	0.0096
422	1458173_at	NA	NA	+	1.3	0.0059
423	1445382_at	NA	NA	+	1.3	0.0074
424	1444286_at	NA	NA	+	1.3	0.0057

#	ID	SYMBOL	GENENAME	EFFECT	FC	P-Value
425	1445508_at	NA	NA	+	1.3	0.0066
426	1433064_at	NA	NA	+	1.3	0.0032
427	1459435_at	NA	NA	+	1.3	0.0044
428	1444841_at	NA	NA	+	1.3	0.0079
429	1460002_at	NA	NA	+	1.3	0.0021
430	1439053_at	NA	NA	+	1.3	0.0030
431	1458127_at	NA	NA	+	1.3	0.0080
432	1434110_x_at	NA	NA	+	1.3	0.0018
433	1458645_at	NA	NA	+	1.3	0.0025
434	1427854_x_at	NA	NA	+	1.3	0.0071
435	1420318_at	NA	NA	+	1.3	0.0087
436	1445834_at	NA	NA	+	1.3	0.0005
437	1458872_at	NA	NA	+	1.3	0.0030
438	1457503_at	NA	NA	+	1.3	0.0094
439	1444912_at	NA	NA	+	1.3	0.0099
440	1442163_at	NA	NA	+	1.3	0.0035
441	1445238_at	NA	NA	+	1.3	0.0060
442	1447092_at	NA	NA	+	1.3	0.0094
443	1457312_at	NA	NA	+	1.3	0.0049
444	1456650_at	NA	NA	+	1.3	0.0073
445	1458138_at	NA	NA	+	1.3	0.0037
446	1443799_at	NA	NA	+	1.3	0.0004
447	1457016_at	NA	NA	+	1.2	0.0087
448	1436259_at	NA	NA	+	1.2	0.0095
449	1445556_at	NA	NA	+	1.2	0.0058
450	1443390_at	NA	NA	+	1.2	0.0024
451	1441332_at	NA	NA	+	1.2	0.0089
452	1441654_at	NA	NA	+	1.2	0.0011
453	1440515_at	NA	NA	+	1.2	0.0059
454	1430590_at	NA	NA	+	1.2	0.0025
455	1460153_at	NA	NA	+	1.2	0.0013
456	1443243_at	NA	NA	+	1.2	0.0033
457	1441472_at	NA	NA	+	1.2	0.0021
458	1440948_at	NA	NA	+	1.2	0.0042
459	1450607_s_at	NA	NA	+	1.2	0.0080
460	1444344_at	NA	NA	+	1.2	0.0071
461	1446894_at	NA	NA	+	1.2	0.0020
462	1439299_at	NA	NA	+	1.2	0.0068
463	1457880_at	NA	NA	+	1.2	0.0085
464	1447430_at	NA	NA	+	1.2	0.0096
465	1444208_at	NA	NA	+	1.2	0.0071
466	1459908_at	NA	NA	+	1.2	0.0082
467	1442184_at	NA	NA	+	1.2	0.0085
468	1458653_at	NA	NA	+	1.2	0.0056
469	1458604_at	NA	NA	+	1.2	0.0090
470	1446875_at	NA	NA	+	1.2	0.0060
471	1442543_at	NA	NA	+	1.2	0.0091
472	1447491_at	NA	NA	+	1.2	0.0034
473	1444750_at	NA	NA	+	1.2	0.0074
474	1444048_at	NA	NA	+	1.2	0.0092
475	1458075_at	NA	NA	+	1.2	0.0086
476	1440266_at	NA	NA	+	1.2	0.0086
477	1441164_at	NA	NA	+	1.2	0.0081
478	1440080_at	NA	NA	+	1.2	0.0091
479	1430788_at	NA	NA	-	1.2	0.0097
480	1426657_s_at	NA	NA	-	1.2	0.0062
481	1451132_at	NA	NA	-	1.2	0.0071
482	1421816_at	NA	NA	-	1.2	0.0085
483	1456861_at	NA	NA	-	1.2	0.0096
484	1450822_at	NA	NA	-	1.2	0.0032
485	1446730_at	NA	NA	-	1.2	0.0094
486	1450882_s_at	NA	NA	-	1.2	0.0079
487	1429154_at	NA	NA	-	1.2	0.0045
488	1415789_a_at	NA	NA	-	1.2	0.0088
489	1440876_at	NA	NA	-	1.2	0.0059
490	1457343_at	NA	NA	-	1.2	0.0045
491	1435150_at	NA	NA	-	1.2	0.0033
492	1445763_at	NA	NA	-	1.2	0.0081
493	1451392_at	NA	NA	-	1.2	0.0020
494	1459660_at	NA	NA	-	1.2	0.0016
495	1450393_a_at	NA	NA	-	1.2	0.0048
496	1440306_at	NA	NA	-	1.2	0.0034
497	1431314_a_at	NA	NA	-	1.2	0.0027
498	1443623_a_at	NA	NA	-	1.3	0.0053
499	1441797_at	NA	NA	-	1.3	0.0078
500	1447479_at	NA	NA	-	1.3	0.0067
501	1442386_at	NA	NA	-	1.3	0.0079
502	1454336_at	NA	NA	-	1.3	0.0040
503	1422068_at	NA	NA	-	1.3	0.0034
504	1457330_at	NA	NA	-	1.3	0.0035
505	1443354_at	NA	NA	-	1.3	0.0008

#	ID	SYMBOL	GENENAME	EFFECT	FC	P-Value
506	1442283_at	NA	NA	-	1.3	0.0041
507	1440512_at	NA	NA	-	1.3	0.0099
508	1457082_at	NA	NA	-	1.3	0.0014
509	1434183_at	NA	NA	-	1.3	0.0029
510	1421787_at	NA	NA	-	1.3	0.0004
511	1435629_at	NA	NA	-	1.3	0.0001
512	1446703_at	NA	NA	-	1.4	0.0053
513	1451522_s_at	NA	NA	-	1.4	0.0040
514	1421895_at	NA	NA	-	1.4	0.0025
515	1446515_at	NA	NA	-	1.4	0.0021
516	1421842_a_at	NA	NA	-	1.4	0.0037
517	1442910_at	NA	NA	-	1.4	0.0023
518	AFFX-r2-Bs-thr-5_s_at	NA	NA	-	1.4	0.0085
519	1456947_at	NA	NA	-	1.4	0.0002
520	1423916_s_at	NA	NA	-	1.4	0.0013
521	AFFX-ThrX-5_at	NA	NA	-	1.4	0.0060
522	1437183_at	NA	NA	-	1.5	0.0020
523	1425174_at	NA	NA	-	1.5	0.0033
524	1441404_at	NA	NA	-	1.8	0.0000
525	1444234_at	Napb	N-ethylmaleimide sensitive fusion protein attachment protein beta	+	1.5	0.0018
526	1424203_at	Ncln	nicalin homolog (zebrafish)	-	1.2	0.0069
527	1423413_at	Ndrg1	N-myc downstream regulated gene 1	-	1.3	0.0041
528	1418881_at	Necab2	N-terminal EF-hand calcium binding protein 2	-	1.2	0.0090
529	1418961_at	Necap2	NECAP endocytosis associated 2	-	1.2	0.0097
530	1450382_at	Nf2	neurofibromatosis 2	-	1.2	0.0044
531	1459909_at	Nfix	nuclear factor I/X	-	1.2	0.0038
532	1423516_a_at	Nid2	nidogen 2	-	1.4	0.0073
533	1420487_at	Nol7	nucleolar protein 7	+	1.2	0.0089
534	1441075_at	Nostrin	nitric oxide synthase trafficker	+	1.2	0.0085
535	1431329_at	Nphp4	nephronophthisis 4 (juvenile) homolog (human)	+	1.3	0.0025
536	1422790_at	Nppc	natriuretic peptide precursor type C	+	1.2	0.0039
537	1427191_at	Npr2	natriuretic peptide receptor 2	-	1.2	0.0022
538	1447211_at	Nrip1	nuclear receptor interacting protein 1	-	1.2	0.0052
539	1455499_at	Nrxn2	neurexin II	-	1.3	0.0092
540	1419433_at	Nthl1	nth (endonuclease III)-like 1 (E.coli)	+	1.2	0.0021
541	1420837_at	Ntrk2	neurotrophic tyrosine kinase, receptor, type 2	-	1.6	0.0003
542	1425070_at	Ntrk3	neurotrophic tyrosine kinase, receptor, type 3	-	1.2	0.0078
543	1416903_at	Nucb1	nucleobindin 1	-	1.3	0.0015
544	1446400_at	Olfr558	olfactory receptor 558	+	1.3	0.0032
545	1422367_at	Olfr70	olfactory receptor 70	-	1.2	0.0075
546	1424990_at	Orai1	ORAI calcium release-activated calcium modulator 1	-	1.2	0.0071
547	1417705_at	Otub1	OTU domain, ubiquitin aldehyde binding 1	-	1.2	0.0088
548	1438985_x_at	Otud5	OTU domain containing 5	+	1.2	0.0036
549	1428953_at	Otud7b	OTU domain containing 7B	-	1.2	0.0034
550	1422034_a_at	Palm	paralemmin	-	1.3	0.0066
551	1421987_at	Papss2	3'-phosphoadenosine 5'-phosphosulfate synthase 2	-	1.2	0.0021
552	1455216_at	Paqr6	progestin and adipoQ receptor family member VI	-	1.2	0.0098
553	1449054_a_at	Pcbp4	poly(rC) binding protein 4	-	1.3	0.0035
554	1422890_at	Pcdh18	protocadherin 18	-	1.3	0.0057
555	1452913_at	Pcp4l1	Purkinje cell protein 4-like 1	-	1.3	0.0031
556	1426184_a_at	Pdcd6ip	programmed cell death 6 interacting protein	-	1.3	0.0064
557	1441967_at	Pddc1	Parkinson disease 7 domain containing 1	-	1.3	0.0028
558	1417603_at	Per2	period homolog 2 (Drosophila)	-	1.3	0.0006
559	1435037_at	Pgap3	post-GPI attachment to proteins 3	-	1.3	0.0038
560	1439527_at	Pgr	progesterone receptor	+	1.2	0.0015
561	1418620_at	Phox2a	paired-like homeobox 2a	+	1.3	0.0027
562	1437637_at	Phtf2	putative homeodomain transcription factor 2	-	1.2	0.0093
563	1421013_at	Pitpnb	phosphatidylinositol transfer protein, beta	-	1.4	0.0035
564	1420307_a_at	Pitpnb	phosphatidylinositol transfer protein, beta	-	1.4	0.0000
565	1435053_s_at	Plekhh1	pleckstrin homology domain containing, family H (with MyTH4 domain) member 1	-	1.4	0.0007
566	1452517_at	Plekhh1	pleckstrin homology domain containing, family H (with MyTH4 domain) member 1	-	1.4	0.0016
567	1444817_at	Plekhh2	pleckstrin homology domain containing, family H (with MyTH4 domain) member 2	+	1.6	0.0002
568	1448945_at	Pllp	plasma membrane proteolipid	-	1.3	0.0008
569	1425467_a_at	Plp1	proteolipid protein (myelin) 1	-	1.4	0.0008
570	1417963_at	Pltp	phospholipid transfer protein	-	1.5	0.0008
571	1418750_at	Plxnb3	plexin B3	-	1.2	0.0081
572	1419298_at	Pon3	paraoxonase 3	-	1.4	0.0005
573	1448565_at	Ppp1r11	protein phosphatase 1, regulatory (inhibitor) subunit 11	-	1.3	0.0054
574	1418086_at	Ppp1r14a	protein phosphatase 1, regulatory (inhibitor) subunit 14A	-	1.3	0.0038
575	1451331_at	Ppp1r1b	protein phosphatase 1, regulatory (inhibitor) subunit 1B	-	1.9	0.0001
576	1415819_a_at	Ppp2r1a	protein phosphatase 2 (formerly 2A), regulatory subunit A (PR 65), alpha isoform	-	1.3	0.0086
577	1425725_s_at	Ppp2r5c	protein phosphatase 2, regulatory subunit B (B56), gamma isoform	-	1.5	0.0006

#	ID	SYMBOL	GENENAME	EFFECT	FC	P-Value
578	1450368_a_at	Ppp3r1	protein phosphatase 3, regulatory subunit B, alpha isoform (calcineurin B, type I)	-	1.4	0.0069
579	1456805_a_at	Ppp4r1l	protein phosphatase 4, regulatory subunit 1-like	+	1.2	0.0087
580	1431361_at	Prcp	prolylcarboxypeptidase (angiotensinase C)	+	1.5	0.0020
581	1452457_a_at	Prkab1	protein kinase, AMP-activated, beta 1 non-catalytic subunit	-	1.3	0.0033
582	1421446_at	Prkcc	protein kinase C, gamma	-	1.4	0.0007
583	1424287_at	Prkx	protein kinase, X-linked	-	1.3	0.0039
584	1431768_a_at	Prmt3	protein arginine N-methyltransferase 3	-	1.3	0.0085
585	1452834_at	Prr5l	proline rich 5 like	-	1.2	0.0082
586	1438500_at	Prrt3	proline-rich transmembrane protein 3	-	1.2	0.0051
587	1432129_a_at	Prrx1	paired related homeobox 1	+	1.3	0.0013
588	1420352_at	Prss22	protease, serine, 22	+	1.2	0.0086
589	1449805_at	Prss29	protease, serine, 29	+	1.3	0.0031
590	1416240_at	Psmb7	proteasome (prosome, macropain) subunit, beta type 7	-	1.3	0.0093
591	1453164_a_at	Ptdss2	phosphatidylserine synthase 2	-	1.3	0.0039
592	1453578_at	Pter	phosphotriesterase related	+	1.3	0.0053
593	1429474_at	Ptgr2	prostaglandin reductase 2	-	1.2	0.0050
594	1452508_x_at	Ptms	parathymosin	-	1.2	0.0049
595	1418182_at	Ptp4a3	protein tyrosine phosphatase 4a3	+	1.3	0.0061
596	1433823_at	Ptpdc1	protein tyrosine phosphatase domain containing 1	-	1.2	0.0022
597	1423448_at	Rab11b	RAB11B, member RAS oncogene family	-	1.2	0.0055
598	1455857_a_at	Rab2b	RAB2B, member RAS oncogene family	-	1.2	0.0079
599	1436923_at	Rab2b	RAB2B, member RAS oncogene family	-	1.3	0.0016
600	1416527_at	Rab32	RAB32, member RAS oncogene family	-	1.3	0.0014
601	1455064_at	Rab36	RAB36, member RAS oncogene family	-	1.2	0.0035
602	1431136_at	Rab36	RAB36, member RAS oncogene family	-	1.3	0.0010
603	1453926_at	Rad54l	RAD54 like (S. cerevisiae)	+	1.4	0.0045
604	1438031_at	Rasgrp3	RAS, guanyl releasing protein 3	-	1.3	0.0030
605	1416354_at	Rbmx	RNA binding motif protein, X chromosome	-	1.2	0.0034
606	1416601_a_at	Rcan1	regulator of calcineurin 1	-	1.4	0.0082
607	1447634_x_at	Rcbtb2	regulator of chromosome condensation (RCC1) and BTB (POZ) domain containing protein 2	+	1.2	0.0088
608	1448860_at	Rem2	rad and gem related GTP binding protein 2	-	1.2	0.0072
609	1457387_at	Repin1	replication initiator 1	+	1.3	0.0034
610	1424715_at	Retsat	retinol saturase (all trans retinol 13,14 reductase)	-	1.2	0.0076
611	1451960_a_at	Rev3l	REV3-like, catalytic subunit of DNA polymerase zeta RAD54 like (S. cerevisiae)	+	1.2	0.0095
612	1421160_a_at	Rfng	RFNG O-fucosylpeptide 3-beta-N-acetylglucosaminyltransferase	-	1.3	0.0013
613	1433586_at	Rgmb	RGM domain family, member B	-	1.2	0.0074
614	1451617_at	Rho	rhodopsin	+	1.3	0.0040
615	1448605_at	Rhoc	ras homolog gene family, member C	-	1.2	0.0084
616	1431684_at	Rlbp1l1	retinaldehyde binding protein 1-like 1	-	1.2	0.0039
617	1431030_a_at	Rnf14	ring finger protein 14	-	1.2	0.0017
618	1458303_at	Rnf165	ring finger protein 165	+	1.2	0.0024
619	1430527_a_at	Rnf167	ring finger protein 167	-	1.3	0.0008
620	1451157_at	Rnf187	ring finger protein 187	-	1.4	0.0013
621	1432478_a_at	Rnf19b	ring finger protein 19B	-	1.3	0.0007
622	1425793_a_at	Rorc	RAR-related orphan receptor gamma	-	1.3	0.0040
623	1419799_at	Rpl27a	ribosomal protein L27A	+	1.3	0.0083
624	1418896_a_at	Rpn2	ribophorin II	-	1.2	0.0019
625	1452383_at	Rps6ka3	ribosomal protein S6 kinase polypeptide 3	+	1.2	0.0088
626	1422268_a_at	Rps6kb2	ribosomal protein S6 kinase, polypeptide 2	-	1.4	0.0001
627	1451293_at	Rrp9	RRP9, small subunit (SSU) processome component, homolog (yeast)	-	1.2	0.0049
628	1425539_a_at	Rtn3	reticulon 3	-	1.3	0.0029
629	1436868_at	Rtn4rl1	reticulon 4 receptor-like 1	-	1.3	0.0009
630	1449246_at	Rundc3a	RUN domain containing 3A	-	1.2	0.0086
631	1431137_at	Rusc1	RUN and SH3 domain containing 1	-	1.2	0.0028
632	1421126_at	Ryr2	ryanodine receptor 2, cardiac	+	1.2	0.0032
633	1456977_at	Samd11	sterile alpha motif domain containing 11	+	1.2	0.0097
634	1456902_at	Satb1	special AT-rich sequence binding protein 1	-	1.2	0.0033
635	1430552_a_at	Sbf1	SET binding factor 1	-	1.3	0.0014
636	1434707_at	Sbf1	SET binding factor 1	-	1.3	0.0039
637	1424709_at	Sc5d	sterol-C5-desaturase (fungal ERG3, delta-5-desaturase) homolog (S. cerevisae)	-	1.3	0.0010
638	1434908_at	Scaf1	SR-related CTD-associated factor 1	-	1.2	0.0034
639	1448404_at	Scamp2	secretory carrier membrane protein 2	-	1.2	0.0085
640	1415823_at	Scd2	stearoyl-Coenzyme A desaturase 2	-	1.4	0.0054
641	1436646_at	Scn2a1	sodium channel, voltage-gated, type II, alpha 1	+	1.4	0.0011
642	1431760_a_at	Sdccag3	serologically defined colon cancer antigen 3	-	1.3	0.0025
643	1428695_at	Sdr39u1	short chain dehydrogenase/reductase family 39U, member 1	-	1.3	0.0064
644	1451908_a_at	Sec14l1	SEC14-like 1 (S. cerevisiae)	-	1.2	0.0083
645	1453014_a_at	Sec31a	Sec31 homolog A (S. cerevisiae)	-	1.2	0.0086
646	1416190_a_at	Sec61a1	Sec61 alpha 1 subunit (S. cerevisiae)	-	1.3	0.0018
647	1459109_at	Sema5a	sema domain, seven thrombospondin repeats (type 1 and type 1-like), transmembrane domain (TM) and short cytoplasmic domain, (semaphorin) 5A	+	1.2	0.0080

#	ID	SYMBOL	GENENAME	EFFECT	FC	P-Value
648	1415828_a_at	Serp1	stress-associated endoplasmic reticulum protein 1	-	1.4	0.0011
649	1416318_at	Serpinb1a	serine (or cysteine) peptidase inhibitor, clade B, member 1a	-	1.3	0.0035
650	1422776_at	Serpinb8	serine (or cysteine) peptidase inhibitor, clade B, member 8	-	1.3	0.0070
651	1420885_a_at	Sez6	seizure related gene 6	-	1.3	0.0005
652	1456040_at	Sf3b2	splicing factor 3b, subunit 2	-	1.2	0.0015
653	1416594_at	Sfrp1	secreted frizzled-related protein 1	+	1.4	0.0082
654	1460187_at	Sfrp1	secreted frizzled-related protein 1	-	1.3	0.0082
655	1449228_at	Sh3gl2	SH3-domain GRB2-like 2	-	1.4	0.0043
656	1451267_at	Sharpin	SHANK-associated RH domain interacting protein	-	1.2	0.0060
657	1424824_at	Slain1	SLAIN motif family, member 1	-	1.2	0.0056
658	1445305_at	Slc10a7	solute carrier family 10 (sodium/bile acid cotransporter family), member 7	+	1.3	0.0055
659	1436989_s_at	Slc12a6	solute carrier family 12, member 6	+	1.2	0.0036
660	1422897_at	Slc22a12	solute carrier family 22 (organic anion/cation transporter), member 12	-	1.4	0.0046
661	1416966_at	Slc22a8	solute carrier family 22 (organic anion transporter), member 8	-	1.3	0.0091
662	1428190_at	Slc25a1	solute carrier family 25 (mitochondrial carrier, citrate transporter), member 1	-	1.2	0.0020
663	1420966_at	Slc25a15	solute carrier family 25 (mitochondrial carrier ornithine transporter), member 15	+	1.2	0.0033
664	1453111_a_at	Slc25a39	solute carrier family 25, member 39	-	1.2	0.0099
665	1422811_at	Slc27a1	solute carrier family 27 (fatty acid transporter), member 1	-	1.2	0.0095
666	1421924_at	Slc2a3	solute carrier family 2 (facilitated glucose transporter), member 3	-	1.2	0.0053
667	1419972_at	Slc35a5	solute carrier family 35, member A5	-	1.3	0.0071
668	1447248_at	Slc39a12	solute carrier family 39 (zinc transporter), member 12	-	1.4	0.0053
669	1438490_at	Slc39a14	solute carrier family 39 (zinc transporter), member 14	-	1.2	0.0098
670	1458394_at	Slc6a17	solute carrier family 6 (neurotransmitter transporter), member 17	-	1.2	0.0078
671	1417150_at	Slc6a4	solute carrier family 6 (neurotransmitter transporter, serotonin), member 4	+	10.6	0.0000
672	1439368_a_at	Slc9a3r2	solute carrier family 9 (sodium/hydrogen exchanger), member 3 regulator 2	-	1.2	0.0066
673	1439369_x_at	Slc9a3r2	solute carrier family 9 (sodium/hydrogen exchanger), member 3 regulator 2	-	1.2	0.0034
674	1431449_at	Slco6d1	solute carrier organic anion transporter family, member 6d1	+	1.3	0.0021
675	1421215_a_at	Slmap	sarcolemma associated protein	-	1.3	0.0067
676	1420030_at	Slu7	SLU7 splicing factor homolog (S. cerevisiae)	+	1.3	0.0058
677	1423077_at	Snx9	sorting nexin 9	-	1.2	0.0094
678	1419329_at	Sorbs3	sorbin and SH3 domain containing 3	-	1.3	0.0068
679	1428338_at	Spata2L	spermatogenesis associated 2-like	-	1.3	0.0049
680	1450618_a_at	Sprr2a	small proline-rich protein 2A	+	1.3	0.0080
681	1422401_at	Sprr3	small proline-rich protein 3	+	1.2	0.0091
682	1428472_at	Spsb1	splA/ryanodine receptor domain and SOCS box containing 1	-	1.2	0.0040
683	1426744_at	Srebf2	sterol regulatory element binding factor 2	-	1.2	0.0082
684	1425351_at	Srxn1	sulfiredoxin 1 homolog (S. cerevisiae)	-	1.3	0.0044
685	1421890_at	St3gal2	ST3 beta-galactoside alpha-2,3-sialyltransferase 2	-	1.3	0.0020
686	1419550_a_at	Stk39	serine/threonine kinase 39, STE20/SPS1 homolog (yeast)	-	1.4	0.0027
687	1419913_at	Strap	serine/threonine kinase receptor associated protein	+	1.5	0.0057
688	1422036_at	Strn	striatin, calmodulin binding protein	+	1.3	0.0007
689	1426343_at	Stt3b	STT3, subunit of the oligosaccharyltransferase complex, homolog B (S. cerevisiae)	-	1.2	0.0093
690	1421606_a_at	Sult4a1	sulfotransferase family 4A, member 1	-	1.3	0.0058
691	1453049_at	Svip	small VCP/p97-interacting protein	-	1.2	0.0046
692	1428685_at	Syce1	synaptonemal complex central element protein 1	+	1.3	0.0016
693	1448216_at	Syngr3	synaptogyrin 3	-	1.3	0.0024
694	1417708_at	Syt3	synaptotagmin III	-	1.3	0.0077
695	1422531_at	Syt5	synaptotagmin V	-	1.4	0.0013
696	1424169_at	Tax1bp3	Tax1 (human T-cell leukemia virus type I) binding protein 3	-	1.5	0.0001
697	1415750_at	Tbl3	transducin (beta)-like 3	-	1.2	0.0030
698	1425158_at	Tbx20	T-box 20	+	1.2	0.0085
699	1424531_a_at	Tcea3	transcription elongation factor A (SII), 3	-	1.3	0.0078
700	1448981_x_at	Tcl1b1	T-cell leukemia/lymphoma 1B, 1	+	1.6	0.0030
701	1423600_a_at	Tcof1	Treacher Collins Franceschetti syndrome 1, homolog	-	1.2	0.0075
702	1420729_at	Tcstv1	2-cell-stage, variable group, member 1	+	1.3	0.0021
703	1421513_at	Tdrd1	tudor domain containing 1	+	1.3	0.0041
704	1418064_at	Tfpt	TCF3 (E2A) fusion partner	-	1.2	0.0071
705	1428425_at	Tgfbrap1	transforming growth factor, beta receptor associated protein 1	-	1.2	0.0079
706	1418765_at	Timd2	T-cell immunoglobulin and mucin domain containing 2	+	1.2	0.0074
707	1448518_at	Timm22	translocase of inner mitochondrial membrane 22 homolog (yeast)	+	1.2	0.0028

#	ID	SYMBOL	GENENAME	EFFECT	FC	P-Value
708	1432282_a_at	Tlcd2	TLC domain containing 2	+	1.3	0.0077
709	1448375_at	Tm9sf3	transmembrane 9 superfamily member 3	-	1.2	0.0039
710	1458372_at	Tmc8	transmembrane channel-like gene family 8	+	1.2	0.0053
711	1451546_s_at	Tmem40	transmembrane protein 40	-	1.2	0.0061
712	1423871_at	Tmem63a	transmembrane protein 63a	-	1.2	0.0054
713	1453285_at	Tmem88	transmembrane protein 88	-	1.3	0.0014
714	1424133_at	Tmem98	transmembrane protein 98	-	1.5	0.0084
715	1423048_a_at	Tollip	toll interacting protein	-	1.3	0.0047
716	1431188_a_at	Tom1	target of myb1 homolog (chicken)	-	1.2	0.0032
717	1436008_at	Tpd52	tumor protein D52	+	1.3	0.0099
718	1449997_at	Tpm3	tropomyosin 3, gamma	-	1.2	0.0052
719	1427567_a_at	Tpm3	tropomyosin 3, gamma	-	1.2	0.0094
720	1439043_at	Tra2a	transformer 2 alpha homolog (Drosophila)	+	1.6	0.0031
721	1425546_a_at	Trf	transferrin	-	1.3	0.0026
722	1451663_a_at	Trim3	tripartite motif-containing 3	-	1.2	0.0082
723	1425621_at	Trim35	tripartite motif-containing 35	-	1.4	0.0005
724	1437314_a_at	Trmt1	TRM1 tRNA methyltransferase 1 homolog (S. cerevisiae)	-	1.2	0.0050
725	1427739_a_at	Trp53	transformation related protein 53	-	1.3	0.0097
726	1452325_at	Trp73	transformation related protein 73	-	1.2	0.0076
727	1418783_at	Trpm5	transient receptor potential cation channel, subfamily M, member 5	+	1.3	0.0074
728	1443392_at	Trpv1	transient receptor potential cation channel, subfamily V, member 1	+	1.6	0.0000
729	1417502_at	Tspan7	tetraspanin 7	-	1.3	0.0073
730	1455414_at	Ttc16	tetratricopeptide repeat domain 16	-	1.2	0.0031
731	1435456_at	Ttc28	tetratricopeptide repeat domain 28	-	1.2	0.0071
732	1433460_at	Ttc7b	tetratricopeptide repeat domain 7B	-	1.3	0.0044
733	1443948_at	Ttc9c	tetratricopeptide repeat domain 9C	-	1.2	0.0095
734	1451694_at	Ttll3	tubulin tyrosine ligase-like family, member 3	+	1.4	0.0011
735	1423221_at	Tubb4	tubulin, beta 4	-	1.2	0.0099
736	1423035_s_at	Txndc17	thioredoxin domain containing 17	-	1.2	0.0068
737	1423036_at	Txndc17	thioredoxin domain containing 17	-	1.3	0.0018
738	1439302_at	Uba6	ubiquitin-like modifier activating enzyme 6	+	1.2	0.0096
739	1448017_at	Ubap2l	ubiquitin associated protein 2-like	-	1.2	0.0085
740	1430177_at	Ube2b	ubiquitin-conjugating enzyme E2B, RAD6 homology (S. cerevisiae)	-	1.4	0.0001
741	1424062_at	Ube2d1	ubiquitin-conjugating enzyme E2D 1, UBC4/5 homolog (yeast)	-	1.2	0.0070
742	1448692_at	Ubqln4	ubiquilin 4	-	1.2	0.0049
743	1435110_at	Unc5b	unc-5 homolog B (C. elegans)	-	1.2	0.0036
744	1420833_at	Vamp2	vesicle-associated membrane protein 2	-	1.4	0.0050
745	1421102_a_at	Vamp3	vesicle-associated membrane protein 3	-	1.4	0.0006
746	1417123_at	Vav3	vav 3 oncogene	-	1.3	0.0012
747	1420909_at	Vegfa	vascular endothelial growth factor A	-	1.2	0.0037
748	1425490_a_at	Wdr13	WD repeat domain 13	-	1.3	0.0049
749	1432217_a_at	Wdr16	WD repeat domain 16	-	1.2	0.0095
750	1429552_at	Wdr16	WD repeat domain 16	-	1.7	0.0007
751	1455278_at	Wdr37	WD repeat domain 37	+	1.2	0.0051
752	1460012_at	Wfdc3	WAP four-disulfide core domain 3	+	1.3	0.0074
753	1453737_at	Wipf2	WAS/WASL interacting protein family, member 2	-	1.3	0.0093
754	1444050_at	Wisp3	WNT1 inducible signaling pathway protein 3	-	1.2	0.0096
755	1431942_at	Wwox	WW domain-containing oxidoreductase	+	1.4	0.0006
756	1443621_at	Xaf1	XIAP associated factor 1	+	7.6	0.0000
757	1443698_at	Xaf1	XIAP associated factor 1	-	1.7	0.0000
758	1420012_at	Xbp1	X-box binding protein 1	+	1.4	0.0035
759	1422532_at	Xpc	xeroderma pigmentosum, complementation group C	-	1.2	0.0076
760	1439005_x_at	Ywhaz	tyrosine 3-monooxygenase/tryptophan 5-monooxygenase activation protein, zeta polypeptide	+	1.3	0.0092
761	1448218_s_at	Ywhaz	tyrosine 3-monooxygenase/tryptophan 5-monooxygenase activation protein, zeta polypeptide	-	1.2	0.0043
762	1419899_at	Zc3h7a	zinc finger CCCH type containing 7 A	+	1.3	0.0014
763	1419955_at	Zfand3	zinc finger, AN1-type domain 3	+	1.2	0.0081
764	1425097_a_at	Zfp106	zinc finger protein 106	-	1.2	0.0046
765	1439698_at	Zfp276	zinc finger protein (C2H2 type) 276	+	1.3	0.0051
766	1452519_a_at	Zfp36	zinc finger protein 36	-	1.2	0.0043
767	1426563_at	Zfp553	zinc finger protein 553	-	1.3	0.0030
768	1436429_at	Zfp606	zinc finger protein 606	-	1.4	0.0018
769	1449691_at	Zfp644	zinc finger protein 644	+	1.3	0.0017
770	1436020_at	Zfp828	zinc finger protein 828	-	1.3	0.0075
771	1449552_at	Zfr	zinc finger RNA binding protein	-	1.4	0.0082
772	1438787_at	Zscan10	zinc finger and SCAN domain containing 10	+	1.2	0.0092
773	1438691_at	Zzef1	zinc finger, ZZ-type with EF hand domain 1	-	1.9	0.0000

5.1.2 Gene expression affected by the environment (prenatal stress versus control)

ID: Affymetrix ID; EFFECT: direction of effect; “+”: gene expression upregulated in prenatally stressed versus control mice; “-“: downregulated in prenatally stressed versus control mice; FC: fold-change in mRNA expression. Genes have been ordered alphabetically.

#	ID	SYMBOL	GENENAME	Effect	FC	P.Value
1	1452437_at	1110021J02Rik	RIKEN cDNA 1110021J02 gene	+	1.5	0.0007
2	1437981_x_at	1110057K04Rik	RIKEN cDNA 1110057K04 gene	+	1.2	0.0016
3	1428922_at	1200009O22Rik	RIKEN cDNA 1200009O22 gene	-	1.2	0.0013
4	1451082_at	1300018I05Rik	RIKEN cDNA 1300018I05 gene	-	1.2	0.0091
5	1447537_at	1500032P08Rik	RIKEN cDNA 1500032P08 gene	+	1.2	0.0092
6	1430261_at	1700024J04Rik	RIKEN cDNA 1700024J04 gene	+	1.1	0.0090
7	1432116_at	1700031F05Rik	RIKEN cDNA 1700031F05 gene	+	1.3	0.0058
8	1441406_at	1700052N19Rik	RIKEN cDNA 1700052N19 gene	+	1.2	0.0044
9	1459809_x_at	1700063D05Rik	RIKEN cDNA 1700063D05 gene	+	1.3	0.0032
10	1442779_at	1700071K01Rik	RIKEN cDNA 1700071K01 gene	-	1.3	0.0031
11	1420681_at	1700120K04Rik	RIKEN cDNA 1700120K04 gene	+	1.2	0.0063
12	1447594_at	1810012K16Rik	RIKEN cDNA 1810012K16 gene	-	1.2	0.0085
13	1430991_at	1810014B01Rik	RIKEN cDNA 1810014B01 gene	+	1.5	0.0005
14	1439561_at	2010012O05Rik	RIKEN cDNA 2010012O05 gene	-	1.1	0.0074
15	1429895_at	2310010G23Rik	RIKEN cDNA 2310010G23 gene	-	1.2	0.0033
16	1432107_at	2310010M20Rik	RIKEN cDNA 2310010M20 gene	-	1.2	0.0094
17	1430446_at	2310057B04Rik	RIKEN cDNA 2310057B04 gene	-	1.2	0.0036
18	1460410_at	2310079F23Rik	RIKEN cDNA 2310079F23 gene	+	1.2	0.0088
19	1435377_at	2410002O22Rik	RIKEN cDNA 2410002O22 gene	+	1.2	0.0034
20	1432500_at	2410006F04Rik	RIKEN cDNA 2410006F04 gene	-	1.2	0.0095
21	1430845_at	2410018L13Rik	RIKEN cDNA 2410018L13 gene	-	1.2	0.0036
22	1420114_s_at	2410022L05Rik	RIKEN cDNA 2410022L05 gene	+	1.4	0.0039
23	1429245_at	2510022D24Rik	RIKEN cDNA 2510022D24 gene	-	1.2	0.0068
24	1453966_at	2610008G14Rik	RIKEN cDNA 2610008G14 gene	+	1.2	0.0073
25	1432606_at	2610012C04Rik	RIKEN cDNA 2610012C04 gene	+	1.2	0.0020
26	1452979_at	2610110G12Rik	RIKEN cDNA 2610110G12 gene	-	1.3	0.0005
27	1428624_at	2810482I07Rik	RIKEN cDNA 2810482I07 gene	+	1.2	0.0062
28	1433387_at	2900022M07Rik	RIKEN cDNA 2900022M07 gene	+	1.4	0.0018
29	1420820_at	2900073G15Rik	RIKEN cDNA 2900073G15 gene	+	1.2	0.0051
30	1430478_at	3110043A19Rik	RIKEN cDNA 3110043A19 gene	-	1.3	0.0068
31	1430841_at	3300002P13Rik	RIKEN cDNA 3300002P13 gene	+	1.2	0.0091
32	1430858_at	4632433K11Rik	RIKEN cDNA 4632433K11 gene	-	1.2	0.0097
33	1430382_at	4833413G10Rik	RIKEN cDNA 4833413G10 gene	-	1.2	0.0007
34	1436524_at	4833438C02Rik	RIKEN cDNA 4833438C02 gene	-	1.3	0.0005
35	1423381_at	4921521F21Rik	RIKEN cDNA 4921521F21 gene	+	1.3	0.0009
36	1453650_at	4930413F20Rik	RIKEN cDNA 4930413F20 gene	-	1.2	0.0095
37	1440349_at	4930420K17Rik	RIKEN cDNA 4930420K17 gene	+	1.1	0.0071
38	1433082_at	4930448K20Rik	glyceraldehyde-3-phosphatedehydrogenase pseudogene	+	1.6	0.0040
39	1429353_a_at	4930511M11Rik	RIKEN cDNA 4930511M11 gene	+	1.2	0.0034
40	1432223_at	4930552N02Rik	RIKEN cDNA 4930552N02 gene	+	1.2	0.0002
41	1428375_at	4932415G12Rik	RIKEN cDNA 4932415G12 gene	-	1.2	0.0024
42	1453828_at	4932422M17Rik	RIKEN cDNA 4932422M17 gene	+	1.2	0.0031
43	1432882_at	4932431P20Rik	RIKEN cDNA 4932431P20 gene	+	1.4	0.0020
44	1432127_at	4933401L05Rik	RIKEN cDNA 4933401L05 gene	+	1.2	0.0096
45	1454101_at	4933401P06Rik	RIKEN cDNA 4933401P06 gene	+	1.2	0.0077
46	1431853_at	4933413C19Rik	RIKEN cDNA 4933413C19 gene	+	1.2	0.0059
47	1432197_at	4933417D19Rik	RIKEN cDNA 4933417D19 gene	+	1.2	0.0048
48	1427065_at	4933439F18Rik	RIKEN cDNA 4933439F18 gene	+	1.2	0.0084
49	1427068_x_at	4933439F18Rik	RIKEN cDNA 4933439F18 gene	+	1.2	0.0010
50	1432935_at	5330433J24Rik	RIKEN cDNA 5330433J24 gene	+	1.3	0.0082
51	1432621_at	5730410E19Rik	RIKEN cDNA 5730410E19 gene	+	1.2	0.0040
52	1447774_x_at	5730469M10Rik	RIKEN cDNA 5730469M10 gene	+	1.2	0.0063
53	1453079_at	5730494M16Rik	RIKEN cDNA 5730494M16 gene	-	1.3	0.0067
54	1431528_at	5830427D02Rik	RIKEN cDNA 5830427D02 gene	+	1.2	0.0004
55	1432998_at	5830462O15Rik	RIKEN cDNA 5830462O15 gene	-	1.3	0.0021
56	1432990_at	5830495A06Rik	RIKEN cDNA 5830495A06 gene	+	1.2	0.0028
57	1446341_at	6030403N03Rik	RIKEN cDNA 6030403N03 gene	+	1.2	0.0088
58	1460522_at	6030458E02Rik	RIKEN cDNA 6030458E02 gene	+	1.2	0.0067
59	1437753_at	6230409E13Rik	RIKEN cDNA 6230409E13 gene	+	1.1	0.0076
60	1456765_at	6430511F03	hypothetical protein 6430511F03	+	1.1	0.0093
61	1452082_at	6430548M08Rik	RIKEN cDNA 6430548M08 gene	-	1.2	0.0006
62	1459051_at	6530418L21Rik	RIKEN cDNA 6530418L21 gene	+	1.2	0.0089
63	1444797_at	8030474K03Rik	RIKEN cDNA 8030474K03 gene	+	1.3	0.0009
64	1454056_at	9030407P20Rik	RIKEN cDNA 9030407P20 gene	-	1.2	0.0098
65	1433101_at	9030419F21Rik	RIKEN cDNA 9030419F21 gene	+	1.2	0.0014

#	ID	SYMBOL	GENENAME	Effect	FC	P.Value
66	1424555_at	9430015G10Rik	RIKEN cDNA 9430015G10 gene	-	1.2	0.0023
67	1435159_at	9430038I01Rik	RIKEN cDNA 9430038I01 gene	-	1.2	0.0058
68	1445167_at	9630001P10Rik	RIKEN cDNA 9630001P10 gene	-	1.3	0.0014
69	1456634_at	9830001H06Rik	RIKEN cDNA 9830001H06 gene	-	1.2	0.0057
70	1433577_at	A730017C20Rik	RIKEN cDNA A730017C20 gene	-	1.2	0.0061
71	1456167_at	AA619741	expressed sequence AA619741	-	1.2	0.0055
72	1451377_a_at	Aaas	achalasia, adrenocortical insufficiency, alacrimia	-	1.2	0.0002
73	1419931_at	Abcb7	ATP-binding cassette, sub-family B (MDR/TAP), member 7	+	1.3	0.0023
74	1423863_at	Abcf2	ATP-binding cassette, sub-family F (GCN20), member 2	-	1.2	0.0042
75	1449827_at	Acan	aggrecan	-	1.2	0.0087
76	1422635_at	Ache	acetylcholinesterase	-	1.3	0.0008
77	1451002_at	Aco2	aconitase 2, mitochondrial	-	1.2	0.0084
78	1425257_at	Acot5	acyl-CoA thioesterase 5	+	1.2	0.0044
79	1418073_at	Acot9	acyl-CoA thioesterase 9	-	1.2	0.0030
80	1419734_at	Actb	actin, beta	-	1.2	0.0009
81	1422564_at	Actl6b	actin-like 6B	-	1.2	0.0082
82	1448327_at	Actn2	actinin alpha 2	-	1.2	0.0053
83	1452057_at	Actr1b	ARP1 actin-related protein 1 homolog B, centractin beta (yeast)	-	1.2	0.0041
84	1448460_at	Acvr1	activin A receptor, type 1	+	1.1	0.0070
85	1416080_at	Adam15	a disintegrin and metallopeptidase domain 15 (metargidin)	-	1.2	0.0055
86	1458197_x_at	Adam1a	a disintegrin and metallopeptidase domain 1a	+	1.2	0.0012
87	1443378_s_at	Adam1a	a disintegrin and metallopeptidase domain 1a	+	1.3	0.0013
88	1427790_at	Adam1a	a disintegrin and metallopeptidase domain 1a	+	1.4	0.0003
89	1416871_at	Adam8	a disintegrin and metallopeptidase domain 8	+	1.3	0.0001
90	1444253_at	Adamts18	a disintegrin-like and metallopeptidase (reprolysin type) with thrombospondin type 1 motif, 18	-	1.3	0.0091
91	1455965_at	Adamts4	a disintegrin-like and metallopeptidase (reprolysin type) with thrombospondin type 1 motif, 4	+	1.3	0.0009
92	1425638_at	Adap2	ArfGAP with dual PH domains 2	-	1.3	0.0011
93	1448490_at	Adck4	aarF domain containing kinase 4	-	1.2	0.0014
94	1420970_at	Adcy7	adenylate cyclase 7	+	1.1	0.0060
95	1430482_at	Adora3	adenosine A3 receptor	+	1.3	0.0012
96	1438158_at	Agbl4	ATP/GTP binding protein-like 4	-	1.2	0.0043
97	1425362_at	Agfg2	ArfGAP with FG repeats 2	+	1.2	0.0009
98	1440138_at	Ahdc1	AT hook, DNA binding motif, containing 1	+	1.3	0.0015
99	1444026_at	AI593442	expressed sequence AI593442	+	1.2	0.0082
100	1416911_a_at	Akirin1	akirin 1	+	1.2	0.0059
101	1448143_at	Aldh2	aldehyde dehydrogenase 2, mitochondrial	+	1.2	0.0028
102	1434987_at	Aldh2	aldehyde dehydrogenase 2, mitochondrial	+	1.3	0.0001
103	1434988_x_at	Aldh2	aldehyde dehydrogenase 2, mitochondrial	+	1.3	0.0001
104	1438941_x_at	Ampd2	adenosine monophosphate deaminase 2 (isoform L)	+	1.2	0.0018
105	1436967_at	Ankrd11	ankyrin repeat domain 11	-	1.2	0.0071
106	1433543_at	Anln	anillin, actin binding protein	+	1.2	0.0062
107	1437895_at	Ano8	anoctamin 8	-	1.2	0.0059
108	1415818_at	Anxa6	annexin A6	-	1.3	0.0029
109	1416134_at	Aplp1	amyloid beta (A4) precursor-like protein 1	-	1.4	0.0066
110	1421889_a_at	Aplp2	amyloid beta (A4) precursor-like protein 2	-	1.2	0.0069
111	1418849_x_at	Aqp7	aquaporin 7	+	1.3	0.0042
112	1434074_x_at	Arf4	ADP-ribosylation factor 4	+	1.3	0.0089
113	1448672_a_at	Arfgap2	ADP-ribosylation factor GTPase activating protein 2	-	1.2	0.0041
114	1431133_at	Arhgap18	Rho GTPase activating protein 18	+	1.1	0.0084
115	1451320_at	Arhgap8	Rho GTPase activating protein 8	+	1.2	0.0049
116	1421164_a_at	Arhgef1	Rho guanine nucleotide exchange factor (GEF) 1	-	1.2	0.0023
117	1418523_at	Arih2	ariadne homolog 2 (Drosophila)	-	1.3	0.0006
118	1424020_at	Arl6ip6	ADP-ribosylation factor-like 6 interacting protein 6	+	1.2	0.0018
119	1428399_a_at	Armc9	armadillo repeat containing 9	-	1.2	0.0099
120	1460703_at	Ascc1	activating signal cointegrator 1 complex subunit 1	-	1.2	0.0097
121	1418292_at	Asna1	arsA arsenite transporter, ATP-binding, homolog 1 (bacterial)	-	1.4	0.0010
122	1430656_a_at	Asnsd1	asparagine synthetase domain containing 1	-	1.1	0.0093
123	1438992_x_at	Atf4	activating transcription factor 4	+	1.3	0.0001
124	1439457_x_at	Atg12	autophagy-related 12 (yeast)	+	1.2	0.0026
125	1435594_at	Atl2	atlastin GTPase 2	-	1.2	0.0057
126	1427481_a_at	Atp1a3	ATPase, Na+/K+ transporting, alpha 3 polypeptide	-	1.4	0.0004
127	1437157_at	Atp1b1	ATPase, Na+/K+ transporting, beta 1 polypeptide	+	1.3	0.0059
128	1437797_at	Atp2a2	ATPase, Ca++ transporting, cardiac muscle, slow twitch 2	+	1.2	0.0032
129	1450124_a_at	Atp2a3	ATPase, Ca++ transporting, ubiquitous	+	1.2	0.0050
130	1444874_at	Atp5g1	ATP synthase, H+ transporting, mitochondrial F0 complex, subunit c (subunit 9), isoform 1	+	1.2	0.0058
131	1437013_x_at	Atp6v0b	ATPase, H+ transporting, lysosomal V0 subunit B	-	1.2	0.0041
132	1425448_x_at	Atp6v0b	ATPase, H+ transporting, lysosomal V0 subunit B	-	1.2	0.0043
133	1448770_a_at	Atpif1	ATPase inhibitory factor 1	+	1.3	0.0043
134	1438294_at	Atxn1	ataxin 1	+	1.2	0.0089
135	1442081_at	AU017455	expressed sequence AU017455	-	1.2	0.0094
136	1442403_at	B130034C11Rik	RIKEN cDNA B130034C11 gene	-	1.3	0.0059
137	1456701_at	B230208H17Rik	RIKEN cDNA B230208H17 gene	+	1.3	0.0044
138	1437433_at	B3galt2	UDP-Gal:betaGlcNAc beta 1,3-galactosyltransferase,	-	1.3	0.0007

#	ID	SYMBOL	GENENAME	Effect	FC	P.Value
			polypeptide 2			
139	1437644_at	B3galt2	UDP-Gal:betaGlcNAc beta 1,3-galactosyltransferase, polypeptide 2	-	1.3	0.0067
140	1448941_at	B4galt2	UDP-Gal:betaGlcNAc beta 1,4- galactosyltransferase, polypeptide 2	-	1.2	0.0073
141	1427230_at	B930041F14Rik	RIKEN cDNA B930041F14 gene	-	1.2	0.0032
142	1425656_a_at	Baiap2	brain-specific angiogenesis inhibitor 1-associated protein 2	-	1.2	0.0090
143	1448221_at	Bat1a	HLA-B-associated transcript 1A	-	1.2	0.0016
144	1423315_at	Bbc3	BCL2 binding component 3	+	1.2	0.0071
145	1460369_at	BC003267	cDNA sequence BC003267	-	1.2	0.0052
146	1425961_at	BC016548	cDNA sequence BC016548	+	1.2	0.0096
147	1423919_at	BC023882	cDNA sequence BC023882	-	1.2	0.0087
148	1424434_at	BC024814	cDNA sequence BC024814	-	1.2	0.0080
149	1437186_at	BC055324	cDNA sequence BC055324	+	1.2	0.0047
150	1444632_at	BC064078	cDNA sequence BC064078	-	1.2	0.0043
151	1417077_at	Bcap29	B-cell receptor-associated protein 29	-	1.2	0.0063
152	1443524_x_at	Bcl10	B-cell leukemia/lymphoma 10	+	1.2	0.0032
153	1420887_a_at	Bcl2l1	BCL2-like 1	-	1.3	0.0053
154	1450732_a_at	Bicd2	bicaudal D homolog 2 (Drosophila)	+	1.3	0.0003
155	1432410_a_at	Bmp7	bone morphogenetic protein 7	-	1.2	0.0086
156	1449211_at	Bpnt1	bisphosphate 3'-nucleotidase 1	+	1.1	0.0074
157	1447941_x_at	Braf	Braf transforming gene	-	1.2	0.0061
158	1416738_at	Brap	BRCA1 associated protein	+	1.3	0.0019
159	1426312_at	Bre	brain and reproductive organ-expressed protein	-	1.2	0.0043
160	1429561_at	Brf2	BRF2, subunit of RNA polymerase III transcription initiation factor, BRF1-like	-	1.2	0.0054
161	1456616_a_at	Bsg	basigin	-	1.3	0.0073
162	1424921_at	Bst2	bone marrow stromal cell antigen 2	+	1.3	0.0051
163	1425884_at	Bxdc1	brix domain containing 1	+	1.3	0.0021
164	1433931_at	C030046I01Rik	RIKEN cDNA C030046I01 gene	-	1.3	0.0010
165	1433932_x_at	C030046I01Rik	RIKEN cDNA C030046I01 gene	-	1.3	0.0003
166	1430501_at	C030047K22Rik	RIKEN cDNA C030047K22 gene	-	1.2	0.0023
167	1442941_at	C77027	expressed sequence C77027	-	1.2	0.0047
168	1460264_at	C81600	expressed sequence C81600	+	1.2	0.0044
169	1417067_s_at	Cabc1	chaperone, ABC1 activity of bc1 complex like (S. pombe)	+	1.2	0.0049
170	1421255_a_at	Cabp1	calcium binding protein 1	-	1.2	0.0091
171	1450520_at	Cacng3	calcium channel, voltage-dependent, gamma subunit 3	-	1.3	0.0004
172	1435146_s_at	Cadm2	cell adhesion molecule 2	+	1.2	0.0016
173	1456934_at	Calb1	calbindin 1	-	1.2	0.0073
174	1449970_at	Capn12	calpain 12	+	1.2	0.0069
175	1418671_at	Capn5	calpain 5	-	1.2	0.0090
176	1434973_at	Car7	carbonic anhydrase 7	-	1.2	0.0020
177	1452484_at	Car7	carbonic anhydrase 7	-	1.2	0.0087
178	1436395_at	Card6	caspase recruitment domain family, member 6	-	1.2	0.0076
179	1452394_at	Cars	cysteinyl-tRNA synthetase	-	1.2	0.0099
180	1441615_at	Cbfa2t2	core-binding factor, runt domain, alpha subunit 2, translocated to, 2 (human)	-	1.2	0.0013
181	1427912_at	Cbr3	carbonyl reductase 3	+	1.2	0.0028
182	1433861_at	Cc2d1b	coiled-coil and C2 domain containing 1B	-	1.2	0.0016
183	1426097_a_at	Ccdc106	coiled-coil domain containing 106	-	1.1	0.0078
184	1434313_at	Ccdc126	coiled-coil domain containing 126	+	1.2	0.0083
185	1439538_at	Ccdc127	coiled-coil domain containing 127	-	1.3	0.0008
186	1451799_at	Ccdc25	coiled-coil domain containing 25	+	1.2	0.0008
187	1438569_at	Ccdc38	coiled-coil domain containing 38	+	1.2	0.0046
188	1439109_at	Ccdc68	coiled-coil domain containing 68	-	1.2	0.0039
189	1453824_at	Ccdc76	coiled-coil domain containing 76	+	1.3	0.0056
190	1453609_s_at	Ccdc9	coiled-coil domain containing 9	-	1.2	0.0087
191	1451395_at	Ccdc92	coiled-coil domain containing 92	-	1.2	0.0074
192	1417266_at	Ccl6	chemokine (C-C motif) ligand 6	+	1.2	0.0099
193	1417420_at	Ccnd1	cyclin D1	+	1.2	0.0089
194	1448229_s_at	Ccnd2	cyclin D2	+	1.2	0.0002
195	1430997_at	Cd47	CD47 antigen (Rh-related antigen, integrin-associated signal transducer)	+	1.2	0.0097
196	1448466_at	Cdca5	cell division cycle associated 5	-	1.2	0.0063
197	1427095_at	Cdcp1	CUB domain containing protein 1	+	1.4	0.0000
198	1418982_at	Cebpa	CCAAT/enhancer binding protein (C/EBP), alpha	-	1.2	0.0013
199	1418901_at	Cebpb	CCAAT/enhancer binding protein (C/EBP), beta	+	1.2	0.0008
200	1424996_at	Cflar	CASP8 and FADD-like apoptosis regulator	+	1.2	0.0031
201	1424528_at	Cgref1	cell growth regulator with EF hand domain 1	-	1.2	0.0016
202	1418816_at	Chmp1b	chromatin modifying protein 1B	+	1.2	0.0009
203	1456722_at	Chrdl1	chordin-like 1	+	1.2	0.0096
204	1448477_at	Chst12	carbohydrate sulfotransferase 12	-	1.2	0.0044
205	1428977_at	Chst8	carbohydrate (N-acetylgalactosamine 4-0) sulfotransferase 8	-	1.2	0.0066
206	1436391_s_at	Clcc1	chloride channel CLIC-like 1	-	1.1	0.0088
207	1418283_at	Cldn4	claudin 4	+	1.2	0.0046
208	1417839_at	Cldn5	claudin 5	+	1.2	0.0093
209	1460039_at	Clec1a	C-type lectin domain family 1, member a	-	1.2	0.0090
210	1427428_at	Clec4g	C-type lectin domain family 4, member g	+	1.2	0.0053
211	1435256_at	Clip3	CAP-GLY domain containing linker protein 3	-	1.2	0.0088

#	ID	SYMBOL	GENENAME	Effect	FC	P.Value
212	1457789_at	Cln3	ceroid lipofuscinosis, neuronal 3, juvenile (Batten, Spielmeyer-Vogt disease)	+	1.2	0.0034
213	1459992_x_at	Cln8	ceroid-lipofuscinosis, neuronal 8	+	1.1	0.0088
214	1416541_at	Clpb	ClpB caseinolytic peptidase B homolog (E. coli)	-	1.2	0.0026
215	1416883_at	Clptm1	cleft lip and palate associated transmembrane protein 1	-	1.2	0.0033
216	1422158_at	Clstn2	calsyntenin 2	-	1.2	0.0089
217	1453411_at	Cmc1	COX assembly mitochondrial protein homolog (S. cerevisiae)	-	1.2	0.0086
218	1423792_a_at	Cmtm6	CKLF-like MARVEL transmembrane domain containing 6	+	1.2	0.0016
219	1422181_at	Cnga2	cyclic nucleotide gated channel alpha 2	+	1.3	0.0008
220	1459783_s_at	Cno	cappuccino	+	1.2	0.0047
221	1443829_x_at	Coasy	Coenzyme A synthase	+	1.2	0.0055
222	1448081_at	Colq	collagen-like tail subunit (single strand of homotrimer) of asymmetric acetylcholinesterase	+	1.2	0.0041
223	1428491_at	Commd10	COMM domain containing 10	-	1.2	0.0060
224	1418701_at	Comt1	catechol-O-methyltransferase 1	-	1.2	0.0077
225	1416017_at	Copg	coatomer protein complex, subunit gamma	-	1.2	0.0084
226	1437039_at	Cops2	COP9 (constitutive photomorphogenic) homolog, subunit 2 (Arabidopsis thaliana)	-	1.3	0.0073
227	1423459_at	Cops2	COP9 (constitutive photomorphogenic) homolog, subunit 2 (Arabidopsis thaliana)	-	1.2	0.0054
228	1429078_a_at	Cops7a	COP9 (constitutive photomorphogenic) homolog, subunit 7a (Arabidopsis thaliana)	-	1.2	0.0046
229	1437364_at	Coq3	coenzyme Q3 homolog, methyltransferase (yeast)	-	1.2	0.0014
230	1434755_at	Coro2b	coronin, actin binding protein, 2B	-	1.3	0.0041
231	1417747_at	Cplx1	complexin 1	-	1.2	0.0011
232	1436383_at	Cplx2	complexin 2	-	1.2	0.0041
233	1449921_s_at	Cpne6	copine VI	-	1.2	0.0020
234	1433715_at	Cpne7	copine VII	-	1.2	0.0041
235	1453356_at	Cpsf7	cleavage and polyadenylation specific factor 7	+	1.3	0.0027
236	1452754_at	Creld2	cysteine-rich with EGF-like domains 2	+	1.3	0.0024
237	1434369_a_at	Cryab	crystallin, alpha B	+	1.2	0.0074
238	1423845_at	Csdc2	cold shock domain containing C2, RNA binding	-	1.3	0.0057
239	1423593_a_at	Csf1r	colony stimulating factor 1 receptor	-	1.2	0.0018
240	1429928_at	Ctag2	cancer/testis antigen 2	+	1.2	0.0054
241	1421315_s_at	Cttn	cortactin	-	1.2	0.0031
242	1435083_at	Ctxn1	cortexin 1	-	1.3	0.0015
243	1441884_x_at	Cx3cl1	chemokine (C-X3-C motif) ligand 1	+	1.2	0.0034
244	1457644_s_at	Cxcl1	chemokine (C-X-C motif) ligand 1	+	1.3	0.0004
245	1417625_s_at	Cxcr7	chemokine (C-X-C motif) receptor 7	+	1.2	0.0098
246	1422185_a_at	Cyb5r3	cytochrome b5 reductase 3	-	1.2	0.0037
247	1426064_at	Cyp3a44	cytochrome P450, family 3, subfamily a, polypeptide 44	+	1.2	0.0070
248	1422533_at	Cyp51	cytochrome P450, family 51	+	1.2	0.0040
249	1419070_at	Cys1	cystin 1	+	1.3	0.0011
250	1419995_at	D10Ertd641e	DNA segment, Chr 10, ERATO Doi 641, expressed	+	1.3	0.0071
251	1443490_at	D3Ertd34e	DNA segment, Chr 3, ERATO Doi 34, expressed	+	1.2	0.0075
252	1448538_a_at	D4Wsu53e	DNA segment, Chr 4, Wayne State University 53, expressed	+	1.2	0.0089
253	1447526_at	D5Ertd255e	DNA segment, Chr 5, ERATO Doi 255, expressed	+	1.2	0.0088
254	1458022_at	D830039M14Rik	RIKEN cDNA D830039M14 gene	-	1.2	0.0024
255	1420695_at	Dach1	dachshund 1 (Drosophila)	-	1.2	0.0087
256	1423446_at	Dapk3	death-associated protein kinase 3	-	1.3	0.0009
257	1418174_at	Dbp	D site albumin promoter binding protein	-	1.2	0.0028
258	1451641_at	Dbr1	debranching enzyme homolog 1 (S. cerevisiae)	+	1.2	0.0049
259	1422521_at	Dctn1	dynactin 1	-	1.2	0.0089
260	1434281_at	Dda1	DET1 and DDB1 associated 1	+	1.1	0.0085
261	1419492_s_at	Defb1	defensin beta 1	+	1.2	0.0091
262	1426732_at	Des	desmin	-	1.2	0.0064
263	1459365_at	Dis3l2	DIS3 mitotic control homolog (S. cerevisiae)-like 2	-	1.2	0.0081
264	1427252_at	Dmrtb1	DMRT-like family B with proline-rich C-terminal, 1	+	1.2	0.0011
265	1421032_a_at	Dnajb12	DnaJ (Hsp40) homolog, subfamily B, member 12	-	1.2	0.0022
266	1449373_at	Dnajc3	DnaJ (Hsp40) homolog, subfamily C, member 3	+	1.2	0.0083
267	1433887_at	Dnajc3	DnaJ (Hsp40) homolog, subfamily C, member 3	+	1.2	0.0041
268	1431215_at	Dnajc6	DnaJ (Hsp40) homolog, subfamily C, member 6	-	1.3	0.0069
269	1427754_a_at	Dnm1	dynamin 1	-	1.3	0.0038
270	1451676_at	Drap1	Dr1 associated protein 1 (negative cofactor 2 alpha)	-	1.2	0.0049
271	1422830_s_at	Drd4	dopamine receptor 4	+	1.3	0.0032
272	1427392_at	Dscaml1	Down syndrome cell adhesion molecule-like 1	-	1.2	0.0094
273	1432196_a_at	Dscaml1	Down syndrome cell adhesion molecule-like 1	-	1.2	0.0075
274	1452912_at	Dscc1	defective in sister chromatid cohesion 1 homolog (S. cerevisiae)	-	1.2	0.0021
275	1426189_at	Dusp15	dual specificity phosphatase-like 15	-	1.2	0.0037
276	1422254_a_at	Dyrk1b	dual-specificity tyrosine-(Y)-phosphorylation regulated kinase 1b	+	1.3	0.0036
277	1438277_at	E130308A19Rik	RIKEN cDNA E130308A19 gene	+	1.4	0.0010
278	1456585_x_at	E130309D02Rik	RIKEN cDNA E130309D02 gene	+	1.2	0.0091
279	1433798_a_at	E330034G19Rik	RIKEN cDNA E330034G19 gene	+	1.2	0.0016
280	1418062_at	Eef1a2	eukaryotic translation elongation factor 1 alpha 2	-	1.2	0.0044
281	1428135_a_at	Eef1d	eukaryotic translation elongation factor 1 delta (guanine nucleotide exchange protein)	+	1.2	0.0060
282	1437229_at	Efhb	EF hand domain family, member B	+	1.3	0.0015

#	ID	SYMBOL	GENENAME	Effect	FC	P.Value
283	1449549_at	Efnb2	ephrin B2	+	1.4	0.0001
284	1438836_at	Eftud2	elongation factor Tu GTP binding domain containing 2	+	1.3	0.0004
285	1427797_s_at	EG665955	predicted gene, EG665955	-	1.3	0.0045
286	1424932_at	Egfr	epidermal growth factor receptor	-	1.1	0.0070
287	1427683_at	Egr2	early growth response 2	+	1.4	0.0032
288	1436329_at	Egr3	early growth response 3	+	1.2	0.0060
289	1436006_at	Eif2ak1	eukaryotic translation initiation factor 2 alpha kinase 1	-	1.1	0.0073
290	1417712_at	Eif2s2	eukaryotic translation initiation factor 2, subunit 2 (beta)	-	1.1	0.0079
291	1455994_x_at	Elovl1	elongation of very long chain fatty acids (FEN1/Elo2, SUR4/Elo3, yeast)-like 1	+	1.2	0.0080
292	1456258_at	Emx2	empty spiracles homolog 2 (Drosophila)	+	1.2	0.0026
293	1434580_at	Enpp4	ectonucleotide pyrophosphatase/phosphodiesterase 4	+	1.2	0.0006
294	1434606_at	Erbb3	v-erb-b2 erythroblastic leukemia viral oncogene homolog 3 (avian)	+	1.2	0.0084
295	1440237_at	Ercc4	excision repair cross-complementing rodent repair deficiency, complementation group 4	-	1.1	0.0061
296	1425265_a_at	Eri3	exoribonuclease 3	-	1.3	0.0021
297	1421244_at	Esr1	estrogen receptor 1 (alpha)	+	1.2	0.0082
298	1451099_at	Esyt1	extended synaptotagmin-like protein 1	-	1.2	0.0042
299	1418462_at	Exosc9	exosome component 9	-	1.2	0.0071
300	1418290_a_at	Ezh1	enhancer of zeste homolog 1 (Drosophila)	+	1.3	0.0083
301	1450779_at	Fabp7	fatty acid binding protein 7, brain	-	1.3	0.0005
302	1449219_at	Fads3	fatty acid desaturase 3	-	1.3	0.0094
303	1429764_at	Fam101b	family with sequence similarity 101, member B	+	1.2	0.0099
304	1436140_at	Fam116b	family with sequence similarity 116, member B	-	1.2	0.0040
305	1433639_at	Fam117a	family with sequence similarity 117, memberA	+	1.2	0.0047
306	1432435_s_at	Fam118b	family with sequence similarity 118, member B	+	1.2	0.0027
307	1457728_at	Fam129c	family with sequence similarity 129, member C	+	1.2	0.0060
308	1447884_x_at	Fam134c	family with sequence similarity 134, member C	+	1.2	0.0077
309	1457246_at	Fam160b2	family with sequence similarity 160, member B2	+	1.2	0.0039
310	1443747_at	Fam48a	family with sequence similarity 48, member A	+	1.3	0.0033
311	1431173_at	Fam53b	family with sequence similarity 53, member B	+	1.2	0.0042
312	1420059_at	Fam54b	family with sequence similarity 54, member B	+	1.4	0.0004
313	1452806_at	Fam57b	family with sequence similarity 57, member B	-	1.2	0.0073
314	1423709_s_at	Farsb	phenylalanyl-tRNA synthetase, beta subunit	-	1.2	0.0081
315	1457232_at	Fbxl21	F-box and leucine-rich repeat protein 21	-	1.2	0.0053
316	1456038_at	Fbxl4	F-box and leucine-rich repeat protein 4	-	1.1	0.0079
317	1426593_a_at	Fbxo22	F-box protein 22	+	1.2	0.0024
318	1447671_x_at	Fbxo6	F-box protein 6	-	1.2	0.0041
319	1436732_s_at	Fbxw8	F-box and WD-40 domain protein 8	-	1.2	0.0039
320	1429991_at	Fezf1	Fez family zinc finger 1	+	1.3	0.0024
321	1425911_a_at	Fgfr1	fibroblast growth factor receptor 1	-	1.3	0.0055
322	1450728_at	Fjx1	four jointed box 1 (Drosophila)	-	1.2	0.0005
323	1416113_at	Fkbp8	FK506 binding protein 8	-	1.3	0.0016
324	1438167_x_at	Flcn	folliculin	+	1.1	0.0047
325	1426677_at	Flna	filamin, alpha	-	1.2	0.0013
326	1417544_a_at	Flot2	flotillin 2	-	1.2	0.0018
327	1440926_at	Flt1	FMS-like tyrosine kinase 1	+	1.2	0.0004
328	1423100_at	Fos	FBJ osteosarcoma oncogene	+	1.8	0.0014
329	1454831_at	Foxn2	forkhead box N2	+	1.2	0.0021
330	1416983_s_at	Foxo1	forkhead box O1	-	1.2	0.0070
331	1438169_a_at	Frmd4b	FERM domain containing 4B	+	1.2	0.0006
332	1449121_at	Fusip1	FUS interacting protein (serine-arginine rich) 1	+	1.2	0.0031
333	1419451_at	Fzr1	fizzy/cell division cycle 20 related 1 (Drosophila)	-	1.2	0.0050
334	1440342_at	G530011O06Rik	RIKEN cDNA G530011O06 gene	+	1.6	0.0057
335	1428245_at	G6pc3	glucose 6 phosphatase, catalytic, 3	-	1.2	0.0033
336	1442120_at	G730007D18Rik	RIKEN cDNA G730007D18 gene	+	1.2	0.0004
337	1421263_at	Gabra3	gamma-aminobutyric acid (GABA) A receptor, subunit alpha 3	-	1.3	0.0036
338	1421629_at	Gabre	gamma-aminobutyric acid (GABA) A receptor, subunit epsilon	+	1.2	0.0081
339	1449773_s_at	Gadd45b	growth arrest and DNA-damage-inducible 45 beta	+	1.2	0.0025
340	1446657_at	Galnt6	UDP-N-acetyl-alpha-D-galactosamine:polypeptide N-acetylgalactosaminyltransferase 6	+	1.2	0.0018
341	1418240_at	Gbp2	guanylate binding protein 2	+	1.2	0.0043
342	1455443_at	Gdap1l1	ganglioside-induced differentiation-associated protein 1-like 1	-	1.3	0.0007
343	1433622_at	Gemin4	gem (nuclear organelle) associated protein 4	-	1.2	0.0093
344	1450835_a_at	Gfra4	glial cell line derived neurotrophic factor family receptor alpha 4	-	1.1	0.0092
345	1457472_at	Gigyf2	GRB10 interacting GYF protein 2	+	1.2	0.0078
346	1428713_s_at	Gins2	GINS complex subunit 2 (Psf2 homolog)	+	1.1	0.0069
347	1445790_at	Gipr	gastric inhibitory polypeptide receptor	+	1.2	0.0044
348	1454759_at	Git1	G protein-coupled receptor kinase-interactor 1	-	1.2	0.0087
349	1422042_at	Gje1	gap junction membrane channel protein epsilon 1	+	1.2	0.0061
350	1445523_at	Gje1	gap junction membrane channel protein epsilon 1	+	1.2	0.0006
351	1437340_x_at	Gkn1	gastrokine 1	+	1.2	0.0046
352	1449006_at	Gla	galactosidase, alpha	-	1.2	0.0018
353	1442089_at	Gm11563	predicted gene 11563	+	1.3	0.0057
354	1435188_at	Gm129	predicted gene 129	-	1.3	0.0047

#	ID	SYMBOL	GENENAME	Effect	FC	P.Value
355	1431971_at	Gm14318	predicted gene 14318	+	1.2	0.0082
356	1459006_a_at	Gm2824	predicted gene 2824	-	1.2	0.0090
357	1455624_at	Gm3764	predicted gene 3764	-	1.3	0.0002
358	1459503_at	Gm3764	predicted gene 3764	+	1.2	0.0088
359	1443460_at	Gm4250	predicted gene 4250	+	1.3	0.0062
360	1460021_at	Gm6658	predicted gene 6658	-	1.2	0.0055
361	1426607_at	Gm7120	predicted gene 7120	+	1.5	0.0026
362	1442246_at	Gm9054	predicted gene 9054	-	1.3	0.0060
363	1453548_at	Gm9558	predicted gene 9558	+	1.3	0.0053
364	1417579_x_at	Gmppa	GDP-mannose pyrophosphorylase A	-	1.2	0.0066
365	1455458_x_at	Gmppa	GDP-mannose pyrophosphorylase A	-	1.1	0.0088
366	1440120_at	Gnb2l1	guanine nucleotide binding protein (G protein), beta polypeptide 2 like 1	+	1.2	0.0030
367	1453297_at	Golga7b	golgi autoantigen, golgin subfamily a, 7B	-	1.2	0.0057
368	1417716_at	Got2	glutamate oxaloacetate transaminase 2, mitochondrial	-	1.2	0.0042
369	1450990_at	Gpc3	glypican 3	-	1.4	0.0030
370	1460123_at	Gpr1	G protein-coupled receptor 1	-	1.2	0.0055
371	1451060_at	Gpr146	G protein-coupled receptor 146	-	1.2	0.0051
372	1434672_at	Gpr22	G protein-coupled receptor 22	-	1.4	0.0003
373	1424613_at	Gprc5b	G protein-coupled receptor, family C, group 5, member B	+	1.2	0.0050
374	1417796_at	Gps2	G protein pathway suppressor 2	-	1.2	0.0040
375	1429387_at	Grap	GRB2-related adaptor protein	-	1.2	0.0052
376	1438866_at	Grin3a	glutamate receptor ionotropic, NMDA3A	-	1.2	0.0049
377	1425626_at	Gstm1	glutathione S-transferase, mu 1	+	1.2	0.0086
378	1424835_at	Gstm4	glutathione S-transferase, mu 4	-	1.2	0.0011
379	1451899_a_at	Gtf2ird1	general transcription factor II I repeat domain-containing 1	-	1.2	0.0024
380	1435735_x_at	H47	histocompatibility 47	+	1.2	0.0025
381	1436152_a_at	Hbxip	hepatitis B virus x interacting protein	+	1.2	0.0061
382	1446415_at	Hebp2	heme binding protein 2	-	1.2	0.0061
383	1442051_at	Hist2h3c1	histone cluster 2, H3c1	+	1.2	0.0034
384	1422155_at	Hist2h3c2	histone cluster 2, H3c2	+	1.3	0.0022
385	1435866_s_at	Hist3h2a	histone cluster 3, H2a	+	1.3	0.0004
386	1420901_a_at	Hk1	hexokinase 1	-	1.2	0.0045
387	1421234_at	Hnf1a	HNF1 homeobox A	+	1.3	0.0036
388	1448408_at	Hps1	Hermansky-Pudlak syndrome 1 homolog (human)	-	1.3	0.0004
389	1452318_a_at	Hspa1b	heat shock protein 1B	+	1.4	0.0014
390	1440575_at	Hspa4	heat shock protein 4	+	1.2	0.0082
391	1447824_x_at	Hspa5	heat shock protein 5	+	1.3	0.0088
392	1427464_s_at	Hspa5	heat shock protein 5	+	1.3	0.0016
393	1416064_a_at	Hspa5	heat shock protein 5	+	1.3	0.0008
394	1431274_a_at	Hspa9	heat shock protein 9	-	1.2	0.0021
395	1417612_at	Ier5	immediate early response 5	+	1.3	0.0048
396	1440169_x_at	Ifnar2	interferon (alpha and beta) receptor 2	+	1.3	0.0011
397	1441259_s_at	Ift122	intraflagellar transport 122 homolog (Chlamydomonas)	+	1.2	0.0087
398	1427351_s_at	Igh-6	immunoglobulin heavy chain 6 (heavy chain of IgM)	-	1.3	0.0078
399	1450091_at	Ighmbp2	immunoglobulin mu binding protein 2	+	1.3	0.0013
400	1420177_at	Igll1	immunoglobulin lambda-like polypeptide 1	-	1.2	0.0012
401	1460675_at	Igsf8	immunoglobulin superfamily, member 8	-	1.2	0.0036
402	1425625_at	Il13ra1	interleukin 13 receptor, alpha 1	+	1.1	0.0096
403	1448950_at	Il1r1	interleukin 1 receptor, type I	+	1.2	0.0061
404	1453305_at	Iqcd	IQ motif containing D	+	1.3	0.0039
405	1422683_at	Irak1bp1	interleukin-1 receptor-associated kinase 1 binding protein 1	-	1.2	0.0089
406	1426111_x_at	Irf3	interferon regulatory factor 3	+	1.2	0.0077
407	1419357_at	Isy1	ISY1 splicing factor homolog (S. cerevisiae)	-	1.2	0.0042
408	1436037_at	Itga4	integrin alpha 4	-	1.2	0.0079
409	1436579_s_at	Itsn1	intersectin 1 (SH3 domain protein 1A)	+	1.2	0.0033
410	1435884_at	Itsn1	intersectin 1 (SH3 domain protein 1A)	+	1.2	0.0020
411	1443724_at	Jph3	junctophilin 3	+	1.2	0.0090
412	1417409_at	Jun	Jun oncogene	+	1.2	0.0053
413	1448023_at	Kalrn	kalirin, RhoGEF kinase	+	1.2	0.0063
414	1457690_at	Kalrn	kalirin, RhoGEF kinase	+	1.2	0.0058
415	1418544_at	Kcnip3	Kv channel interacting protein 3, calsenilin	-	1.4	0.0044
416	1421342_at	Kcns2	K+ voltage-gated channel, subfamily S, 2	+	1.2	0.0094
417	1429741_at	Kcnv1	potassium channel, subfamily V, member 1	-	1.2	0.0036
418	1417205_at	Kdelr2	KDEL (Lys-Asp-Glu-Leu) endoplasmic reticulum protein retention receptor 2	-	1.2	0.0017
419	1440346_at	Kdm6b	KDM1 lysine (K)-specific demethylase 6B	+	1.3	0.0055
420	1450108_at	Kif1a	kinesin family member 1A	-	1.2	0.0045
421	1426493_a_at	Kifc2	kinesin family member C2	-	1.3	0.0012
422	1421312_a_at	Kifc2	kinesin family member C2	-	1.2	0.0058
423	1448117_at	Kitl	kit ligand	-	1.3	0.0054
424	1448164_at	Klhdc3	kelch domain containing 3	-	1.3	0.0001
425	1424887_at	Klhdc4	kelch domain containing 4	-	1.2	0.0059
426	1425664_at	Klhl20	kelch-like 20 (Drosophila)	-	1.2	0.0095
427	1435575_at	Kntc1	kinetochore associated 1	-	1.2	0.0043
428	1435472_at	Kremen1	kringle containing transmembrane protein 1	+	1.1	0.0087
429	1430669_at	Krtap4-7	keratin associated protein 4-7	+	1.2	0.0057
430	1425141_at	Lactb2	lactamase, beta 2	-	1.2	0.0091

#	ID	SYMBOL	GENENAME	Effect	FC	P.Value
431	1436915_x_at	Laptm4b	lysosomal-associated protein transmembrane 4B	+	1.2	0.0022
432	1438633_x_at	Lasp1	LIM and SH3 protein 1	+	1.2	0.0063
433	1439479_at	Lct	lactase	+	1.2	0.0017
434	1450383_at	Ldlr	low density lipoprotein receptor	-	1.3	0.0002
435	1436900_x_at	Leprot	leptin receptor overlapping transcript	+	1.2	0.0044
436	1435499_at	Letm2	leucine zipper-EF-hand containing transmembrane protein 2	-	1.1	0.0096
437	1422662_at	Lgals8	lectin, galactose binding, soluble 8	-	1.1	0.0083
438	1456838_at	Lingo3	leucine rich repeat and Ig domain containing 3	-	1.2	0.0090
439	1431492_at	Lipn	lipase, family member N	+	1.3	0.0088
440	1428129_at	Lman1	lectin, mannose-binding, 1	+	1.2	0.0020
441	1444491_at	LOC100042150	similar to NTAK alpha2	+	1.2	0.0023
442	1454666_at	LOC100046855	similar to BKLF	+	1.1	0.0088
443	1455557_at	LOC553095	hypothetical LOC553095	+	1.2	0.0084
444	1429863_at	Lonrf3	LON peptidase N-terminal domain and ring finger 3	+	1.2	0.0094
445	1440207_at	Lpcat4	lysophosphatidylcholine acyltransferase 4	-	1.2	0.0078
446	1444669_at	Lrfn1	leucine rich repeat and fibronectin type III domain containing 1	-	1.2	0.0089
447	1436083_at	Lrp3	low density lipoprotein receptor-related protein 3	-	1.2	0.0019
448	1426288_at	Lrp4	low density lipoprotein receptor-related protein 4	+	1.2	0.0013
449	1455883_a_at	Lrrtm1	leucine rich repeat transmembrane neuronal 1	+	1.2	0.0084
450	1428437_at	Lsm14a	LSM14 homolog A (SCD6, S. cerevisiae)	+	1.1	0.0097
451	1453304_s_at	Ly6e	lymphocyte antigen 6 complex, locus E	-	1.3	0.0009
452	1447945_at	Maf	avian musculoaponeurotic fibrosarcoma (v-maf) AS42 oncogene homolog	-	1.2	0.0056
453	1428112_at	Manf	mesencephalic astrocyte-derived neurotrophic factor	+	1.2	0.0034
454	1453712_a_at	Map2k5	mitogen-activated protein kinase kinase 5	-	1.2	0.0098
455	1421416_at	Map2k7	mitogen-activated protein kinase kinase 7	+	1.2	0.0038
456	1443540_at	Map3k1	mitogen-activated protein kinase kinase kinase 1	+	1.2	0.0092
457	1447667_x_at	Map3k4	mitogen-activated protein kinase kinase kinase 4	+	1.1	0.0098
458	1455441_at	Map3k7	mitogen-activated protein kinase kinase kinase 7	-	1.2	0.0048
459	1427079_at	Mapre3	microtubule-associated protein, RP/EB family, member 3	-	1.4	0.0001
460	1455346_at	Masp1	mannan-binding lectin serine peptidase 1	-	1.2	0.0062
461	1455978_a_at	Matn2	matrilin 2	+	1.2	0.0045
462	1449490_at	Mbd4	methyl-CpG binding domain protein 4	+	1.2	0.0028
463	1418787_at	Mbl2	mannose-binding lectin (protein C) 2	-	1.1	0.0068
464	1456381_x_at	Mcl1	myeloid cell leukemia sequence 1	+	1.2	0.0089
465	1416006_at	Mdk	midkine	-	1.3	0.0036
466	1425585_at	Med12	mediator of RNA polymerase II transcription, subunit 12 homolog (yeast)	-	1.2	0.0069
467	1456785_at	Med14	mediator complex subunit 14	-	1.2	0.0057
468	1416826_a_at	Med20	mediator complex subunit 20	+	1.3	0.0025
469	1426758_s_at	Meg3	maternally expressed 3	-	1.2	0.0083
470	1423984_a_at	Meis3	Meis homeobox 3	-	1.2	0.0071
471	1426837_at	Metap1	methionyl aminopeptidase 1	-	1.2	0.0069
472	1453983_a_at	Mett10d	methyltransferase 10 domain containing	+	1.2	0.0067
473	1447683_x_at	Mettl1	methyltransferase like 1	-	1.2	0.0050
474	1416358_at	Mfsd10	major facilitator superfamily domain containing 10	-	1.2	0.0061
475	1444199_at	Mfsd4	major facilitator superfamily domain containing 4	+	1.2	0.0070
476	1417120_at	Miip	migration and invasion inhibitory protein	-	1.2	0.0076
477	1454014_a_at	Mkks	McKusick-Kaufman syndrome protein	+	1.2	0.0062
478	1427283_at	Mll1	myeloid/lymphoid or mixed-lineage leukemia 1	-	1.2	0.0072
479	1459611_at	Mpp3	membrane protein, palmitoylated 3 (MAGUK p55 subfamily member 3)	-	1.2	0.0077
480	1418356_at	Mpst	mercaptopyruvate sulfurtransferase	+	1.2	0.0058
481	1428167_a_at	Mpzl1	myelin protein zero-like 1	+	1.3	0.0000
482	1417146_at	Mri1	methylthioribose-1-phosphate isomerase homolog (S. cerevisiae)	-	1.2	0.0035
483	1460354_a_at	Mrpl13	mitochondrial ribosomal protein L13	+	1.1	0.0045
484	1444306_at	Msi1	Musashi homolog 1(Drosophila)	+	1.2	0.0019
485	1460566_at	Mtap1a	microtubule-associated protein 1 A	-	1.2	0.0030
486	1429894_a_at	Mtap7	microtubule-associated protein 7	+	1.2	0.0080
487	1449199_at	Muc1	mucin 1, transmembrane	-	1.2	0.0035
488	1430539_at	Mxra7	matrix-remodelling associated 7	+	1.2	0.0080
489	1427769_x_at	Myl3	myosin, light polypeptide 3	+	1.3	0.0077
490	1460159_at	Mysm1	myb-like, SWIRM and MPN domains 1	-	1.3	0.0049
491	1446957_s_at	N4bp1	NEDD4 binding protein 1	+	1.2	0.0063
492	1435269_at	N6amt2	N-6 adenine-specific DNA methyltransferase 2 (putative)	-	1.2	0.0021
493	1455869_at	NA	NA	-	1.8	0.0009
494	1435353_a_at	NA	NA	-	1.6	0.0057
495	1431213_a_at	NA	NA	-	1.5	0.0037
496	1423916_s_at	NA	NA	-	1.4	0.0008
497	1434270_at	NA	NA	-	1.4	0.0003
498	1440030_at	NA	NA	-	1.4	0.0074
499	1450455_s_at	NA	NA	-	1.3	0.0055
500	1456160_at	NA	NA	-	1.3	0.0077
501	1422319_at	NA	NA	-	1.3	0.0002
502	1437183_at	NA	NA	-	1.3	0.0067
503	1459062_x_at	NA	NA	-	1.3	0.0033

#	ID	SYMBOL	GENENAME	Effect	FC	P.Value
504	1447559_at	NA	NA	-	1.3	0.0007
505	1420084_at	NA	NA	-	1.3	0.0011
506	1429546_at	NA	NA	-	1.3	0.0010
507	1440055_at	NA	NA	-	1.3	0.0074
508	1417524_at	NA	NA	-	1.3	0.0027
509	1444495_at	NA	NA	-	1.3	0.0004
510	1446571_at	NA	NA	-	1.3	0.0021
511	1440380_at	NA	NA	-	1.3	0.0094
512	1440099_at	NA	NA	-	1.2	0.0069
513	1442386_at	NA	NA	-	1.2	0.0054
514	1441472_at	NA	NA	-	1.2	0.0007
515	1457920_at	NA	NA	-	1.2	0.0019
516	1418768_at	NA	NA	-	1.2	0.0026
517	1459590_at	NA	NA	-	1.2	0.0017
518	1446182_at	NA	NA	-	1.2	0.0071
519	1448796_s_at	NA	NA	-	1.2	0.0092
520	1455503_at	NA	NA	-	1.2	0.0097
521	1415896_x_at	NA	NA	-	1.2	0.0021
522	1445110_at	NA	NA	-	1.2	0.0055
523	1415895_at	NA	NA	-	1.2	0.0022
524	1445564_at	NA	NA	-	1.2	0.0061
525	1443707_at	NA	NA	-	1.2	0.0029
526	1421181_at	NA	NA	-	1.2	0.0013
527	1444510_at	NA	NA	-	1.2	0.0020
528	1447223_at	NA	NA	-	1.2	0.0027
529	1443544_at	NA	NA	-	1.2	0.0030
530	1421063_s_at	NA	NA	-	1.2	0.0015
531	1426040_a_at	NA	NA	-	1.2	0.0028
532	1452100_at	NA	NA	-	1.2	0.0032
533	1440755_at	NA	NA	-	1.2	0.0065
534	1443038_at	NA	NA	-	1.2	0.0062
535	1436599_at	NA	NA	-	1.2	0.0037
536	1445717_at	NA	NA	-	1.2	0.0099
537	1438780_at	NA	NA	-	1.2	0.0054
538	1419794_at	NA	NA	-	1.2	0.0087
539	1458324_x_at	NA	NA	-	1.2	0.0044
540	1427968_at	NA	NA	-	1.2	0.0096
541	1445485_at	NA	NA	-	1.2	0.0085
542	1445603_at	NA	NA	-	1.2	0.0066
543	1441164_at	NA	NA	-	1.2	0.0048
544	1446372_at	NA	NA	-	1.2	0.0093
545	1435716_x_at	NA	NA	-	1.2	0.0051
546	1458341_x_at	NA	NA	-	1.2	0.0065
547	1460072_at	NA	NA	-	1.1	0.0082
548	1442087_at	NA	NA	+	1.1	0.0081
549	1459367_at	NA	NA	+	1.1	0.0067
550	1454639_x_at	NA	NA	+	1.1	0.0051
551	1434848_at	NA	NA	+	1.1	0.0052
552	1445569_at	NA	NA	+	1.1	0.0076
553	1438553_x_at	NA	NA	+	1.1	0.0058
554	1442681_at	NA	NA	+	1.2	0.0093
555	1443050_at	NA	NA	+	1.2	0.0065
556	1444971_at	NA	NA	+	1.2	0.0078
557	1435129_at	NA	NA	+	1.2	0.0063
558	1459285_at	NA	NA	+	1.2	0.0055
559	1445590_at	NA	NA	+	1.2	0.0099
560	1447000_at	NA	NA	+	1.2	0.0091
561	1438596_at	NA	NA	+	1.2	0.0064
562	1439683_at	NA	NA	+	1.2	0.0070
563	1458406_at	NA	NA	+	1.2	0.0040
564	1444473_at	NA	NA	+	1.2	0.0045
565	1445729_at	NA	NA	+	1.2	0.0045
566	1457637_at	NA	NA	+	1.2	0.0083
567	1457247_at	NA	NA	+	1.2	0.0036
568	1424972_at	NA	NA	+	1.2	0.0083
569	1453682_at	NA	NA	+	1.2	0.0073
570	1437026_at	NA	NA	+	1.2	0.0069
571	1449760_at	NA	NA	+	1.2	0.0090
572	1438908_at	NA	NA	+	1.2	0.0029
573	1443354_at	NA	NA	+	1.2	0.0046
574	1439600_at	NA	NA	+	1.2	0.0065
575	1446784_at	NA	NA	+	1.2	0.0045
576	1445529_at	NA	NA	+	1.2	0.0097
577	1423585_at	NA	NA	+	1.2	0.0070
578	1420128_s_at	NA	NA	+	1.2	0.0079
579	1425872_at	NA	NA	+	1.2	0.0075
580	1447958_at	NA	NA	+	1.2	0.0047
581	1434589_x_at	NA	NA	+	1.2	0.0038
582	1442929_at	NA	NA	+	1.2	0.0029
583	1434150_a_at	NA	NA	+	1.2	0.0061
584	1442527_at	NA	NA	+	1.2	0.0062

#	ID	SYMBOL	GENENAME	Effect	FC	P.Value
585	1435311_s_at	NA	NA	+	1.2	0.0011
586	1459071_at	NA	NA	+	1.2	0.0019
587	1447176_at	NA	NA	+	1.2	0.0047
588	1444057_at	NA	NA	+	1.2	0.0056
589	1457132_at	NA	NA	+	1.2	0.0037
590	1458692_at	NA	NA	+	1.2	0.0012
591	1458598_at	NA	NA	+	1.2	0.0020
592	1458494_at	NA	NA	+	1.2	0.0057
593	1436687_x_at	NA	NA	+	1.2	0.0005
594	1459733_at	NA	NA	+	1.2	0.0086
595	1445735_at	NA	NA	+	1.2	0.0031
596	1459419_at	NA	NA	+	1.2	0.0060
597	1422096_at	NA	NA	+	1.2	0.0030
598	1442435_at	NA	NA	+	1.2	0.0069
599	1446335_at	NA	NA	+	1.2	0.0074
600	1438931_s_at	NA	NA	+	1.2	0.0009
601	1439053_at	NA	NA	+	1.2	0.0082
602	1439265_at	NA	NA	+	1.2	0.0083
603	1438622_x_at	NA	NA	+	1.2	0.0005
604	1445755_at	NA	NA	+	1.2	0.0086
605	1447560_at	NA	NA	+	1.2	0.0060
606	1456909_at	NA	NA	+	1.2	0.0006
607	1458805_at	NA	NA	+	1.3	0.0011
608	1432828_at	NA	NA	+	1.3	0.0092
609	1437767_s_at	NA	NA	+	1.3	0.0009
610	1437455_a_at	NA	NA	+	1.3	0.0021
611	1447479_at	NA	NA	+	1.3	0.0028
612	1447511_at	NA	NA	+	1.3	0.0055
613	1447454_at	NA	NA	+	1.3	0.0077
614	1434029_at	NA	NA	+	1.3	0.0095
615	1456687_at	NA	NA	+	1.3	0.0024
616	1445262_at	NA	NA	+	1.3	0.0066
617	1457015_at	NA	NA	+	1.3	0.0001
618	1443770_x_at	NA	NA	+	1.3	0.0024
619	1422416_s_at	NA	NA	+	1.3	0.0008
620	1419946_s_at	NA	NA	+	1.3	0.0020
621	1438009_at	NA	NA	+	1.3	0.0002
622	1420287_at	NA	NA	+	1.3	0.0007
623	1441530_at	NA	NA	+	1.3	0.0057
624	1449790_at	NA	NA	+	1.3	0.0026
625	1458629_at	NA	NA	+	1.4	0.0017
626	1445977_at	NA	NA	+	1.4	0.0002
627	1444913_at	NA	NA	+	1.4	0.0021
628	1420094_at	NA	NA	+	1.4	0.0001
629	1419937_at	NA	NA	+	1.4	0.0001
630	1454284_at	NA	NA	+	1.4	0.0002
631	1459066_at	NA	NA	+	1.5	0.0026
632	1437729_at	NA	NA	+	1.5	0.0018
633	1449727_x_at	NA	NA	+	1.5	0.0015
634	1419915_at	NA	NA	+	1.6	0.0003
635	1449788_at	NA	NA	+	1.6	0.0002
636	1454378_at	NA	NA	+	1.8	0.0035
637	1420968_at	Nacc1	nucleus accumbens associated 1, BEN and BTB (POZ) domain containing	+	1.2	0.0020
638	1418570_at	Ncstn	nicastrin	-	1.2	0.0071
639	1453565_at	Ndufab1	NADH dehydrogenase (ubiquinone) 1, alpha/beta subcomplex, 1	+	1.2	0.0095
640	1428160_at	Ndufab1	NADH dehydrogenase (ubiquinone) 1, alpha/beta subcomplex, 1	+	1.3	0.0040
641	1431670_at	Ndufc2	NADH dehydrogenase (ubiquinone) 1, subcomplex unknown, 2	+	1.3	0.0048
642	1418881_at	Necab2	N-terminal EF-hand calcium binding protein 2	-	1.2	0.0050
643	1425714_a_at	Nfam1	Nfat activating molecule with ITAM motif 1	+	1.3	0.0007
644	1455891_at	Nhedc1	Na+/H+ exchanger domain containing 1	+	1.3	0.0033
645	1429145_at	Nhlrc2	NHL repeat containing 2	+	1.2	0.0035
646	1456467_s_at	Nlk	nemo like kinase	+	1.1	0.0067
647	1424899_at	Nmnat3	nicotinamide nucleotide adenylyltransferase 3	+	1.2	0.0073
648	1423506_a_at	Nnat	neuronatin	-	1.4	0.0013
649	1416105_at	Nnt	nicotinamide nucleotide transhydrogenase	-	1.2	0.0088
650	1420487_at	Nol7	nucleolar protein 7	+	1.2	0.0076
651	1453114_at	Nol9	nucleolar protein 9	+	1.2	0.0087
652	1425151_a_at	Noxo1	NADPH oxidase organizer 1	-	1.2	0.0037
653	1432416_a_at	Npm1	nucleophosmin 1	-	1.2	0.0034
654	1452107_s_at	Npnt	nephronectin	+	1.2	0.0027
655	1427191_at	Npr2	natriuretic peptide receptor 2	-	1.3	0.0001
656	1454167_at	Nr2c2	nuclear receptor subfamily 2, group C, member 2	+	1.2	0.0022
657	1457635_s_at	Nr3c1	nuclear receptor subfamily 3, group C, member 1	+	1.2	0.0079
658	1434640_at	Nrsn2	neurensin 2	-	1.3	0.0039
659	1455499_at	Nrxn2	neurexin II	-	1.4	0.0008
660	1455387_at	Nufip2	nuclear fragile X mental retardation protein interacting protein 2	+	1.4	0.0004

#	ID	SYMBOL	GENENAME	Effect	FC	P.Value
661	1435216_a_at	Odf2	outer dense fiber of sperm tails 2	-	1.2	0.0087
662	1455796_x_at	Olfm1	olfactomedin 1	+	1.1	0.0074
663	1426512_at	Olfm3	olfactomedin 3	-	1.3	0.0005
664	1455743_at	Olfml2a	olfactomedin-like 2A	+	1.3	0.0054
665	1418212_at	Omg	oligodendrocyte myelin glycoprotein	-	1.1	0.0086
666	1458350_at	Opa3	optic atrophy 3 (human)	+	1.2	0.0081
667	1459402_at	Oprm1	opioid receptor, mu 1	+	1.2	0.0032
668	1424235_at	Ormdl2	ORM1-like 2 (S. cerevisiae)	+	1.2	0.0055
669	1449627_at	Osbpl6	oxysterol binding protein-like 6	+	1.3	0.0008
670	1425540_at	Otc	ornithine transcarbamylase	-	1.3	0.0037
671	1448817_at	Otub1	OTU domain, ubiquitin aldehyde binding 1	-	1.2	0.0010
672	1417575_at	Otub2	OTU domain, ubiquitin aldehyde binding 2	+	1.2	0.0015
673	1452094_at	P4ha1	procollagen-proline, 2-oxoglutarate 4-dioxygenase (proline 4-hydroxylase), alpha 1 polypeptide	+	1.2	0.0032
674	1460265_at	Pa2g4	proliferation-associated 2G4	+	1.2	0.0018
675	1449381_a_at	Pacsin1	protein kinase C and casein kinase substrate in neurons 1	-	1.3	0.0009
676	1455216_at	Paqr6	progestin and adipoQ receptor family member VI	-	1.2	0.0085
677	1449975_a_at	Park2	Parkinson disease (autosomal recessive, juvenile) 2, parkin	-	1.2	0.0008
678	1434363_x_at	Paxip1	PAX interacting (with transcription-activation domain) protein 1	+	1.2	0.0053
679	1427956_at	Pcgf1	polycomb group ring finger 1	-	1.2	0.0004
680	1432108_at	Pcgf6	polycomb group ring finger 6	+	1.2	0.0050
681	1454120_a_at	Pcgf6	polycomb group ring finger 6	+	1.2	0.0010
682	1425824_a_at	Pcsk4	proprotein convertase subtilisin/kexin type 4	-	1.2	0.0033
683	1415956_a_at	Pctk1	PCTAIRE-motif protein kinase 1	-	1.3	0.0040
684	1449151_at	Pctk3	PCTAIRE-motif protein kinase 3	-	1.3	0.0010
685	1460263_at	Pdcd6ip	programmed cell death 6 interacting protein	+	1.3	0.0007
686	1425100_a_at	Pde6g	phosphodiesterase 6G, cGMP-specific, rod, gamma	+	1.3	0.0029
687	1428308_at	Pdrg1	p53 and DNA damage regulated 1	+	1.2	0.0076
688	1438358_x_at	Pfdn5	prefoldin 5	+	1.1	0.0052
689	1439148_a_at	Pfkl	phosphofructokinase, liver, B-type	-	1.2	0.0073
690	1449018_at	Pfn1	profilin 1	-	1.3	0.0017
691	1437239_x_at	Phc2	polyhomeotic-like 2 (Drosophila)	+	1.2	0.0010
692	1418620_at	Phox2a	paired-like homeobox 2a	+	1.5	0.0000
693	1427903_at	Phpt1	phosphohistidine phosphatase 1	-	1.2	0.0068
694	1421284_at	Pign	phosphatidylinositol glycan anchor biosynthesis, class N	+	1.2	0.0065
695	1437594_x_at	Pigt	phosphatidylinositol glycan anchor biosynthesis, class T	+	1.4	0.0017
696	1455284_x_at	Pigx	phosphatidylinositol glycan anchor biosynthesis, class X	+	1.2	0.0027
697	1425514_at	Pik3r1	phosphatidylinositol 3-kinase, regulatory subunit, polypeptide 1 (p85 alpha)	+	1.2	0.0049
698	1424954_a_at	Pip5k1c	phosphatidylinositol-4-phosphate 5-kinase, type 1 gamma	-	1.2	0.0085
699	1420307_a_at	Pitpnb	phosphatidylinositol transfer protein, beta	-	1.3	0.0001
700	1452940_x_at	Pitpnc1	phosphatidylinositol transfer protein, cytoplasmic 1	+	1.2	0.0049
701	1454838_s_at	Pkdcc	protein kinase domain containing, cytoplasmic	+	1.2	0.0034
702	1434820_s_at	Pkig	protein kinase inhibitor, gamma	+	1.2	0.0024
703	1417308_at	Pkm2	pyruvate kinase, muscle	-	1.2	0.0077
704	1426208_x_at	Plagl1	pleiomorphic adenoma gene-like 1	-	1.3	0.0080
705	1417963_at	Pltp	phospholipid transfer protein	-	1.3	0.0092
706	1448757_at	Pml	promyelocytic leukemia	+	1.2	0.0053
707	1416378_at	Pnkp	polynucleotide kinase 3'- phosphatase	-	1.2	0.0024
708	1433431_at	Pnlip	pancreatic lipase	+	1.3	0.0087
709	1455622_at	Podxl2	podocalyxin-like 2	-	1.2	0.0056
710	1420910_at	Ppap2c	phosphatidic acid phosphatase type 2C	+	1.4	0.0029
711	1428344_at	Ppapdc2	phosphatidic acid phosphatase type 2 domain containing 2	-	1.2	0.0016
712	1451943_a_at	Ppm1a	protein phosphatase 1A, magnesium dependent, alpha isoform	-	1.2	0.0058
713	1416618_at	Ppox	protoporphyrinogen oxidase	-	1.2	0.0061
714	1431328_at	Ppp1cb	protein phosphatase 1, catalytic subunit, beta isoform	+	1.2	0.0024
715	1448565_at	Ppp1r11	protein phosphatase 1, regulatory (inhibitor) subunit 11	-	1.3	0.0016
716	1424554_at	Ppp1r8	protein phosphatase 1, regulatory (inhibitor) subunit 8	-	1.3	0.0050
717	1415819_a_at	Ppp2r1a	protein phosphatase 2 (formerly 2A), regulatory subunit A (PR 65), alpha isoform	-	1.4	0.0009
718	1420034_at	Ppp2r2d	protein phosphatase 2, regulatory subunit B, delta isoform	+	1.4	0.0099
719	1455198_a_at	Ppp2r3d	protein phosphatase 2 (formerly 2A), regulatory subunit B'', delta	-	1.2	0.0023
720	1440189_at	Ppp2r5a	protein phosphatase 2, regulatory subunit B (B56), alpha isoform	+	1.2	0.0051
721	1434205_at	Ppp2r5c	protein phosphatase 2, regulatory subunit B (B56), gamma isoform	+	1.2	0.0075
722	1439942_at	Prep	prolyl endopeptidase	-	1.2	0.0002
723	1424119_at	Prkab1	protein kinase, AMP-activated, beta 1 non-catalytic subunit	-	1.1	0.0081
724	1433533_x_at	Prkag1	protein kinase, AMP-activated, gamma 1 non-catalytic subunit	+	1.1	0.0076
725	1421446_at	Prkcc	protein kinase C, gamma	-	1.3	0.0014
726	1422657_at	Prl5a1	prolactin family 5, subfamily a, member 1	+	1.2	0.0023

#	ID	SYMBOL	GENENAME	Effect	FC	P.Value
727	1454789_x_at	Prpf6	PRP6 pre-mRNA splicing factor 6 homolog (yeast)	+	1.2	0.0091
728	1432129_a_at	Prrx1	paired related homeobox 1	+	1.2	0.0027
729	1433573_x_at	Prss2	protease, serine, 2	+	1.2	0.0061
730	1417682_a_at	Prss2	protease, serine, 2	+	1.2	0.0037
731	1454607_s_at	Psat1	phosphoserine aminotransferase 1	+	1.1	0.0078
732	1420052_x_at	Psmb1	proteasome (prosome, macropain) subunit, beta type 1	+	1.2	0.0021
733	1420053_at	Psmb1	proteasome (prosome, macropain) subunit, beta type 1	+	1.2	0.0036
734	1416240_at	Psmb7	proteasome (prosome, macropain) subunit, beta type 7	-	1.3	0.0063
735	1453854_at	Ptar1	protein prenyltransferase alpha subunit repeat containing 1	+	1.2	0.0056
736	1417263_at	Ptgs2	prostaglandin-endoperoxide synthase 2	-	1.2	0.0028
737	1428707_at	Ptms	parathymosin	-	1.2	0.0056
738	1428708_x_at	Ptms	parathymosin	-	1.2	0.0040
739	1438058_s_at	Ptov1	prostate tumor over expressed gene 1	-	1.2	0.0098
740	1418181_at	Ptp4a3	protein tyrosine phosphatase 4a3	-	1.2	0.0019
741	1454726_s_at	Ptpdc1	protein tyrosine phosphatase domain containing 1	-	1.2	0.0082
742	1416588_at	Ptprn	protein tyrosine phosphatase, receptor type, N	-	1.2	0.0010
743	1420131_s_at	Pttg1ip	pituitary tumor-transforming 1 interacting protein	+	1.2	0.0031
744	1420132_s_at	Pttg1ip	pituitary tumor-transforming 1 interacting protein	+	1.2	0.0038
745	1450819_at	Pvrl1	poliovirus receptor-related 1	+	1.2	0.0028
746	1451253_at	Pxk	PX domain containing serine/threonine kinase	-	1.2	0.0027
747	1423448_at	Rab11b	RAB11B, member RAS oncogene family	-	1.2	0.0073
748	1417214_at	Rab27b	RAB27b, member RAS oncogene family	-	1.2	0.0030
749	1455857_a_at	Rab2b	RAB2B, member RAS oncogene family	-	1.2	0.0005
750	1422589_at	Rab3a	RAB3A, member RAS oncogene family	-	1.3	0.0018
751	1425266_a_at	Rap1gds1	RAP1, GTP-GDP dissociation stimulator 1	-	1.2	0.0072
752	1427975_at	Rasl10a	RAS-like, family 10, member A	+	1.3	0.0046
753	1452091_a_at	Rbm28	RNA binding motif protein 28	+	1.1	0.0086
754	1429169_at	Rbm3	RNA binding motif protein 3	+	1.3	0.0025
755	1418245_a_at	Rbm9	RNA binding motif protein 9	+	1.2	0.0088
756	1416354_at	Rbmx	RNA binding motif protein, X chromosome	-	1.2	0.0052
757	1443922_at	Rcor3	REST corepressor 3	-	1.2	0.0082
758	1424386_at	Reep2	receptor accessory protein 2	-	1.2	0.0058
759	1421160_a_at	Rfng	RFNG O-fucosylpeptide 3-beta-N-acetylglucosaminyltransferase	-	1.2	0.0040
760	1419310_s_at	Rfxank	regulatory factor X-associated ankyrin-containing protein	-	1.2	0.0095
761	1425245_a_at	Rgs11	regulator of G-protein signaling 11	-	1.2	0.0050
762	1453129_a_at	Rgs12	regulator of G-protein signaling 12	-	1.2	0.0053
763	1422238_at	Rhbdd2	rhomboid domain containing 2	+	1.2	0.0086
764	1448605_at	Rhoc	ras homolog gene family, member C	-	1.2	0.0077
765	1428710_at	Rit1	Ras-like without CAAX 1	+	1.2	0.0023
766	1440526_at	Rltpr	RGD motif, leucine rich repeats, tropomodulin domain and proline-rich containing	-	1.2	0.0090
767	1439583_x_at	Rltpr	RGD motif, leucine rich repeats, tropomodulin domain and proline-rich containing	-	1.2	0.0046
768	1442441_at	Rnasek	ribonuclease, RNase K	-	1.3	0.0054
769	1456108_x_at	Rnf112	ring finger protein 112	+	1.2	0.0016
770	1437949_x_at	Rnf114	ring finger protein 114	+	1.2	0.0049
771	1431030_a_at	Rnf14	ring finger protein 14	-	1.2	0.0033
772	1430527_a_at	Rnf167	ring finger protein 167	-	1.2	0.0025
773	1459877_x_at	Rnf185	ring finger protein 185	+	1.2	0.0020
774	1455051_at	Rnf31	ring finger protein 31	-	1.2	0.0029
775	1436634_at	Robo3	roundabout homolog 3 (Drosophila)	+	1.3	0.0037
776	1434635_at	Rph3a	rabphilin 3A	-	1.1	0.0077
777	1429759_at	Rps6ka6	ribosomal protein S6 kinase polypeptide 6	-	1.3	0.0001
778	1422268_a_at	Rps6kb2	ribosomal protein S6 kinase, polypeptide 2	-	1.3	0.0004
779	1434624_x_at	Rps9	ribosomal protein S9	+	1.2	0.0084
780	1453253_a_at	Rpusd1	RNA pseudouridylate synthase domain containing 1	-	1.2	0.0029
781	1429442_at	Rpusd2	RNA pseudouridylate synthase domain containing 2	+	1.2	0.0085
782	1443187_at	Rspo3	R-spondin 3 homolog (Xenopus laevis)	-	1.3	0.0001
783	1449246_at	Rundc3a	RUN domain containing 3A	-	1.2	0.0070
784	1431137_at	Rusc1	RUN and SH3 domain containing 1	-	1.2	0.0047
785	1438017_at	Rusc1	RUN and SH3 domain containing 1	-	1.2	0.0092
786	1452533_at	Ryr3	ryanodine receptor 3	-	1.3	0.0096
787	1440185_x_at	Sae1	SUMO1 activating enzyme subunit 1	+	1.2	0.0007
788	1436306_at	Saps1	SAPS domain family, member 1	-	1.2	0.0059
789	1454030_at	Saps3	SAPS domain family, member 3	+	1.3	0.0014
790	1445644_at	Sarm1	sterile alpha and HEAT/Armadillo motif containing 1	+	1.2	0.0078
791	1434707_at	Sbf1	SET binding factor 1	-	1.2	0.0071
792	1443762_s_at	Sbf2	SET binding factor 2	+	1.2	0.0082
793	1451190_a_at	Sbk1	SH3-binding kinase 1	+	1.2	0.0036
794	1434908_at	Scaf1	SR-related CTD-associated factor 1	-	1.3	0.0003
795	1436044_at	Scn7a	sodium channel, voltage-gated, type VII, alpha	-	1.3	0.0017
796	1419975_at	Scp2	sterol carrier protein 2, liver	+	1.2	0.0064
797	1457310_x_at	Scrt2	scratch homolog 2, zinc finger protein (Drosophila)	-	1.2	0.0052
798	1418206_at	Sdf2l1	stromal cell-derived factor 2-like 1	+	1.4	0.0006
799	1428695_at	Sdr39u1	short chain dehydrogenase/reductase family 39U, member 1	-	1.3	0.0013
800	1449202_at	Sema4g	sema domain, immunoglobulin domain (Ig), transmembrane domain (TM) and short cytoplasmic	-	1.3	0.0009

#	ID	SYMBOL	GENENAME	Effect	FC	P.Value
			domain, (semaphorin) 4G			
801	1435963_at	Sema5b	sema domain, seven thrombospondin repeats (type 1 and type 1-like), transmembrane domain (TM) and short cytoplasmic domain, (semaphorin) 5B	-	1.2	0.0057
802	1448790_at	Sema6b	sema domain, transmembrane domain (TM), and cytoplasmic domain, (semaphorin) 6B	-	1.2	0.0068
803	1454610_at	sept7	septin 7	-	1.2	0.0048
804	1423866_at	Serpina3k	serine (or cysteine) peptidase inhibitor, clade A, member 3K	+	1.2	0.0040
805	1420885_a_at	Sez6	seizure related gene 6	-	1.2	0.0015
806	1456040_at	Sf3b2	splicing factor 3b, subunit 2	-	1.2	0.0049
807	1423796_at	Sfpq	splicing factor proline/glutamine rich (polypyrimidine tract binding protein associated)	+	1.2	0.0042
808	1454683_at	Sfrs8	splicing factor, arginine/serine-rich 8	+	1.3	0.0080
809	1426423_at	Shmt2	serine hydroxymethyltransferase 2 (mitochondrial)	-	1.2	0.0086
810	1428493_at	Sipa1l3	signal-induced proliferation-associated 1 like 3	+	1.1	0.0062
811	1426441_at	Slc11a2	solute carrier family 11 (proton-coupled divalent metal ion transporters), member 2	-	1.3	0.0012
812	1436989_s_at	Slc12a6	solute carrier family 12, member 6	+	1.3	0.0005
813	1428986_at	Slc17a7	solute carrier family 17 (sodium-dependent inorganic phosphate cotransporter), member 7	-	1.3	0.0063
814	1425950_at	Slc17a9	solute carrier family 17, member 9	+	1.2	0.0085
815	1422203_at	Slc18a3	solute carrier family 18 (vesicular monoamine), member 3	-	1.3	0.0069
816	1452653_at	Slc25a22	solute carrier family 25 (mitochondrial carrier, glutamate), member 22	-	1.2	0.0025
817	1421445_at	Slc26a3	solute carrier family 26, member 3	-	1.2	0.0022
818	1416639_at	Slc2a5	solute carrier family 2 (facilitated glucose transporter), member 5	+	1.2	0.0026
819	1448741_at	Slc3a1	solute carrier family 3, member 1	+	1.2	0.0033
820	1428065_at	Slc44a2	solute carrier family 44, member 2	-	1.2	0.0039
821	1436137_at	Slc6a17	solute carrier family 6 (neurotransmitter transporter), member 17	-	1.2	0.0043
822	1455760_at	Slc9a5	solute carrier family 9 (sodium/hydrogen exchanger), member 5	-	1.2	0.0033
823	1448377_at	Slpi	secretory leukocyte peptidase inhibitor	+	1.2	0.0082
824	1435856_x_at	Smarcb1	SWI/SNF related, matrix associated, actin dependent regulator of chromatin, subfamily b, member 1	+	1.2	0.0011
825	1448913_at	Smarcd1	SWI/SNF related, matrix associated, actin dependent regulator of chromatin, subfamily d, member 1	-	1.2	0.0082
826	1429531_at	Smpd4	sphingomyelin phosphodiesterase 4	+	1.2	0.0046
827	1432043_at	Smu1	smu-1 suppressor of mec-8 and unc-52 homolog (C. elegans)	-	1.2	0.0096
828	1451722_s_at	Smyd5	SET and MYND domain containing 5	-	1.2	0.0025
829	1452713_a_at	Snrnp40	small nuclear ribonucleoprotein 40 (U5)	+	1.2	0.0021
830	1449840_at	Sntb2	syntrophin, basic 2	+	1.3	0.0003
831	1430037_at	Snx27	sorting nexin family member 27	+	1.3	0.0009
832	1433449_at	Snx32	sorting nexin 32	-	1.2	0.0038
833	1453002_at	Sox11	SRY-box containing gene 11	+	1.3	0.0091
834	1453125_at	Sox11	SRY-box containing gene 11	+	1.3	0.0086
835	1436790_a_at	Sox11	SRY-box containing gene 11	+	1.3	0.0005
836	1433575_at	Sox4	SRY-box containing gene 4	+	1.2	0.0071
837	1458332_x_at	Sox4	SRY-box containing gene 4	+	1.3	0.0022
838	1432495_at	Sox7	SRY-box containing gene 7	+	1.3	0.0037
839	1418180_at	Sp1	trans-acting transcription factor 1	+	1.2	0.0061
840	1454656_at	Spata13	spermatogenesis associated 13	+	1.3	0.0014
841	1427889_at	Spna2	spectrin alpha 2	-	1.2	0.0087
842	1435026_at	Spock2	sparc/osteonectin, cwcv and kazal-like domains proteoglycan 2	-	1.3	0.0092
843	1422307_at	Sppl3	signal peptide peptidase 3	+	1.2	0.0027
844	1423160_at	Spred1	sprouty protein with EVH-1 domain 1, related sequence	+	1.1	0.0097
845	1445669_at	Spry4	sprouty homolog 4 (Drosophila)	+	1.3	0.0017
846	1447806_s_at	Srpk3	serine/arginine-rich protein specific kinase 3	+	1.2	0.0095
847	1450045_at	Srrm1	serine/arginine repetitive matrix 1	+	1.2	0.0043
848	1419360_a_at	Ss18	synovial sarcoma translocation, Chromosome 18	+	1.1	0.0077
849	1419361_at	Ss18	synovial sarcoma translocation, Chromosome 18	+	1.2	0.0055
850	1449843_at	St8sia2	ST8 alpha-N-acetyl-neuraminide alpha-2,8-sialyltransferase 2	+	1.2	0.0068
851	1423530_at	Stk32c	serine/threonine kinase 32C	+	1.2	0.0099
852	1433186_at	Strada	STE20-related kinase adaptor alpha	+	1.2	0.0067
853	1419913_at	Strap	serine/threonine kinase receptor associated protein	+	1.5	0.0057
854	1416449_x_at	Stxbp2	syntaxin binding protein 2	-	1.2	0.0007
855	1425749_at	Stxbp6	syntaxin binding protein 6 (amisyn)	+	1.2	0.0002
856	1449534_at	Sycp3	synaptonemal complex protein 3	+	1.2	0.0098
857	1431798_a_at	Syde1	synapse defective 1, Rho GTPase, homolog 1 (C. elegans)	-	1.2	0.0003
858	1451484_a_at	Syn1	synapsin I	-	1.3	0.0028
859	1448280_at	Syp	synaptophysin	-	1.2	0.0019
860	1417708_at	Syt3	synaptotagmin III	-	1.2	0.0060
861	1422531_at	Syt5	synaptotagmin V	-	1.3	0.0026
862	1441927_at	Syt7	synaptotagmin VII	+	1.2	0.0017

#	ID	SYMBOL	GENENAME	Effect	FC	P.Value
863	1431883_at	Tac1	tachykinin 1	-	1.3	0.0090
864	1425694_at	Tbx5	T-box 5	-	1.2	0.0035
865	1420123_at	Tcta	T-cell leukemia translocation altered gene	-	1.1	0.0094
866	1430912_a_at	Tectb	tectorin beta	-	1.2	0.0055
867	1452264_at	Tenc1	tensin like C1 domain-containing phosphatase	-	1.3	0.0013
868	1439464_s_at	Tex10	testis expressed gene 10	+	1.2	0.0028
869	1418064_at	Tfpt	TCF3 (E2A) fusion partner	-	1.3	0.0013
870	1419314_at	Tinag	tubulointerstitial nephritis antigen	-	1.2	0.0042
871	1436244_a_at	Tle2	transducin-like enhancer of split 2, homolog of Drosophila E(spl)	-	1.3	0.0008
872	1451996_at	Tm2d1	TM2 domain containing 1	+	1.3	0.0095
873	1425079_at	Tm6sf2	transmembrane 6 superfamily member 2	+	1.3	0.0038
874	1438504_x_at	Tm7sf3	transmembrane 7 superfamily member 3	+	1.2	0.0076
875	1430818_at	Tmc1	transmembrane channel-like gene family 1	+	1.2	0.0090
876	1458372_at	Tmc8	transmembrane channel-like gene family 8	+	1.2	0.0033
877	1441890_x_at	Tmeff1	transmembrane protein with EGF-like and two follistatin-like domains 1	+	1.2	0.0026
878	1456057_x_at	Tmem109	transmembrane protein 109	+	1.2	0.0090
879	1441880_x_at	Tmem149	transmembrane protein 149	+	1.2	0.0029
880	1428899_at	Tmem182	transmembrane protein 182	-	1.2	0.0047
881	1452053_a_at	Tmem33	transmembrane protein 33	+	1.2	0.0051
882	1425568_a_at	Tmem33	transmembrane protein 33	+	1.2	0.0053
883	1449677_s_at	Tmem38b	transmembrane protein 38B	+	1.2	0.0019
884	1452825_at	Tmem59l	transmembrane protein 59-like	-	1.2	0.0028
885	1432008_at	Tmem86b	transmembrane protein 86B	+	1.3	0.0065
886	1458305_at	Tmtc3	transmembrane and tetratricopeptide repeat containing 3	-	1.2	0.0007
887	1416342_at	Tnc	tenascin C	-	1.2	0.0033
888	1422231_a_at	Tnfrsf25	tumor necrosis factor receptor superfamily, member 25	+	1.4	0.0012
889	1460469_at	Tnfrsf9	tumor necrosis factor receptor superfamily, member 9	+	1.2	0.0022
890	1431188_a_at	Tom1	target of myb1 homolog (chicken)	-	1.2	0.0005
891	1439043_at	Tra2a	transformer 2 alpha homolog (Drosophila)	+	1.6	0.0008
892	1449571_at	Trhr	thyrotropin releasing hormone receptor	-	1.5	0.0091
893	1451663_a_at	Trim3	tripartite motif-containing 3	-	1.2	0.0019
894	1416118_at	Trim59	tripartite motif-containing 59	+	1.2	0.0027
895	1453599_at	Trim71	tripartite motif-containing 71	+	1.2	0.0047
896	1459581_at	Trp63	transformation related protein 63	+	1.2	0.0044
897	1449431_at	Trpc6	transient receptor potential cation channel, subfamily C, member 6	+	1.2	0.0080
898	1427642_at	Trpm6	transient receptor potential cation channel, subfamily M, member 6	+	1.2	0.0061
899	1434849_at	Tspyl2	TSPY-like 2	-	1.2	0.0022
900	1433460_at	Ttc7b	tetratricopeptide repeat domain 7B	-	1.2	0.0062
901	1427284_a_at	Ttpa	tocopherol (alpha) transfer protein	-	1.2	0.0093
902	1427838_at	Tubb2a	tubulin, beta 2A	+	1.2	0.0027
903	1423221_at	Tubb4	tubulin, beta 4	-	1.3	0.0051
904	1439440_x_at	Twf2	twinfilin, actin-binding protein, homolog 2 (Drosophila)	+	1.2	0.0043
905	1439184_s_at	Txndc17	thioredoxin domain containing 17	+	1.2	0.0010
906	1448116_at	Uba1	ubiquitin-like modifier activating enzyme 1	-	1.2	0.0025
907	1437278_a_at	Uba2	ubiquitin-like modifier activating enzyme 2	+	1.1	0.0055
908	1454373_x_at	Ubc	ubiquitin C	+	1.5	0.0029
909	1452054_at	Ube2w	ubiquitin-conjugating enzyme E2W (putative)	+	1.2	0.0032
910	1448692_at	Ubqln4	ubiquilin 4	-	1.2	0.0009
911	1448260_at	Uchl1	ubiquitin carboxy-terminal hydrolase L1	-	1.2	0.0014
912	1439028_at	Ufm1	ubiquitin-fold modifier 1	+	1.3	0.0023
913	1439211_at	Umodl1	uromodulin-like 1	-	1.2	0.0094
914	1426681_at	Unk	unkempt homolog (Drosophila)	-	1.2	0.0061
915	1425023_at	Usp3	ubiquitin specific peptidase 3	-	1.2	0.0083
916	1453162_at	Utp11l	UTP11-like, U3 small nucleolar ribonucleoprotein, (yeast)	+	1.2	0.0063
917	1421863_at	Vamp1	vesicle-associated membrane protein 1	-	1.2	0.0082
918	1448472_at	Vars	valyl-tRNA synthetase	-	1.2	0.0005
919	1420909_at	Vegfa	vascular endothelial growth factor A	+	1.2	0.0024
920	1419417_at	Vegfc	vascular endothelial growth factor C	-	1.2	0.0068
921	1438881_at	Vezt	vezatin, adherens junctions transmembrane protein	-	1.2	0.0096
922	1452489_at	Vps11	vacuolar protein sorting 11 (yeast)	+	1.2	0.0072
923	1450055_at	Vsnl1	visinin-like 1	-	1.2	0.0066
924	1451230_a_at	Wbp5	WW domain binding protein 5	-	1.1	0.0086
925	1456645_at	Wdr25	WD repeat domain 25	-	1.2	0.0090
926	1452392_a_at	Wipi1	WD repeat domain, phosphoinositide interacting 1	+	1.3	0.0056
927	1457499_at	Wwp2	WW domain containing E3 ubiquitin protein ligase 2	+	1.2	0.0075
928	1437155_a_at	Wwtr1	WW domain containing transcription regulator 1	+	1.2	0.0025
929	1420012_at	Xbp1	X-box binding protein 1	+	1.6	0.0002
930	1439411_a_at	Xpo7	exportin 7	+	1.2	0.0098
931	1438839_a_at	Ywhae	tyrosine 3-monooxygenase/tryptophan 5-monooxygenase activation protein, epsilon polypeptide	-	1.2	0.0078
932	1436981_a_at	Ywhaz	tyrosine 3-monooxygenase/tryptophan 5-monooxygenase activation protein, zeta polypeptide	+	1.3	0.0053
933	1439005_x_at	Ywhaz	tyrosine 3-monooxygenase/tryptophan 5-monooxygenase activation protein, zeta polypeptide	+	1.4	0.0006
934	1422570_at	Yy1	YY1 transcription factor	-	1.2	0.0071

#	ID	SYMBOL	GENENAME	Effect	FC	P.Value
935	1453175_at	Zbtb25	zinc finger and BTB domain containing 25	-	1.2	0.0030
936	1426999_at	Zc3h14	zinc finger CCCH type containing 14	-	1.2	0.0060
937	1437355_at	Zcchc5	zinc finger, CCHC domain containing 5	-	1.3	0.0084
938	1433748_at	Zdhhc18	zinc finger, DHHC domain containing 18	+	1.2	0.0100
939	1416084_at	Zfand5	zinc finger, AN1-type domain 5	-	1.2	0.0087
940	1425010_at	Zfp119	zinc finger protein 119	-	1.2	0.0062
941	1428170_at	Zfp180	zinc finger protein 180	+	1.2	0.0026
942	1433953_at	Zfp277	zinc finger protein 277	-	1.2	0.0042
943	1455638_at	Zfp319	zinc finger protein 319	+	1.2	0.0069
944	1420110_s_at	Zfp334	zinc finger protein 334	-	1.2	0.0077
945	1422528_a_at	Zfp36l1	zinc finger protein 36, C3H type-like 1	+	1.3	0.0001
946	1421139_a_at	Zfp386	zinc finger protein 386 (Kruppel-like)	-	1.3	0.0093
947	1436081_a_at	Zfp414	zinc finger protein 414	-	1.3	0.0023
948	1425058_at	Zfp472	zinc finger protein 472	-	1.2	0.0033
949	1429634_at	Zfp580	zinc finger protein 580	-	1.2	0.0029
950	1449691_at	Zfp644	zinc finger protein 644	+	1.3	0.0042
951	1434720_at	Zfp652	zinc finger protein 652	+	1.2	0.0015
952	1454986_at	Zfp668	zinc finger protein 668	-	1.2	0.0098
953	1428687_at	Zfp687	zinc finger protein 687	-	1.1	0.0098
954	1451902_at	Zfp758	zinc finger protein 758	-	1.3	0.0064
955	1452623_at	Zfp759	zinc finger protein 759	-	1.2	0.0013
956	1426292_at	Zfp790	zinc finger protein 790	+	1.1	0.0096
957	1427499_at	Zfp81	zinc finger protein 81	-	1.2	0.0077
958	1438079_at	Zfp867	zinc finger protein 867	-	1.2	0.0009
959	1425531_at	Znhit1	zinc finger, HIT domain containing 1	-	1.2	0.0080
960	1433869_at	Zxdc	ZXD family zinc finger C	-	1.1	0.0055

5.1.3 Gene expression regulated at the gene × environment level

ID: Affymetrix ID; FC: fold-change in mRNA expression. Genes have been ordered alphabetically.

#	ID	SYMBOL	GENENAME	FC	P-Value
1	1457715_at	1010001B22Rik	RIKEN cDNA 1010001B22 gene	2.3	0.006
2	1454286_at	1110004M10Rik	RIKEN cDNA 1110004M10 gene	1.6	0.003
3	1430012_at	1110050K14Rik	RIKEN cDNA 1110050K14 gene	1.4	0.008
4	1438288_x_at	1110059G02Rik	RIKEN cDNA 1110059G02 gene	1.6	0.004
5	1422722_at	1700001K19Rik	RIKEN cDNA 1700001K19 gene	1.8	0.004
6	1451061_at	1700018B24Rik	enhancer of rudimentary homolog pseudogene	1.6	0.007
7	1442779_at	1700071K01Rik	RIKEN cDNA 1700071K01 gene	1.9	0.002
8	1447798_at	1700123O21Rik	RIKEN cDNA 1700123O21 gene	2.7	0.003
9	1430612_at	1810033B17Rik	RIKEN cDNA 1810033B17 gene	1.4	0.007
10	1430280_at	1810062G17Rik	RIKEN cDNA 1810062G17 gene	1.6	0.006
11	1447576_at	2010001K21Rik	RIKEN cDNA 2010001K21 gene	1.9	0.000
12	1430878_at	2210406H18Rik	RIKEN cDNA 2210406H18 gene	1.6	0.002
13	1453174_at	2310076G13Rik	RIKEN cDNA 2310076G13 gene	1.7	0.009
14	1430195_at	2810043O03Rik	RIKEN cDNA 2810043O03 gene	1.5	0.006
15	1444703_at	2810403D21Rik	RIKEN cDNA 2810403D21 gene	1.4	0.003
16	1433266_at	2810416A17Rik	RIKEN cDNA 2810416A17 gene	1.9	0.004
17	1432824_at	2900018N21Rik	RIKEN cDNA 2900018N21 gene	1.7	0.008
18	1433387_at	2900022M07Rik	RIKEN cDNA 2900022M07 gene	2.5	0.000
19	1431703_at	2900027M19Rik	RIKEN cDNA 2900027M19 gene	2.1	0.007
20	1432944_at	2900046L07Rik	RIKEN cDNA 2900046L07 gene	1.6	0.008
21	1453456_at	2900084O13Rik	RIKEN cDNA 2900084O13 gene	2.0	0.003
22	1454478_at	3100002H20Rik	RIKEN cDNA 3100002H20 gene	1.5	0.007
23	1432686_at	4833406M21Rik	RIKEN cDNA 4833406M21 gene	1.7	0.008
24	1430622_at	4833423F13Rik	RIKEN cDNA 4833423F13 gene	1.6	0.010
25	1430467_at	4921511H03Rik	RIKEN cDNA 4921511H03 gene	1.5	0.009
26	1430722_at	4921515J06Rik	RIKEN cDNA 4921515J06 gene	1.3	0.009
27	1440467_at	4922501C03Rik	RIKEN cDNA 4922501C03 gene	1.7	0.003
28	1440349_at	4930420K17Rik	RIKEN cDNA 4930420K17 gene	1.6	0.000
29	1433234_at	4930424E08Rik	RIKEN cDNA 4930424E08 gene	1.4	0.008
30	1431954_x_at	4930431C11Rik	RIKEN cDNA 4930431C11 gene	1.7	0.002
31	1431628_at	4930435H24Rik	RIKEN cDNA 4930435H24 gene	1.5	0.005
32	1442152_at	4930513N10Rik	RIKEN cDNA 4930513N10 gene	1.6	0.002
33	1433320_at	4930519N06Rik	RIKEN cDNA 4930519N06 gene	1.6	0.005
34	1440783_at	4930529M08Rik	RIKEN cDNA 4930529M08 gene	1.8	0.009
35	1431660_at	4930564D02Rik	RIKEN cDNA 4930564D02 gene	1.5	0.005
36	1439684_at	4930570G19Rik	RIKEN cDNA 4930570G19 gene	1.8	0.000
37	1430175_at	4930588G05Rik	RIKEN cDNA 4930588G05 gene	1.6	0.004
38	1436219_at	4933403F05Rik	RIKEN cDNA 4933403F05 gene	1.4	0.009
39	1453893_at	4933412O06Rik	RIKEN cDNA 4933412O06 gene	1.4	0.003
40	1431571_at	4933437I04Rik	RIKEN cDNA 4933437I04 gene	1.9	0.002
41	1427065_at	4933439F18Rik	RIKEN cDNA 4933439F18 gene	1.6	0.002
42	1431248_at	5031426D15Rik	RIKEN cDNA 5031426D15 gene	1.9	0.007
43	1431473_at	5330423I11Rik	RIKEN cDNA 5330423I11 gene	1.7	0.003
44	1439179_a_at	5830405N20Rik	RIKEN cDNA 5830405N20 gene	1.6	0.010

#	ID	SYMBOL	GENENAME	FC	P-Value
45	1456296_at	5830418K08Rik	RIKEN cDNA 5830418K08 gene	1.8	0.009
46	1432696_at	5830431M20Rik	RIKEN cDNA 5830431M20 gene	1.6	0.001
47	1439512_at	5830444B04Rik	RIKEN cDNA 5830444B04 gene	1.6	0.009
48	1430585_at	5930436O19Rik	RIKEN cDNA 5930436O19 gene	1.4	0.002
49	1433202_at	6030400A10Rik	RIKEN cDNA 6030400A10 gene	1.6	0.009
50	1431242_at	6330575P09Rik	RIKEN cDNA 6330575P09 gene	1.5	0.003
51	1434797_at	6720469N11Rik	RIKEN cDNA 6720469N11 gene	1.6	0.004
52	1433184_at	6720477C19Rik	RIKEN cDNA 6720477C19 gene	1.9	0.009
53	1440542_at	7420416P09Rik	RIKEN cDNA 7420416P09 gene	1.3	0.009
54	1430877_at	8030425K09Rik	RIKEN cDNA 8030425K09 gene	1.6	0.005
55	1444797_at	8030474K03Rik	RIKEN cDNA 8030474K03 gene	1.6	0.002
56	1453638_at	9030420J04Rik	RIKEN cDNA 9030420J04 gene	1.4	0.005
57	1433002_at	9030613N10Rik	RIKEN cDNA 9030613N10 gene	1.7	0.005
58	1433261_at	9430052A13Rik	RIKEN cDNA 9430052A13 gene	1.7	0.007
59	1431491_at	9430087N24Rik	RIKEN cDNA 9430087N24 gene	1.6	0.010
60	1433195_at	9530006O14Rik	RIKEN cDNA 9530006O14 gene	1.6	0.003
61	1458113_at	9530019H20Rik	RIKEN cDNA 9530019H20 gene	1.5	0.002
62	1441179_at	9530020O07Rik	RIKEN cDNA 9530020O07 gene	1.5	0.004
63	1445167_at	9630001P10Rik	RIKEN cDNA 9630001P10 gene	1.5	0.004
64	1458123_at	9630002A11Rik	RIKEN cDNA 9630002A11 gene	1.9	0.002
65	1443127_at	9630021D06Rik	RIKEN cDNA 9630021D06 gene	2.3	0.000
66	1456634_at	9830001H06Rik	RIKEN cDNA 9830001H06 gene	1.5	0.003
67	1440671_at	A130012E19Rik	RIKEN cDNA A130012E19 gene	1.5	0.002
68	1443457_at	A230055J12Rik	RIKEN cDNA A230055J12 gene	1.5	0.006
69	1454278_at	A430105D02Rik	RIKEN cDNA A430105D02 gene	1.6	0.005
70	1440884_s_at	A530047J11Rik	RIKEN cDNA A530047J11 gene	1.7	0.002
71	1455203_at	A930003A15Rik	RIKEN cDNA A930003A15 gene	1.4	0.007
72	1459349_at	A930011G23Rik	RIKEN cDNA A930011G23 gene	1.5	0.002
73	1459391_at	Abca5	ATP-binding cassette, sub-family A (ABC1), member 5	1.7	0.004
74	1456812_at	Abcd2	ATP-binding cassette, sub-family D (ALD), member 2	1.6	0.002
75	1453474_at	Abhd15	abhydrolase domain containing 15	1.6	0.009
76	1446433_at	Acbd5	acyl-Coenzyme A binding domain containing 5	1.5	0.003
77	1441975_at	Acpp	acid phosphatase, prostate	1.6	0.006
78	1437382_at	Acvr2a	activin receptor IIA	1.5	0.004
79	1448539_a_at	Acy3	aspartoacylase (aminoacylase) 3	1.5	0.003
80	1452595_at	Adamts4	a disintegrin-like and metallopeptidase (reprolysin type) with	1.6	0.001
81	1451932_a_at	Adamtsl4	ADAMTS-like 4	1.4	0.007
82	1416225_at	Adh1	alcohol dehydrogenase 1 (class I)	1.7	0.004
83	1438759_x_at	Adi1	acireductone dioxygenase 1	1.4	0.009
84	1446463_at	Adnp2	ADNP homeobox 2	1.5	0.004
85	1435719_at	AI448984	expressed sequence AI448984	1.7	0.008
86	1438716_at	AI451617	expressed sequence AI451617	1.9	0.003
87	1460003_at	AI956758	expressed sequence AI956758	2.1	0.003
88	1442703_at	AK220484	cDNA sequence AK220484	1.5	0.004
89	1439066_at	Angpt1	angiopoietin 1	1.8	0.003
90	1450085_at	Angptl2	angiopoietin-like 2	1.4	0.005
91	1447259_at	Ank3	ankyrin 3, epithelial	1.6	0.005
92	1437768_at	Ankib1	ankyrin repeat and IBR domain containing 1	1.6	0.001
93	1443887_at	Ankrd13c	ankyrin repeat domain 13c	1.6	0.003
94	1451837_at	Ap3b2	adaptor-related protein complex 3, beta 2 subunit	1.8	0.004
95	1443112_at	Api5	apoptosis inhibitor 5	1.7	0.006
96	1418069_at	Apoc2	apolipoprotein C-II	1.5	0.010
97	1418853_at	Apon	apolipoprotein N	2.2	0.001
98	1450460_at	Aqp3	aquaporin 3	1.5	0.002
99	1419549_at	Arg1	arginase, liver	1.4	0.007
100	1457410_at	Arhgap5	Rho GTPase activating protein 5	1.6	0.005
101	1451867_x_at	Arhgap6	Rho GTPase activating protein 6	2.2	0.001
102	1441022_at	Arih1	ariadne ubiquitin-conjugating enzyme E2 binding protein homolog 1	1.4	0.007
103	1441190_at	Arpc5l	actin related protein 2/3 complex, subunit 5-like	1.6	0.009
104	1438921_at	Atr	ataxia telangiectasia and Rad3 related	1.9	0.006
105	1458945_at	AU015148	expressed sequence AU015148	1.6	0.005
106	1459155_at	AU015696	expressed sequence AU015696	1.4	0.006
107	1424266_s_at	AU018778	expressed sequence AU018778	1.6	0.002
108	1443399_at	AU021001	expressed sequence AU021001	1.8	0.000
109	1418604_at	Avpr1a	arginine vasopressin receptor 1A	1.9	0.001
110	1430000_at	B230117O15Rik	RIKEN cDNA B230117O15 gene	1.6	0.001
111	1442028_at	B4galnt2	beta-1,4-N-acetyl-galactosaminyl transferase 2	1.5	0.005
112	1440781_at	B830007D08Rik	RIKEN cDNA B830007D08 gene	2.5	0.005
113	1458376_at	B930025B16Rik	RIKEN cDNA B930025B16 gene	1.9	0.002
114	1446681_at	BB086117	expressed sequence BB086117	1.6	0.002
115	1436585_at	BB182297	expressed sequence BB182297	1.7	0.001
116	1427041_at	BC013712	cDNA sequence BC013712	1.5	0.004
117	1437264_at	BC051142	cDNA sequence BC051142	1.8	0.001
118	1424814_a_at	Bcl2l14	BCL2-like 14 (apoptosis facilitator)	2.1	0.005
119	1422745_at	Bicd2	bicaudal D homolog 2 (Drosophila)	1.5	0.007
120	1420683_at	Bnipl	BCL2/adenovirus E1B 19kD interacting protein like	1.3	0.006
121	1426129_at	Brms1	breast cancer metastasis-suppressor 1	1.5	0.004
122	1439329_a_at	Brsk2	BR serine/threonine kinase 2	1.9	0.009
123	1435953_at	Btaf1	BTAF1 RNA polymerase II, B-TFIID transcription factor-associated,	1.4	0.008
124	1454342_at	C030007D22Rik	RIKEN cDNA C030007D22 gene	1.6	0.008
125	1432200_at	C030044M21Rik	RIKEN cDNA C030044M21 gene	1.6	0.002
126	1438905_x_at	C030046I01Rik	RIKEN cDNA C030046I01 gene	1.6	0.009

#	ID	SYMBOL	GENENAME	FC	P-Value
127	1416051_at	C2	complement component 2 (within H-2S)	1.4	0.004
128	1444340_at	C230066G23Rik	RIKEN cDNA C230066G23 gene	1.5	0.005
129	1457656_s_at	C230085N15Rik	RIKEN cDNA C230085N15 gene	1.9	0.001
130	1438125_at	C230085N15Rik	RIKEN cDNA C230085N15 gene	1.4	0.005
131	1432423_a_at	C530008M17Rik	RIKEN cDNA C530008M17 gene	1.4	0.006
132	1441394_at	C76554	expressed sequence C76554	1.6	0.004
133	1444445_at	C77648	expressed sequence C77648	1.5	0.007
134	1447182_at	C77815	expressed sequence C77815	2.1	0.000
135	1442566_at	C78878	expressed sequence C78878	1.5	0.001
136	1447507_at	C80406	expressed sequence C80406	1.5	0.006
137	1441477_at	Calu	calumenin	1.5	0.003
138	1422659_at	Camk2d	calcium/calmodulin-dependent protein kinase II, delta	1.6	0.009
139	1439843_at	Camk4	calcium/calmodulin-dependent protein kinase IV	1.8	0.006
140	1432628_at	Cbx3	chromobox homolog 3 (Drosophila HP1 gamma)	1.9	0.003
141	1441886_at	Ccdc79	coiled-coil domain containing 79	1.5	0.004
142	1436789_at	Ccnjl	cyclin J-like	1.5	0.006
143	1421188_at	Ccr2	chemokine (C-C motif) receptor 2	1.5	0.003
144	1427736_a_at	Ccrl2	chemokine (C-C motif) receptor-like 2	1.5	0.004
145	1423760_at	Cd44	CD44 antigen	1.7	0.004
146	1427095_at	Cdcp1	CUB domain containing protein 1	1.5	0.003
147	1460045_at	Cdh7	cadherin 7, type 2	1.8	0.001
148	1419497_at	Cdkn1b	cyclin-dependent kinase inhibitor 1B	1.7	0.002
149	1425912_at	Cep164	centrosomal protein 164	1.5	0.005
150	1425642_at	Cep290	centrosomal protein 290	1.8	0.009
151	1419320_at	Chst5	carbohydrate (N-acetylglucosamine 6-O) sulfotransferase 5	1.6	0.001
152	1425200_at	Clcc1	chloride channel CLIC-like 1	1.4	0.005
153	1421698_a_at	Col19a1	collagen, type XIX, alpha 1	1.6	0.002
154	1440911_at	Col23a1	collagen, type XXIII, alpha 1	1.7	0.007
155	1419703_at	Col5a3	collagen, type V, alpha 3	1.6	0.005
156	1421373_at	Cox4i2	cytochrome c oxidase subunit IV isoform 2	1.5	0.002
157	1419960_at	Cphx	cytoplasmic polyadenylated homeobox	1.6	0.004
158	1443909_at	Cstf3	cleavage stimulation factor, 3' pre-RNA, subunit 3	1.8	0.004
159	1422680_at	Ctr9	Ctr9, Paf1/RNA polymerase II complex component, homolog (S.	1.4	0.003
160	1417590_at	Cyp27a1	cytochrome P450, family 27, subfamily a, polypeptide 1	1.5	0.004
161	1438581_at	Cytsa	cytospin A	1.6	0.005
162	1457304_at	D13Ertd787e	DNA segment, Chr 13, ERATO Doi 787, expressed	1.7	0.005
163	1457004_at	D15Wsu169e	DNA segment, Chr 15, Wayne State University 169, expressed	1.7	0.006
164	1446564_at	D18Ertd169e	DNA segment, Chr 18, ERATO Doi 169, expressed	2.0	0.002
165	1441229_at	D230019N24Rik	RIKEN cDNA D230019N24 gene	1.5	0.006
166	1441558_at	D230044B12Rik	RIKEN cDNA D230044B12 gene	1.7	0.002
167	1438222_at	D2Ertd612e	DNA segment, Chr 2, ERATO Doi 612, expressed	1.8	0.008
168	1439691_at	D5Ertd579e	DNA segment, Chr 5, ERATO Doi 579, expressed	1.4	0.004
169	1438788_at	D5Wsu152e	DNA segment, Chr 5, Wayne State University 152, expressed	1.6	0.004
170	1444292_at	D7Ertd143e	DNA segment, Chr 7, ERATO Doi 143, expressed	1.4	0.004
171	1424860_at	D930016D06Rik	RIKEN cDNA D930016D06 gene	1.7	0.007
172	1424861_at	D930016D06Rik	RIKEN cDNA D930016D06 gene	1.6	0.009
173	1457012_at	Dbx1	developing brain homeobox 1	1.4	0.007
174	1446190_at	Dclk1	doublecortin-like kinase 1	1.8	0.007
175	1458361_at	Dclre1c	DNA cross-link repair 1C, PSO2 homolog (S. cerevisiae)	1.7	0.001
176	1458614_at	Dcp1b	DCP1 decapping enzyme homolog b (S. cerevisiae)	1.6	0.001
177	1418139_at	Dcx	doublecortin	1.4	0.008
178	1445798_at	Dlg1	discs, large homolog 1 (Drosophila)	1.7	0.001
179	1440639_at	Dlgap1	discs, large (Drosophila) homolog-associated protein 1	1.4	0.008
180	1420335_at	Dmc1	DMC1 dosage suppressor of mck1 homolog, meiosis-specific	1.4	0.003
181	1420221_at	Dnajc21	DnaJ (Hsp40) homolog, subfamily C, member 21	1.8	0.001
182	1452638_s_at	Dnm1l	dynamin 1-like	1.6	0.003
183	1449052_a_at	Dnmt3b	DNA methyltransferase 3B	1.5	0.004
184	1418351_a_at	Dnmt3b	DNA methyltransferase 3B	1.5	0.007
185	1436661_at	Dpp10	dipeptidylpeptidase 10	1.6	0.003
186	1437272_at	Dpy19l2	dpy-19-like 2 (C. elegans)	1.5	0.001
187	1434534_at	Dsc3	desmocollin 3	1.7	0.003
188	1445710_x_at	Duxbl	double homeobox B-like	1.8	0.009
189	1454393_at	Dzip3	DAZ interacting protein 3, zinc finger	1.5	0.006
190	1430386_at	E030024N20Rik	peptidylprolyl isomerase A pseudogene 8	1.4	0.009
191	1439571_at	E230008J23Rik	RIKEN cDNA E230008J23 gene	1.7	0.005
192	1424561_at	Ece2	endothelin converting enzyme 2	1.5	0.001
193	1421900_at	Eif2ak1	eukaryotic translation initiation factor 2 alpha kinase 1	1.6	0.002
194	1420491_at	Eif2s1	eukaryotic translation initiation factor 2, subunit 1 alpha	1.7	0.007
195	1434489_at	Elmo3	engulfment and cell motility 3, ced-12 homolog (C. elegans)	1.6	0.006
196	1447857_at	Enox1	ecto-NOX disulfide-thiol exchanger 1	1.6	0.006
197	1419276_at	Enpp1	ectonucleotide pyrophosphatase/phosphodiesterase 1	1.6	0.009
198	1421406_at	Entpd7	ectonucleoside triphosphate diphosphohydrolase 7	1.4	0.008
199	1444150_at	Epb4.1	erythrocyte protein band 4.1	2.2	0.001
200	1456481_at	Esyt3	extended synaptotagmin-like protein 3	1.6	0.001
201	1449305_at	F10	coagulation factor X	1.4	0.008
202	1436374_x_at	F11r	F11 receptor	1.8	0.004
203	1421595_at	Fam184b	family with sequence similarity 184, member B	1.4	0.008
204	1435282_at	Fam189a2	family with sequence similarity 189, member A2	1.6	0.002
205	1447475_at	Fam189a2	family with sequence similarity 189, member A2	1.6	0.003
206	1432884_at	Fam23a	family with sequence similarity 23, member A	1.6	0.004
207	1452513_a_at	Fanca	Fanconi anemia, complementation group A	1.7	0.006
208	1449141_at	Fblim1	filamin binding LIM protein 1	1.5	0.006

#	ID	SYMBOL	GENENAME	FC	P-Value
209	1438336_at	Fbxw11	F-box and WD-40 domain protein 11	1.6	0.006
210	1426090_a_at	Fert2	fer (fms/fps related) protein kinase, testis specific 2	1.5	0.006
211	1426041_a_at	Fgd4	FYVE, RhoGEF and PH domain containing 4	1.4	0.009
212	1429310_at	Flrt3	fibronectin leucine rich transmembrane protein 3	1.5	0.006
213	1419924_at	Fnip1	folliculin interacting protein 1	1.5	0.009
214	1425291_at	Foxj1	forkhead box J1	2.0	0.008
215	1456367_at	Fut8	fucosyltransferase 8	1.7	0.007
216	1434788_at	Fzd3	frizzled homolog 3 (Drosophila)	1.5	0.007
217	1449730_s_at	Fzd3	frizzled homolog 3 (Drosophila)	1.4	0.007
218	1441911_x_at	Gart	phosphoribosylglycinamide formyltransferase	1.6	0.007
219	1449232_at	Gata1	GATA binding protein 1	1.6	0.006
220	1418904_at	Gfpt1	glutamine fructose-6-phosphate transaminase 1	1.4	0.006
221	1416715_at	Gjb3	gap junction protein, beta 3	1.6	0.001
222	1457933_at	Gm1964	predicted gene 1964	1.4	0.003
223	1459561_at	Gm3924	predicted gene 3924	1.4	0.009
224	1453869_at	Gm5085	predicted gene 5085	1.5	0.008
225	1439156_at	Gm962	predicted gene 962	1.5	0.005
226	1438888_at	Gmcl1	germ cell-less homolog 1 (Drosophila)	1.5	0.010
227	1435978_at	Gmppa	GDP-mannose pyrophosphorylase A	1.4	0.009
228	1422817_at	Gp5	glycoprotein 5 (platelet)	1.6	0.005
229	1448303_at	Gpnmb	glycoprotein (transmembrane) nmb	1.5	0.003
230	1434725_at	Gramd1c	GRAM domain containing 1C	1.5	0.005
231	1435722_at	Gria4	glutamate receptor, ionotropic, AMPA4 (alpha 4)	1.6	0.005
232	1439286_at	Grik2	glutamate receptor, ionotropic, kainate 2 (beta 2)	1.6	0.005
233	1434007_at	Gyltl1b	glycosyltransferase-like 1B	1.8	0.005
234	1438858_x_at	H2-Aa	histocompatibility 2, class II antigen A, alpha	2.1	0.006
235	1434572_at	Hdac9	histone deacetylase 9	1.3	0.005
236	1456631_at	Heatr7b1	HEAT repeat containing 7B1	1.7	0.002
237	1440656_at	Hecw1	HECT, C2 and WW domain containing E3 ubiquitin protein ligase 1	1.7	0.001
238	1450049_a_at	Hira	histone cell cycle regulation defective homolog A (S. cerevisiae)	1.8	0.004
239	1443020_at	Hmbox1	homeobox containing 1	1.5	0.008
240	1438532_at	Hmcn1	hemicentin 1	1.5	0.003
241	1435157_at	Hook3	hook homolog 3 (Drosophila)	1.6	0.003
242	1452400_a_at	Hoxa11as	HOXA11 antisense RNA (non-protein coding)	1.5	0.009
243	1427362_x_at	Hoxc6	homeo box C6	1.5	0.007
244	1431099_at	Hoxd8	homeo box D8	1.7	0.006
245	1422919_at	Hrasls	HRAS-like suppressor	1.6	0.005
246	1425786_a_at	Hsf4	heat shock transcription factor 4	1.4	0.008
247	1452956_a_at	Ifi27l1	interferon, alpha-inducible protein 27 like 1	1.5	0.010
248	1425120_x_at	Ifi27l2b	interferon, alpha-inducible protein 27 like 2B	1.5	0.005
249	1417292_at	Ifi47	interferon gamma inducible protein 47	1.5	0.003
250	1421992_a_at	Igfbp4	insulin-like growth factor binding protein 4	1.5	0.006
251	1427850_x_at	Igh-VJ558	immunoglobulin heavy chain (J558 family)	2.9	0.009
252	1425454_a_at	Il12a	interleukin 12a	1.5	0.004
253	1422397_a_at	Il15ra	interleukin 15 receptor, alpha chain	1.5	0.008
254	1426566_s_at	Il17re	interleukin 17 receptor E	1.4	0.007
255	1421843_at	Il1rap	interleukin 1 receptor accessory protein	1.5	0.005
256	1420462_at	Il1rapl2	interleukin 1 receptor accessory protein-like 2	2.1	0.003
257	1449864_at	Il4	interleukin 4	1.4	0.009
258	1446750_at	Impact	imprinted and ancient	1.4	0.005
259	1460491_at	Invs	inversin	1.8	0.001
260	1427387_a_at	Itgb4	integrin beta 4	1.5	0.003
261	1431416_a_at	Jam2	junction adhesion molecule 2	1.5	0.009
262	1458161_at	Kcnq1ot1	KCNQ1 overlapping transcript 1	1.7	0.002
263	1457482_at	Kdm5b	lysine (K)-specific demethylase 5B	1.3	0.010
264	1415855_at	Kitl	kit ligand	1.7	0.006
265	1425192_at	Klhl25	kelch-like 25 (Drosophila)	1.4	0.009
266	1425123_at	Klhl36	kelch-like 36 (Drosophila)	1.7	0.010
267	1420770_at	Klk1b24	kallikrein 1-related peptidase b24	1.9	0.007
268	1455888_at	Lingo2	leucine rich repeat and Ig domain containing 2	1.5	0.006
269	1416304_at	Litaf	LPS-induced TN factor	1.7	0.006
270	1443907_at	Lnpep	leucyl/cystinyl aminopeptidase	1.8	0.007
271	1438127_at	LOC552906	hypothetical LOC552906	1.5	0.003
272	1442320_at	LOC553096	hypothetical LOC553096	1.6	0.006
273	1445422_at	LOC621549	hypothetical protein LOC621549	1.6	0.001
274	1426110_a_at	Lpar1	lysophosphatidic acid receptor 1	1.5	0.007
275	1434761_at	Lrrtm3	leucine rich repeat transmembrane neuronal 3	1.4	0.003
276	1453528_at	Lta4h	leukotriene A4 hydrolase	1.6	0.005
277	1449789_x_at	Ly6g6c	lymphocyte antigen 6 complex, locus G6C	1.5	0.008
278	1447684_at	Lzic	leucine zipper and CTNNBIP1 domain containing	1.6	0.001
279	1426648_at	Mapkapk2	MAP kinase-activated protein kinase 2	1.3	0.010
280	1459387_at	Mast4	microtubule associated serine/threonine kinase family member 4	1.6	0.004
281	1417675_a_at	Mdn1	midasin homolog (yeast)	1.5	0.003
282	1438538_at	Mecp2	methyl CpG binding protein 2	1.6	0.006
283	1440091_at	Meis2	Meis homeobox 2	2.1	0.001
284	1458919_at	Mkln1	muskelin 1, intracellular mediator containing kelch motifs	1.7	0.008
285	1441535_at	Mllt3	myeloid/lymphoid or mixed-lineage leukemia (trithorax homolog,	1.8	0.002
286	1440920_at	Mmp14	matrix metallopeptidase 14 (membrane-inserted)	1.6	0.004
287	1441185_at	Msi2	Musashi homolog 2 (Drosophila)	1.5	0.009
288	1449559_at	Msx2	homeobox, msh-like 2	1.5	0.009
289	1445151_at	Mtf2	metal response element binding transcription factor 2	1.7	0.008
290	1420466_at	Mucl1	mucin-like 1	1.5	0.001

#	ID	SYMBOL	GENENAME	FC	P-Value
291	1454946_at	Mybl2	myeloblastosis oncogene-like 2	1.4	0.003
292	1447150_at	Mycbp2	MYC binding protein 2	1.7	0.008
293	1459679_s_at	Myo1b	myosin IB	1.8	0.002
294	1446407_at	Mysm1	myb-like, SWIRM and MPN domains 1	1.5	0.007
295	1430599_at	Myt1l	myelin transcription factor 1-like	1.9	0.008
296	1457804_at	NA	NA	3.1	0.000
297	1418638_at	NA	NA	2.7	0.000
298	1425174_at	NA	NA	2.6	0.001
299	1440425_at	NA	NA	2.5	0.007
300	1445090_at	NA	NA	2.5	0.000
301	1460097_at	NA	NA	2.5	0.000
302	1442491_at	NA	NA	2.4	0.001
303	1439290_at	NA	NA	2.3	0.000
304	1443237_at	NA	NA	2.3	0.003
305	1444622_at	NA	NA	2.3	0.000
306	1459126_at	NA	NA	2.3	0.001
307	1440630_at	NA	NA	2.2	0.008
308	1443179_at	NA	NA	2.1	0.007
309	1446571_at	NA	NA	2.1	0.000
310	1459675_at	NA	NA	2.1	0.008
311	1439123_at	NA	NA	2.1	0.000
312	1439412_at	NA	NA	2.1	0.001
313	1457973_at	NA	NA	2.0	0.004
314	1446799_at	NA	NA	2.0	0.002
315	1442622_at	NA	NA	2.0	0.001
316	1458230_at	NA	NA	2.0	0.000
317	1460158_at	NA	NA	2.0	0.002
318	1457322_at	NA	NA	2.0	0.010
319	1443751_at	NA	NA	2.0	0.000
320	1447527_at	NA	NA	2.0	0.000
321	1456787_at	NA	NA	2.0	0.008
322	1443238_at	NA	NA	2.0	0.001
323	1458360_at	NA	NA	1.9	0.001
324	1441718_at	NA	NA	1.9	0.000
325	1441629_at	NA	NA	1.9	0.009
326	1440650_at	NA	NA	1.9	0.007
327	1439195_at	NA	NA	1.9	0.002
328	1430477_s_at	NA	NA	1.9	0.003
329	1443161_at	NA	NA	1.9	0.010
330	1420068_at	NA	NA	1.9	0.005
331	1441584_at	NA	NA	1.9	0.005
332	1442715_at	NA	NA	1.9	0.007
333	1439929_at	NA	NA	1.8	0.002
334	1427841_at	NA	NA	1.8	0.002
335	1438072_at	NA	NA	1.8	0.002
336	1446406_at	NA	NA	1.8	0.005
337	1457370_at	NA	NA	1.8	0.000
338	1459238_at	NA	NA	1.8	0.002
339	1440465_at	NA	NA	1.8	0.003
340	1458135_at	NA	NA	1.8	0.001
341	1445779_at	NA	NA	1.8	0.005
342	1439711_at	NA	NA	1.8	0.003
343	1440810_x_at	NA	NA	1.8	0.008
344	1457367_at	NA	NA	1.8	0.009
345	1442924_at	NA	NA	1.8	0.001
346	1443075_at	NA	NA	1.8	0.002
347	1439336_at	NA	NA	1.8	0.008
348	1458556_at	NA	NA	1.8	0.007
349	1446809_at	NA	NA	1.8	0.002
350	1446286_at	NA	NA	1.8	0.004
351	1447060_at	NA	NA	1.8	0.001
352	1443410_at	NA	NA	1.8	0.005
353	1443396_at	NA	NA	1.8	0.001
354	1455977_x_at	NA	NA	1.8	0.000
355	1444126_at	NA	NA	1.8	0.008
356	1443018_at	NA	NA	1.8	0.001
357	1447378_at	NA	NA	1.8	0.002
358	1447546_s_at	NA	NA	1.8	0.006
359	1458018_at	NA	NA	1.8	0.003
360	1459702_at	NA	NA	1.8	0.010
361	1442620_at	NA	NA	1.8	0.005
362	1444869_at	NA	NA	1.7	0.001
363	1431237_at	NA	NA	1.7	0.006
364	1443628_at	NA	NA	1.7	0.004
365	1440728_at	NA	NA	1.7	0.003
366	1442910_at	NA	NA	1.7	0.007
367	1447312_at	NA	NA	1.7	0.003
368	1444345_at	NA	NA	1.7	0.002
369	1459746_at	NA	NA	1.7	0.001
370	1456720_at	NA	NA	1.7	0.006
371	1443270_at	NA	NA	1.7	0.005
372	1447581_at	NA	NA	1.7	0.006

#	ID	SYMBOL	GENENAME	FC	P-Value
373	1449787_at	NA	NA	1.7	0.009
374	1440682_at	NA	NA	1.7	0.003
375	1445336_at	NA	NA	1.7	0.004
376	1449601_x_at	NA	NA	1.7	0.002
377	1436449_at	NA	NA	1.7	0.003
378	1458586_at	NA	NA	1.7	0.003
379	1440660_at	NA	NA	1.7	0.000
380	1419801_x_at	NA	NA	1.7	0.001
381	1419937_at	NA	NA	1.7	0.005
382	1427572_at	NA	NA	1.7	0.007
383	1421674_at	NA	NA	1.7	0.008
384	1458290_at	NA	NA	1.7	0.007
385	1443389_at	NA	NA	1.7	0.009
386	1447062_at	NA	NA	1.7	0.001
387	1458075_at	NA	NA	1.7	0.000
388	1438891_at	NA	NA	1.7	0.002
389	1443072_at	NA	NA	1.7	0.005
390	1446447_at	NA	NA	1.7	0.002
391	1446515_at	NA	NA	1.7	0.008
392	1442049_at	NA	NA	1.7	0.010
393	1440694_at	NA	NA	1.7	0.006
394	1443606_at	NA	NA	1.6	0.006
395	1459409_at	NA	NA	1.6	0.004
396	1443164_at	NA	NA	1.6	0.007
397	1442886_at	NA	NA	1.6	0.009
398	1440954_at	NA	NA	1.6	0.007
399	1442126_at	NA	NA	1.6	0.006
400	1446223_at	NA	NA	1.6	0.001
401	1444609_at	NA	NA	1.6	0.004
402	1446327_at	NA	NA	1.6	0.004
403	1459278_at	NA	NA	1.6	0.007
404	1457175_at	NA	NA	1.6	0.001
405	1459703_at	NA	NA	1.6	0.004
406	1458309_at	NA	NA	1.6	0.002
407	1443138_at	NA	NA	1.6	0.005
408	1455385_at	NA	NA	1.6	0.008
409	1443166_at	NA	NA	1.6	0.010
410	1458002_at	NA	NA	1.6	0.002
411	1438813_at	NA	NA	1.6	0.001
412	1420062_at	NA	NA	1.6	0.001
413	1441538_at	NA	NA	1.6	0.006
414	1445567_at	NA	NA	1.6	0.005
415	1458885_at	NA	NA	1.6	0.002
416	AFFX-r2-Bs-phe-	NA	NA	1.6	0.008
417	1445020_at	NA	NA	1.6	0.004
418	1437219_at	NA	NA	1.6	0.005
419	1456933_at	NA	NA	1.6	0.002
420	1444069_at	NA	NA	1.6	0.010
421	1444735_at	NA	NA	1.6	0.002
422	1444732_at	NA	NA	1.6	0.000
423	1440657_at	NA	NA	1.6	0.004
424	1438543_at	NA	NA	1.6	0.005
425	1444641_at	NA	NA	1.6	0.008
426	1453615_at	NA	NA	1.6	0.005
427	1446488_at	NA	NA	1.6	0.002
428	1457617_at	NA	NA	1.6	0.008
429	1443445_at	NA	NA	1.6	0.002
430	1456688_at	NA	NA	1.6	0.007
431	1442704_at	NA	NA	1.6	0.005
432	1445379_at	NA	NA	1.6	0.003
433	1449652_at	NA	NA	1.6	0.005
434	1438762_at	NA	NA	1.6	0.005
435	1443799_at	NA	NA	1.6	0.001
436	1444365_at	NA	NA	1.6	0.008
437	1446324_at	NA	NA	1.6	0.008
438	1459485_at	NA	NA	1.6	0.002
439	1441203_at	NA	NA	1.5	0.004
440	1440433_at	NA	NA	1.5	0.005
441	1436082_at	NA	NA	1.5	0.007
442	1446104_at	NA	NA	1.5	0.005
443	1459571_at	NA	NA	1.5	0.007
444	1443697_at	NA	NA	1.5	0.010
445	1441498_at	NA	NA	1.5	0.007
446	1436087_at	NA	NA	1.5	0.008
447	1459008_at	NA	NA	1.5	0.009
448	1441392_at	NA	NA	1.5	0.004
449	1458916_at	NA	NA	1.5	0.007
450	1443232_at	NA	NA	1.5	0.004
451	1438393_at	NA	NA	1.5	0.001
452	1441775_at	NA	NA	1.5	0.010
453	1442509_at	NA	NA	1.5	0.006
454	1441351_at	NA	NA	1.5	0.002

#	ID	SYMBOL	GENENAME	FC	P-Value
455	1441425_at	NA	NA	1.5	0.001
456	1457847_at	NA	NA	1.5	0.005
457	1447096_at	NA	NA	1.5	0.004
458	1447322_at	NA	NA	1.5	0.007
459	1443526_at	NA	NA	1.5	0.002
460	1447144_at	NA	NA	1.5	0.008
461	1449580_s_at	NA	NA	1.5	0.005
462	1446138_at	NA	NA	1.5	0.010
463	1444458_at	NA	NA	1.5	0.005
464	1440511_at	NA	NA	1.5	0.010
465	1447123_at	NA	NA	1.5	0.004
466	1458946_at	NA	NA	1.5	0.003
467	1427600_at	NA	NA	1.5	0.005
468	1435839_at	NA	NA	1.5	0.002
469	1443983_at	NA	NA	1.5	0.005
470	1458328_x_at	NA	NA	1.5	0.010
471	1445869_at	NA	NA	1.5	0.006
472	1440196_at	NA	NA	1.5	0.004
473	1458257_at	NA	NA	1.5	0.005
474	1444772_at	NA	NA	1.5	0.007
475	1445129_at	NA	NA	1.5	0.006
476	1441674_at	NA	NA	1.5	0.009
477	1441701_at	NA	NA	1.5	0.007
478	1441267_at	NA	NA	1.5	0.003
479	1458357_x_at	NA	NA	1.5	0.006
480	1441475_at	NA	NA	1.5	0.004
481	1446504_at	NA	NA	1.5	0.004
482	1427827_at	NA	NA	1.4	0.004
483	1439652_at	NA	NA	1.4	0.006
484	1446412_at	NA	NA	1.4	0.006
485	1441299_at	NA	NA	1.4	0.003
486	1447661_at	NA	NA	1.4	0.009
487	1444971_at	NA	NA	1.4	0.005
488	1457938_at	NA	NA	1.4	0.007
489	1422948_s_at	NA	NA	1.4	0.010
490	1445561_at	NA	NA	1.4	0.010
491	1446422_at	NA	NA	1.4	0.010
492	1459689_at	NA	NA	1.4	0.005
493	1458891_at	NA	NA	1.4	0.006
494	1459371_at	NA	NA	1.4	0.009
495	1447951_at	NA	NA	1.4	0.003
496	1443024_at	NA	NA	1.4	0.008
497	1440533_at	NA	NA	1.4	0.007
498	1441164_at	NA	NA	1.4	0.007
499	1456223_at	NA	NA	1.4	0.007
500	1432638_at	NA	NA	1.4	0.009
501	1458432_at	NA	NA	1.4	0.004
502	1442241_at	NA	NA	1.4	0.009
503	1456928_at	NA	NA	1.4	0.008
504	1456669_at	NA	NA	1.4	0.009
505	1456801_at	NA	NA	1.4	0.006
506	1450822_at	NA	NA	1.3	0.008
507	1441020_at	NA	NA	1.3	0.009
508	1441444_at	Nbeal1	neurobeachin like 1	1.6	0.002
509	1448428_at	Nbl1	neuroblastoma, suppression of tumorigenicity 1	1.4	0.007
510	1448746_at	Nbn	nibrin	1.4	0.006
511	1439556_at	Ncam1	neural cell adhesion molecule 1	1.7	0.004
512	1450976_at	Ndrg1	N-myc downstream regulated gene 1	1.6	0.004
513	1444003_at	Neurl3	neuralized homolog 3 homolog (Drosophila)	1.4	0.009
514	1447549_x_at	Ninj1	ninjurin 1	1.4	0.006
515	1434275_at	Nkd2	naked cuticle 2 homolog (Drosophila)	1.5	0.007
516	1437660_at	Nktr	natural killer tumor recognition sequence	1.8	0.000
517	1422346_at	Nkx2-1	NK2 homeobox 1	1.4	0.008
518	1427420_at	Nkx6-2	NK6 homeobox 2	1.6	0.007
519	1441447_at	Nol4	nucleolar protein 4	2.0	0.001
520	1422142_at	Nphs1	nephrosis 1 homolog, nephrin (human)	1.9	0.008
521	1428534_at	Nr2c2ap	nuclear receptor 2C2-associated protein	1.4	0.007
522	1421515_at	Nr6a1	nuclear receptor subfamily 6, group A, member 1	1.6	0.001
523	1456773_at	Nupl2	nucleoporin like 2	1.4	0.007
524	1429753_at	Nxph4	neurexophilin 4	1.8	0.005
525	1454424_at	Odz2	odd Oz/ten-m homolog 2 (Drosophila)	1.9	0.001
526	1422370_at	Olfr49	olfactory receptor 49	1.5	0.007
527	1451710_at	Oscar	osteoclast associated receptor	1.7	0.006
528	1423002_at	Pag1	phosphoprotein associated with glycosphingolipid microdomains 1	1.5	0.006
529	1446159_at	Pak7	p21 protein (Cdc42/Rac)-activated kinase 7	2.0	0.002
530	1444317_at	Pcdh15	protocadherin 15	1.6	0.009
531	1450263_at	Pcdhb5	protocadherin beta 5	1.5	0.007
532	1427160_at	Pcf11	cleavage and polyadenylation factor subunit homolog (S. cerevisiae)	1.4	0.008
533	1446272_at	Pctk2	PCTAIRE-motif protein kinase 2	1.7	0.002
534	1436966_at	Peli2	pellino 2	1.4	0.009
535	1453283_at	Pgm1	phosphoglucomutase 1	1.4	0.008
536	1439527_at	Pgr	progesterone receptor	1.4	0.005

#	ID	SYMBOL	GENENAME	FC	P-Value
537	1441145_at	Phf21a	PHD finger protein 21A	1.6	0.007
538	1454999_at	Phf21b	PHD finger protein 21B	1.4	0.008
539	1438535_at	Phip	pleckstrin homology domain interacting protein	1.7	0.005
540	1457640_x_at	Pigs	phosphatidylinositol glycan anchor biosynthesis, class S	1.5	0.007
541	1451335_at	Plac8	placenta-specific 8	1.6	0.001
542	1452517_at	Plekhh1	pleckstrin homology domain containing, family H (with MyTH4	1.7	0.008
543	1418595_at	Plin4	perilipin 4	1.5	0.003
544	1450952_at	Pln	phospholamban	1.4	0.005
545	1425371_at	Polb	polymerase (DNA directed), beta	1.5	0.005
546	1427094_at	Pole2	polymerase (DNA directed), epsilon 2 (p59 subunit)	1.5	0.006
547	1453420_at	Pou5f2	POU domain class 5, transcription factor 2	1.7	0.004
548	1435861_at	Ppfia1	protein tyrosine phosphatase, receptor type, f polypeptide (PTPRF),	1.7	0.007
549	1419681_a_at	Prok2	prokineticin 2	1.8	0.005
550	1446560_at	Prss23	protease, serine, 23	1.9	0.000
551	1425549_at	Psen1	presenilin 1	1.4	0.005
552	1450375_at	Pspn	persephin	1.6	0.007
553	1448816_at	Ptgis	prostaglandin I2 (prostacyclin) synthase	1.7	0.007
554	1449798_at	Rab3c	RAB3C, member RAS oncogene family	1.8	0.000
555	1417620_at	Rac2	RAS-related C3 botulinum substrate 2	1.8	0.000
556	1435826_at	Rad18	RAD18 homolog (S. cerevisiae)	1.4	0.004
557	1442775_at	Rangap1	RAN GTPase activating protein 1	1.4	0.004
558	1438828_at	Rapgef6	Rap guanine nucleotide exchange factor (GEF) 6	1.8	0.009
559	1429024_at	Rbm20	RNA binding motif protein 20	1.6	0.009
560	1443715_at	Rbm24	RNA binding motif protein 24	1.5	0.003
561	1444765_at	Rbpms	RNA binding protein gene with multiple splicing	1.6	0.004
562	1456105_at	Rc3h2	ring finger and CCCH-type zinc finger domains 2	1.4	0.009
563	1457019_s_at	Rdh14	retinol dehydrogenase 14 (all-trans and 9-cis)	1.4	0.005
564	1418892_at	Rhoj	ras homolog gene family, member J	1.6	0.001
565	1449914_at	Ribc1	RIB43A domain with coiled-coils 1	1.6	0.002
566	1429490_at	Rif1	Rap1 interacting factor 1 homolog (yeast)	1.9	0.003
567	1429491_s_at	Rif1	Rap1 interacting factor 1 homolog (yeast)	1.9	0.005
568	1434684_at	Rin3	Ras and Rab interactor 3	1.6	0.002
569	1431100_at	Rinl	Ras and Rab interactor-like	1.4	0.006
570	1452361_at	Rnf20	ring finger protein 20	1.5	0.003
571	1441162_at	Rock1	Rho-associated coiled-coil containing protein kinase 1	1.5	0.007
572	1440310_at	Runx1t1	runt-related transcription factor 1; translocated to, 1 (cyclin D-	1.8	0.003
573	1439161_at	Saps3	SAPS domain family, member 3	1.6	0.004
574	1441573_at	Scmh1	sex comb on midleg homolog 1	1.8	0.006
575	1436646_at	Scn2a1	sodium channel, voltage-gated, type II, alpha 1	1.7	0.004
576	1459269_at	Sdr39u1	short chain dehydrogenase/reductase family 39U, member 1	1.6	0.003
577	1441636_at	Sec14l5	SEC14-like 5 (S. cerevisiae)	1.4	0.008
578	1448415_a_at	Sema3b	sema domain, immunoglobulin domain (Ig), short basic domain,	2.4	0.008
579	1425840_a_at	Sema3f	sema domain, immunoglobulin domain (Ig), short basic domain,	1.4	0.010
580	1435946_at	Sepsecs	Sep (O-phosphoserine) tRNA:Sec (selenocysteine) tRNA synthase	1.5	0.003
581	1431300_at	Sgip1	SH3-domain GRB2-like (endophilin) interacting protein 1	1.7	0.008
582	1426551_at	Sidt1	SID1 transmembrane family, member 1	1.4	0.005
583	1449163_at	Sigirr	single immunoglobulin and toll-interleukin 1 receptor (TIR) domain	1.5	0.007
584	1456508_at	Skint10	selection and upkeep of intraepithelial T cells 10	1.7	0.004
585	1425570_at	Slamf1	signaling lymphocytic activation molecule family member 1	1.5	0.005
586	1420445_at	Slc16a8	solute carrier family 16 (monocarboxylic acid transporters), member	2.0	0.007
587	1420966_at	Slc25a15	solute carrier family 25 (mitochondrial carrier ornithine transporter),	1.6	0.002
588	1445528_at	Slc28a3	solute carrier family 28 (sodium-coupled nucleoside transporter),	1.8	0.000
589	1422788_at	Slc43a3	solute carrier family 43, member 3	1.5	0.006
590	1451055_at	Slc45a2	solute carrier family 45, member 2	1.7	0.001
591	1444242_at	Slco2a1	solute carrier organic anion transporter family, member 2a1	1.5	0.009
592	1422771_at	Smad6	MAD homolog 6 (Drosophila)	1.9	0.000
593	1458479_at	Smc2	structural maintenance of chromosomes 2	1.7	0.006
594	1428539_at	Smg1	SMG1 homolog, phosphatidylinositol 3-kinase-related kinase (C.	1.6	0.007
595	1426320_at	Snx29	sorting nexin 29	1.8	0.006
596	1423077_at	Snx9	sorting nexin 9	1.5	0.007
597	1437865_at	Spata13	spermatogenesis associated 13	1.5	0.003
598	1421277_at	Spna1	spectrin alpha 1	1.4	0.006
599	1441653_at	Srcap	Snf2-related CREBBP activator protein	2.0	0.008
600	1425829_a_at	Steap4	STEAP family member 4	1.5	0.005
601	1427291_at	Sycp1	synaptonemal complex protein 1	1.4	0.009
602	1431798_a_at	Syde1	synapse defective 1, Rho GTPase, homolog 1 (C. elegans)	1.4	0.004
603	1421248_at	Syn3	synapsin III	1.5	0.006
604	1438282_at	Syt1	synaptotagmin I	2.0	0.002
605	1439090_at	Tbc1d23	TBC1 domain family, member 23	1.6	0.002
606	1421909_at	Tcf20	transcription factor 20	1.9	0.002
607	1445895_at	Tcrb-V8.2	T-cell receptor beta, variable 8.2	1.6	0.007
608	1423224_at	Tctn2	tectonic family member 2	1.6	0.001
609	1425169_at	Tessp2	testis serine protease 2	1.9	0.001
610	1452978_at	Tmem138	transmembrane protein 138	1.4	0.010
611	1441811_x_at	Tmem176a	transmembrane protein 176A	1.6	0.005
612	1456963_at	Tmem214	transmembrane protein 214	1.5	0.008
613	1460451_at	Tmem52	transmembrane protein 52	1.6	0.009
614	1458106_at	Tmem60	transmembrane protein 60	1.6	0.007
615	1458342_at	Tmem90a	transmembrane protein 90a	1.5	0.008
616	1456344_at	Tnc	tenascin C	1.5	0.001
617	1418424_at	Tnfaip6	tumor necrosis factor alpha induced protein 6	1.6	0.004
618	1430259_at	Tnfrsf11a	tumor necrosis factor receptor superfamily, member 11a	1.5	0.003

#	ID	SYMBOL	GENENAME	FC	P-Value
619	1417291_at	Tnfrsf1a	tumor necrosis factor receptor superfamily, member 1a	1.4	0.006
620	1448951_at	Tnfrsf1b	tumor necrosis factor receptor superfamily, member 1b	1.4	0.007
621	1450272_at	Tnfsf8	tumor necrosis factor (ligand) superfamily, member 8	1.4	0.009
622	1450813_a_at	Tnni1	troponin I, skeletal, slow 1	1.8	0.002
623	1421998_at	Tor3a	torsin family 3, member A	1.5	0.007
624	1439043_at	Tra2a	transformer 2 alpha homolog (Drosophila)	2.2	0.008
625	1425161_a_at	Trabd	TraB domain containing	1.7	0.002
626	1439910_a_at	Tradd	TNFRSF1A-associated via death domain	1.6	0.007
627	1449571_at	Trhr	thyrotropin releasing hormone receptor	3.3	0.001
628	1443989_at	Trim9	tripartite motif-containing 9	1.4	0.009
629	1430920_at	Trmt11	tRNA methyltransferase 11 homolog (S. cerevisiae)	1.7	0.006
630	1442316_x_at	Trp53bp1	transformation related protein 53 binding protein 1	1.6	0.003
631	1431355_s_at	Trpm7	transient receptor potential cation channel, subfamily M, member 7	1.7	0.000
632	1445727_at	Ube3a	ubiquitin protein ligase E3A	1.4	0.010
633	1418132_a_at	Ubfd1	ubiquitin family domain containing 1	1.5	0.009
634	1437022_at	Ubn2	ubinuclein 2	1.6	0.005
635	1426105_a_at	Ubxn11	UBX domain protein 11	1.6	0.002
636	1450001_a_at	Ush1c	Usher syndrome 1C homolog (human)	1.7	0.003
637	1428193_at	Usp9x	ubiquitin specific peptidase 9, X chromosome	1.6	0.009
638	1438579_at	Utp14b	UTP14, U3 small nucleolar ribonucleoprotein, homolog B (yeast)	1.6	0.002
639	1451314_a_at	Vcam1	vascular cell adhesion molecule 1	1.7	0.002
640	1455299_at	Vgll3	vestigial like 3 (Drosophila)	3.6	0.000
641	1453593_at	Vgll3	vestigial like 3 (Drosophila)	2.3	0.002
642	1444050_at	Wisp3	WNT1 inducible signaling pathway protein 3	1.4	0.006
643	1443924_at	Wnk3	WNK lysine deficient protein kinase 3	1.6	0.007
644	1437822_at	Yme1l1	YME1-like 1 (S. cerevisiae)	1.8	0.005
645	1431781_at	Ypel1	yippee-like 1 (Drosophila)	1.6	0.009
646	1422570_at	Yy1	YY1 transcription factor	1.5	0.009
647	1438269_at	Zbtb38	zinc finger and BTB domain containing 38	1.9	0.009
648	1425097_a_at	Zfp106	zinc finger protein 106	1.7	0.000
649	1438479_at	Zfp213	zinc finger protein 213	1.9	0.004
650	1456023_at	Zfp846	zinc finger protein 846	1.4	0.003
651	1455290_at	Znrf2	zinc and ring finger 2	1.5	0.003

5.1.4 DNA methylation affected by the genotype (5-Htt+/- versus wild-type).

Effect: direction of effect; “+”: DNA methylation upregulated in 5-Htt+/- versus wild-type mice; “-“: downregulated in 5-Htt+/- versus wild type mice. Genes have been ordered alphabetically by symbol.

#	Feature	Symbol	Genename	Effect
1	ENSMUSG00000046840	0610008F07Rik	RIKEN cDNA 0610008F07 gene [Source:MGI Symbol;Acc:MGI:1915564]	-
2	ENSMUSG00000060512	0610040J01Rik	RIKEN cDNA 0610040J01 gene [Source:MGI Symbol;Acc:MGI:1923511]	-
3	ENSMUSG00000052105	1110012J17Rik	RIKEN cDNA 1110012J17 gene [Source:MGI Symbol;Acc:MGI:1915867]	+
4	ENSMUSG00000031509	1700016D06Rik	RIKEN cDNA 1700016D06 gene [Source:MGI Symbol;Acc:MGI:1923663]	+
5	ENSMUSG00000037535	1700021A07Rik	RIKEN cDNA 1700021A07 gene [Source:MGI Symbol;Acc:MGI:1924174]	+
6	ENSMUSG00000041707	1810011H11Rik	RIKEN cDNA 1810011H11 gene [Source:MGI Symbol;Acc:MGI:1916319]	+
7	ENSMUSG00000076437	2700094K13Rik	RIKEN cDNA 2700094K13 gene [Source:MGI Symbol;Acc:MGI:1919907]	+
8	ENSMUSG00000043833	2900005J15Rik	RIKEN cDNA 2900005J15 gene [Source:MGI Symbol;Acc:MGI:1914511]	+
9	ENSMUSG00000034689	4921530L21Rik	RIKEN cDNA 4921530L21 gene [Source:MGI Symbol;Acc:MGI:1913982]	+
10	ENSMUSG00000043633	4930412F15Rik	RIKEN cDNA 4930412F15 gene [Source:MGI Symbol;Acc:MGI:2441678]	-
11	ENSMUSG00000050883	4930523C07Rik	RIKEN cDNA 4930523C07 gene [Source:MGI Symbol;Acc:MGI:1914897]	-
12	ENSMUSG00000051758	4930544M13Rik	RIKEN cDNA 4930544M13 gene [Source:MGI Symbol;Acc:MGI:1922411]	+
13	ENSMUSG00000028801	4930555I21Rik	RIKEN cDNA 4930555I21 gene [Source:MGI Symbol;Acc:MGI:1926056]	-
14	ENSMUSG00000049506	4933407P14Rik	RIKEN cDNA 4933407P14 gene [Source:MGI Symbol;Acc:MGI:3045264]	-
15	ENSMUSG00000046591	5730590G19Rik	RIKEN cDNA 5730590G19 gene [Source:MGI Symbol;Acc:MGI:1924261]	+
16	ENSMUSG00000030982	9030624J02Rik	RIKEN cDNA 9030624J02 gene [Source:MGI Symbol;Acc:MGI:1918767]	-
17	ENSMUSG00000044350	9030625A04Rik	RIKEN cDNA 9030625A04 gene [Source:MGI Symbol;Acc:MGI:2445077]	-
18	ENSMUSG00000044350	9030625A04Rik	RIKEN cDNA 9030625A04 gene [Source:MGI Symbol;Acc:MGI:2445077]	+
19	ENSMUSG00000047878	A4galt	alpha 1,4-galactosyltransferase [Source:MGI Symbol;Acc:MGI:3512453]	-
20	ENSMUSG00000054057	A930004D18Rik	RIKEN cDNA A930004D18 gene [Source:MGI Symbol;Acc:MGI:1925190]	+
21	ENSMUSG00000027380	Acoxl	acyl-Coenzyme A oxidase-like [Source:MGI Symbol;Acc:MGI:1921371]	+
22	ENSMUSG00000028093	Acp6	acid phosphatase 6, lysophosphatidic [Source:MGI Symbol;Acc:MGI:1931010]	+
23	ENSMUSG00000022039	Adam2	a disintegrin and metallopeptidase domain 2 [Source:MGI Symbol;Acc:MGI:1340894]	+
24	ENSMUSG00000043468	Adam30	a disintegrin and metallopeptidase domain 30 [Source:MGI Symbol;Acc:MGI:1918328]	+
25	ENSMUSG00000022449	Adamts20	a disintegrin-like and metallopeptidase (reprolysin type) with thrombospondin type 1 motif, 20 [Source:MGI Symbol;Acc:MGI:2660628]	-
26	ENSMUSG00000043635	Adamts3	a disintegrin-like and metallopeptidase (reprolysin type) with thrombospondin type 1 motif, 3 [Source:MGI Symbol;Acc:MGI:3045353]	-
27	ENSMUSG00000057134	Ado	2-aminoethanethiol (cysteamine) dioxygenase [Source:MGI Symbol;Acc:MGI:2685083]	+
28	ENSMUSG00000061603	Akap6	A kinase (PRKA) anchor protein 6 [Source:MGI Symbol;Acc:MGI:3050566]	-
29	ENSMUSG00000010025	Aldh3a2	aldehyde dehydrogenase family 3, subfamily A2 [Source:MGI Symbol;Acc:MGI:1353452]	+
30	ENSMUSG00000025172	Ankrd2	ankyrin repeat domain 2 (stretch responsive muscle) [Source:MGI Symbol;Acc:MGI:1861447]	+
31	ENSMUSG00000032231	Anxa2	annexin A2 [Source:MGI Symbol;Acc:MGI:88246]	-
32	ENSMUSG00000073705	Apitd1	apoptosis-inducing, TAF9-like domain 1 [Source:MGI Symbol;Acc:MGI:1917178]	+
33	ENSMUSG00000030051	Aplf	aprataxin and PNKP like factor [Source:MGI Symbol;Acc:MGI:1919353]	+

34	ENSMUSG00000021895	Arhgef3	Rho guanine nucleotide exchange factor (GEF) 3 [Source:MGI Symbol;Acc:MGI:1918954]	+
35	ENSMUSG00000015709	Arnt2	aryl hydrocarbon receptor nuclear translocator 2 [Source:MGI Symbol;Acc:MGI:107188]	+
36	ENSMUSG00000036995	Asap3	ArfGAP with SH3 domain, ankyrin repeat and PH domain 3 [Source:MGI Symbol;Acc:MGI:2684986]	-
37	ENSMUSG00000021619	Atg10	autophagy-related 10 (yeast) [Source:MGI Symbol;Acc:MGI:1914045]	+
38	ENSMUSG00000034780	B3galt1	UDP-Gal:betaGlcNAc beta 1,3-galactosyltransferase, polypeptide 1 [Source:MGI Symbol;Acc:MGI:1349403]	+
39	ENSMUSG00000022641	Bbx	bobby sox homolog (Drosophila) [Source:MGI Symbol;Acc:MGI:1917758]	+
40	ENSMUSG00000044937	BC030307	cDNA sequence BC030307 [Source:MGI Symbol;Acc:MGI:2387653]	+
41	ENSMUSG00000034773	BC030867	cDNA sequence BC030867 [Source:MGI Symbol;Acc:MGI:2387601]	-
42	ENSMUSG00000021763	BC067074	cDNA sequence BC067074 [Source:MGI Symbol;Acc:MGI:3040697]	+
43	ENSMUSG00000027381	Bcl2l11	BCL2-like 11 (apoptosis facilitator) [Source:MGI Symbol;Acc:MGI:1197519]	+
44	ENSMUSG00000021835	Bmp4	bone morphogenetic protein 4 [Source:MGI Symbol;Acc:MGI:88180]	+
45	ENSMUSG00000052430	Bmpr1b	bone morphogenetic protein receptor, type 1B [Source:MGI Symbol;Acc:MGI:107191]	+
46	ENSMUSG00000067998	Bpifb9a	BPI fold containing family B, member 9A [Source:MGI Symbol;Acc:MGI:3767993]	+
47	ENSMUSG00000038658	C030046E11Rik	RIKEN cDNA C030046E11 gene [Source:MGI Symbol;Acc:MGI:1924893]	-
48	ENSMUSG00000046491	C1qtnf2	C1q and tumor necrosis factor related protein 2 [Source:MGI Symbol;Acc:MGI:1916433]	-
49	ENSMUSG00000040552	C3ar1	complement component 3a receptor 1 [Source:MGI Symbol;Acc:MGI:1097680]	+
50	ENSMUSG00000036438	Calm2	calmodulin 2 [Source:MGI Symbol;Acc:MGI:103250]	-
51	ENSMUSG00000063130	Calml3	calmodulin-like 3 [Source:MGI Symbol;Acc:MGI:1917655]	+
52	ENSMUSG00000028745	Capzb	capping protein (actin filament) muscle Z-line, beta [Source:MGI Symbol;Acc:MGI:104652]	-
53	ENSMUSG00000027187	Cat	catalase [Source:MGI Symbol;Acc:MGI:88271]	+
54	ENSMUSG00000026676	Ccdc3	coiled-coil domain containing 3 [Source:MGI Symbol;Acc:MGI:1921436]	-
55	ENSMUSG00000039977	Ccdc67	coiled-coil domain containing 67 [Source:MGI Symbol;Acc:MGI:2443026]	-
56	ENSMUSG00000079227	Ccr5	chemokine (C-C motif) receptor 5 [Source:MGI Symbol;Acc:MGI:107182]	-
57	ENSMUSG00000027863	Cd2	CD2 antigen [Source:MGI Symbol;Acc:MGI:88320]	-
58	ENSMUSG00000030798	Cd37	CD37 antigen [Source:MGI Symbol;Acc:MGI:88330]	-
59	ENSMUSG00000024081	Cebpz	CCAAT/enhancer binding protein zeta [Source:MGI Symbol;Acc:MGI:109386]	+
60	ENSMUSG00000036403	Cep135	centrosomal protein 135 [Source:MGI Symbol;Acc:MGI:2681869]	+
61	ENSMUSG00000028298	Cga	glycoprotein hormones, alpha subunit [Source:MGI Symbol;Acc:MGI:88390]	-
62	ENSMUSG00000036960	Clca5	chloride channel calcium activated 5 [Source:MGI Symbol;Acc:MGI:2139758]	-
63	ENSMUSG00000000605	Clcn4-2	chloride channel 4-2 [Source:MGI Symbol;Acc:MGI:104571]	-
64	ENSMUSG00000038070	Cntln	centlein, centrosomal protein [Source:MGI Symbol;Acc:MGI:2443104]	+
65	ENSMUSG00000033063	Cntnap3	contactin associated protein-like 3 [Source:MGI Symbol;Acc:MGI:3588199]	+
66	ENSMUSG00000025196	Cpn1	carboxypeptidase N, polypeptide 1 [Source:MGI Symbol;Acc:MGI:2135874]	+
67	ENSMUSG00000006134	Crkl	v-crk sarcoma virus CT10 oncogene homolog (avian)-like [Source:MGI Symbol;Acc:MGI:104686]	+
68	ENSMUSG00000046707	Csnk2a2	casein kinase 2, alpha prime polypeptide [Source:MGI Symbol;Acc:MGI:88547]	+
69	ENSMUSG00000032359	Ctsh	cathepsin H [Source:MGI Symbol;Acc:MGI:107285]	+
70	ENSMUSG00000021477	Ctsl	cathepsin L [Source:MGI Symbol;Acc:MGI:88564]	+
71	ENSMUSG00000029380	Cxcl1	chemokine (C-X-C motif) ligand 1 [Source:MGI Symbol;Acc:MGI:108068]	+
72	ENSMUSG00000044365	Cxxc4	CXXC finger 4 [Source:MGI Symbol;Acc:MGI:2442112]	+
73	ENSMUSG00000027015	Cybrd1	cytochrome b reductase 1 [Source:MGI Symbol;Acc:MGI:2654575]	-
74	ENSMUSG00000020075	Ddx21	DEAD (Asp-Glu-Ala-Asp) box polypeptide 21 [Source:MGI Symbol;Acc:MGI:1860494]	+
75	ENSMUSG00000070291	Ddx43	DEAD (Asp-Glu-Ala-Asp) box polypeptide 43 [Source:MGI Symbol;Acc:MGI:3642857]	+
76	ENSMUSG00000074681	Defb23	defensin beta 23 [Source:MGI Symbol;Acc:MGI:3644405]	-
77	ENSMUSG00000021697	Depdc1b	DEP domain containing 1B [Source:MGI Symbol;Acc:MGI:2145425]	+
78	ENSMUSG00000022419	Deptor	DEP domain containing MTOR-interacting protein [Source:MGI Symbol;Acc:MGI:2146322]	-
79	ENSMUSG00000030986	Dhx32	DEAH (Asp-Glu-Ala-His) box polypeptide 32 [Source:MGI Symbol;Acc:MGI:2141813]	-
80	ENSMUSG00000004099	Dnmt1	DNA methyltransferase (cytosine-5) 1 [Source:MGI Symbol;Acc:MGI:94912]	+
81	ENSMUSG00000052085	Dock8	dedicator of cytokinesis 8 [Source:MGI Symbol;Acc:MGI:1921396]	-
82	ENSMUSG00000052085	Dock8	dedicator of cytokinesis 8 [Source:MGI Symbol;Acc:MGI:1921396]	+
83	ENSMUSG00000039661	Dusp26	dual specificity phosphatase 26 (putative) [Source:MGI Symbol;Acc:MGI:1914209]	+
84	ENSMUSG00000016477	E2f3	E2F transcription factor 3 [Source:MGI Symbol;Acc:MGI:1096340]	-
85	ENSMUSG00000048029	Eno4	enolase 4 [Source:MGI Symbol;Acc:MGI:2441717]	-
86	ENSMUSG00000001946	Esam	endothelial cell-specific adhesion molecule [Source:MGI Symbol;Acc:MGI:1916774]	-
87	ENSMUSG00000019768	Esr1	estrogen receptor 1 (alpha) [Source:MGI Symbol;Acc:MGI:1352467]	+
88	ENSMUSG00000011831	Evi5	ecotropic viral integration site 5 [Source:MGI Symbol;Acc:MGI:104736]	+
89	ENSMUSG00000017897	Eya2	eyes absent 2 homolog (Drosophila) [Source:MGI Symbol;Acc:MGI:109341]	+
90	ENSMUSG00000062196	Fabp5l2	fatty acid binding protein 5-like 2 [Source:MGI Symbol;Acc:MGI:3644282]	-
91	ENSMUSG00000020405	Fabp6	fatty acid binding protein 6, ileal (gastrotropin) [Source:MGI Symbol;Acc:MGI:96565]	+
92	ENSMUSG00000070471	Fam194a	family with sequence similarity 194, member A [Source:MGI Symbol;Acc:MGI:3588212]	-
93	ENSMUSG00000022378	Fam49b	family with sequence similarity 49, member B [Source:MGI Symbol;Acc:MGI:1923520]	+
94	ENSMUSG00000053111	Fank1	fibronectin type 3 and ankyrin repeat domains 1 [Source:MGI Symbol;Acc:MGI:1914180]	-
95	ENSMUSG00000005371	Fbxo11	F-box protein 11 [Source:MGI Symbol;Acc:MGI:2147134]	+
96	ENSMUSG00000005320	Fgfr4	fibroblast growth factor receptor 4 [Source:MGI Symbol;Acc:MGI:95525]	+
97	ENSMUSG00000056602	Fry	furry homolog (Drosophila) [Source:MGI Symbol;Acc:MGI:2443895]	-
98	ENSMUSG00000030049	Gkn2	gastrokine 2 [Source:MGI Symbol;Acc:MGI:1913534]	+
99	ENSMUSG00000059659	Gm10069	predicted gene 10069 [Source:MGI Symbol;Acc:MGI:3641875]	-
100	ENSMUSG00000061062	Gm10093	predicted pseudogene 10093 [Source:MGI Symbol;Acc:MGI:3704479]	-
101	ENSMUSG00000066180	Gm10155	predicted gene 10155 [Source:MGI Symbol;Acc:MGI:3642914]	-
102	ENSMUSG00000070713	Gm10282	predicted pseudogene 10282 [Source:MGI Symbol;Acc:MGI:3704312]	-
103	ENSMUSG00000070511	Gm10295	predicted gene 10295 [Source:MGI Symbol;Acc:MGI:3642770]	-
104	ENSMUSG00000081758	Gm11460	predicted gene 11460 [Source:MGI Symbol;Acc:MGI:3649774]	+
105	ENSMUSG00000082410	Gm12011	predicted gene 12011 [Source:MGI Symbol;Acc:MGI:3651574]	-
106	ENSMUSG00000072834	Gm12298	predicted gene 12298 [Source:MGI Symbol;Acc:MGI:3649680]	-
107	ENSMUSG00000043770	Gm12481	predicted gene 12481 [Source:MGI Symbol;Acc:MGI:3650743]	-
108	ENSMUSG00000084159	Gm12696	predicted gene 12696 [Source:MGI Symbol;Acc:MGI:3649288]	-
109	ENSMUSG00000081136	Gm12990	predicted gene 12990 [Source:MGI Symbol;Acc:MGI:3651107]	+
110	ENSMUSG00000080802	Gm13804	predicted gene 13804 [Source:MGI Symbol;Acc:MGI:3651562]	-
111	ENSMUSG00000081196	Gm13858	predicted gene 13858 [Source:MGI Symbol;Acc:MGI:3649681]	+
112	ENSMUSG00000081991	Gm13859	predicted gene 13859 [Source:MGI Symbol;Acc:MGI:3649465]	+
113	ENSMUSG00000081422	Gm14282	predicted gene 14282 [Source:MGI Symbol;Acc:MGI:3709350]	-

114	ENSMUSG00000079261	Gm15217	predicted gene 15217 [Source:MGI Symbol;Acc:MGI:3705233]	+
115	ENSMUSG00000010529	Gm266	predicted gene 266 [Source:MGI Symbol;Acc:MGI:2685112]	-
116	ENSMUSG00000066491	Gm6265	predicted pseudogene 6265 [Source:MGI Symbol;Acc:MGI:3649160]	-
117	ENSMUSG00000072407	Gm6419	predicted gene 6419 [Source:MGI Symbol;Acc:MGI:3647564]	+
118	ENSMUSG00000046411	Gm6816	predicted gene 6816 [Source:MGI Symbol;Acc:MGI:3648347]	-
119	ENSMUSG00000081259	Gm6893	predicted gene 6893 [Source:MGI Symbol;Acc:MGI:3645616]	-
120	ENSMUSG00000024437	Gm8615	predicted pseudogene 8615 [Source:MGI Symbol;Acc:MGI:3647532]	-
121	ENSMUSG00000062458	Gm8623	predicted gene 8623 [Source:MGI Symbol;Acc:MGI:3644689]	+
122	ENSMUSG00000062458	Gm8623	predicted gene 8623 [Source:MGI Symbol;Acc:MGI:3644689]	+
123	ENSMUSG00000062896	Gm9154	predicted gene 9154 [Source:MGI Symbol;Acc:MGI:3646595]	+
124	ENSMUSG00000038594	Gm9766	predicted gene 9766 [Source:MGI Symbol;Acc:MGI:3642684]	-
125	ENSMUSG00000053749	Gm9920	predicted gene 9920 [Source:MGI Symbol;Acc:MGI:3642228]	-
126	ENSMUSG00000028850	Gpatch3	G patch domain containing 3 [Source:MGI Symbol;Acc:MGI:2442492]	+
127	ENSMUSG00000028848	Gpn2	GPN-loop GTPase 2 [Source:MGI Symbol;Acc:MGI:2140368]	+
128	ENSMUSG00000034450	Gulo	gulonolactone (L-) oxidase [Source:MGI Symbol;Acc:MGI:1353434]	+
129	ENSMUSG00000006930	Hap1	huntingtin-associated protein 1 [Source:MGI Symbol;Acc:MGI:1261831]	+
130	ENSMUSG00000035181	Heatr5a	HEAT repeat containing 5A [Source:MGI Symbol;Acc:MGI:2444133]	-
131	ENSMUSG00000068851	Hist4h4	histone cluster 4, H4 [Source:MGI Symbol;Acc:MGI:2448443]	+
132	ENSMUSG00000021379	Id4	inhibitor of DNA binding 4 [Source:MGI Symbol;Acc:MGI:99414]	-
133	ENSMUSG00000037801	Iqch	IQ motif containing H [Source:MGI Symbol;Acc:MGI:1925500]	-
134	ENSMUSG00000059883	Irak4	interleukin-1 receptor-associated kinase 4 [Source:MGI Symbol;Acc:MGI:2182474]	+
135	ENSMUSG00000027087	Itgav	integrin alpha V [Source:MGI Symbol;Acc:MGI:96608]	+
136	ENSMUSG00000057963	Itpk1	inositol 1,3,4-triphosphate 5/6 kinase [Source:MGI Symbol;Acc:MGI:2446159]	-
137	ENSMUSG00000040606	Kazn	kazrin, periplakin interacting protein [Source:MGI Symbol;Acc:MGI:1918779]	-
138	ENSMUSG00000032034	Kcnj5	potassium inwardly-rectifying channel, subfamily J, member 5 [Source:MGI Symbol;Acc:MGI:104755]	+
139	ENSMUSG00000021375	Kif13a	kinesin family member 13A [Source:MGI Symbol;Acc:MGI:1098264]	-
140	ENSMUSG00000050382	Kif7	kinesin family member 7 [Source:MGI Symbol;Acc:MGI:1098239]	+
141	ENSMUSG00000029414	Kntc1	kinetochore associated 1 [Source:MGI Symbol;Acc:MGI:2673709]	+
142	ENSMUSG00000006777	Krt23	keratin 23 [Source:MGI Symbol;Acc:MGI:2148866]	-
143	ENSMUSG00000022986	Krt75	keratin 75 [Source:MGI Symbol;Acc:MGI:1923500]	+
144	ENSMUSG00000030124	Lag3	lymphocyte-activation gene 3 [Source:MGI Symbol;Acc:MGI:106588]	-
145	ENSMUSG00000024063	Lbh	limb-bud and heart [Source:MGI Symbol;Acc:MGI:1925139]	+
146	ENSMUSG00000048058	Ldlrad3	low density lipoprotein receptor class A domain containing 3 [Source:MGI Symbol;Acc:MGI:2138856]	+
147	ENSMUSG00000020140	Lgr5	leucine rich repeat containing G protein coupled receptor 5 [Source:MGI Symbol;Acc:MGI:1341817]	+
148	ENSMUSG00000050217	Lgsn	lengsin, lens protein with glutamine synthetase domain [Source:MGI Symbol;Acc:MGI:2672844]	-
149	ENSMUSG00000029228	Lnx1	ligand of numb-protein X 1 [Source:MGI Symbol;Acc:MGI:1278335]	-
150	ENSMUSG00000025185	Loxl4	lysyl oxidase-like 4 [Source:MGI Symbol;Acc:MGI:1914823]	+
151	ENSMUSG00000041673	Lrrc18	leucine rich repeat containing 18 [Source:MGI Symbol;Acc:MGI:1914830]	+
152	ENSMUSG00000045854	Lyrm2	LYR motif containing 2 [Source:MGI Symbol;Acc:MGI:1917573]	+
153	ENSMUSG00000028164	Manba	mannosidase, beta A, lysosomal [Source:MGI Symbol;Acc:MGI:88175]	+
154	ENSMUSG00000021028	Mbip	MAP3K12 binding inhibitory protein 1 [Source:MGI Symbol;Acc:MGI:1918320]	-
155	ENSMUSG00000058006	Mdn1	midasin homolog (yeast) [Source:MGI Symbol;Acc:MGI:1926159]	+
156	ENSMUSG00000018160	Med1	mediator complex subunit 1 [Source:MGI Symbol;Acc:MGI:1100846]	-
157	ENSMUSG00000034258	Mfsd7c	major facilitator superfamily domain containing 7C [Source:MGI Symbol;Acc:MGI:2384974]	-
158	ENSMUSG00000054612	Mgmt	O-6-methylguanine-DNA methyltransferase [Source:MGI Symbol;Acc:MGI:96977]	-
159	ENSMUSG00000030218	Mgp	matrix Gla protein [Source:MGI Symbol;Acc:MGI:96976]	+
160	ENSMUSG00000065497	Mir410	microRNA 410 [Source:MGI Symbol;Acc:MGI:3619398]	-
161	ENSMUSG00000038437	Mllt6	myeloid/lymphoid or mixed-lineage leukemia (trithorax homolog, Drosophila); translocated to, 6 [Source:MGI Symbol;Acc:MGI:1935145]	-
162	ENSMUSG00000026303	Mlph	melanophilin [Source:MGI Symbol;Acc:MGI:2176380]	+
163	ENSMUSG00000003948	Mmd	monocyte to macrophage differentiation-associated [Source:MGI Symbol;Acc:MGI:1914718]	-
164	ENSMUSG00000057440	Mpp7	membrane protein, palmitoylated 7 (MAGUK p55 subfamily member 7) [Source:MGI Symbol;Acc:MGI:1922989]	-
165	ENSMUSG00000057388	Mrpl18	mitochondrial ribosomal protein L18 [Source:MGI Symbol;Acc:MGI:1914931]	+
166	ENSMUSG00000034729	Mrps10	mitochondrial ribosomal protein S10 [Source:MGI Symbol;Acc:MGI:1928139]	+
167	ENSMUSG00000021731	Mrps30	mitochondrial ribosomal protein S30 [Source:MGI Symbol;Acc:MGI:1926237]	+
168	ENSMUSG00000005370	Msh6	mutS homolog 6 (E. coli) [Source:MGI Symbol;Acc:MGI:1343961]	+
169	ENSMUSG00000028158	Mttp	microsomal triglyceride transfer protein [Source:MGI Symbol;Acc:MGI:106926]	+
170	ENSMUSG00000032508	Myd88	myeloid differentiation primary response gene 88 [Source:MGI Symbol;Acc:MGI:108005]	-
171	ENSMUSG00000039057	Myo16	myosin XVI [Source:MGI Symbol;Acc:MGI:2685951]	+
172	ENSMUSG00000074151	Nlrc5	NLR family, CARD domain containing 5 [Source:MGI Symbol;Acc:MGI:3612191]	-
173	ENSMUSG00000026751	Nr5a1	nuclear receptor subfamily 5, group A, member 1 [Source:MGI Symbol;Acc:MGI:1346833]	-
174	ENSMUSG00000026751	Nr5a1	nuclear receptor subfamily 5, group A, member 1 [Source:MGI Symbol;Acc:MGI:1346833]	-
175	ENSMUSG00000070192	n-R5s58	nuclear encoded rRNA 5S 58 [Source:MGI Symbol;Acc:MGI:4421903]	-
176	ENSMUSG00000075069	Olfr1264	olfactory receptor 1264 [Source:MGI Symbol;Acc:MGI:3031098]	-
177	ENSMUSG00000035626	Olfr1509	olfactory receptor 1509 [Source:MGI Symbol;Acc:MGI:3031343]	-
178	ENSMUSG00000060640	Olfr1512	olfactory receptor 1512 [Source:MGI Symbol;Acc:MGI:3031346]	+
179	ENSMUSG00000032987	Olfr281	olfactory receptor 281 [Source:MGI Symbol;Acc:MGI:3030115]	-
180	ENSMUSG00000056184	Olfr283	olfactory receptor 283 [Source:MGI Symbol;Acc:MGI:3030117]	+
181	ENSMUSG00000078624	Olfr613	olfactory receptor 613 [Source:MGI Symbol;Acc:MGI:3030447]	-
182	ENSMUSG00000046173	Pabpc6	poly(A) binding protein, cytoplasmic 6 [Source:MGI Symbol;Acc:MGI:1914793]	-
183	ENSMUSG00000047307	Pcdhb13	protocadherin beta 13 [Source:MGI Symbol;Acc:MGI:2136748]	+
184	ENSMUSG00000073591	Pcdhb22	protocadherin beta 22 [Source:MGI Symbol;Acc:MGI:2136760]	+
185	ENSMUSG00000020388	Pdlim4	PDZ and LIM domain 4 [Source:MGI Symbol;Acc:MGI:1353470]	+
186	ENSMUSG00000028085	Pet112l	PET112-like (yeast) [Source:MGI Symbol;Acc:MGI:2442496]	+
187	ENSMUSG00000048070	Pirt	phosphoinositide-interacting regulator of transient receptor potential channels [Source:MGI Symbol;Acc:MGI:2443635]	-
188	ENSMUSG00000034462	Pkd2	polycystic kidney disease 2 [Source:MGI Symbol;Acc:MGI:1099818]	+

189	ENSMUSG00000024247	Pkdcc	protein kinase domain containing, cytoplasmic [Source:MGI Symbol;Acc:MGI:2147077]	+
190	ENSMUSG00000058908	Pla2g2a	phospholipase A2, group IIA (platelets, synovial fluid) [Source:MGI Symbol;Acc:MGI:104642]	+
191	ENSMUSG00000041193	Pla2g5	phospholipase A2, group V [Source:MGI Symbol;Acc:MGI:101899]	+
192	ENSMUSG00000019817	Plagl1	pleiomorphic adenoma gene-like 1 [Source:MGI Symbol;Acc:MGI:1100874]	-
193	ENSMUSG00000003363	Pld3	phospholipase D family, member 3 [Source:MGI Symbol;Acc:MGI:1333782]	+
194	ENSMUSG00000038583	Pln	phospholamban [Source:MGI Symbol;Acc:MGI:97622]	-
195	ENSMUSG00000018217	Pmp22	peripheral myelin protein 22 [Source:MGI Symbol;Acc:MGI:97631]	+
196	ENSMUSG00000025608	Podxl	podocalyxin-like [Source:MGI Symbol;Acc:MGI:1351317]	+
197	ENSMUSG00000029649	Pomp	proteasome maturation protein [Source:MGI Symbol;Acc:MGI:1913787]	-
198	ENSMUSG00000029649	Pomp	proteasome maturation protein [Source:MGI Symbol;Acc:MGI:1913787]	+
199	ENSMUSG00000048349	Pou4f1	POU domain, class 4, transcription factor 1 [Source:MGI Symbol;Acc:MGI:102525]	+
200	ENSMUSG00000031570	Ppapdc1b	phosphatidic acid phosphatase type 2 domain containing 1B [Source:MGI Symbol;Acc:MGI:1919160]	-
201	ENSMUSG00000029167	Ppargc1a	peroxisome proliferative activated receptor, gamma, coactivator 1 alpha [Source:MGI Symbol;Acc:MGI:1342774]	+
202	ENSMUSG00000046794	Ppp1r3b	protein phosphatase 1, regulatory (inhibitor) subunit 3B [Source:MGI Symbol;Acc:MGI:2177268]	+
203	ENSMUSG00000021816	Ppp3cb	protein phosphatase 3, catalytic subunit, beta isoform [Source:MGI Symbol;Acc:MGI:107163]	-
204	ENSMUSG00000038151	Prdm1	PR domain containing 1, with ZNF domain [Source:MGI Symbol;Acc:MGI:99655]	+
205	ENSMUSG00000042496	Prdm10	PR domain containing 10 [Source:MGI Symbol;Acc:MGI:2682952]	-
206	ENSMUSG00000015748	Prpf3	PRP3 pre-mRNA processing factor 3 homolog (yeast) [Source:MGI Symbol;Acc:MGI:1918017]	-
207	ENSMUSG00000026604	Ptpn14	protein tyrosine phosphatase, non-receptor type 14 [Source:MGI Symbol;Acc:MGI:102467]	+
208	ENSMUSG00000029128	Rab28	RAB28, member RAS oncogene family [Source:MGI Symbol;Acc:MGI:1917285]	-
209	ENSMUSG00000055069	Rab39	RAB39, member RAS oncogene family [Source:MGI Symbol;Acc:MGI:2442855]	+
210	ENSMUSG00000003411	Rab3b	RAB3B, member RAS oncogene family [Source:MGI Symbol;Acc:MGI:1917158]	+
211	ENSMUSG00000029576	Radil	Ras association and DIL domains [Source:MGI Symbol;Acc:MGI:2443088]	+
212	ENSMUSG00000045110	Rassf8	Ras association (RalGDS/AF-6) domain family (N-terminal) member 8 [Source:MGI Symbol;Acc:MGI:1918573]	-
213	ENSMUSG00000030259	Rassf8	Ras association (RalGDS/AF-6) domain family (N-terminal) member 8 [Source:MGI Symbol;Acc:MGI:1918573]	-
214	ENSMUSG00000037627	Rgs22	regulator of G-protein signalling 22 [Source:MGI Symbol;Acc:MGI:3613651]	-
215	ENSMUSG00000070661	Rnf186	ring finger protein 186 [Source:MGI Symbol;Acc:MGI:1914075]	-
216	ENSMUSG00000022120	Rnf219	ring finger protein 219 [Source:MGI Symbol;Acc:MGI:1919736]	+
217	ENSMUSG00000061167	Rpl15-ps3	ribosomal protein L15, pseudogene 3 [Source:MGI Symbol;Acc:MGI:3782952]	+
218	ENSMUSG00000062456	Rpl9-ps6	ribosomal protein L9, pseudogene 6 [Source:MGI Symbol;Acc:MGI:3642682]	+
219	ENSMUSG00000038387	Rras	Harvey rat sarcoma oncogene, subgroup R [Source:MGI Symbol;Acc:MGI:98179]	-
220	ENSMUSG00000022952	Runx1	runt related transcription factor 1 [Source:MGI Symbol;Acc:MGI:99852]	+
221	ENSMUSG00000028133	Rwdd3	RWD domain containing 3 [Source:MGI Symbol;Acc:MGI:1920420]	+
222	ENSMUSG00000051984	Sec31b	Sec31 homolog B (S. cerevisiae) [Source:MGI Symbol;Acc:MGI:2685187]	-
223	ENSMUSG00000067001	Serpinb7	serine (or cysteine) peptidase inhibitor, clade B, member 7 [Source:MGI Symbol;Acc:MGI:2151053]	+
224	ENSMUSG00000023764	Sfi1	Sfi1 homolog, spindle assembly associated (yeast) [Source:MGI Symbol;Acc:MGI:1926137]	+
225	ENSMUSG00000050010	Shisa3	shisa homolog 3 (Xenopus laevis) [Source:MGI Symbol;Acc:MGI:3041225]	+
226	ENSMUSG00000024597	Slc12a2	solute carrier family 12, member 2 [Source:MGI Symbol;Acc:MGI:101924]	+
227	ENSMUSG00000020102	Slc16a7	solute carrier family 16 (monocarboxylic acid transporters), member 7 [Source:MGI Symbol;Acc:MGI:1330284]	+
228	ENSMUSG00000067144	Slc22a7	solute carrier family 22 (organic anion transporter), member 7 [Source:MGI Symbol;Acc:MGI:1859559]	-
229	ENSMUSG00000043885	Slc36a4	solute carrier family 36 (proton/amino acid symporter), member 4 [Source:MGI Symbol;Acc:MGI:2442595]	+
230	ENSMUSG00000028360	Slc44a5	solute carrier family 44, member 5 [Source:MGI Symbol;Acc:MGI:3035141]	-
231	ENSMUSG00000025880	Smad7	MAD homolog 7 (Drosophila) [Source:MGI Symbol;Acc:MGI:1100518]	+
232	ENSMUSG00000031993	Snx19	sorting nexin 19 [Source:MGI Symbol;Acc:MGI:1921581]	-
233	ENSMUSG00000017733	Spinlw1	serine protease inhibitor-like, with Kunitz and WAP domains 1 (eppin) [Source:MGI Symbol;Acc:MGI:1922776]	+
234	ENSMUSG00000039911	Spsb1	splA/ryanodine receptor domain and SOCS box containing 1 [Source:MGI Symbol;Acc:MGI:1921896]	+
235	ENSMUSG00000057286	St6galnac2	ST6 (alpha-N-acetyl-neuraminyl-2,3-beta-galactosyl-1,3)-N-acetylgalactosaminide alpha-2,6-sialyltransferase 2 [Source:MGI Symbol;Acc:MGI:107553]	-
236	ENSMUSG00000033855	Ston1	stonin 1 [Source:MGI Symbol;Acc:MGI:1924307]	+
237	ENSMUSG00000006342	Susd2	sushi domain containing 2 [Source:MGI Symbol;Acc:MGI:1918983]	+
238	ENSMUSG00000059602	Syn3	synapsin III [Source:MGI Symbol;Acc:MGI:1351334]	-
239	ENSMUSG00000054321	Taf4b	TAF4B RNA polymerase II, TATA box binding protein (TBP)-associated factor [Source:MGI Symbol;Acc:MGI:2152345]	-
240	ENSMUSG00000052302	Tbc1d30	TBC1 domain family, member 30 [Source:MGI Symbol;Acc:MGI:1921944]	+
241	ENSMUSG00000020115	Tbk1	TANK-binding kinase 1 [Source:MGI Symbol;Acc:MGI:1929658]	+
242	ENSMUSG00000001604	Tcea3	transcription elongation factor A (SII), 3 [Source:MGI Symbol;Acc:MGI:1196908]	-
243	ENSMUSG00000024246	Thumpd2	THUMP domain containing 2 [Source:MGI Symbol;Acc:MGI:1919417]	+
244	ENSMUSG00000020044	Timp3	tissue inhibitor of metalloproteinase 3 [Source:MGI Symbol;Acc:MGI:98754]	-
245	ENSMUSG00000027995	Tlr2	toll-like receptor 2 [Source:MGI Symbol;Acc:MGI:1346060]	-
246	ENSMUSG00000069763	Tmem100	transmembrane protein 100 [Source:MGI Symbol;Acc:MGI:1915138]	-
247	ENSMUSG00000036826	Tmem149	transmembrane protein 149 [Source:MGI Symbol;Acc:MGI:3655979]	+
248	ENSMUSG00000040616	Tmem51	transmembrane protein 51 [Source:MGI Symbol;Acc:MGI:2384874]	-
249	ENSMUSG00000023153	Tmem52	transmembrane protein 52 [Source:MGI Symbol;Acc:MGI:1916921]	+
250	ENSMUSG00000048764	Tmprss11f	transmembrane protease, serine 11f [Source:MGI Symbol;Acc:MGI:2442348]	+
251	ENSMUSG00000079451	Tmprss11g	transmembrane protease, serine 11g [Source:MGI Symbol;Acc:MGI:2444058]	+
252	ENSMUSG00000050043	Tmx2	thioredoxin-related transmembrane protein 2 [Source:MGI Symbol;Acc:MGI:1914208]	+
253	ENSMUSG00000035274	Tpbg	trophoblast glycoprotein [Source:MGI Symbol;Acc:MGI:1341264]	+
254	ENSMUSG00000064043	Trerf1	transcriptional regulating factor 1 [Source:MGI Symbol;Acc:MGI:2442086]	+
255	ENSMUSG00000027857	Tshb	thyroid stimulating hormone, beta subunit [Source:MGI Symbol;Acc:MGI:98848]	+
256	ENSMUSG00000066637	Ttc32	tetratricopeptide repeat domain 32 [Source:MGI Symbol;Acc:MGI:1922766]	-
257	ENSMUSG00000051747	Ttn	titin [Source:MGI Symbol;Acc:MGI:98864]	-

258	ENSMUSG00000007805	Twist2	twist homolog 2 (Drosophila) [Source:MGI Symbol;Acc:MGI:104685]	-
259	ENSMUSG00000078765	U2af1l4	U2 small nuclear RNA auxiliary factor 1-like 4 [Source:MGI Symbol;Acc:MGI:2678374]	+
260	ENSMUSG00000032596	Uba7	ubiquitin-like modifier activating enzyme 7 [Source:MGI Symbol;Acc:MGI:1349462]	+
261	ENSMUSG00000035186	Ubd	ubiquitin D [Source:MGI Symbol;Acc:MGI:1344410]	-
262	ENSMUSG00000025939	Ube2w	ubiquitin-conjugating enzyme E2W (putative) [Source:MGI Symbol;Acc:MGI:1914049]	-
263	ENSMUSG00000025171	Ubtd1	ubiquitin domain containing 1 [Source:MGI Symbol;Acc:MGI:2385092]	+
264	ENSMUSG00000054814	Usp46	ubiquitin specific peptidase 46 [Source:MGI Symbol;Acc:MGI:1916977]	+
265	ENSMUSG00000034235	Usp54	ubiquitin specific peptidase 54 [Source:MGI Symbol;Acc:MGI:1926037]	-
266	ENSMUSG00000051506	Wdfy4	WD repeat and FYVE domain containing 4 [Source:MGI Symbol;Acc:MGI:3584510]	+
267	ENSMUSG00000035560	Wdr20b	WD repeat domain 20b [Source:MGI Symbol;Acc:MGI:1918198]	+
268	ENSMUSG00000066643	Wdr35	WD repeat domain 35 [Source:MGI Symbol;Acc:MGI:1921932]	-
269	ENSMUSG00000042660	Wdr55	WD repeat domain 55 [Source:MGI Symbol;Acc:MGI:1915186]	-
270	ENSMUSG00000054823	Whsc1l1	Wolf-Hirschhorn syndrome candidate 1-like 1 (human) [Source:MGI Symbol;Acc:MGI:2142581]	-
271	ENSMUSG00000034667	Xpot	exportin, tRNA (nuclear export receptor for tRNAs) [Source:MGI Symbol;Acc:MGI:1920442]	+
272	ENSMUSG00000063935	Zar1	zygote arrest 1 [Source:MGI Symbol;Acc:MGI:2180337]	+
273	ENSMUSG00000056586	Zar1l	zygote arrest 1-like [Source:MGI Symbol;Acc:MGI:3690051]	+
274	ENSMUSG00000033454	Zbtb1	zinc finger and BTB domain containing 1 [Source:MGI Symbol;Acc:MGI:2442326]	+
275	ENSMUSG00000049321	Zfp2	zinc finger protein 2 [Source:MGI Symbol;Acc:MGI:99167]	-
276	ENSMUSG00000052056	Zfp217	zinc finger protein 217 [Source:MGI Symbol;Acc:MGI:2685408]	+
277	ENSMUSG00000024420	Zfp521	zinc finger protein 521 [Source:MGI Symbol;Acc:MGI:95459]	-
278	ENSMUSG00000024420	Zfp521	zinc finger protein 521 [Source:MGI Symbol;Acc:MGI:95459]	-
279	ENSMUSG00000054967	Zfp647	zinc finger protein 647 [Source:MGI Symbol;Acc:MGI:3052806]	+
280	ENSMUSG00000071285	Zfp87	zinc finger protein 87 [Source:MGI Symbol;Acc:MGI:107768]	+
281	ENSMUSG00000037492	Zmat4	zinc finger, matrin type 4 [Source:MGI Symbol;Acc:MGI:2443497]	-
282	ENSMUSG00000021945	Zmym2	zinc finger, MYM-type 2 [Source:MGI Symbol;Acc:MGI:1923257]	+
283	ENSMUSG00000065634		Small nucleolar RNA SNORA24 [Source:RFAM;Acc:RF00399]	-
284	ENSMUSG00000065942		U6 spliceosomal RNA [Source:RFAM;Acc:RF00026]	-
285	ENSMUSG00000077094			+
286	ENSMUSG00000065240		U6 spliceosomal RNA [Source:RFAM;Acc:RF00026]	+

5.1.5 DNA methylation affected by the environment (prenatal stress versus control).

Effect: direction of effect; “+”: DNA methylation upregulated in prenatally stressed versus control mice; “-“: downregulated in prenatally stressed versus control mice. Genes have been ordered alphabetically.

#	Feature	Symbol	Genename	Effect
1	ENSMUSG00000040591	1110051M20Rik	RIKEN cDNA 1110051M20 gene [Source:MGI Symbol;Acc:MGI:1915079]	+
2	ENSMUSG00000063447	1700013N18Rik	RIKEN cDNA 1700013N18 gene [Source:MGI Symbol;Acc:MGI:1920568]	+
3	ENSMUSG00000037910	1700018B24Rik	RIKEN cDNA 1700018B24 gene [Source:MGI Symbol;Acc:MGI:1913582]	-
4	ENSMUSG00000030623	1700019G06Rik	RIKEN cDNA 1700019G06 gene [Source:MGI Symbol;Acc:MGI:1916654]	-
5	ENSMUSG00000045350	1700030F18Rik	RIKEN cDNA 1700030F18 gene [Source:MGI Symbol;Acc:MGI:1919527]	+
6	ENSMUSG00000055833	1700034H15Rik	RIKEN cDNA 1700034H15 gene [Source:MGI Symbol;Acc:MGI:1921515]	+
7	ENSMUSG00000062760	1810041L15Rik	RIKEN cDNA 1810041L15 gene [Source:MGI Symbol;Acc:MGI:1919551]	+
8	ENSMUSG00000021290	2010107E04Rik	RIKEN cDNA 2010107E04 gene [Source:MGI Symbol;Acc:MGI:1917507]	+
9	ENSMUSG00000013643	2210415F13Rik	RIKEN cDNA 2210415F13 gene [Source:MGI Symbol;Acc:MGI:1917413]	+
10	ENSMUSG00000071540	3425401B19Rik	RIKEN cDNA 3425401B19 gene [Source:MGI Symbol;Acc:MGI:3588196]	+
11	ENSMUSG00000052779	4833418N17Rik	RIKEN cDNA 4833418N17 gene [Source:MGI Symbol;Acc:MGI:1921157]	+
12	ENSMUSG00000044544	4921513I03Rik	RIKEN cDNA 4921513I03 gene [Source:MGI Symbol;Acc:MGI:1918124]	+
13	ENSMUSG00000079177	4930417G10Rik	RIKEN cDNA 4930417G10 gene [Source:MGI Symbol;Acc:MGI:1922105]	-
14	ENSMUSG00000052407	4930473A06Rik	RIKEN cDNA 4930473A06 gene [Source:MGI Symbol;Acc:MGI:1922152]	+
15	ENSMUSG00000029331	4930522N08Rik	RIKEN cDNA 4930522N08 gene [Source:MGI Symbol;Acc:MGI:1922344]	+
16	ENSMUSG00000043986	4932411G14Rik	RIKEN cDNA 4932411G14 gene [Source:MGI Symbol;Acc:MGI:3045260]	+
17	ENSMUSG00000029586	4933411G11Rik	RIKEN cDNA 4933411G11Rik gene [Source:MGI Symbol;Acc:MGI:3612701]	-
18	ENSMUSG00000048665	A430010J10Rik	RIKEN cDNA A430010J10 gene [Source:MGI Symbol;Acc:MGI:2442501]	+
19	ENSMUSG00000037953	A4gnt	alpha-1,4-N-acetylglucosaminyltransferase [Source:MGI Symbol;Acc:MGI:2143261]	+
20	ENSMUSG00000028970	Abcb1b	ATP-binding cassette, sub-family B (MDR/TAP), member 1B [Source:MGI Symbol;Acc:MGI:97568]	+
21	ENSMUSG00000032849	Abcc4	ATP-binding cassette, sub-family C (CFTR/MRP), member 4 [Source:MGI Symbol;Acc:MGI:2443111]	+
22	ENSMUSG00000043487	Acot6	acyl-CoA thioesterase 6 [Source:MGI Symbol;Acc:MGI:1921287]	+
23	ENSMUSG00000067416	Actl9	actin-like 9 [Source:MGI Symbol;Acc:MGI:1916731]	+
24	ENSMUSG00000056413	Adap1	ArfGAP with dual PH domains 1 [Source:MGI Symbol;Acc:MGI:2442201]	-
25	ENSMUSG00000019986	Ahi1	Abelson helper integration site 1 [Source:MGI Symbol;Acc:MGI:87971]	+
26	ENSMUSG00000040554	Aipl1	aryl hydrocarbon receptor-interacting protein-like 1 [Source:MGI Symbol;Acc:MGI:2148800]	+
27	ENSMUSG00000039058	Ak5	adenylate kinase 5 [Source:MGI Symbol;Acc:MGI:2677491]	+
28	ENSMUSG00000066406	Akap13	A kinase (PRKA) anchor protein 13 [Source:MGI Symbol;Acc:MGI:2676556]	+
29	ENSMUSG00000028737	Aldh4a1	aldehyde dehydrogenase 4 family, member A1 [Source:MGI Symbol;Acc:MGI:2443883]	+
30	ENSMUSG00000070385	Ampd1	adenosine monophosphate deaminase 1 [Source:MGI Symbol;Acc:MGI:88015]	+
31	ENSMUSG00000024803	Ankrd1	ankyrin repeat domain 1 (cardiac muscle) [Source:MGI Symbol;Acc:MGI:1097717]	+
32	ENSMUSG00000007827	Ankrd26	ankyrin repeat domain 26 [Source:MGI Symbol;Acc:MGI:1917887]	+
33	ENSMUSG00000021950	Anxa8	annexin A8 [Source:MGI Symbol;Acc:MGI:1201374]	+
34	ENSMUSG00000071847	Apcdd1	adenomatosis polyposis coli down-regulated 1 [Source:MGI Symbol;Acc:MGI:3513977]	+
35	ENSMUSG00000074625	Arhgap40	Rho GTPase activating protein 40 [Source:MGI Symbol;Acc:MGI:3649852]	+
36	ENSMUSG00000054901	Arhgef33	Rho guanine nucleotide exchange factor (GEF) 33 [Source:MGI Symbol;Acc:MGI:2685787]	+
37	ENSMUSG00000033952	Aspm	asp (abnormal spindle)-like, microcephaly associated (Drosophila) [Source:MGI Symbol;Acc:MGI:1334448]	+
38	ENSMUSG00000073043	Atoh1	atonal homolog 1 (Drosophila) [Source:MGI Symbol;Acc:MGI:104654]	+

39	ENSMUSG00000074804	AU015228	expressed sequence AU015228 [Source:MGI Symbol;Acc:MGI:2139152]	+
40	ENSMUSG00000074166	AW146154	expressed sequence AW146154 [Source:MGI Symbol;Acc:MGI:2142212]	+
41	ENSMUSG00000044633	B530045E10Rik	RIKEN cDNA B530045E10 gene [Source:MGI Symbol;Acc:MGI:2445145]	+
42	ENSMUSG00000049792	Bag5	BCL2-associated athanogene 5 [Source:MGI Symbol;Acc:MGI:1917619]	+
43	ENSMUSG00000006010	BC003331	cDNA sequence BC003331 [Source:MGI Symbol;Acc:MGI:2385108]	+
44	ENSMUSG00000027580	BC006779	cDNA sequence BC006779 [Source:MGI Symbol;Acc:MGI:2385169]	-
45	ENSMUSG00000074052	BC048644	cDNA sequence BC048644 [Source:MGI Symbol;Acc:MGI:3039566]	+
46	ENSMUSG00000047841	BC051628	cDNA sequence BC051628 [Source:MGI Symbol;Acc:MGI:3051572]	-
47	ENSMUSG00000021763	BC067074	cDNA sequence BC067074 [Source:MGI Symbol;Acc:MGI:3040697]	+
48	ENSMUSG00000059439	Bcas3	breast carcinoma amplified sequence 3 [Source:MGI Symbol;Acc:MGI:2385848]	-
49	ENSMUSG00000028191	Bcl10	B cell leukemia/lymphoma 10 [Source:MGI Symbol;Acc:MGI:1337994]	-
50	ENSMUSG00000021835	Bmp4	bone morphogenetic protein 4 [Source:MGI Symbol;Acc:MGI:88180]	+
51	ENSMUSG00000025105	Bnc1	basonuclin 1 [Source:MGI Symbol;Acc:MGI:1097164]	+
52	ENSMUSG00000015943	Bola1	bolA-like 1 (E. coli) [Source:MGI Symbol;Acc:MGI:1916418]	+
53	ENSMUSG00000032056	Btg4	B cell translocation gene 4 [Source:MGI Symbol;Acc:MGI:1860140]	+
54	ENSMUSG00000037469	C330005M16Rik	RIKEN cDNA C330005M16 gene [Source:MGI Symbol;Acc:MGI:2142121]	+
55	ENSMUSG00000035031	C8a	complement component 8, alpha polypeptide [Source:MGI Symbol;Acc:MGI:2668347]	+
56	ENSMUSG00000033033	Calhm2	calcium homeostasis modulator 2 [Source:MGI Symbol;Acc:MGI:1919941]	+
57	ENSMUSG00000056158	Car10	carbonic anhydrase 10 [Source:MGI Symbol;Acc:MGI:1919855]	+
58	ENSMUSG00000027555	Car13	carbonic anhydrase 13 [Source:MGI Symbol;Acc:MGI:1931322]	+
59	ENSMUSG00000056228	Cars2	cysteinyl-tRNA synthetase 2 (mitochondrial)(putative) [Source:MGI Symbol;Acc:MGI:1919191]	-
60	ENSMUSG00000025076	Casp7	caspase 7 [Source:MGI Symbol;Acc:MGI:109383]	-
61	ENSMUSG00000025150	Cbr2	carbonyl reductase 2 [Source:MGI Symbol;Acc:MGI:107200]	-
62	ENSMUSG00000080793	Cbx3-ps3	chromobox homolog 3 (Drosophila HP1 gamma), pseudogene 3 [Source:MGI Symbol;Acc:MGI:1890540]	+
63	ENSMUSG00000022833	Ccdc14	coiled-coil domain containing 14 [Source:MGI Symbol;Acc:MGI:2443448]	+
64	ENSMUSG00000050685	Ccdc54	coiled-coil domain containing 54 [Source:MGI Symbol;Acc:MGI:1916589]	+
65	ENSMUSG00000027793	Ccna1	cyclin A1 [Source:MGI Symbol;Acc:MGI:108042]	+
66	ENSMUSG00000064039	Ccr1l1	chemokine (C-C motif) receptor 1-like 1 [Source:MGI Symbol;Acc:MGI:104617]	+
67	ENSMUSG00000021624	Cd180	CD180 antigen [Source:MGI Symbol;Acc:MGI:1194924]	-
68	ENSMUSG00000030342	Cd9	CD9 antigen [Source:MGI Symbol;Acc:MGI:88348]	-
69	ENSMUSG00000078284	Cdc73	cell division cycle 73, Paf1/RNA polymerase II complex component, homolog (S. cerevisiae) [Source:MGI Symbol;Acc:MGI:2384876]	-
70	ENSMUSG00000021803	Cdhr1	cadherin-related family member 1 [Source:MGI Symbol;Acc:MGI:2157782]	+
71	ENSMUSG00000030878	Cdr2	cerebellar degeneration-related 2 [Source:MGI Symbol;Acc:MGI:1100885]	-
72	ENSMUSG00000041491	Cep78	centrosomal protein 78 [Source:MGI Symbol;Acc:MGI:1924386]	+
73	ENSMUSG00000022945	Chaf1b	chromatin assembly factor 1, subunit B (p60) [Source:MGI Symbol;Acc:MGI:1314881]	+
74	ENSMUSG00000060002	Chpt1	choline phosphotransferase 1 [Source:MGI Symbol;Acc:MGI:2384841]	+
75	ENSMUSG00000045613	Chrm2	cholinergic receptor, muscarinic 2, cardiac [Source:MGI Symbol;Acc:MGI:88397]	+
76	ENSMUSG00000029516	Cit	citron [Source:MGI Symbol;Acc:MGI:105313]	+
77	ENSMUSG00000029516	Cit	citron [Source:MGI Symbol;Acc:MGI:105313]	+
78	ENSMUSG00000032473	Cldn18	claudin 18 [Source:MGI Symbol;Acc:MGI:1929209]	+
79	ENSMUSG00000023959	Clic5	chloride intracellular channel 5 [Source:MGI Symbol;Acc:MGI:1917912]	+
80	ENSMUSG00000032452	Clstn2	calsyntenin 2 [Source:MGI Symbol;Acc:MGI:1929897]	+
81	ENSMUSG00000025545	Clybl	citrate lyase beta like [Source:MGI Symbol;Acc:MGI:1916884]	+
82	ENSMUSG00000067220	Cnga1	cyclic nucleotide gated channel alpha 1 [Source:MGI Symbol;Acc:MGI:88436]	+
83	ENSMUSG00000001435	Col18a1	collagen, type XVIII, alpha 1 [Source:MGI Symbol;Acc:MGI:88451]	-
84	ENSMUSG00000005220	Corin	corin [Source:MGI Symbol;Acc:MGI:1349451]	+
85	ENSMUSG00000018727	Cpsf4l	cleavage and polyadenylation specific factor 4-like [Source:MGI Symbol;Acc:MGI:1277182]	+
86	ENSMUSG00000052955	Cpvl	carboxypeptidase, vitellogenic-like [Source:MGI Symbol;Acc:MGI:1918537]	+
87	ENSMUSG00000001767	Crnkl1	Crn, crooked neck-like 1 (Drosophila) [Source:MGI Symbol;Acc:MGI:1914127]	+
88	ENSMUSG00000044636	Csrnp2	cysteine-serine-rich nuclear protein 2 [Source:MGI Symbol;Acc:MGI:2386852]	+
89	ENSMUSG00000060843	Ctnna3	catenin (cadherin associated protein), alpha 3 [Source:MGI Symbol;Acc:MGI:2661445]	+
90	ENSMUSG00000038545	Cul7	cullin 7 [Source:MGI Symbol;Acc:MGI:1913765]	+
91	ENSMUSG00000018541	Cwc25	CWC25 spliceosome-associated protein homolog (S. cerevisiae) [Source:MGI Symbol;Acc:MGI:1914730]	+
92	ENSMUSG00000028194	Ddah1	dimethylarginine dimethylaminohydrolase 1 [Source:MGI Symbol;Acc:MGI:1916469]	-
93	ENSMUSG00000021500	Ddx46	DEAD (Asp-Glu-Ala-Asp) box polypeptide 46 [Source:MGI Symbol;Acc:MGI:1920895]	+
94	ENSMUSG00000022210	Dhrs4	dehydrogenase/reductase (SDR family) member 4 [Source:MGI Symbol;Acc:MGI:90169]	-
95	ENSMUSG00000017830	Dhx58	DEXH (Asp-Glu-X-His) box polypeptide 58 [Source:MGI Symbol;Acc:MGI:1931560]	+
96	ENSMUSG00000034931	Dhx8	DEAH (Asp-Glu-Ala-His) box polypeptide 8 [Source:MGI Symbol;Acc:MGI:1306823]	+
97	ENSMUSG00000022429	Dmc1	DMC1 dosage suppressor of mck1 homolog, meiosis-specific homologous recombination (yeast) [Source:MGI Symbol;Acc:MGI:105393]	+
98	ENSMUSG00000036875	Dna2	DNA replication helicase 2 homolog (yeast) [Source:MGI Symbol;Acc:MGI:2443732]	+
99	ENSMUSG00000005237	Dnahc2	dynein, axonemal, heavy chain 2 [Source:MGI Symbol;Acc:MGI:107731]	+
100	ENSMUSG00000030708	Dnajb13	DnaJ (Hsp40) related, subfamily B, member 13 [Source:MGI Symbol;Acc:MGI:1916637]	+
101	ENSMUSG00000022560	Dnajc13	DnaJ (Hsp40) homolog, subfamily C, member 13 [Source:MGI Symbol;Acc:MGI:2676368]	+
102	ENSMUSG00000025195	Dnmbp	dynamin binding protein [Source:MGI Symbol;Acc:MGI:1917352]	+
103	ENSMUSG00000058325	Dock1	dedicator of cytokinesis 1 [Source:MGI Symbol;Acc:MGI:2429765]	+
104	ENSMUSG00000025558	Dock9	dedicator of cytokinesis 9 [Source:MGI Symbol;Acc:MGI:106321]	+
105	ENSMUSG00000041035	Dpcd	deleted in primary ciliary dyskinesia [Source:MGI Symbol;Acc:MGI:1924407]	+
106	ENSMUSG00000022705	Drd3	dopamine receptor D3 [Source:MGI Symbol;Acc:MGI:94925]	+
107	ENSMUSG00000022191	Drosha	drosha, ribonuclease type III [Source:MGI Symbol;Acc:MGI:1261425]	+
108	ENSMUSG00000035064	Eef2k	eukaryotic elongation factor-2 kinase [Source:MGI Symbol;Acc:MGI:1195261]	+
109	ENSMUSG00000040659	Efhd2	EF hand domain containing 2 [Source:MGI Symbol;Acc:MGI:106504]	+
110	ENSMUSG00000036893	Ehmt1	euchromatic histone methyltransferase 1 [Source:MGI Symbol;Acc:MGI:1924933]	+
111	ENSMUSG00000021364	Elovl2	elongation of very long chain fatty acids (FEN1/Elo2, SUR4/Elo3, yeast)-like 2 [Source:MGI Symbol;Acc:MGI:1858960]	+
112	ENSMUSG00000039167	Eltd1	EGF, latrophilin seven transmembrane domain containing 1 [Source:MGI Symbol;Acc:MGI:2655562]	+
113	ENSMUSG00000058070	Eml1	echinoderm microtubule associated protein like 1 [Source:MGI Symbol;Acc:MGI:1915769]	+
114	ENSMUSG00000048029	Eno4	enolase 4 [Source:MGI Symbol;Acc:MGI:2441717]	+

115	ENSMUSG00000024140	Epas1	endothelial PAS domain protein 1 [Source:MGI Symbol;Acc:MGI:109169]	+
116	ENSMUSG00000015766	Eps8	epidermal growth factor receptor pathway substrate 8 [Source:MGI Symbol;Acc:MGI:104684]	+
117	ENSMUSG00000032035	Ets1	E26 avian leukemia oncogene 1, 5' domain [Source:MGI Symbol;Acc:MGI:95455]	+
118	ENSMUSG00000011831	Evi5	ecotropic viral integration site 5 [Source:MGI Symbol;Acc:MGI:104736]	+
119	ENSMUSG00000053799	Exoc6	exocyst complex component 6 [Source:MGI Symbol;Acc:MGI:1351611]	+
120	ENSMUSG00000056069	Fam105a	family with sequence similarity 105, member A [Source:MGI Symbol;Acc:MGI:2687281]	+
121	ENSMUSG00000049119	Fam110b	family with sequence similarity 110, member B [Source:MGI Symbol;Acc:MGI:1916593]	+
122	ENSMUSG00000036800	Fam135b	family with sequence similarity 135, member B [Source:MGI Symbol;Acc:MGI:1917613]	+
123	ENSMUSG00000036501	Fam13b	family with sequence similarity 13, member B [Source:MGI Symbol;Acc:MGI:2447834]	+
124	ENSMUSG00000046500	Fam19a4	family with sequence similarity 19, member A4 [Source:MGI Symbol;Acc:MGI:2444563]	+
125	ENSMUSG00000041471	Fam35a	family with sequence similarity 35, member A [Source:MGI Symbol;Acc:MGI:1922948]	-
126	ENSMUSG00000044576	Fam59b	family with sequence similarity 59, member B [Source:MGI Symbol;Acc:MGI:2685290]	+
127	ENSMUSG00000004031	Fam5b	family with sequence similarity 5, member B [Source:MGI Symbol;Acc:MGI:2443333]	+
128	ENSMUSG00000027086	Fastkd1	FAST kinase domains 1 [Source:MGI Symbol;Acc:MGI:2444596]	-
129	ENSMUSG00000047539	Fbxo28	F-box protein 28 [Source:MGI Symbol;Acc:MGI:1261890]	+
130	ENSMUSG00000058715	Fcer1g	Fc receptor, IgE, high affinity I, gamma polypeptide [Source:MGI Symbol;Acc:MGI:95496]	+
131	ENSMUSG00000048373	Fgfbp1	fibroblast growth factor binding protein 1 [Source:MGI Symbol;Acc:MGI:1096350]	+
132	ENSMUSG00000033860	Fgg	fibrinogen gamma chain [Source:MGI Symbol;Acc:MGI:95526]	+
133	ENSMUSG00000051435	Fhad1	forkhead-associated (FHA) phosphopeptide binding domain 1 [Source:MGI Symbol;Acc:MGI:1920323]	-
134	ENSMUSG00000051435	Fhad1	forkhead-associated (FHA) phosphopeptide binding domain 1 [Source:MGI Symbol;Acc:MGI:1920323]	+
135	ENSMUSG00000075012	Fjx1	four jointed box 1 (Drosophila) [Source:MGI Symbol;Acc:MGI:1341907]	+
136	ENSMUSG00000024222	Fkbp5	FK506 binding protein 5 [Source:MGI Symbol;Acc:MGI:104670]	+
137	ENSMUSG00000040013	Fkbp6	FK506 binding protein 6 [Source:MGI Symbol;Acc:MGI:2137612]	+
138	ENSMUSG00000061175	Fnip2	folliculin interacting protein 2 [Source:MGI Symbol;Acc:MGI:2683054]	+
139	ENSMUSG00000067199	Frat1	frequently rearranged in advanced T cell lymphomas [Source:MGI Symbol;Acc:MGI:109450]	+
140	ENSMUSG00000048285	Frmd6	FERM domain containing 6 [Source:MGI Symbol;Acc:MGI:2442579]	+
141	ENSMUSG00000022148	Fyb	FYN binding protein [Source:MGI Symbol;Acc:MGI:1346327]	+
142	ENSMUSG00000021943	Gdf10	growth differentiation factor 10 [Source:MGI Symbol;Acc:MGI:95684]	-
143	ENSMUSG00000050953	Gja1	gap junction protein, alpha 1 [Source:MGI Symbol;Acc:MGI:95713]	+
144	ENSMUSG00000038257	Glra3	glycine receptor, alpha 3 subunit [Source:MGI Symbol;Acc:MGI:95749]	+
145	ENSMUSG00000036401	Glt6d1	glycosyltransferase 6 domain containing 1 [Source:MGI Symbol;Acc:MGI:1918353]	+
146	ENSMUSG00000066543	Gm10166	predicted pseudogene 10166 [Source:MGI Symbol;Acc:MGI:3641818]	+
147	ENSMUSG00000069885	Gm10281	predicted gene 10281 [Source:MGI Symbol;Acc:MGI:3642652]	+
148	ENSMUSG00000071222	Gm10320	predicted pseudogene 10320 [Source:MGI Symbol;Acc:MGI:3642323]	+
149	ENSMUSG00000071532	Gm10335	predicted gene 10335 [Source:MGI Symbol;Acc:MGI:3641693]	+
150	ENSMUSG00000072589	Gm10371	predicted gene 10371 [Source:MGI Symbol;Acc:MGI:3642716]	+
151	ENSMUSG00000074517	Gm10710	predicted gene 10710 [Source:MGI Symbol;Acc:MGI:3642896]	+
152	ENSMUSG00000074603	Gm10729	predicted gene 10729 [Source:MGI Symbol;Acc:MGI:3642905]	+
153	ENSMUSG00000074674	Gm10742	predicted gene 10742 [Source:MGI Symbol;Acc:MGI:3642301]	-
154	ENSMUSG00000075591	Gm10874	predicted gene 10874 [Source:MGI Symbol;Acc:MGI:3704261]	-
155	ENSMUSG00000084358	Gm11352	predicted gene 11352 [Source:MGI Symbol;Acc:MGI:3649796]	+
156	ENSMUSG00000044639	Gm11507	predicted gene 11507 [Source:MGI Symbol;Acc:MGI:3650927]	+
157	ENSMUSG00000081647	Gm13022	predicted gene 13022 [Source:MGI Symbol;Acc:MGI:3651775]	+
158	ENSMUSG00000082795	Gm13193	predicted gene 13193 [Source:MGI Symbol;Acc:MGI:3651271]	-
159	ENSMUSG00000081037	Gm13929	predicted gene 13929 [Source:MGI Symbol;Acc:MGI:3649396]	+
160	ENSMUSG00000084067	Gm14269	predicted gene 14269 [Source:MGI Symbol;Acc:MGI:3650060]	+
161	ENSMUSG00000074655	Gm1527	predicted gene 1527 [Source:MGI Symbol;Acc:MGI:2686373]	-
162	ENSMUSG00000083500	Gm15470	predicted gene 15470 [Source:MGI Symbol;Acc:MGI:3641891]	+
163	ENSMUSG00000082203	Gm15636	predicted gene 15636 [Source:MGI Symbol;Acc:MGI:3783080]	+
164	ENSMUSG00000019767	Gm221	predicted gene 221 [Source:MGI Symbol;Acc:MGI:2685067]	+
165	ENSMUSG00000078967	Gm3272	predicted pseudogene 3272 [Source:MGI Symbol;Acc:MGI:3781450]	+
166	ENSMUSG00000056797	Gm4889	predicted gene 4889 [Source:MGI Symbol;Acc:MGI:3647233]	+
167	ENSMUSG00000066626	Gm5121	predicted gene 5121 [Source:MGI Symbol;Acc:MGI:3647258]	+
168	ENSMUSG00000050190	Gm5346	predicted gene 5346 [Source:MGI Symbol;Acc:MGI:3647273]	+
169	ENSMUSG00000049414	Gm5417	predicted gene 5417 [Source:MGI Symbol;Acc:MGI:3648626]	+
170	ENSMUSG00000059301	Gm5434	predicted gene 5434 [Source:MGI Symbol;Acc:MGI:3646221]	+
171	ENSMUSG00000071035	Gm5499	predicted pseudogene 5499 [Source:MGI Symbol;Acc:MGI:3643804]	-
172	ENSMUSG00000059040	Gm5506	predicted gene 5506 [Source:MGI Symbol;Acc:MGI:3648653]	+
173	ENSMUSG00000022187	Gm5546	predicted gene 5546 [Source:MGI Symbol;Acc:MGI:3648205]	+
174	ENSMUSG00000080866	Gm5687	predicted gene 5687 [Source:MGI Symbol;Acc:MGI:3644274]	+
175	ENSMUSG00000011350	Gm5893	predicted gene 5893 [Source:MGI Symbol;Acc:MGI:3645761]	+
176	ENSMUSG00000081111	Gm5913	predicted gene 5913 [Source:MGI Symbol;Acc:MGI:3648292]	+
177	ENSMUSG00000081052	Gm6305	predicted gene 6305 [Source:MGI Symbol;Acc:MGI:3644967]	+
178	ENSMUSG00000068964	Gm6361	predicted gene 6361 [Source:MGI Symbol;Acc:MGI:3646180]	+
179	ENSMUSG00000062687	Gm6531	predicted gene 6531 [Source:MGI Symbol;Acc:MGI:3643620]	+
180	ENSMUSG00000072722	Gm6588	predicted gene 6588 [Source:MGI Symbol;Acc:MGI:3648937]	+
181	ENSMUSG00000059114	Gm6772	predicted gene 6772 [Source:MGI Symbol;Acc:MGI:3646959]	-
182	ENSMUSG00000046411	Gm6816	predicted gene 6816 [Source:MGI Symbol;Acc:MGI:3648347]	+
183	ENSMUSG00000066553	Gm6969	predicted pseudogene 6969 [Source:MGI Symbol;Acc:MGI:3645320]	-
184	ENSMUSG00000074261	Gm7092	predicted gene 7092 [Source:MGI Symbol;Acc:MGI:3646269]	+
185	ENSMUSG00000071909	Gm806	predicted gene 806 [Source:MGI Symbol;Acc:MGI:2685652]	+
186	ENSMUSG00000074913	Gm815	predicted gene 815 [Source:MGI Symbol;Acc:MGI:2685661]	+
187	ENSMUSG00000059814	Gm8355	predicted pseudogene 8355 [Source:MGI Symbol;Acc:MGI:3645191]	+
188	ENSMUSG00000024429	Gnl1	guanine nucleotide binding protein-like 1 [Source:MGI Symbol;Acc:MGI:95764]	+
189	ENSMUSG00000029255	Gnrhr	gonadotropin releasing hormone receptor [Source:MGI Symbol;Acc:MGI:95790]	+
190	ENSMUSG00000034243	Golgb1	golgi autoantigen, golgin subfamily b, macrogolgin 1 [Source:MGI Symbol;Acc:MGI:1099447]	-
191	ENSMUSG00000034243	Golgb1	golgi autoantigen, golgin subfamily b, macrogolgin 1 [Source:MGI Symbol;Acc:MGI:1099447]	+
192	ENSMUSG00000080935	Got2-ps1	glutamate oxaloacetate transaminase 2, mitochondrial, pseudogene 1 [Source:MGI Symbol;Acc:MGI:104721]	-
193	ENSMUSG00000034621	Gpatch8	G patch domain containing 8 [Source:MGI Symbol;Acc:MGI:1918667]	+

194	ENSMUSG00000041293	Gpr110	G protein-coupled receptor 110 [Source:MGI Symbol;Acc:MGI:1924846]	+
195	ENSMUSG00000039116	Gpr126	G protein-coupled receptor 126 [Source:MGI Symbol;Acc:MGI:1916151]	+
196	ENSMUSG00000022286	Grhl2	grainyhead-like 2 (Drosophila) [Source:MGI Symbol;Acc:MGI:2182543]	+
197	ENSMUSG00000035637	Grhpr	glyoxylate reductase/hydroxypyruvate reductase [Source:MGI Symbol;Acc:MGI:1923488]	-
198	ENSMUSG00000016503	Gtf3a	general transcription factor III A [Source:MGI Symbol;Acc:MGI:1913846]	+
199	ENSMUSG00000053624	Gykl1	glycerol kinase-like 1 [Source:MGI Symbol;Acc:MGI:891990]	+
200	ENSMUSG00000044927	H1fx	H1 histone family, member X [Source:MGI Symbol;Acc:MGI:2685307]	-
201	ENSMUSG00000022367	Has2	hyaluronan synthase 2 [Source:MGI Symbol;Acc:MGI:107821]	+
202	ENSMUSG00000022831	Hcls1	hematopoietic cell specific Lyn substrate 1 [Source:MGI Symbol;Acc:MGI:104568]	-
203	ENSMUSG00000022831	Hcls1	hematopoietic cell specific Lyn substrate 1 [Source:MGI Symbol;Acc:MGI:104568]	+
204	ENSMUSG00000025857	Heatr2	HEAT repeat containing 2 [Source:MGI Symbol;Acc:MGI:3616079]	+
205	ENSMUSG00000035247	Hectd1	HECT domain containing 1 [Source:MGI Symbol;Acc:MGI:2384768]	+
206	ENSMUSG00000075254	Heg1	HEG homolog 1 (zebrafish) [Source:MGI Symbol;Acc:MGI:1924696]	+
207	ENSMUSG00000066842	Hmcn1	hemicentin 1 [Source:MGI Symbol;Acc:MGI:2685047]	+
208	ENSMUSG00000031844	Hsd17b2	hydroxysteroid (17-beta) dehydrogenase 2 [Source:MGI Symbol;Acc:MGI:1096386]	+
209	ENSMUSG00000045336	Hsfy2	heat shock transcription factor, Y linked 2 [Source:MGI Symbol;Acc:MGI:1918316]	+
210	ENSMUSG00000032115	Hyou1	hypoxia up-regulated 1 [Source:MGI Symbol;Acc:MGI:108030]	+
211	ENSMUSG00000041025	Iffo2	intermediate filament family orphan 2 [Source:MGI Symbol;Acc:MGI:2140675]	+
212	ENSMUSG00000027776	Il12a	interleukin 12a [Source:MGI Symbol;Acc:MGI:96539]	+
213	ENSMUSG00000018341	Il12rb2	interleukin 12 receptor, beta 2 [Source:MGI Symbol;Acc:MGI:1270861]	-
214	ENSMUSG00000020383	Il13	interleukin 13 [Source:MGI Symbol;Acc:MGI:96541]	+
215	ENSMUSG00000050222	Il17d	interleukin 17D [Source:MGI Symbol;Acc:MGI:2446510]	-
216	ENSMUSG00000016524	Il19	interleukin 19 [Source:MGI Symbol;Acc:MGI:1890472]	+
217	ENSMUSG00000020007	Il20ra	interleukin 20 receptor, alpha [Source:MGI Symbol;Acc:MGI:3605069]	+
218	ENSMUSG00000032178	Ilf3	interleukin enhancer binding factor 3 [Source:MGI Symbol;Acc:MGI:1339973]	-
219	ENSMUSG00000035804	Ins1	insulin I [Source:MGI Symbol;Acc:MGI:96572]	+
220	ENSMUSG00000025133	Ints4	integrator complex subunit 4 [Source:MGI Symbol;Acc:MGI:1917164]	+
221	ENSMUSG00000020918	Kat2a	K(lysine) acetyltransferase 2A [Source:MGI Symbol;Acc:MGI:1343101]	+
222	ENSMUSG00000037579	Kcnh3	potassium voltage-gated channel, subfamily H (eag-related), member 3 [Source:MGI Symbol;Acc:MGI:1341723]	+
223	ENSMUSG00000030499	Kctd15	potassium channel tetramerisation domain containing 15 [Source:MGI Symbol;Acc:MGI:2385276]	+
224	ENSMUSG00000018476	Kdm6b	KDM1 lysine (K)-specific demethylase 6B [Source:MGI Symbol;Acc:MGI:2448492]	+
225	ENSMUSG00000032254	Kif23	kinesin family member 23 [Source:MGI Symbol;Acc:MGI:1919069]	+
226	ENSMUSG00000044938	Klhl31	kelch-like 31 (Drosophila) [Source:MGI Symbol;Acc:MGI:3045305]	+
227	ENSMUSG00000014543	Klra17	killer cell lectin-like receptor, subfamily A, member 17 [Source:MGI Symbol;Acc:MGI:2180674]	+
228	ENSMUSG00000020913	Krt24	keratin 24 [Source:MGI Symbol;Acc:MGI:1922956]	+
229	ENSMUSG00000002900	Lamb1	laminin B1 [Source:MGI Symbol;Acc:MGI:96743]	+
230	ENSMUSG00000024493	Lars	leucyl-tRNA synthetase [Source:MGI Symbol;Acc:MGI:1913808]	-
231	ENSMUSG00000030510	Lass3	LAG1 homolog, ceramide synthase 3 [Source:MGI Symbol;Acc:MGI:2681008]	+
232	ENSMUSG00000021539	Lect2	leukocyte cell-derived chemotaxin 2 [Source:MGI Symbol;Acc:MGI:1278342]	+
233	ENSMUSG00000057722	Lepr	leptin receptor [Source:MGI Symbol;Acc:MGI:104993]	-
234	ENSMUSG00000034394	Lif	leukemia inhibitory factor [Source:MGI Symbol;Acc:MGI:96787]	-
235	ENSMUSG00000027070	Lrp2	low density lipoprotein receptor-related protein 2 [Source:MGI Symbol;Acc:MGI:95794]	-
236	ENSMUSG00000054720	Lrrc8c	leucine rich repeat containing 8 family, member C [Source:MGI Symbol;Acc:MGI:2140839]	+
237	ENSMUSG00000061143	Maml3	mastermind like 3 (Drosophila) [Source:MGI Symbol;Acc:MGI:2389461]	+
238	ENSMUSG00000021754	Map3k1	mitogen-activated protein kinase kinase kinase 1 [Source:MGI Symbol;Acc:MGI:1346872]	+
239	ENSMUSG00000034751	Mast4	microtubule associated serine/threonine kinase family member 4 [Source:MGI Symbol;Acc:MGI:1918885]	-
240	ENSMUSG00000041859	Mcm3	minichromosome maintenance deficient 3 (S. cerevisiae) [Source:MGI Symbol;Acc:MGI:101845]	+
241	ENSMUSG00000041390	Mdfic	MyoD family inhibitor domain containing [Source:MGI Symbol;Acc:MGI:104611]	+
242	ENSMUSG00000036466	Megf11	multiple EGF-like-domains 11 [Source:MGI Symbol;Acc:MGI:1920951]	+
243	ENSMUSG00000054619	Mettl7a1	methyltransferase like 7A1 [Source:MGI Symbol;Acc:MGI:1916523]	+
244	ENSMUSG00000065406	Mirlet7i	microRNA let7i [Source:MGI Symbol;Acc:MGI:2676802]	+
245	ENSMUSG00000025609	Mkln1	muskelin 1, intracellular mediator containing kelch motifs [Source:MGI Symbol;Acc:MGI:1351638]	+
246	ENSMUSG00000034602	Mon2	MON2 homolog (yeast) [Source:MGI Symbol;Acc:MGI:1914324]	+
247	ENSMUSG00000039456	Morc3	microrchidia 3 [Source:MGI Symbol;Acc:MGI:2136841]	+
248	ENSMUSG00000026621	Mosc1	MOCO sulphurase C-terminal domain containing 1 [Source:MGI Symbol;Acc:MGI:1913362]	+
249	ENSMUSG00000032459	Mrps22	mitochondrial ribosomal protein S22 [Source:MGI Symbol;Acc:MGI:1928137]	+
250	ENSMUSG00000054256	Msi1	Musashi homolog 1(Drosophila) [Source:MGI Symbol;Acc:MGI:107376]	+
251	ENSMUSG00000016510	Mtif3	mitochondrial translational initiation factor 3 [Source:MGI Symbol;Acc:MGI:1923616]	+
252	ENSMUSG00000028116	Myoz2	myozenin 2 [Source:MGI Symbol;Acc:MGI:1913063]	+
253	ENSMUSG00000027977	Ndst3	N-deacetylase/N-sulfotransferase (heparan glucosaminyl) 3 [Source:MGI Symbol;Acc:MGI:1932544]	+
254	ENSMUSG00000020022	Ndufa12	NADH dehydrogenase (ubiquinone) 1 alpha subcomplex, 12 [Source:MGI Symbol;Acc:MGI:1913664]	+
255	ENSMUSG00000013593	Ndufs2	NADH dehydrogenase (ubiquinone) Fe-S protein 2 [Source:MGI Symbol;Acc:MGI:2385112]	+
256	ENSMUSG00000026950	Neb	nebulin [Source:MGI Symbol;Acc:MGI:97292]	+
257	ENSMUSG00000072889	Nfxl1	nuclear transcription factor, X-box binding-like 1 [Source:MGI Symbol;Acc:MGI:1923646]	+
258	ENSMUSG00000000120	Ngfr	nerve growth factor receptor (TNFR superfamily, member 16) [Source:MGI Symbol;Acc:MGI:97323]	+
259	ENSMUSG00000039835	Nhsl1	NHS-like 1 [Source:MGI Symbol;Acc:MGI:106390]	+
260	ENSMUSG00000028992	Nmnat1	nicotinamide nucleotide adenylyltransferase 1 [Source:MGI Symbol;Acc:MGI:1913704]	-
261	ENSMUSG00000029361	Nos1	nitric oxide synthase 1, neuronal [Source:MGI Symbol;Acc:MGI:97360]	+
262	ENSMUSG00000047911	Npm2	nucleophosmin/nucleoplasmin 2 [Source:MGI Symbol;Acc:MGI:1890811]	+
263	ENSMUSG00000005897	Nr2c1	nuclear receptor subfamily 2, group C, member 1 [Source:MGI Symbol;Acc:MGI:1352465]	+
264	ENSMUSG00000024109	Nrxn1	neurexin I [Source:MGI Symbol;Acc:MGI:1096391]	+
265	ENSMUSG00000021595	Nsun2	NOL1/NOP2/Sun domain family member 2 [Source:MGI Symbol;Acc:MGI:107252]	-
266	ENSMUSG00000054027	Nt5dc3	5'-nucleotidase domain containing 3 [Source:MGI Symbol;Acc:MGI:3513266]	+
267	ENSMUSG00000035351	Nup37	nucleoporin 37 [Source:MGI Symbol;Acc:MGI:1919964]	+
268	ENSMUSG00000075592	Nynrin	NYN domain and retroviral integrase containing [Source:MGI Symbol;Acc:MGI:2652872]	-
269	ENSMUSG00000075592	Nynrin	NYN domain and retroviral integrase containing [Source:MGI Symbol;Acc:MGI:2652872]	+
270	ENSMUSG00000035963	Odf3l2	outer dense fiber of sperm tails 3-like 2 [Source:MGI Symbol;Acc:MGI:2686003]	+

271	ENSMUSG00000075158	Olfr1111	olfactory receptor 1111 [Source:MGI Symbol;Acc:MGI:3030945]	+
272	ENSMUSG00000059504	Olfr314	olfactory receptor 314 [Source:MGI Symbol;Acc:MGI:3030148]	-
273	ENSMUSG00000060549	Olfr488	olfactory receptor 488 [Source:MGI Symbol;Acc:MGI:3030322]	+
274	ENSMUSG00000045591	Olig3	oligodendrocyte transcription factor 3 [Source:MGI Symbol;Acc:MGI:2149955]	+
275	ENSMUSG00000050121	Opalin	oligodendrocytic myelin paranodal and inner loop protein [Source:MGI Symbol;Acc:MGI:2657025]	+
276	ENSMUSG00000021799	Opn4	opsin 4 (melanopsin) [Source:MGI Symbol;Acc:MGI:1353425]	-
277	ENSMUSG00000044252	Osbpl1a	oxysterol binding protein-like 1A [Source:MGI Symbol;Acc:MGI:1927551]	+
278	ENSMUSG00000018906	P4ha2	procollagen-proline, 2-oxoglutarate 4-dioxygenase (proline 4-hydroxylase), alpha II polypeptide [Source:MGI Symbol;Acc:MGI:894286]	+
279	ENSMUSG00000016664	Pacsin2	protein kinase C and casein kinase substrate in neurons 2 [Source:MGI Symbol;Acc:MGI:1345153]	+
280	ENSMUSG00000038683	Pak1ip1	PAK1 interacting protein 1 [Source:MGI Symbol;Acc:MGI:1915333]	+
281	ENSMUSG00000046526	Pard3b	par-3 partitioning defective 3 homolog B (C. elegans) [Source:MGI Symbol;Acc:MGI:1919301]	-
282	ENSMUSG00000052062	Pard3b	par-3 partitioning defective 3 homolog B (C. elegans) [Source:MGI Symbol;Acc:MGI:1919301]	-
283	ENSMUSG00000022439	Parvg	parvin, gamma [Source:MGI Symbol;Acc:MGI:2158329]	+
284	ENSMUSG00000022439	Parvg	parvin, gamma [Source:MGI Symbol;Acc:MGI:2158329]	+
285	ENSMUSG00000007440	Pcdha9	protocadherin alpha 4 [Source:MGI Symbol;Acc:MGI:1298406]	+
286	ENSMUSG00000045062	Pcdhb7	protocadherin beta 7 [Source:MGI Symbol;Acc:MGI:2136741]	+
287	ENSMUSG00000023036	Pcdhgb6	protocadherin gamma subfamily A, 9 [Source:MGI Symbol;Acc:MGI:1935226]	+
288	ENSMUSG00000023036	Pcdhgb6	protocadherin gamma subfamily A, 9 [Source:MGI Symbol;Acc:MGI:1935226]	+
289	ENSMUSG00000020553	Pctp	phosphatidylcholine transfer protein [Source:MGI Symbol;Acc:MGI:107375]	+
290	ENSMUSG00000025137	Pcyt2	phosphate cytidylyltransferase 2, ethanolamine [Source:MGI Symbol;Acc:MGI:1915921]	+
291	ENSMUSG00000025047	Pdcd11	programmed cell death 11 [Source:MGI Symbol;Acc:MGI:1341788]	+
292	ENSMUSG00000031595	Pdgfrl	platelet-derived growth factor receptor-like [Source:MGI Symbol;Acc:MGI:1916047]	+
293	ENSMUSG00000035357	Pdzrn3	PDZ domain containing RING finger 3 [Source:MGI Symbol;Acc:MGI:1933157]	+
294	ENSMUSG00000017781	Pitpna	phosphatidylinositol transfer protein, alpha [Source:MGI Symbol;Acc:MGI:99887]	-
295	ENSMUSG00000014503	Pkd2l2	polycystic kidney disease 2-like 2 [Source:MGI Symbol;Acc:MGI:1858231]	+
296	ENSMUSG00000058908	Pla2g2a	phospholipase A2, group IIA (platelets, synovial fluid) [Source:MGI Symbol;Acc:MGI:104642]	+
297	ENSMUSG00000041193	Pla2g5	phospholipase A2, group V [Source:MGI Symbol;Acc:MGI:101899]	+
298	ENSMUSG00000027695	Pld1	phospholipase D1 [Source:MGI Symbol;Acc:MGI:109585]	-
299	ENSMUSG00000002733	Plekha3	pleckstrin homology domain-containing, family A (phosphoinositide binding specific) member 3 [Source:MGI Symbol;Acc:MGI:1932515]	-
300	ENSMUSG00000028917	Plekhm2	pleckstrin homology domain containing, family M (with RUN domain) member 2 [Source:MGI Symbol;Acc:MGI:1916832]	-
301	ENSMUSG00000074785	Plxnc1	plexin C1 [Source:MGI Symbol;Acc:MGI:1890127]	+
302	ENSMUSG00000046008	Pnlip	pancreatic lipase [Source:MGI Symbol;Acc:MGI:97722]	+
303	ENSMUSG00000018868	Pnpla5	patatin-like phospholipase domain containing 5 [Source:MGI Symbol;Acc:MGI:1923022]	-
304	ENSMUSG00000067279	Ppp1r3c	protein phosphatase 1, regulatory (inhibitor) subunit 3C [Source:MGI Symbol;Acc:MGI:1858229]	+
305	ENSMUSG00000014039	Prdm15	PR domain containing 15 [Source:MGI Symbol;Acc:MGI:1930121]	-
306	ENSMUSG00000029513	Prkab1	protein kinase, AMP-activated, beta 1 non-catalytic subunit [Source:MGI Symbol;Acc:MGI:1336167]	+
307	ENSMUSG00000030069	Prok2	prokineticin 2 [Source:MGI Symbol;Acc:MGI:1354178]	+
308	ENSMUSG00000038500	Prr3	proline-rich polypeptide 3 [Source:MGI Symbol;Acc:MGI:1922460]	+
309	ENSMUSG00000027978	Prss12	protease, serine, 12 neurotrypsin (motopsin) [Source:MGI Symbol;Acc:MGI:1100881]	+
310	ENSMUSG00000024116	Prss21	protease, serine, 21 [Source:MGI Symbol;Acc:MGI:1916698]	+
311	ENSMUSG00000039405	Prss23	protease, serine, 23 [Source:MGI Symbol;Acc:MGI:1923703]	-
312	ENSMUSG00000044664	Prss42	protease, serine, 42 [Source:MGI Symbol;Acc:MGI:2665280]	+
313	ENSMUSG00000028378	Ptgr1	prostaglandin reductase 1 [Source:MGI Symbol;Acc:MGI:1914353]	+
314	ENSMUSG00000028378	Ptgr1	prostaglandin reductase 1 [Source:MGI Symbol;Acc:MGI:1914353]	+
315	ENSMUSG00000021009	Ptpn21	protein tyrosine phosphatase, non-receptor type 21 [Source:MGI Symbol;Acc:MGI:1344406]	+
316	ENSMUSG00000045378	Pxt1	peroxisomal, testis specific 1 [Source:MGI Symbol;Acc:MGI:1916557]	+
317	ENSMUSG00000079477	Rab7	RAB7, member RAS oncogene family [Source:MGI Symbol;Acc:MGI:105068]	-
318	ENSMUSG00000038569	Rad9b	RAD9 homolog B (S. cerevisiae) [Source:MGI Symbol;Acc:MGI:2385231]	+
319	ENSMUSG00000039607	Rbms3	RNA binding motif, single stranded interacting protein [Source:MGI Symbol;Acc:MGI:2444477]	+
320	ENSMUSG00000005251	Ripk4	receptor-interacting serine-threonine kinase 4 [Source:MGI Symbol;Acc:MGI:1919638]	-
321	ENSMUSG00000022236	Ropn1l	ropporin 1-like [Source:MGI Symbol;Acc:MGI:2182357]	+
322	ENSMUSG00000071269	Rpl9-ps4	ribosomal protein L9, pseudogene 4 [Source:MGI Symbol;Acc:MGI:3704410]	+
323	ENSMUSG00000007892	Rplp1	ribosomal protein, large, P1 [Source:MGI Symbol;Acc:MGI:1927099]	+
324	ENSMUSG00000040952	Rps19	ribosomal protein S19 [Source:MGI Symbol;Acc:MGI:1333780]	+
325	ENSMUSG00000020649	Rrm2	ribonucleotide reductase M2 [Source:MGI Symbol;Acc:MGI:98181]	-
326	ENSMUSG00000005846	Rsl1d1	ribosomal L1 domain containing 1 [Source:MGI Symbol;Acc:MGI:1913659]	+
327	ENSMUSG00000037846	Rtkn2	rhotekin 2 [Source:MGI Symbol;Acc:MGI:2158417]	+
328	ENSMUSG00000037846	Rtkn2	rhotekin 2 [Source:MGI Symbol;Acc:MGI:2158417]	+
329	ENSMUSG00000031665	Sall1	sal-like 1 (Drosophila) [Source:MGI Symbol;Acc:MGI:1889585]	+
330	ENSMUSG00000031665	Sall1	sal-like 1 (Drosophila) [Source:MGI Symbol;Acc:MGI:1889585]	+
331	ENSMUSG00000027547	Sall4	sal-like 4 (Drosophila) [Source:MGI Symbol;Acc:MGI:2139360]	+
332	ENSMUSG00000048652	Samd13	sterile alpha motif domain containing 13 [Source:MGI Symbol;Acc:MGI:2686498]	+
333	ENSMUSG00000021838	Samd4	sterile alpha motif domain containing 4 [Source:MGI Symbol;Acc:MGI:1921730]	+
334	ENSMUSG00000051860	Samd7	sterile alpha motif domain containing 7 [Source:MGI Symbol;Acc:MGI:1923203]	+
335	ENSMUSG00000028236	Sdr16c5	short chain dehydrogenase/reductase family 16C, member 5 [Source:MGI Symbol;Acc:MGI:2668443]	+
336	ENSMUSG00000051984	Sec31b	Sec31 homolog B (S. cerevisiae) [Source:MGI Symbol;Acc:MGI:2685187]	+
337	ENSMUSG00000024548	Setbp1	SET binding protein 1 [Source:MGI Symbol;Acc:MGI:1933199]	+
338	ENSMUSG00000058153	Sez6l	seizure related 6 homolog like [Source:MGI Symbol;Acc:MGI:1935121]	+
339	ENSMUSG00000022097	Sftpc	surfactant associated protein C [Source:MGI Symbol;Acc:MGI:109517]	+
340	ENSMUSG00000025138	Sirt7	sirtuin 7 (silent mating type information regulation 2, homolog) 7 (S. cerevisiae) [Source:MGI Symbol;Acc:MGI:2385849]	+
341	ENSMUSG00000057399	Ska2l-ps	spindle and kinetochore associated complex subunit 2-like, pseudogene [Source:MGI Symbol;Acc:MGI:3643639]	+
342	ENSMUSG00000025557	Slc15a1	solute carrier family 15 (oligopeptide transporter), member 1 [Source:MGI Symbol;Acc:MGI:1861376]	+
343	ENSMUSG00000022199	Slc22a17	solute carrier family 22 (organic cation transporter), member 17 [Source:MGI Symbol;Acc:MGI:1926225]	-

344	ENSMUSG00000071253	Slc25a16	solute carrier family 25 (mitochondrial carrier, Graves disease autoantigen), member 16 [Source:MGI Symbol;Acc:MGI:1920382]	+
345	ENSMUSG00000037434	Slc30a1	solute carrier family 30 (zinc transporter), member 1 [Source:MGI Symbol;Acc:MGI:1345281]	+
346	ENSMUSG00000032122	Slc37a2	solute carrier family 37 (glycerol-3-phosphate transporter), member 2 [Source:MGI Symbol;Acc:MGI:1929693]	+
347	ENSMUSG00000022464	Slc38a4	solute carrier family 38, member 4 [Source:MGI Symbol;Acc:MGI:1916604]	+
348	ENSMUSG00000022464	Slc38a4	solute carrier family 38, member 4 [Source:MGI Symbol;Acc:MGI:1916604]	+
349	ENSMUSG00000022464	Slc38a4	solute carrier family 38, member 4 [Source:MGI Symbol;Acc:MGI:1916604]	+
350	ENSMUSG00000031596	Slc7a2	solute carrier family 7 (cationic amino acid transporter, y+ system), member 2 [Source:MGI Symbol;Acc:MGI:99828]	+
351	ENSMUSG00000024921	Smarca2	SWI/SNF related, matrix associated, actin dependent regulator of chromatin, subfamily a, member 2 [Source:MGI Symbol;Acc:MGI:99603]	+
352	ENSMUSG00000042364	Snx18	sorting nexin 18 [Source:MGI Symbol;Acc:MGI:2137642]	+
353	ENSMUSG00000051910	Sox6	SRY-box containing gene 6 [Source:MGI Symbol;Acc:MGI:98368]	-
354	ENSMUSG00000046957	Spz1	spermatogenic leucine zipper 1 [Source:MGI Symbol;Acc:MGI:1930801]	+
355	ENSMUSG00000047963	Stbd1	starch binding domain 1 [Source:MGI Symbol;Acc:MGI:1261768]	+
356	ENSMUSG00000020954	Strn3	striatin, calmodulin binding protein 3 [Source:MGI Symbol;Acc:MGI:2151064]	+
357	ENSMUSG00000032437	Stt3b	STT3, subunit of the oligosaccharyltransferase complex, homolog B (S. cerevisiae) [Source:MGI Symbol;Acc:MGI:1915542]	+
358	ENSMUSG00000038486	Sv2a	synaptic vesicle glycoprotein 2 a [Source:MGI Symbol;Acc:MGI:1927139]	+
359	ENSMUSG00000039215	Svs1	seminal vesicle secretory protein 1 [Source:MGI Symbol;Acc:MGI:2682321]	+
360	ENSMUSG00000063450	Syne2	synaptic nuclear envelope 2 [Source:MGI Symbol;Acc:MGI:2449316]	+
361	ENSMUSG00000050315	Synpo2	synaptopodin 2 [Source:MGI Symbol;Acc:MGI:2153070]	+
362	ENSMUSG00000058159	T2	brachyury 2 [Source:MGI Symbol;Acc:MGI:104658]	+
363	ENSMUSG00000020872	Tac4	tachykinin 4 [Source:MGI Symbol;Acc:MGI:1931130]	-
364	ENSMUSG00000021177	Tdp1	tyrosyl-DNA phosphodiesterase 1 [Source:MGI Symbol;Acc:MGI:1920036]	+
365	ENSMUSG00000040943	Tet2	tet methylcytosine dioxygenase 2 [Source:MGI Symbol;Acc:MGI:2443298]	+
366	ENSMUSG00000040548	Tex2	testis expressed gene 2 [Source:MGI Symbol;Acc:MGI:102465]	+
367	ENSMUSG00000054474	Thnsl2	threonine synthase-like 2 (bacterial) [Source:MGI Symbol;Acc:MGI:3041254]	-
368	ENSMUSG00000025013	Tll2	tolloid-like 2 [Source:MGI Symbol;Acc:MGI:1346044]	+
369	ENSMUSG00000062545	Tlr12	toll-like receptor 12 [Source:MGI Symbol;Acc:MGI:3045221]	+
370	ENSMUSG00000029483	Tmem132b	transmembrane protein 132B [Source:MGI Symbol;Acc:MGI:3609245]	-
371	ENSMUSG00000024754	Tmem2	transmembrane protein 2 [Source:MGI Symbol;Acc:MGI:1890373]	+
372	ENSMUSG00000036019	Tmtc2	transmembrane and tetratricopeptide repeat containing 2 [Source:MGI Symbol;Acc:MGI:1914057]	-
373	ENSMUSG00000031529	Tnks	tankyrase, TRF1-interacting ankyrin-related ADP-ribose polymerase [Source:MGI Symbol;Acc:MGI:1341087]	-
374	ENSMUSG00000000296	Tpd52l1	tumor protein D52-like 1 [Source:MGI Symbol;Acc:MGI:1298386]	+
375	ENSMUSG00000006005	Tpr	translocated promoter region [Source:MGI Symbol;Acc:MGI:1922066]	+
376	ENSMUSG00000026875	Traf1	TNF receptor-associated factor 1 [Source:MGI Symbol;Acc:MGI:101836]	-
377	ENSMUSG00000033209	Ttc28	tetratricopeptide repeat domain 28 [Source:MGI Symbol;Acc:MGI:2140873]	+
378	ENSMUSG00000033209	Ttc28	tetratricopeptide repeat domain 28 [Source:MGI Symbol;Acc:MGI:2140873]	+
379	ENSMUSG00000051747	Ttn	titin [Source:MGI Symbol;Acc:MGI:98864]	-
380	ENSMUSG00000054892	Txk	TXK tyrosine kinase [Source:MGI Symbol;Acc:MGI:102960]	+
381	ENSMUSG00000022615	Tymp	thymidine phosphorylase [Source:MGI Symbol;Acc:MGI:1920212]	+
382	ENSMUSG00000041765	Ubac2	ubiquitin associated domain containing 2 [Source:MGI Symbol;Acc:MGI:1916139]	+
383	ENSMUSG00000030884	Uqcrc2	ubiquinol cytochrome c reductase core protein 2 [Source:MGI Symbol;Acc:MGI:1914253]	+
384	ENSMUSG00000030979	Uros	uroporphyrinogen III synthase [Source:MGI Symbol;Acc:MGI:98917]	+
385	ENSMUSG00000031826	Usp10	ubiquitin specific peptidase 10 [Source:MGI Symbol;Acc:MGI:894652]	+
386	ENSMUSG00000051527	Usp29	ubiquitin specific peptidase 29 [Source:MGI Symbol;Acc:MGI:1888998]	+
387	ENSMUSG00000033653	Vps8	vacuolar protein sorting 8 homolog (S. cerevisiae) [Source:MGI Symbol;Acc:MGI:2146407]	+
388	ENSMUSG00000037890	Wdr19	WD repeat domain 19 [Source:MGI Symbol;Acc:MGI:2443231]	+
389	ENSMUSG00000035295	Wdr38	WD repeat domain 38 [Source:MGI Symbol;Acc:MGI:1923896]	+
390	ENSMUSG00000073434	Wdr90	WD repeat domain 90 [Source:MGI Symbol;Acc:MGI:1921267]	+
391	ENSMUSG00000040154	Wfdc5	WAP four-disulfide core domain 5 [Source:MGI Symbol;Acc:MGI:2384800]	+
392	ENSMUSG00000022100	Xpo7	exportin 7 [Source:MGI Symbol;Acc:MGI:1929705]	+
393	ENSMUSG00000034667	Xpot	exportin, tRNA (nuclear export receptor for tRNAs) [Source:MGI Symbol;Acc:MGI:1920442]	+
394	ENSMUSG00000035649	Zcchc7	zinc finger, CCHC domain containing 7 [Source:MGI Symbol;Acc:MGI:2442912]	-
395	ENSMUSG00000022335	Zfat	zinc finger and AT hook domain containing [Source:MGI Symbol;Acc:MGI:2681865]	+
396	ENSMUSG00000022335	Zfat	zinc finger and AT hook domain containing [Source:MGI Symbol;Acc:MGI:2681865]	+
397	ENSMUSG00000038872	Zfhx3	zinc finger homeobox 3 [Source:MGI Symbol;Acc:MGI:99948]	-
398	ENSMUSG00000030446	Zfp273	zinc finger protein 273 [Source:MGI Symbol;Acc:MGI:3036278]	+
399	ENSMUSG00000028840	Zfp593	zinc finger protein 593 [Source:MGI Symbol;Acc:MGI:1915290]	+
400	ENSMUSG00000027667	Zfp639	zinc finger protein 639 [Source:MGI Symbol;Acc:MGI:1915028]	+
401	ENSMUSG00000027551	Zfp64	zinc finger protein 64 [Source:MGI Symbol;Acc:MGI:107342]	+
402	ENSMUSG00000039501	Znfx1	zinc finger, NFX1-type containing 1 [Source:MGI Symbol;Acc:MGI:2138982]	+
403	ENSMUSG00000077407		Small nucleolar RNA SNORA17 [Source:RFAM;Acc:RF00560]	-
404	ENSMUSG00000077320		Small nucleolar RNA SNORA17 [Source:RFAM;Acc:RF00560]	-
405	ENSMUSG00000080679			+
406	ENSMUSG00000065767		U2 spliceosomal RNA [Source:RFAM;Acc:RF00004]	+
407	ENSMUSG00000064386		U6 spliceosomal RNA [Source:RFAM;Acc:RF00026]	+
408	ENSMUSG00000065339		U6 spliceosomal RNA [Source:RFAM;Acc:RF00026]	+
409	ENSMUSG00000064644		U6 spliceosomal RNA [Source:RFAM;Acc:RF00026]	+
410	ENSMUSG00000080355			+
411	ENSMUSG00000080506			+
412	ENSMUSG00000065240		U6 spliceosomal RNA [Source:RFAM;Acc:RF00026]	+
413	ENSMUSG00000080460		mmu-mir-1194 [Source:miRBase;Acc:MI0006299]	+
414	ENSMUSG00000065360		Small nucleolar RNA SNORA32 [Source:RFAM;Acc:RF00421]	+
415	ENSMUSG00000076961			+

5.1.6 DNA methylation regulated at the gene × environment level.

Genes have been ordered alphabetically.

#	Feature	Symbol	Genename	Effect
1	ENSMUSG00000021470	0610007P08Rik	RIKEN cDNA 0610007P08 gene [Source:MGI Symbol;Acc:MGI:1923501]	-
2	ENSMUSG00000021252	0610007P14Rik	RIKEN cDNA 0610007P14 gene [Source:MGI Symbol;Acc:MGI:1915571]	-
3	ENSMUSG00000026154	1110058L19Rik	RIKEN cDNA 1110058L19 gene [Source:MGI Symbol;Acc:MGI:1915252]	-
4	ENSMUSG00000057816	1700007G11Rik	RIKEN cDNA 1700007G11 gene [Source:MGI Symbol;Acc:MGI:1916571]	-
5	ENSMUSG00000029766	1700012A03Rik	RIKEN cDNA 1700012A03 gene [Source:MGI Symbol;Acc:MGI:1923632]	-
6	ENSMUSG00000072878	1700123L14Rik	RIKEN cDNA 1700123L14 gene [Source:MGI Symbol;Acc:MGI:1925732]	-
7	ENSMUSG00000078607	1810010H24Rik	RIKEN cDNA 1810010H24 gene [Source:MGI Symbol;Acc:MGI:1916316]	+
8	ENSMUSG00000041707	1810011H11Rik	RIKEN cDNA 1810011H11 gene [Source:MGI Symbol;Acc:MGI:1916319]	+
9	ENSMUSG00000021040	1810035L17Rik	RIKEN cDNA 1810035L17 gene [Source:MGI Symbol;Acc:MGI:1916394]	-
10	ENSMUSG00000051606	2010001K21Rik	RIKEN cDNA 2010001K21 gene [Source:MGI Symbol;Acc:MGI:1917079]	-
11	ENSMUSG00000049916	2610318N02Rik	RIKEN cDNA 2610318N02 gene [Source:MGI Symbol;Acc:MGI:1917708]	-
12	ENSMUSG00000021041	2700073G19Rik	RIKEN cDNA 2700073G19 gene [Source:MGI Symbol;Acc:MGI:1919868]	-
13	ENSMUSG00000026388	3110009E18Rik	RIKEN cDNA 3110009E18 gene [Source:MGI Symbol;Acc:MGI:1920353]	+
14	ENSMUSG00000074224	4932431P20Rik	RIKEN cDNA 4932431P20 gene [Source:MGI Symbol;Acc:MGI:2149781]	+
15	ENSMUSG00000050709	4932442E05Rik	RIKEN cDNA 4932442E05 gene [Source:MGI Symbol;Acc:MGI:1921665]	-
16	ENSMUSG00000067613	5430421N21Rik	RIKEN cDNA 5430421N21 gene [Source:MGI Symbol;Acc:MGI:3690448]	-
17	ENSMUSG00000045968	5830403L16Rik	RIKEN cDNA 5830403L16 gene [Source:MGI Symbol;Acc:MGI:1923273]	+
18	ENSMUSG00000031960	Aars	alanyl-tRNA synthetase [Source:MGI Symbol;Acc:MGI:2384560]	+
19	ENSMUSG00000028093	Acp6	acid phosphatase 6, lysophosphatidic [Source:MGI Symbol;Acc:MGI:1931010]	+
20	ENSMUSG00000035783	Acta2	actin, alpha 2, smooth muscle, aorta [Source:MGI Symbol;Acc:MGI:87909]	+
21	ENSMUSG00000029313	Aff1	AF4/FMR2 family, member 1 [Source:MGI Symbol;Acc:MGI:1100819]	-
22	ENSMUSG00000025754	Agbl1	ATP/GTP binding protein-like 1 [Source:MGI Symbol;Acc:MGI:3646469]	-
23	ENSMUSG00000026246	Alppl2	alkaline phosphatase, placental-like 2 [Source:MGI Symbol;Acc:MGI:108009]	-
24	ENSMUSG00000060096	Amd-ps3	S-adenosylmethionine decarboxylase, pseudogene 3 [Source:MGI Symbol;Acc:MGI:3704487]	-
25	ENSMUSG00000069601	Ank3	ankyrin 3, epithelial [Source:MGI Symbol;Acc:MGI:88026]	-
26	ENSMUSG00000021866	Anxa11	annexin A11 [Source:MGI Symbol;Acc:MGI:108481]	+
27	ENSMUSG00000028411	Aptx	aprataxin [Source:MGI Symbol;Acc:MGI:1913658]	+
28	ENSMUSG00000028427	Aqp7	aquaporin 7 [Source:MGI Symbol;Acc:MGI:1314647]	+
29	ENSMUSG00000030220	Arhgdib	Rho, GDP dissociation inhibitor (GDI) beta [Source:MGI Symbol;Acc:MGI:101940]	+
30	ENSMUSG00000054901	Arhgef33	Rho guanine nucleotide exchange factor (GEF) 33 [Source:MGI Symbol;Acc:MGI:2685787]	-
31	ENSMUSG00000019947	Arid5b	AT rich interactive domain 5B (MRF1-like) [Source:MGI Symbol;Acc:MGI:2175912]	+
32	ENSMUSG00000030651	Art2b	ADP-ribosyltransferase 2b [Source:MGI Symbol;Acc:MGI:107545]	+
33	ENSMUSG00000038997	Asb17	ankyrin repeat and SOCS box-containing 17 [Source:MGI Symbol;Acc:MGI:1914022]	-
34	ENSMUSG00000076441	Ass1	argininosuccinate synthetase 1 [Source:MGI Symbol;Acc:MGI:88090]	+
35	ENSMUSG00000041341	Atg2b	ATG2 autophagy related 2 homolog B (S. cerevisiae) [Source:MGI Symbol;Acc:MGI:1923809]	-
36	ENSMUSG00000038160	Atg5	autophagy-related 5 (yeast) [Source:MGI Symbol;Acc:MGI:1277186]	-
37	ENSMUSG00000055415	Atp10b	ATPase, class V, type 10B [Source:MGI Symbol;Acc:MGI:2442688]	-
38	ENSMUSG00000038600	Atp6v0a4	ATPase, H+ transporting, lysosomal V0 subunit A4 [Source:MGI Symbol;Acc:MGI:2153480]	-
39	ENSMUSG00000028541	B4galt2	UDP-Gal:betaGlcNAc beta 1,4- galactosyltransferase, polypeptide 2 [Source:MGI Symbol;Acc:MGI:1858493]	+
40	ENSMUSG00000033722	BC034090	cDNA sequence BC034090 [Source:MGI Symbol;Acc:MGI:2672904]	+
41	ENSMUSG00000048186	Bend7	BEN domain containing 7 [Source:MGI Symbol;Acc:MGI:2443100]	-
42	ENSMUSG00000075411	Bin2	bridging integrator 2 [Source:MGI Symbol;Acc:MGI:3611448]	+
43	ENSMUSG00000040481	Bptf	bromodomain PHD finger transcription factor [Source:MGI Symbol;Acc:MGI:2444008]	+
44	ENSMUSG00000040302	C030048B08Rik	RIKEN cDNA C030048B08 gene [Source:MGI Symbol;Acc:MGI:2442653]	+
45	ENSMUSG00000036896	C1qc	complement component 1, q subcomponent, C chain [Source:MGI Symbol;Acc:MGI:88225]	+
46	ENSMUSG00000020196	Cabin1	calcineurin binding protein 1 [Source:MGI Symbol;Acc:MGI:1298375]	-
47	ENSMUSG00000020866	Cacna1g	calcium channel, voltage-dependent, T type, alpha 1G subunit [Source:MGI Symbol;Acc:MGI:1201678]	-
48	ENSMUSG00000044566	Cage1	cancer antigen 1 [Source:MGI Symbol;Acc:MGI:1918463]	-
49	ENSMUSG00000025076	Casp7	caspase 7 [Source:MGI Symbol;Acc:MGI:109383]	+
50	ENSMUSG00000074570	Cass4	Cas scaffolding protein family member 4 [Source:MGI Symbol;Acc:MGI:2444482]	-
51	ENSMUSG00000074570	Cass4	Cas scaffolding protein family member 4 [Source:MGI Symbol;Acc:MGI:2444482]	+
52	ENSMUSG00000038498	Catsper1	cation channel, sperm associated 1 [Source:MGI Symbol;Acc:MGI:2179947]	-
53	ENSMUSG00000040525	Cblc	Casitas B-lineage lymphoma c [Source:MGI Symbol;Acc:MGI:1931457]	+
54	ENSMUSG00000078588	Ccdc24	coiled-coil domain containing 24 [Source:MGI Symbol;Acc:MGI:2685874]	+
55	ENSMUSG00000030577	Cd22	CD22 antigen [Source:MGI Symbol;Acc:MGI:88322]	-
56	ENSMUSG00000033102	Cdc14b	CDC14 cell division cycle 14 homolog B (S. cerevisiae) [Source:MGI Symbol;Acc:MGI:2441808]	-
57	ENSMUSG00000029205	Chrna9	cholinergic receptor, nicotinic, alpha polypeptide 9 [Source:MGI Symbol;Acc:MGI:1202403]	-
58	ENSMUSG00000029205	Chrna9	cholinergic receptor, nicotinic, alpha polypeptide 9 [Source:MGI Symbol;Acc:MGI:1202403]	-
59	ENSMUSG00000050520	Cldn8	claudin 8 [Source:MGI Symbol;Acc:MGI:1859286]	+
60	ENSMUSG00000001829	Clpb	ClpB caseinolytic peptidase B homolog (E. coli) [Source:MGI Symbol;Acc:MGI:1100517]	-
61	ENSMUSG00000025064	Col17a1	collagen, type XVII, alpha 1 [Source:MGI Symbol;Acc:MGI:88450]	-
62	ENSMUSG00000022483	Col2a1	collagen, type II, alpha 1 [Source:MGI Symbol;Acc:MGI:88452]	-

63	ENSMUSG00000029034	Cpsf3l	cleavage and polyadenylation specific factor 3-like [Source:MGI Symbol;Acc:MGI:1919207]	+
64	ENSMUSG00000029625	Cpsf4	cleavage and polyadenylation specific factor 4 [Source:MGI Symbol;Acc:MGI:1861602]	+
65	ENSMUSG00000022723	Crybg3	beta-gamma crystallin domain containing 3 [Source:MGI Symbol;Acc:MGI:2676311]	-
66	ENSMUSG00000037815	Ctnna1	catenin (cadherin associated protein), alpha 1 [Source:MGI Symbol;Acc:MGI:88274]	-
67	ENSMUSG00000026726	Cubn	cubilin (intrinsic factor-cobalamin receptor) [Source:MGI Symbol;Acc:MGI:1931256]	-
68	ENSMUSG00000026726	Cubn	cubilin (intrinsic factor-cobalamin receptor) [Source:MGI Symbol;Acc:MGI:1931256]	-
69	ENSMUSG00000041134	Cyyr1	cysteine and tyrosine-rich protein 1 [Source:MGI Symbol;Acc:MGI:2152187]	-
70	ENSMUSG00000013539	D16H22S680E	DNA segment, Chr 16, human D22S680E, expressed [Source:MGI Symbol;Acc:MGI:101825]	-
71	ENSMUSG00000063455	D630045J12Rik	RIKEN cDNA D630045J12 gene [Source:MGI Symbol;Acc:MGI:2669829]	-
72	ENSMUSG00000030225	Dera	2-deoxyribose-5-phosphate aldolase homolog (C. elegans) [Source:MGI Symbol;Acc:MGI:1913762]	+
73	ENSMUSG00000022209	Dhrs2	dehydrogenase/reductase member 2 [Source:MGI Symbol;Acc:MGI:1918662]	-
74	ENSMUSG00000021094	Dhrs7	dehydrogenase/reductase (SDR family) member 7 [Source:MGI Symbol;Acc:MGI:1913625]	-
75	ENSMUSG00000027655	Dhx35	DEAH (Asp-Glu-Ala-His) box polypeptide 35 [Source:MGI Symbol;Acc:MGI:1918965]	-
76	ENSMUSG00000038060	Dlec1	deleted in lung and esophageal cancer 1 [Source:MGI Symbol;Acc:MGI:2443671]	+
77	ENSMUSG00000033987	Dnahc17	dynein, axonemal, heavy chain 17 [Source:MGI Symbol;Acc:MGI:1917176]	-
78	ENSMUSG00000052273	Dnahc3	dynein, axonemal, heavy chain 3 [Source:MGI Symbol;Acc:MGI:2683040]	-
79	ENSMUSG00000052861	Dnahc6	dynein, axonemal, heavy chain 6 [Source:MGI Symbol;Acc:MGI:107744]	-
80	ENSMUSG00000024963	Dnajc4	DnaJ (Hsp40) homolog, subfamily C, member 4 [Source:MGI Symbol;Acc:MGI:1927346]	-
81	ENSMUSG00000046323	Dppa3	developmental pluripotency-associated 3 [Source:MGI Symbol;Acc:MGI:1920958]	+
82	ENSMUSG00000034467	Dynlrb2	dynein light chain roadblock-type 2 [Source:MGI Symbol;Acc:MGI:1922715]	-
83	ENSMUSG00000042156	Dzip1	DAZ interacting protein 1 [Source:MGI Symbol;Acc:MGI:1914311]	-
84	ENSMUSG00000054116	E130116L18Rik	RIKEN cDNA E130116L18 gene [Source:MGI Symbol;Acc:MGI:1925120]	-
85	ENSMUSG00000050666	E130203B14Rik	RIKEN cDNA E130203B14 gene [Source:MGI Symbol;Acc:MGI:2444633]	-
86	ENSMUSG00000043019	Edem3	ER degradation enhancer, mannosidase alpha-like 3 [Source:MGI Symbol;Acc:MGI:1914217]	-
87	ENSMUSG00000034994	Eef2	eukaryotic translation elongation factor 2 [Source:MGI Symbol;Acc:MGI:95288]	-
88	ENSMUSG00000042961	Egflam	EGF-like, fibronectin type III and laminin G domains [Source:MGI Symbol;Acc:MGI:2146149]	+
89	ENSMUSG00000016554	Eif3d	eukaryotic translation initiation factor 3, subunit D [Source:MGI Symbol;Acc:MGI:1933181]	-
90	ENSMUSG00000022468	Endou	endonuclease, polyU-specific [Source:MGI Symbol;Acc:MGI:97746]	-
91	ENSMUSG00000031483	Erlin2	ER lipid raft associated 2 [Source:MGI Symbol;Acc:MGI:2387215]	-
92	ENSMUSG00000013089	Etv5	ets variant gene 5 [Source:MGI Symbol;Acc:MGI:1096867]	-
93	ENSMUSG00000017897	Eya2	eyes absent 2 homolog (Drosophila) [Source:MGI Symbol;Acc:MGI:109341]	+
94	ENSMUSG00000031444	F10	coagulation factor X [Source:MGI Symbol;Acc:MGI:103107]	+
95	ENSMUSG00000052125	F730043M19Rik	RIKEN cDNA F730043M19 gene [Source:MGI Symbol;Acc:MGI:2443237]	-
96	ENSMUSG00000026153	Fam135a	family with sequence similarity 135, member A [Source:MGI Symbol;Acc:MGI:1915437]	-
97	ENSMUSG00000035420	Fam170a	family with sequence similarity 170, member A [Source:MGI Symbol;Acc:MGI:2684939]	-
98	ENSMUSG00000059187	Fam19a1	family with sequence similarity 19, member A1 [Source:MGI Symbol;Acc:MGI:2443695]	-
99	ENSMUSG00000027751	Fam48a	family with sequence similarity 48, member A [Source:MGI Symbol;Acc:MGI:1929651]	+
100	ENSMUSG00000027654	Fam83d	family with sequence similarity 83, member D [Source:MGI Symbol;Acc:MGI:1919128]	-
101	ENSMUSG00000070047	Fat1	FAT tumor suppressor homolog 1 (Drosophila) [Source:MGI Symbol;Acc:MGI:109168]	+
102	ENSMUSG00000069805	Fbp1	fructose bisphosphatase 1 [Source:MGI Symbol;Acc:MGI:95492]	-
103	ENSMUSG00000030811	Fbxl19	F-box and leucine-rich repeat protein 19 [Source:MGI Symbol;Acc:MGI:3039600]	+
104	ENSMUSG00000059994	Fcrl1	Fc receptor-like 1 [Source:MGI Symbol;Acc:MGI:2442862]	+
105	ENSMUSG00000000183	Fgf6	fibroblast growth factor 6 [Source:MGI Symbol;Acc:MGI:95520]	-
106	ENSMUSG00000036053	Fmnl2	formin-like 2 [Source:MGI Symbol;Acc:MGI:1918659]	-
107	ENSMUSG00000034227	Foxj1	forkhead box J1 [Source:MGI Symbol;Acc:MGI:1347474]	+
108	ENSMUSG00000016552	Foxred2	FAD-dependent oxidoreductase domain containing 2 [Source:MGI Symbol;Acc:MGI:106315]	-
109	ENSMUSG00000044674	Fzd1	frizzled homolog 1 (Drosophila) [Source:MGI Symbol;Acc:MGI:1196625]	+
110	ENSMUSG00000038072	Galnt11	UDP-N-acetyl-alpha-D-galactosamine:polypeptide N-acetylgalactosaminyltransferase 11 [Source:MGI Symbol;Acc:MGI:2444392]	-
111	ENSMUSG00000031608	Galnt7	UDP-N-acetyl-alpha-D-galactosamine: polypeptide N-acetylgalactosaminyltransferase 7 [Source:MGI Symbol;Acc:MGI:1349449]	-
112	ENSMUSG00000074802	Gas2l3	growth arrest-specific 2 like 3 [Source:MGI Symbol;Acc:MGI:1918780]	-
113	ENSMUSG00000023333	Gcm1	glial cells missing homolog 1 (Drosophila) [Source:MGI Symbol;Acc:MGI:108045]	+
114	ENSMUSG00000079260	Glb1	galactosidase, beta 1 [Source:MGI Symbol;Acc:MGI:88151]	-
115	ENSMUSG00000052942	Glis3	GLIS family zinc finger 3 [Source:MGI Symbol;Acc:MGI:2444289]	-
116	ENSMUSG00000000263	Glra1	glycine receptor, alpha 1 subunit [Source:MGI Symbol;Acc:MGI:95747]	-
117	ENSMUSG00000062279	Gm10237	predicted gene 10237 [Source:MGI Symbol;Acc:MGI:3641816]	-
118	ENSMUSG00000069518	Gm10271	predicted gene 10271 [Source:MGI Symbol;Acc:MGI:3642827]	+
119	ENSMUSG00000070528	Gm10297	predicted pseudogene 10297 [Source:MGI Symbol;Acc:MGI:3642512]	-
120	ENSMUSG00000081758	Gm11460	predicted gene 11460 [Source:MGI Symbol;Acc:MGI:3649774]	+
121	ENSMUSG00000083008	Gm12053	predicted gene 12053 [Source:MGI Symbol;Acc:MGI:3652155]	-
122	ENSMUSG00000084006	Gm14245	predicted gene 14245 [Source:MGI Symbol;Acc:MGI:3651254]	-
123	ENSMUSG00000084013	Gm14270	predicted gene 14270 [Source:MGI Symbol;Acc:MGI:3649849]	-
124	ENSMUSG00000081142	Gm15497	predicted gene 15497 [Source:MGI Symbol;Acc:MGI:3782944]	-
125	ENSMUSG00000083772	Gm15566	predicted gene 15566 [Source:MGI Symbol;Acc:MGI:3783015]	-
126	ENSMUSG00000084126	Gm15844	predicted gene 15844 [Source:MGI Symbol;Acc:MGI:3802079]	-
127	ENSMUSG00000062758	Gm16477	predicted pseudogene 16477 [Source:MGI Symbol;Acc:MGI:3646779]	-
128	ENSMUSG00000034057	Gm239	predicted gene 239 [Source:MGI Symbol;Acc:MGI:2685085]	-
129	ENSMUSG00000058174	Gm5148	predicted gene 5148 [Source:MGI Symbol;Acc:MGI:3646006]	-
130	ENSMUSG00000058622	Gm5265	predicted pseudogene 5265 [Source:MGI Symbol;Acc:MGI:3643416]	+
131	ENSMUSG00000067106	Gm5529	predicted pseudogene 5529 [Source:MGI Symbol;Acc:MGI:3646377]	-
132	ENSMUSG00000084218	Gm8145	predicted gene 8145 [Source:MGI Symbol;Acc:MGI:3644272]	-
133	ENSMUSG00000020656	Grhl1	grainyhead-like 1 (Drosophila) [Source:MGI Symbol;Acc:MGI:2182540]	-
134	ENSMUSG00000025421	Hdhd2	haloacid dehalogenase-like hydrolase domain containing 2 [Source:MGI	-

			Symbol;Acc:MGI:1924237]	
135	ENSMUSG00000050244	Heatr1	HEAT repeat containing 1 [Source:MGI Symbol;Acc:MGI:2442524]	-
136	ENSMUSG00000055632	Hmcn2	hemicentin 2 [Source:MGI Symbol;Acc:MGI:2677838]	+
137	ENSMUSG00000007850	Hnrnph1	heterogeneous nuclear ribonucleoprotein H1 [Source:MGI Symbol;Acc:MGI:1891925]	+
138	ENSMUSG00000021538	Il9	interleukin 9 [Source:MGI Symbol;Acc:MGI:96563]	-
139	ENSMUSG00000020227	Irak3	interleukin-1 receptor-associated kinase 3 [Source:MGI Symbol;Acc:MGI:1921164]	+
140	ENSMUSG00000042284	Itga1	integrin alpha 1 [Source:MGI Symbol;Acc:MGI:96599]	+
141	ENSMUSG00000015533	Itga2	integrin alpha 2 [Source:MGI Symbol;Acc:MGI:96600]	+
142	ENSMUSG00000039672	Kcne2	potassium voltage-gated channel, Isk-related subfamily, gene 2 [Source:MGI Symbol;Acc:MGI:1891123]	-
143	ENSMUSG00000034402	Kcnh5	potassium voltage-gated channel, subfamily H (eag-related), member 5 [Source:MGI Symbol;Acc:MGI:3584508]	-
144	ENSMUSG00000030247	Kcnj8	potassium inwardly-rectifying channel, subfamily J, member 8 [Source:MGI Symbol;Acc:MGI:1100508]	-
145	ENSMUSG00000032254	Kif23	kinesin family member 23 [Source:MGI Symbol;Acc:MGI:1919069]	-
146	ENSMUSG00000044294	Krt84	keratin 84 [Source:MGI Symbol;Acc:MGI:96700]	-
147	ENSMUSG00000050239	Krtap24-1	keratin associated protein 24-1 [Source:MGI Symbol;Acc:MGI:2685158]	+
148	ENSMUSG00000056706	Krtap7-1	keratin associated protein 7-1 [Source:MGI Symbol;Acc:MGI:1918613]	-
149	ENSMUSG00000043501	Lgals2	lectin, galactose-binding, soluble 2 [Source:MGI Symbol;Acc:MGI:895068]	-
150	ENSMUSG00000057554	Lgals8	lectin, galactose binding, soluble 8 [Source:MGI Symbol;Acc:MGI:1928481]	-
151	ENSMUSG00000033794	Lpcat2b	lysophosphatidylcholine acyltransferase 2B [Source:MGI Symbol;Acc:MGI:1918152]	+
152	ENSMUSG00000028184	Lphn2	latrophilin 2 [Source:MGI Symbol;Acc:MGI:2139714]	-
153	ENSMUSG00000020593	Lpin1	lipin 1 [Source:MGI Symbol;Acc:MGI:1891340]	-
154	ENSMUSG00000024120	Lrpprc	leucine-rich PPR-motif containing [Source:MGI Symbol;Acc:MGI:1919666]	-
155	ENSMUSG00000026765	Lypd6b	LY6/PLAUR domain containing 6B [Source:MGI Symbol;Acc:MGI:1919147]	-
156	ENSMUSG00000055435	Maf	avian musculoaponeurotic fibrosarcoma (v-maf) AS42 oncogene homolog [Source:MGI Symbol;Acc:MGI:96909]	-
157	ENSMUSG00000056972	Magel2	melanoma antigen, family L, 2 [Source:MGI Symbol;Acc:MGI:1351648]	+
158	ENSMUSG00000024863	Mbl2	mannose-binding lectin (protein C) 2 [Source:MGI Symbol;Acc:MGI:96924]	-
159	ENSMUSG00000041607	Mbp	myelin basic protein [Source:MGI Symbol;Acc:MGI:96925]	+
160	ENSMUSG00000025956	Mettl21a	methyltransferase like 21A [Source:MGI Symbol;Acc:MGI:1914349]	-
161	ENSMUSG00000054612	Mgmt	O-6-methylguanine-DNA methyltransferase [Source:MGI Symbol;Acc:MGI:96977]	-
162	ENSMUSG00000054612	Mgmt	O-6-methylguanine-DNA methyltransferase [Source:MGI Symbol;Acc:MGI:96977]	+
163	ENSMUSG00000065464	Mir185	microRNA 185 [Source:MGI Symbol;Acc:MGI:2676849]	-
164	ENSMUSG00000005417	Mprip	myosin phosphatase Rho interacting protein [Source:MGI Symbol;Acc:MGI:1349438]	+
165	ENSMUSG00000052727	Mtap1b	microtubule-associated protein 1B [Source:MGI Symbol;Acc:MGI:1306778]	+
166	ENSMUSG00000031698	Mylk3	myosin light chain kinase 3 [Source:MGI Symbol;Acc:MGI:2443063]	-
167	ENSMUSG00000024049	Myom1	myomesin 1 [Source:MGI Symbol;Acc:MGI:1341430]	-
168	ENSMUSG00000041794	Myrip	myosin VIIA and Rab interacting protein [Source:MGI Symbol;Acc:MGI:2384407]	-
169	ENSMUSG00000035121	Neil2	nei like 2 (E. coli) [Source:MGI Symbol;Acc:MGI:2686058]	+
170	ENSMUSG00000056749	Nfil3	nuclear factor, interleukin 3, regulated [Source:MGI Symbol;Acc:MGI:109495]	+
171	ENSMUSG00000038146	Notch3	Notch gene homolog 3 (Drosophila) [Source:MGI Symbol;Acc:MGI:99460]	-
172	ENSMUSG00000065771	n-R5s54	nuclear encoded rRNA 5S 54 [Source:MGI Symbol;Acc:MGI:4421899]	+
173	ENSMUSG00000032311	Nrg4	neuregulin 4 [Source:MGI Symbol;Acc:MGI:1933833]	-
174	ENSMUSG00000059974	Ntm	neurotrimin [Source:MGI Symbol;Acc:MGI:2446259]	+
175	ENSMUSG00000054200	O3far1	omega-3 fatty acid receptor 1 [Source:MGI Symbol;Acc:MGI:2147577]	-
176	ENSMUSG00000026790	Odf2	outer dense fiber of sperm tails 2 [Source:MGI Symbol;Acc:MGI:1098824]	+
177	ENSMUSG00000022026	Olfm4	olfactomedin 4 [Source:MGI Symbol;Acc:MGI:2685142]	+
178	ENSMUSG00000047286	Olfr370	olfactory receptor 370 [Source:MGI Symbol;Acc:MGI:3030204]	-
179	ENSMUSG00000043948	Olfr691	olfactory receptor 691 [Source:MGI Symbol;Acc:MGI:3030525]	-
180	ENSMUSG00000045306	Olfr734	olfactory receptor 734 [Source:MGI Symbol;Acc:MGI:3030568]	-
181	ENSMUSG00000043964	Orai3	ORAI calcium release-activated calcium modulator 3 [Source:MGI Symbol;Acc:MGI:3039586]	+
182	ENSMUSG00000020051	Pah	phenylalanine hydroxylase [Source:MGI Symbol;Acc:MGI:97473]	-
183	ENSMUSG00000034422	Parp14	poly (ADP-ribose) polymerase family, member 14 [Source:MGI Symbol;Acc:MGI:1919489]	+
184	ENSMUSG00000063687	Pcdhb5	protocadherin beta 5 [Source:MGI Symbol;Acc:MGI:2136739]	-
185	ENSMUSG00000048371	Pdp2	pyruvate dehyrogenase phosphatase catalytic subunit 2 [Source:MGI Symbol;Acc:MGI:1918878]	+
186	ENSMUSG00000047652	Pea15b	phosphoprotein enriched in astrocytes 15B [Source:MGI Symbol;Acc:MGI:3525016]	-
187	ENSMUSG00000005907	Pex1	peroxisomal biogenesis factor 1 [Source:MGI Symbol;Acc:MGI:1918632]	+
188	ENSMUSG00000003464	Pex19	peroxisomal biogenesis factor 19 [Source:MGI Symbol;Acc:MGI:1334458]	+
189	ENSMUSG00000007946	Phox2a	paired-like homeobox 2a [Source:MGI Symbol;Acc:MGI:106633]	-
190	ENSMUSG00000055108	Phxr2	per-hexamer repeat gene 2 [Source:MGI Symbol;Acc:MGI:104524]	+
191	ENSMUSG00000023791	Pigx	phosphatidylinositol glycan anchor biosynthesis, class X [Source:MGI Symbol;Acc:MGI:1919334]	-
192	ENSMUSG00000024014	Pim1	proviral integration site 1 [Source:MGI Symbol;Acc:MGI:97584]	+
193	ENSMUSG00000031903	Pla2g15	phospholipase A2, group XV [Source:MGI Symbol;Acc:MGI:2178076]	+
194	ENSMUSG00000058908	Pla2g2a	phospholipase A2, group IIA (platelets, synovial fluid) [Source:MGI Symbol;Acc:MGI:104642]	-
195	ENSMUSG00000041193	Pla2g5	phospholipase A2, group V [Source:MGI Symbol;Acc:MGI:101899]	-
196	ENSMUSG00000002733	Plekha3	pleckstrin homology domain-containing, family A (phosphoinositide binding specific) member 3 [Source:MGI Symbol;Acc:MGI:1932515]	-
197	ENSMUSG00000002733	Plekha3	pleckstrin homology domain-containing, family A (phosphoinositide binding specific) member 3 [Source:MGI Symbol;Acc:MGI:1932515]	+
198	ENSMUSG00000018217	Pmp22	peripheral myelin protein 22 [Source:MGI Symbol;Acc:MGI:97631]	+
199	ENSMUSG00000019952	Poc1b	POC1 centriolar protein homolog B (Chlamydomonas) [Source:MGI Symbol;Acc:MGI:1918511]	+
200	ENSMUSG00000038425	Poli	polymerase (DNA directed), iota [Source:MGI Symbol;Acc:MGI:1347081]	-
201	ENSMUSG00000016982	Pom121l2	POM121 membrane glycoprotein-like 2 (rat) [Source:MGI Symbol;Acc:MGI:2684870]	+
202	ENSMUSG00000002588	Pon1	paraoxonase 1 [Source:MGI Symbol;Acc:MGI:103295]	+
203	ENSMUSG00000016487	Ppfibp1	PTPRF interacting protein, binding protein 1 (liprin beta 1) [Source:MGI Symbol;Acc:MGI:1914783]	-

204	ENSMUSG00000022771	Ppil2	peptidylprolyl isomerase (cyclophilin)-like 2 [Source:MGI Symbol;Acc:MGI:2447857]	-
205	ENSMUSG00000002930	Ppp1r17	protein phosphatase 1, regulatory subunit 17 [Source:MGI Symbol;Acc:MGI:1333876]	+
206	ENSMUSG00000032827	Ppp1r9a	protein phosphatase 1, regulatory (inhibitor) subunit 9A [Source:MGI Symbol;Acc:MGI:2442401]	+
207	ENSMUSG00000031445	Proz	protein Z, vitamin K-dependent plasma glycoprotein [Source:MGI Symbol;Acc:MGI:1860488]	+
208	ENSMUSG00000039449	Prpf18	PRP18 pre-mRNA processing factor 18 homolog (yeast) [Source:MGI Symbol;Acc:MGI:1914479]	+
209	ENSMUSG00000061136	Prpf40a	PRP40 pre-mRNA processing factor 40 homolog A (yeast) [Source:MGI Symbol;Acc:MGI:1860512]	-
210	ENSMUSG00000050762	Prss27	protease, serine, 27 [Source:MGI Symbol;Acc:MGI:2450123]	+
211	ENSMUSG00000044664	Prss42	protease, serine, 42 [Source:MGI Symbol;Acc:MGI:2665280]	-
212	ENSMUSG00000030465	Psd3	pleckstrin and Sec7 domain containing 3 [Source:MGI Symbol;Acc:MGI:1918215]	+
213	ENSMUSG00000030603	Psmc4	proteasome (prosome, macropain) 26S subunit, ATPase, 4 [Source:MGI Symbol;Acc:MGI:1346093]	+
214	ENSMUSG00000034573	Ptpn13	protein tyrosine phosphatase, non-receptor type 13 [Source:MGI Symbol;Acc:MGI:103293]	-
215	ENSMUSG00000034573	Ptpn13	protein tyrosine phosphatase, non-receptor type 13 [Source:MGI Symbol;Acc:MGI:103293]	-
216	ENSMUSG00000028149	Rap1gds1	RAP1, GTP-GDP dissociation stimulator 1 [Source:MGI Symbol;Acc:MGI:2385189]	+
217	ENSMUSG00000022951	Rcan1	regulator of calcineurin 1 [Source:MGI Symbol;Acc:MGI:1890564]	+
218	ENSMUSG00000040121	Rep15	RAB15 effector protein [Source:MGI Symbol;Acc:MGI:1913782]	-
219	ENSMUSG00000024143	Rhoq	ras homolog gene family, member Q [Source:MGI Symbol;Acc:MGI:1931553]	+
220	ENSMUSG00000021428	Riok1	RIO kinase 1 (yeast) [Source:MGI Symbol;Acc:MGI:1918590]	-
221	ENSMUSG00000039328	Rnf122	ring finger protein 122 [Source:MGI Symbol;Acc:MGI:1916117]	-
222	ENSMUSG00000052949	Rnf157	ring finger protein 157 [Source:MGI Symbol;Acc:MGI:2442484]	+
223	ENSMUSG00000058761	Rnf169	ring finger protein 169 [Source:MGI Symbol;Acc:MGI:1920257]	-
224	ENSMUSG00000032850	Rnft2	ring finger protein, transmembrane 2 [Source:MGI Symbol;Acc:MGI:2442859]	+
225	ENSMUSG00000061684	Rpl21-ps8	ribosomal protein L21, pseudogene 8 [Source:MGI Symbol;Acc:MGI:3648345]	+
226	ENSMUSG00000078126	Rpl23a-ps3	ribosomal protein L23A, pseudogene 3 [Source:MGI Symbol;Acc:MGI:3781353]	-
227	ENSMUSG00000070519	Rpl35a-ps6	ribosomal protein L35A, pseudogene 6 [Source:MGI Symbol;Acc:MGI:3704258]	-
228	ENSMUSG00000026727	Rsu1	Ras suppressor protein 1 [Source:MGI Symbol;Acc:MGI:103040]	-
229	ENSMUSG00000032417	Rwdd2a	RWD domain containing 2A [Source:MGI Symbol;Acc:MGI:1916769]	-
230	ENSMUSG00000032511	Scn5a	sodium channel, voltage-gated, type V, alpha [Source:MGI Symbol;Acc:MGI:98251]	-
231	ENSMUSG00000023030	Slc11a2	solute carrier family 11 (proton-coupled divalent metal ion transporters), member 2 [Source:MGI Symbol;Acc:MGI:1345279]	-
232	ENSMUSG00000059336	Slc14a1	solute carrier family 14 (urea transporter), member 1 [Source:MGI Symbol;Acc:MGI:1351654]	-
233	ENSMUSG00000027359	Slc27a2	solute carrier family 27 (fatty acid transporter), member 2 [Source:MGI Symbol;Acc:MGI:1347099]	+
234	ENSMUSG00000026614	Slc30a10	solute carrier family 30, member 10 [Source:MGI Symbol;Acc:MGI:2685058]	-
235	ENSMUSG00000030089	Slc41a3	solute carrier family 41, member 3 [Source:MGI Symbol;Acc:MGI:1918949]	-
236	ENSMUSG00000079020	Slc45a4	solute carrier family 45, member 4 [Source:MGI Symbol;Acc:MGI:2146236]	+
237	ENSMUSG00000031904	Slc7a6	solute carrier family 7 (cationic amino acid transporter, y+ system), member 6 [Source:MGI Symbol;Acc:MGI:2142598]	+
238	ENSMUSG00000001158	Snrnp27	small nuclear ribonucleoprotein 27 (U4/U6.U5) [Source:MGI Symbol;Acc:MGI:1913868]	+
239	ENSMUSG00000020867	Spata20	spermatogenesis associated 20 [Source:MGI Symbol;Acc:MGI:2183449]	-
240	ENSMUSG00000005233	Spc25	SPC25, NDC80 kinetochore complex component, homolog (S. cerevisiae) [Source:MGI Symbol;Acc:MGI:1913692]	-
241	ENSMUSG00000046957	Spz1	spermatogenic leucine zipper 1 [Source:MGI Symbol;Acc:MGI:1930801]	+
242	ENSMUSG00000030224	Strap	serine/threonine kinase receptor associated protein [Source:MGI Symbol;Acc:MGI:1329037]	+
243	ENSMUSG00000027882	Stxbp3a	syntaxin binding protein 3A [Source:MGI Symbol;Acc:MGI:107362]	-
244	ENSMUSG00000030101	Sumf1	sulfatase modifying factor 1 [Source:MGI Symbol;Acc:MGI:1889844]	-
245	ENSMUSG00000030554	Synm	synemin, intermediate filament protein [Source:MGI Symbol;Acc:MGI:2661187]	-
246	ENSMUSG00000024985	Tcf7l2	transcription factor 7 like 2, T cell specific, HMG box [Source:MGI Symbol;Acc:MGI:1202879]	+
247	ENSMUSG00000024613	Tcof1	Treacher Collins Franceschetti syndrome 1, homolog [Source:MGI Symbol;Acc:MGI:892003]	-
248	ENSMUSG00000023949	Tcte1	t-complex-associated testis expressed 1 [Source:MGI Symbol;Acc:MGI:98640]	+
249	ENSMUSG00000021953	Tdh	L-threonine dehydrogenase [Source:MGI Symbol;Acc:MGI:1926231]	-
250	ENSMUSG00000037705	Tecta	tectorin alpha [Source:MGI Symbol;Acc:MGI:109575]	+
251	ENSMUSG00000029287	Tgfbr3	transforming growth factor, beta receptor III [Source:MGI Symbol;Acc:MGI:104637]	-
252	ENSMUSG00000029829	Tmem213	transmembrane protein 213 [Source:MGI Symbol;Acc:MGI:1924772]	-
253	ENSMUSG00000079580	Tmem217	transmembrane protein 217 [Source:MGI Symbol;Acc:MGI:3646280]	-
254	ENSMUSG00000076860	Trav17	T cell receptor alpha variable 17 [Source:MGI Symbol;Acc:MGI:3702128]	-
255	ENSMUSG00000051747	Ttn	titin [Source:MGI Symbol;Acc:MGI:98864]	-
256	ENSMUSG00000051747	Ttn	titin [Source:MGI Symbol;Acc:MGI:98864]	+
257	ENSMUSG00000043262	Uevld	UEV and lactate/malate dehyrogenase domains [Source:MGI Symbol;Acc:MGI:1860490]	-
258	ENSMUSG00000040936	Ulk4	unc-51-like kinase 4 (C. elegans) [Source:MGI Symbol;Acc:MGI:1921622]	-
259	ENSMUSG00000028963	Uts2	urotensin 2 [Source:MGI Symbol;Acc:MGI:1346329]	-
260	ENSMUSG00000024962	Vegfb	vascular endothelial growth factor B [Source:MGI Symbol;Acc:MGI:106199]	-
261	ENSMUSG00000035284	Vps13c	vacuolar protein sorting 13C (yeast) [Source:MGI Symbol;Acc:MGI:2444207]	+
262	ENSMUSG00000024312	Wdr46	WD repeat domain 46 [Source:MGI Symbol;Acc:MGI:1931871]	-
263	ENSMUSG00000029442	Wdr66	WD repeat domain 66 [Source:MGI Symbol;Acc:MGI:1918495]	-
264	ENSMUSG00000031563	Wwc2	WW, C2 and coiled-coil domain containing 2 [Source:MGI Symbol;Acc:MGI:1261872]	-
265	ENSMUSG00000026469	Xpr1	xenotropic and polytropic retrovirus receptor 1 [Source:MGI Symbol;Acc:MGI:97932]	+
266	ENSMUSG00000034333	Zbed4	zinc finger, BED domain containing 4 [Source:MGI Symbol;Acc:MGI:2682302]	-
267	ENSMUSG00000038872	Zfhx3	zinc finger homeobox 3 [Source:MGI Symbol;Acc:MGI:99948]	-
268	ENSMUSG00000038872	Zfhx3	zinc finger homeobox 3 [Source:MGI Symbol;Acc:MGI:99948]	-
269	ENSMUSG00000050919	Zfp366	zinc finger protein 366 [Source:MGI Symbol;Acc:MGI:2178429]	+
270	ENSMUSG00000024420	Zfp521	zinc finger protein 521 [Source:MGI Symbol;Acc:MGI:95459]	-

271	ENSMUSG00000058291	Zfp68	zinc finger protein 68 [Source:MGI Symbol;Acc:MGI:1344427]	-
272	ENSMUSG00000000823	Znf512b	zinc finger protein 512B [Source:MGI Symbol;Acc:MGI:2685478]	-
273	ENSMUSG00000064629		U6 spliceosomal RNA [Source:RFAM;Acc:RF00026]	-
274	ENSMUSG00000076190			-
275	ENSMUSG00000077526		Small nucleolar RNA SNORA65 [Source:RFAM;Acc:RF00302]	-
276	ENSMUSG00000084706		7SK RNA [Source:RFAM;Acc:RF00100]	-

5.1.7 WTPS good performers in the FST versus all WTC

All genes that have a FC < 1.5 and a p-value < 0.01 are shown. ID: Affymetrix ID; EFFECT: direction of effect; “+”: gene expression upregulated in the WTPS good performers versus WT control mice; “-“: downregulated in WTPS good performers versus WT control mice; FC: fold-change in mRNA expression. Genes have been ordered alphabetically.

FC<1.5; p<0.01

#	ID	SYMBOL	GENENAME	Effect	FC	P.Value
1	1447218_at	1110003F02Rik	RIKEN cDNA 1110003F02 gene	+	1,6	0,002
2	1438288_x_at	1110059G02Rik	RIKEN cDNA 1110059G02 gene	+	1,6	0,003
3	1436203_a_at	1110059G02Rik	RIKEN cDNA 1110059G02 gene	+	1,6	0,004
4	1422722_at	1700001K19Rik	RIKEN cDNA 1700001K19 gene	+	1,7	0,005
5	1428984_a_at	1700012B09Rik	RIKEN cDNA 1700012B09 gene	+	2,1	0,004
6	1432528_at	1700021P04Rik	RIKEN cDNA 1700021P04 gene	-	2,0	0,002
7	1453320_at	1700027A23Rik	RIKEN cDNA 1700027A23 gene	+	2,3	0,005
8	1447798_at	1700123O21Rik	RIKEN cDNA 1700123O21 gene	+	2,6	0,001
9	1430991_at	1810014B01Rik	RIKEN cDNA 1810014B01 gene	+	1,6	0,008
10	1441252_at	2010001A14Rik	RIKEN cDNA 2010001A14 gene	-	1,5	0,003
11	1447576_at	2010001K21Rik	RIKEN cDNA 2010001K21 gene	+	1,6	0,003
12	1425147_at	2410075B13Rik	RIKEN cDNA 2410075B13 gene	-	1,6	0,005
13	1453519_at	2610037D02Rik	RIKEN cDNA 2610037D02 gene	+	1,5	0,004
14	1452979_at	2610110G12Rik	RIKEN cDNA 2610110G12 gene	-	1,6	0,001
15	1431912_at	2700089I24Rik	RIKEN cDNA 2700089I24 gene	-	1,5	0,002
16	1432758_at	2900011L18Rik	RIKEN cDNA 2900011L18 gene	+	1,6	0,008
17	1445673_at	2900052N01Rik	RIKEN cDNA 2900052N01 gene	+	1,5	0,009
18	1420820_at	2900073G15Rik	RIKEN cDNA 2900073G15 gene	+	1,5	0,008
19	1430691_at	4632411P08Rik	RIKEN cDNA 4632411P08 gene	+	1,6	0,009
20	1433142_at	4921504P05Rik	RIKEN cDNA 4921504P05 gene	+	1,6	0,006
21	1433404_at	4930423O20Rik	RIKEN cDNA 4930423O20 gene	+	1,6	0,003
22	1431954_x_at	4930431C11Rik	RIKEN cDNA 4930431C11 gene	+	1,7	0,003
23	1433136_at	4930432H08Rik	RIKEN cDNA 4930432H08 gene	+	1,7	0,003
24	1430727_at	4930432O21Rik	RIKEN cDNA 4930432O21 gene	+	1,9	0,003
25	1454135_at	4930458K08Rik	RIKEN cDNA 4930458K08 gene	+	2,0	0,003
26	1433320_at	4930519N06Rik	RIKEN cDNA 4930519N06 gene	+	1,5	0,003
27	1453828_at	4932422M17Rik	RIKEN cDNA 4932422M17 gene	+	1,6	0,001
28	1460539_at	4933404K13Rik	RIKEN cDNA 4933404K13 gene	+	1,6	0,002
29	1453873_at	4933421H06Rik	RIKEN cDNA 4933421H06 gene	+	1,7	0,008
30	1446883_at	4933427D06Rik	RIKEN cDNA 4933427D06 gene	+	1,7	0,003
31	1433386_at	4933428C20Rik	RIKEN cDNA 4933428C20 gene	+	1,6	0,001
32	1431571_at	4933437I04Rik	RIKEN cDNA 4933437I04 gene	-	1,7	0,004
33	1431473_at	5330423I11Rik	RIKEN cDNA 5330423I11 gene	-	1,7	0,002
34	1429208_at	5730408K05Rik	RIKEN cDNA 5730408K05 gene	+	2,0	0,003
35	1433376_at	5830445D09Rik	RIKEN cDNA 5830445D09 gene	+	1,5	0,002
36	1454482_at	5830474E16Rik	RIKEN cDNA 5830474E16 gene	+	1,7	0,003
37	1454425_at	5830495A06Rik	RIKEN cDNA 5830495A06 gene	+	1,5	0,008
38	1460522_at	6030458E02Rik	RIKEN cDNA 6030458E02 gene	+	1,7	0,000
39	1433807_at	6720463M24Rik	RIKEN cDNA 6720463M24 gene	-	1,6	0,006
40	1444797_at	8030474K03Rik	RIKEN cDNA 8030474K03 gene	+	1,6	0,004
41	1432241_at	9030205G03Rik	RIKEN cDNA 9030205G03 gene	-	1,7	0,004
42	1441179_at	9530020O07Rik	RIKEN cDNA 9530020O07 gene	+	1,6	0,002
43	1443127_at	9630021D06Rik	RIKEN cDNA 9630021D06 gene	-	2,0	0,003
44	1432212_at	A1cf	APOBEC1 complementation factor	+	1,6	0,004
45	1457461_at	A630039O03Rik	RIKEN cDNA A630039O03 gene	+	3,1	0,001
46	1446519_at	A730091E23Rik	RIKEN cDNA A730091E23 gene	+	1,6	0,009
47	1459349_at	A930011G23Rik	RIKEN cDNA A930011G23 gene	-	1,6	0,001
48	1446463_at	Adnp2	ADNP homeobox 2	+	1,5	0,004
49	1438716_at	AI451617	expressed sequence AI451617	+	1,7	0,001
50	1428785_at	Amotl1	angiomotin-like 1	+	1,6	0,004
51	1451867_x_at	Arhgap6	Rho GTPase activating protein 6	-	1,9	0,002
52	1452304_a_at	Arhgef5	Rho guanine nucleotide exchange factor (GEF) 5	+	1,5	0,009
53	1441144_at	Arr3	arrestin 3, retinal	+	1,6	0,003
54	1427759_a_at	Art5	ADP-ribosyltransferase 5	+	1,6	0,002

55	1418774_a_at	Atp7a	ATPase, Cu++ transporting, alpha polypeptide	+	1,7	0,004
56	1457752_at	AU014876	expressed sequence AU014876	+	1,5	0,004
57	1418604_at	Avpr1a	arginine vasopressin receptor 1A	+	1,8	0,001
58	1456295_at	B230114P17Rik	RIKEN cDNA B230114P17 gene	+	1,6	0,002
59	1436585_at	BB182297	expressed sequence BB182297	-	1,5	0,003
60	1437262_x_at	Bcas2	breast carcinoma amplified sequence 2	+	1,8	0,005
61	1424814_a_at	Bcl2l14	BCL2-like 14 (apoptosis facilitator)	+	2,1	0,007
62	1450624_at	Bhmt	betaine-homocysteine methyltransferase	+	1,9	0,007
63	1439329_a_at	Brsk2	BR serine/threonine kinase 2	+	1,9	0,008
64	1440881_at	Brwd3	bromodomain and WD repeat domain containing 3	+	1,5	0,005
65	1454342_at	C030007D22Rik	RIKEN cDNA C030007D22 gene	+	1,5	0,008
66	1439194_at	C030048H21Rik	RIKEN cDNA C030048H21 gene	+	1,5	0,007
67	1455416_at	C130021I20Rik	Riken cDNA C130021I20 gene	+	1,7	0,002
68	1445890_at	C230079E05Rik	RIKEN cDNA C230079E05 gene	+	1,7	0,001
69	1441279_at	C430002E04Rik	RIKEN cDNA C430002E04 gene	+	1,5	0,008
70	1440510_at	C430002N11Rik	RIKEN cDNA C430002N11 gene	+	1,6	0,003
71	1447182_at	C77815	expressed sequence C77815	-	1,6	0,003
72	1446941_at	C78505	expressed sequence C78505	+	1,6	0,007
73	1447762_x_at	Car12	carbonic anyhydrase 12	+	1,9	0,007
74	1433607_at	Cbln4	cerebellin 4 precursor protein	-	1,6	0,006
75	1432628_at	Cbx3	chromobox homolog 3 (Drosophila HP1 gamma)	+	1,8	0,001
76	1427657_at	Ccdc134	coiled-coil domain containing 134	+	1,5	0,007
77	1442573_at	Ccdc76	coiled-coil domain containing 76	+	1,5	0,007
78	1417925_at	Ccl22	chemokine (C-C motif) ligand 22	+	1,6	0,002
79	1423760_at	Cd44	CD44 antigen	-	1,7	0,004
80	1427095_at	Cdcp1	CUB domain containing protein 1	+	1,7	0,002
81	1460045_at	Cdh7	cadherin 7, type 2	-	1,7	0,003
82	1424845_a_at	Cep68	centrosomal protein 68	-	1,9	0,000
83	1447214_at	Chrna9	cholinergic receptor, nicotinic, alpha polypeptide 9	+	1,6	0,003
84	1456911_at	Clasp2	CLIP associating protein 2	-	1,8	0,001
85	1418283_at	Cldn4	claudin 4	+	1,6	0,009
86	1417845_at	Cldn6	claudin 6	+	1,8	0,004
87	1439427_at	Cldn9	claudin 9	+	1,7	0,007
88	1416541_at	Clpb	ClpB caseinolytic peptidase B homolog (E. coli)	-	1,5	0,002
89	1418237_s_at	Col18a1	collagen, type XVIII, alpha 1	+	1,5	0,004
90	1440911_at	Col23a1	collagen, type XXIII, alpha 1	-	1,5	0,009
91	1425772_at	Col4a4	collagen, type IV, alpha 4	+	1,6	0,004
92	1452250_a_at	Col6a2	collagen, type VI, alpha 2	-	1,7	0,007
93	1420280_x_at	Col9a3	collagen, type IX, alpha 3	+	2,8	0,009
94	1433715_at	Cpne7	copine VII	-	1,5	0,001
95	1418930_at	Cxcl10	chemokine (C-X-C motif) ligand 10	+	2,8	0,006
96	1436467_at	D230004N17Rik	RIKEN cDNA D230004N17 gene	-	1,6	0,006
97	1445183_s_at	D7Ertd523e	DNA segment, Chr 7, ERATO Doi 523, expressed	+	1,5	0,003
98	1457905_at	D7Ertd59e	DNA segment, Chr 7, ERATO Doi 59, expressed	+	2,1	0,008
99	1444014_at	D830025C05Rik	RIKEN cDNA D830025C05 gene	-	1,7	0,005
100	1423805_at	Dab2	disabled homolog 2 (Drosophila)	+	1,8	0,002
101	1421864_at	Dbil5	diazepam binding inhibitor-like 5	+	1,6	0,007
102	1443525_at	Dbx2	developing brain homeobox 2	-	1,5	0,002
103	1441503_at	Dcdc2a	doublecortin domain containing 2a	+	2,1	0,003
104	1449368_at	Dcn	decorin	-	1,5	0,002
105	1418028_at	Dct	dopachrome tautomerase	+	2,1	0,001
106	1422037_at	Dlx3	distal-less homeobox 3	+	1,7	0,005
107	1438763_at	Dnahc2	dynein, axonemal, heavy chain 2	+	1,6	0,003
108	1436296_x_at	Dnaic2	dynein, axonemal, intermediate chain 2	+	1,7	0,001
109	1420221_at	Dnajc21	DnaJ (Hsp40) homolog, subfamily C, member 21	+	1,6	0,001
110	1452638_s_at	Dnm1l	dynamin 1-like	-	1,6	0,004
111	1422641_at	Dok5	docking protein 5	-	1,5	0,005
112	1422830_s_at	Drd4	dopamine receptor 4	+	1,6	0,008
113	1436111_at	E030011K20Rik	RIKEN cDNA E030011K20 gene	+	1,5	0,006
114	1443677_at	E030011O05Rik	RIKEN cDNA E030011O05 gene	+	1,5	0,005
115	1442768_at	E130112L23Rik	RIKEN cDNA E130112L23 gene	+	1,6	0,003
116	1433798_a_at	E330034G19Rik	RIKEN cDNA E330034G19 gene	+	1,5	0,003
117	1422586_at	Ecel1	endothelin converting enzyme-like 1	-	1,8	0,001
118	1441924_x_at	Edn3	endothelin 3	+	2,1	0,005
119	1447760_x_at	Ehf	ets homologous factor	+	1,7	0,003
120	1420491_at	Eif2s1	eukaryotic translation initiation factor 2, subunit 1 alpha	+	1,7	0,003
121	1417563_at	Eif4ebp1	eukaryotic translation initiation factor 4E binding protein 1	+	1,6	0,007
122	1416916_at	Elf3	E74-like factor 3	+	1,6	0,004
123	1445886_at	Elk3	ELK3, member of ETS oncogene family	-	1,6	0,002
124	1434489_at	Elmo3	engulfment and cell motility 3, ced-12 homolog (C. elegans)	+	1,6	0,005
125	1441891_x_at	Elovl7	ELOVL family member 7, elongation of long chain fatty acids (yeast)	+	2,8	0,002
126	1441091_at	Elovl7	ELOVL family member 7, elongation of long chain fatty acids (yeast)	+	2,5	0,001
127	1424098_at	Elovl7	ELOVL family member 7, elongation of long chain fatty acids (yeast)	+	2,3	0,002
128	1424097_at	Elovl7	ELOVL family member 7, elongation of long chain fatty acids (yeast)	+	2,2	0,002
129	1440354_at	Elovl7	ELOVL family member 7, elongation of long chain fatty acids (yeast)	+	2,1	0,004
130	1440312_at	Elovl7	ELOVL family member 7, elongation of long chain fatty acids (yeast)	+	2,0	0,000
131	1425353_at	Enpp3	ectonucleotide pyrophosphatase/phosphodiesterase 3	-	1,5	0,003
132	1424765_at	Eps15l1	epidermal growth factor receptor pathway substrate 15-like 1	+	1,6	0,001
133	1449280_at	Esm1	endothelial cell-specific molecule 1	+	1,5	0,005
134	1422027_a_at	Ets1	E26 avian leukemia oncogene 1, 5' domain	+	1,8	0,001
135	1436374_x_at	F11r	F11 receptor	+	1,7	0,003
136	1429889_at	Faim3	Fas apoptotic inhibitory molecule 3	+	1,6	0,004

137	1436685_at	Fam181a	family with sequence similarity 181, member A	+	1,6	0,001
138	1437137_at	Fam70a	family with sequence similarity 70, member A	-	1,9	0,001
139	1436948_a_at	Fam70a	family with sequence similarity 70, member A	-	1,6	0,006
140	1452513_a_at	Fanca	Fanconi anemia, complementation group A	+	1,6	0,005
141	1417552_at	Fap	fibroblast activation protein	+	2,5	0,006
142	1438954_x_at	Figf	c-fos induced growth factor	-	1,7	0,002
143	1455280_at	Frem1	Fras1 related extracellular matrix protein 1	+	1,8	0,007
144	1417343_at	Fxyd6	FXYD domain-containing ion transport regulator 6	-	1,5	0,005
145	1455443_at	Gdap1l1	ganglioside-induced differentiation-associated protein 1-like 1	-	1,6	0,002
146	1460613_x_at	Gh	growth hormone	-	128,6	0,005
147	1437522_x_at	Gh	growth hormone	-	92,3	0,007
148	1456595_x_at	Gh	growth hormone	-	89,7	0,007
149	1445790_at	Gipr	gastric inhibitory polypeptide receptor	+	1,5	0,009
150	1445523_at	Gje1	gap junction membrane channel protein epsilon 1	+	1,6	0,002
151	1457429_s_at	Gm106	predicted gene 106	+	2,0	0,006
152	1442089_at	Gm11563	predicted gene 11563	+	1,6	0,008
153	1453869_at	Gm5085	predicted gene 5085	-	1,6	0,002
154	1437703_at	Gm5164	predicted gene 5164	+	1,5	0,008
155	1438768_at	Gm7544	predicted gene 7544	+	1,5	0,009
156	1457555_at	Gpr151	G protein-coupled receptor 151	+	2,9	0,003
157	1460275_at	Gpr3	G-protein coupled receptor 3	-	1,8	0,001
158	1417894_at	Gpr97	G protein-coupled receptor 97	+	1,5	0,007
159	1435722_at	Gria4	glutamate receptor, ionotropic, AMPA4 (alpha 4)	-	1,6	0,008
160	1435290_x_at	H2-Aa	histocompatibility 2, class II antigen A, alpha	+	2,9	0,002
161	1438858_x_at	H2-Aa	histocompatibility 2, class II antigen A, alpha	+	2,3	0,000
162	1452431_s_at	H2-Aa	histocompatibility 2, class II antigen A, alpha	+	2,2	0,001
163	1451721_a_at	H2-Ab1	histocompatibility 2, class II antigen A, beta 1	+	2,2	0,000
164	1450648_s_at	H2-Ab1	histocompatibility 2, class II antigen A, beta 1	+	2,0	0,000
165	1448716_at	Hba-x	hemoglobin X, alpha-like embryonic chain in Hba complex	+	1,9	0,004
166	1419407_at	Hc	hemolytic complement	+	1,7	0,002
167	1454713_s_at	Hdc	histidine decarboxylase	+	1,5	0,003
168	1448812_at	Hpcal1	hippocalcin-like 1	-	1,6	0,006
169	1448408_at	Hps1	Hermansky-Pudlak syndrome 1 homolog (human)	-	1,5	0,003
170	1422919_at	Hrasls	HRAS-like suppressor	+	1,6	0,001
171	1428640_at	Hsf2bp	heat shock transcription factor 2 binding protein	+	1,9	0,003
172	1425120_x_at	Ifi27l2b	interferon, alpha-inducible protein 27 like 2B	+	1,5	0,002
173	1437103_at	Igf2bp2	insulin-like growth factor 2 mRNA binding protein 2	+	1,6	0,005
174	1419042_at	Iigp1	interferon inducible GTPase 1	+	1,7	0,002
175	1421843_at	Il1rap	interleukin 1 receptor accessory protein	+	1,5	0,002
176	1418697_at	Inmt	indolethylamine N-methyltransferase	+	1,7	0,001
177	1418676_at	Isl2	insulin related protein 2 (islet 2)	+	1,5	0,009
178	1459621_at	Itsn1	intersectin 1 (SH3 domain protein 1A)	+	1,9	0,002
179	1450515_at	Kcnj11	potassium inwardly rectifying channel, subfamily J, member 11	+	1,5	0,009
180	1425437_a_at	Kcnk7	potassium channel, subfamily K, member 7	+	1,6	0,002
181	1425558_at	Klc3	kinesin light chain 3	+	1,6	0,008
182	1452909_at	Klhdc10	kelch domain containing 10	+	1,9	0,000
183	1425664_at	Klhl20	kelch-like 20 (Drosophila)	-	1,5	0,002
184	1435575_at	Kntc1	kinetochore associated 1	-	1,7	0,000
185	1419230_at	Krt12	keratin 12	-	1,7	0,003
186	1449387_at	Krt33a	keratin 33A	+	1,9	0,001
187	1432474_a_at	Krtcap3	keratinocyte associated protein 3	+	1,5	0,006
188	1420677_x_at	Lce1a1	late cornified envelope 1A1	+	1,7	0,002
189	1443907_at	Lnpep	leucyl/cystinyl aminopeptidase	+	1,5	0,009
190	1444019_at	Lrrc19	leucine rich repeat containing 19	+	1,5	0,005
191	1450009_at	Ltf	lactotransferrin	+	1,6	0,006
192	1423607_at	Lum	lumican	+	1,8	0,003
193	1443540_at	Map3k1	mitogen-activated protein kinase kinase kinase 1	+	1,5	0,007
194	1430994_at	March5	membrane-associated ring finger (C3HC4) 5	+	1,6	0,004
195	1453264_at	Marveld3	MARVEL (membrane-associating) domain containing 3	+	2,4	0,000
196	1459387_at	Mast4	microtubule associated serine/threonine kinase family member 4	+	1,5	0,006
197	1419558_at	Mdm4	transformed mouse 3T3 cell double minute 4	+	1,5	0,003
198	1422295_at	Mecom	MDS1 and EVI1 complex locus	+	1,5	0,009
199	1442302_at	Mpg	N-methylpurine-DNA glycosylase	-	1,7	0,001
200	1450867_at	Mrpl17	mitochondrial ribosomal protein L17	+	1,7	0,000
201	1445151_at	Mtf2	metal response element binding transcription factor 2	+	1,5	0,002
202	1446189_at	Myst4	MYST histone acetyltransferase monocytic leukemia 4	-	1,8	0,000
203	1423561_at	Nell2	NEL-like 2 (chicken)	-	1,6	0,002
204	1423516_a_at	Nid2	nidogen 2	+	1,8	0,004
205	1423506_a_at	Nnat	neuronatin	-	1,7	0,007
206	1438483_at	Nos1	nitric oxide synthase 1, neuronal	-	1,6	0,003
207	1416160_at	Nr2f2	nuclear receptor subfamily 2, group F, member 2	-	1,8	0,003
208	1436475_at	Nr2f2	nuclear receptor subfamily 2, group F, member 2	-	1,6	0,004
209	1433422_at	Nr4a2	nuclear receptor subfamily 4, group A, member 2	+	1,7	0,008
210	1420799_at	Ntsr1	neurotensin receptor 1	-	1,8	0,000
211	1428439_at	Nub1	negative regulator of ubiquitin-like proteins 1	+	1,7	0,003
212	1424339_at	Oasl1	2'-5' oligoadenylate synthetase-like 1	+	1,5	0,009
213	1455743_at	Olfml2a	olfactomedin-like 2A	+	1,6	0,001
214	1422370_at	Olfr49	olfactory receptor 49	+	1,6	0,003
215	1420578_at	Optc	opticin	+	1,6	0,001
216	1449627_at	Osbpl6	oxysterol binding protein-like 6	+	1,7	0,000
217	1460719_a_at	P2rx1	purinergic receptor P2X, ligand-gated ion channel, 1	+	1,5	0,005
218	1448433_a_at	Pcolce	procollagen C-endopeptidase enhancer protein	+	1,9	0,004

219	1425100_a_at	Pde6g	phosphodiesterase 6G, cGMP-specific, rod, gamma	+	1,8	0,007
220	1418407_at	Pde8a	phosphodiesterase 8A	+	1,5	0,009
221	1418620_at	Phox2a	paired-like homeobox 2a	+	1,7	0,003
222	1437594_x_at	Pigt	phosphatidylinositol glycan anchor biosynthesis, class T	+	1,5	0,008
223	1448558_a_at	Pla2g4a	phospholipase A2, group IVA (cytosolic, calcium-dependent)	+	1,5	0,003
224	1418595_at	Plin4	perilipin 4	+	1,5	0,009
225	1451475_at	Plxnd1	plexin D1	-	1,5	0,004
226	1429224_at	Pnma1	paraneoplastic antigen MA1	-	1,6	0,002
227	1439806_at	Pogk	pogo transposable element with KRAB domain	-	1,8	0,001
228	1427835_at	Pou2f1	POU domain, class 2, transcription factor 1	+	1,6	0,003
229	1429667_at	Pou4f1	POU domain, class 4, transcription factor 1	+	1,6	0,004
230	1435861_at	Ppfia1	protein tyrosine phosphatase, receptor type, f polypeptide (PTPRF), interacting protein, alpha 1	+	1,6	0,001
231	1416322_at	Prelp	proline arginine-rich end leucine-rich repeat	+	1,5	0,007
232	1429287_a_at	Prl	prolactin	-	112,2	0,008
233	1419681_a_at	Prok2	prokineticin 2	-	1,6	0,003
234	1417682_a_at	Prss2	protease, serine, 2	+	1,6	0,002
235	1418078_at	Psme3	proteaseome (prosome, macropain) 28 subunit, 3	-	1,6	0,004
236	1431680_a_at	Ptprk	protein tyrosine phosphatase, receptor type, K	-	1,6	0,002
237	1439628_x_at	Rab38	RAB38, member of RAS oncogene family	+	1,6	0,005
238	1417620_at	Rac2	RAS-related C3 botulinum substrate 2	+	1,7	0,004
239	1432604_at	Rbl1	retinoblastoma-like 1 (p107)	+	1,8	0,001
240	1438021_at	Rbm47	RNA binding motif protein 47	+	3,2	0,005
241	1448754_at	Rbp1	retinol binding protein 1, cellular	+	1,7	0,006
242	1430128_a_at	Reep6	receptor accessory protein 6	-	1,6	0,003
243	1449465_at	Reln	reelin	-	1,5	0,001
244	1453129_a_at	Rgs12	regulator of G-protein signaling 12	-	1,5	0,002
245	1436634_at	Robo3	roundabout homolog 3 (Drosophila)	+	1,6	0,005
246	1429759_at	Rps6ka6	ribosomal protein S6 kinase polypeptide 6	-	1,6	0,001
247	1426123_a_at	Rrbp1	ribosome binding protein 1	+	1,7	0,005
248	1450280_a_at	Rrh	retinal pigment epithelium derived rhodopsin homolog	+	1,8	0,002
249	1436058_at	Rsad2	radical S-adenosyl methionine domain containing 2	+	1,8	0,001
250	1417643_at	Rsph1	radial spoke head 1 homolog (Chlamydomonas)	+	1,8	0,001
251	1447880_x_at	S1pr2	sphingosine-1-phosphate receptor 2	+	1,8	0,003
252	1456608_at	Sac3d1	SAC3 domain containing 1	+	1,7	0,007
253	1436002_at	Scube3	signal peptide, CUB domain, EGF-like 3	+	1,8	0,007
254	1431795_a_at	Sema3b	sema domain, immunoglobulin domain (Ig), short basic domain, secreted, (semaphorin) 3B	+	1,5	0,003
255	1424923_at	Serpina3g	serine (or cysteine) peptidase inhibitor, clade A, member 3G	-	1,7	0,006
256	1456733_x_at	Serpinh1	serine (or cysteine) peptidase inhibitor, clade H, member 1	+	1,8	0,007
257	1445719_at	Sf3a1	splicing factor 3a, subunit 1	+	1,6	0,003
258	1418460_at	Sh3d19	SH3 domain protein D19	+	1,6	0,001
259	1456971_at	Slc1a7	solute carrier family 1 (glutamate transporter), member 7	+	1,9	0,004
260	1417809_at	Slc22a18	solute carrier family 22 (organic cation transporter), member 18	+	1,8	0,002
261	1423279_at	Slc34a1	solute carrier family 34 (sodium phosphate), member 1	+	1,6	0,001
262	1422771_at	Smad6	MAD homolog 6 (Drosophila)	+	1,8	0,000
263	1449840_at	Sntb2	syntrophin, basic 2	+	1,7	0,002
264	1438492_at	Socs7	suppressor of cytokine signaling 7	+	1,6	0,004
265	1457780_at	Stx11	syntaxin 11	+	1,6	0,002
266	1435058_x_at	Stxbp3a	syntaxin binding protein 3A	+	1,7	0,007
267	1459770_at	Taok1	TAO kinase 1	+	7,0	0,007
268	1429427_s_at	Tcf7l2	transcription factor 7-like 2, T-cell specific, HMG-box	+	2,3	0,004
269	1445895_at	Tcrb-V8.2	T-cell receptor beta, variable 8.2	+	1,7	0,002
270	1425009_at	Tcte2	t-complex-associated testis expressed 2	-	1,5	0,005
271	1431816_at	Tex9	testis expressed gene 9	+	1,7	0,008
272	1456250_x_at	Tgfbi	transforming growth factor, beta induced	+	2,4	0,002
273	1415871_at	Tgfbi	transforming growth factor, beta induced	+	1,6	0,008
274	1440150_at	Tgm3	transglutaminase 3, E polypeptide	+	1,7	0,001
275	1436423_at	Themis	thymocyte selection associated	+	1,6	0,008
276	1436244_a_at	Tle2	transducin-like enhancer of split 2, homolog of Drosophila E(spl)	-	1,6	0,005
277	1454688_x_at	Tmed10	transmembrane emp24-like trafficking protein 10 (yeast)	+	1,8	0,009
278	1443556_at	Tmem140	transmembrane protein 140	+	1,9	0,002
279	1458106_at	Tmem60	transmembrane protein 60	+	1,6	0,007
280	1432506_at	Tmem86b	transmembrane protein 86B	+	1,6	0,003
281	1455848_at	Tmprss11a	transmembrane protease, serine 11a	+	6,8	0,000
282	1418424_at	Tnfaip6	tumor necrosis factor alpha induced protein 6	+	1,7	0,002
283	1460469_at	Tnfrsf9	tumor necrosis factor receptor superfamily, member 9	+	1,5	0,003
284	1425635_at	Tnk1	tyrosine kinase, non-receptor, 1	+	1,5	0,003
285	1447518_at	Tpx2	TPX2, microtubule-associated protein homolog (Xenopus laevis)	+	1,7	0,002
286	1439539_at	Tram2	translocating chain-associating membrane protein 2	-	2,3	0,001
287	1451158_at	Trip12	thyroid hormone receptor interactor 12	+	1,5	0,002
288	1440696_at	Trnp1	TMF1-regulated nuclear protein 1	+	1,8	0,007
289	1441966_at	Trpm3	transient receptor potential cation channel, subfamily M, member 3	+	2,4	0,006
290	1456251_x_at	Tspo	translocator protein	+	1,6	0,006
291	1421485_at	Ttbk2	tau tubulin kinase 2	+	1,8	0,004
292	1429416_at	Ttc9b	tetratricopeptide repeat domain 9B	-	1,5	0,009
293	1455780_at	Ttll6	tubulin tyrosine ligase-like family, member 6	+	1,7	0,002
294	1419518_at	Tuba8	tubulin, alpha 8	-	1,7	0,002
295	1453082_at	Tulp3	tubby-like protein 3	+	1,5	0,004
296	1451314_a_at	Vcam1	vascular cell adhesion molecule 1	+	1,7	0,000
297	1455299_at	Vgll3	vestigial like 3 (Drosophila)	-	2,3	0,003
298	1453593_at	Vgll3	vestigial like 3 (Drosophila)	-	2,3	0,001

299	1443621_at	Xaf1	XIAP associated factor 1	+	2,9	0,000
300	1453866_a_at	Xk	Kell blood group precursor (McLeod phenotype) homolog	+	1,6	0,008
301	1438269_at	Zbtb38	zinc finger and BTB domain containing 38	+	1,6	0,008
302	1425097_a_at	Zfp106	zinc finger protein 106	+	1,6	0,002
303	1422528_a_at	Zfp36l1	zinc finger protein 36, C3H type-like 1	+	1,6	0,001
304	1458026_at	Zfp462	zinc finger protein 462	-	1,7	0,004

5.1.8 HETPS good performers in the FST versus all HETC

All genes that have a FC < 1.5 and a p-value < 0.01 are shown. ID: Affymetrix ID; EFFECT: direction of effect; “+”: gene expression upregulated in the HETPS good performers versus HET control mice; “-“: downregulated in HETPS good performers versus HET control mice; FC: fold-change in mRNA expression. Genes have been ordered alphabetically.

#	ID	SYMBOL	GENENAME	Effect	FC	P.Value
1	1419333_at	1110008J03Rik	RIKEN cDNA 1110008J03 gene	-	1,6	0,003
2	1447369_at	1190005F20Rik	RIKEN cDNA 1190005F20 gene	-	1,8	0,004
3	1450007_at	1500003O03Rik	RIKEN cDNA 1500003O03 gene	-	1,8	0,005
4	1447439_at	1700023E05Rik	RIKEN cDNA 1700023E05 gene	+	1,5	0,007
5	1433334_at	1700024P12Rik	RIKEN cDNA 1700024P12 gene	-	2,0	0,001
6	1450999_a_at	1700029H14Rik	RIKEN cDNA 1700029H14 gene	-	1,6	0,002
7	1442779_at	1700071K01Rik	RIKEN cDNA 1700071K01 gene	-	1,8	0,008
8	1430991_at	1810014B01Rik	RIKEN cDNA 1810014B01 gene	+	1,7	0,004
9	1433023_at	2310068G24Rik	RIKEN cDNA 2310068G24 gene	+	1,6	0,002
10	1432737_at	2810026P18Rik	RIKEN cDNA 2810026P18 gene	-	2,1	0,001
11	1432824_at	2900018N21Rik	RIKEN cDNA 2900018N21 gene	-	1,8	0,003
12	1433387_at	2900022M07Rik	RIKEN cDNA 2900022M07 gene	+	2,3	0,000
13	1430858_at	4632433K11Rik	RIKEN cDNA 4632433K11 gene	-	1,6	0,003
14	1436524_at	4833438C02Rik	RIKEN cDNA 4833438C02 gene	-	1,8	0,001
15	1442152_at	4930513N10Rik	RIKEN cDNA 4930513N10 gene	-	1,5	0,003
16	1431855_at	4930570E03Rik	RIKEN cDNA 4930570E03 gene	+	1,5	0,007
17	1454522_at	4930573G07Rik	RIKEN cDNA 4930573G07 gene	-	1,7	0,006
18	1442611_at	4930592C13Rik	RIKEN cDNA 4930592C13 gene	-	1,7	0,006
19	1454477_at	5530401A10Rik	RIKEN cDNA 5530401A10 gene	+	1,6	0,002
20	1430362_at	5730409N24Rik	RIKEN cDNA 5730409N24 gene	+	1,6	0,003
21	1444614_x_at	6430537H07Rik	RIKEN cDNA 6430537H07 gene	-	1,7	0,001
22	1431158_at	8430406H22Rik	RIKEN cDNA 8430406H22 gene	+	1,5	0,001
23	1453561_x_at	8430431K14Rik	RIKEN cDNA 8430431K14 gene	-	1,6	0,008
24	1445639_at	9130014G24Rik	RIKEN cDNA 9130014G24 gene	-	1,6	0,004
25	1432213_at	9530047P18Rik	RIKEN cDNA 9530047P18 gene	-	4,7	0,000
26	1458123_at	9630002A11Rik	RIKEN cDNA 9630002A11 gene	+	1,6	0,004
27	1456167_at	AA619741	expressed sequence AA619741	-	1,5	0,006
28	1449827_at	Acan	aggrecan	-	1,6	0,005
29	1452057_at	Actr1b	ARP1 actin-related protein 1 homolog B, centractin beta (yeast)	-	1,5	0,002
30	1457168_at	AI225934	expressed sequence AI225934	+	1,7	0,001
31	1422000_at	Akr1c12	aldo-keto reductase family 1, member C12	-	2,3	0,004
32	1450497_at	Apc2	adenomatosis polyposis coli 2	-	1,5	0,006
33	1443112_at	Api5	apoptosis inhibitor 5	+	1,8	0,001
34	1418292_at	Asna1	arsA arsenite transporter, ATP-binding, homolog 1 (bacterial)	-	1,7	0,007
35	1435597_at	Atad5	ATPase family, AAA domain containing 5	+	1,6	0,005
36	1438921_at	Atr	ataxia telangiectasia and Rad3 related	+	1,7	0,009
37	1418991_at	Bak1	BCL2-antagonist/killer 1	-	1,8	0,000
38	1456287_at	BB236558	expressed sequence BB236558	-	1,6	0,005
39	1420887_a_at	Bcl2l1	BCL2-like 1	-	1,6	0,002
40	1439936_at	BE949265	cDNA sequence BE949265	+	1,5	0,008
41	1451386_at	Blvrb	biliverdin reductase B (flavin reductase (NADPH))	-	1,5	0,006
42	1457664_x_at	C2	complement component 2 (within H-2S)	-	1,5	0,008
43	1457656_s_at	C230085N15Rik	RIKEN cDNA C230085N15 gene	+	1,7	0,006
44	1422190_at	C5ar1	complement component 5a receptor 1	-	1,5	0,004
45	1447182_at	C77815	expressed sequence C77815	+	1,7	0,002
46	1441734_at	Camk2a	calcium/calmodulin-dependent protein kinase II alpha	-	1,5	0,003
47	1422105_at	Cd3e	CD3 antigen, epsilon polypeptide	-	2,3	0,002
48	1441312_at	Cnnm1	cyclin M1	-	1,5	0,003
49	1429928_at	Ctag2	cancer/testis antigen 2	+	1,5	0,002
50	1459475_at	D10Ertd761e	DNA segment, Chr 10, ERATO Doi 761, expressed	+	1,7	0,004
51	1449368_at	Dcn	decorin	-	1,6	0,001
52	1446169_at	Dgcr8	DiGeorge syndrome critical region gene 8	+	1,6	0,005
53	1445798_at	Dlg1	discs, large homolog 1 (Drosophila)	+	1,6	0,003
54	1459791_at	Dnajc1	DnaJ (Hsp40) homolog, subfamily C, member 1	+	1,7	0,007
55	1434534_at	Dsc3	desmocollin 3	+	1,6	0,009
56	1439098_at	E230013L22Rik	RIKEN cDNA E230013L22 gene	-	1,7	0,007
57	1449549_at	Efnb2	ephrin B2	+	1,5	0,005

58	1424960_at	Epn3	epsin 3	-	1,5	0,006
59	1441212_at	Fam92a	family with sequence similarity 92, member A	+	1,5	0,004
60	1449528_at	Figf	c-fos induced growth factor	-	1,6	0,006
61	1415939_at	Fmod	fibromodulin	-	1,7	0,004
62	1456084_x_at	Fmod	fibromodulin	-	1,5	0,007
63	1440605_at	Fscn2	fascin homolog 2, actin-bundling protein, retinal (Strongylocentrotus purpuratus)	-	1,5	0,005
64	1431971_at	Gm14318	predicted gene 14318	+	1,6	0,004
65	1450990_at	Gpc3	glypican 3	-	2,0	0,000
66	1434007_at	Gyltl1b	glycosyltransferase-like 1B	-	1,8	0,008
67	1459343_at	Heatr6	HEAT repeat containing 6	-	2,6	0,000
68	1428641_at	Hsf2bp	heat shock transcription factor 2 binding protein	-	2,0	0,008
69	1419212_at	Icosl	icos ligand	-	1,5	0,005
70	1455223_at	Igf2bp1	insulin-like growth factor 2 mRNA binding protein 1	+	1,8	0,001
71	1433156_at	Kcnip1	Kv channel-interacting protein 1	+	1,6	0,004
72	1421462_a_at	Lepre1	leprecan 1	-	1,7	0,000
73	1431251_at	Lrrc3	leucine rich repeat containing 3	-	1,6	0,005
74	1427079_at	Mapre3	microtubule-associated protein, RP/EB family, member 3	-	1,6	0,003
75	1440966_at	March7	membrane-associated ring finger (C3HC4) 7	+	1,6	0,002
76	1453264_at	Marveld3	MARVEL (membrane-associating) domain containing 3	-	1,7	0,002
77	1419629_at	Mesp2	mesoderm posterior 2	-	1,5	0,009
78	1434447_at	Met	met proto-oncogene	-	1,6	0,003
79	1420092_at	Morc3	microrchidia 3	+	1,7	0,001
80	1416236_a_at	Mpzl2	myelin protein zero-like 2	-	1,6	0,009
81	1455104_at	Mxd1	MAX dimerization protein 1	-	1,7	0,001
82	1422961_at	Nat3	N-acetyltransferase 3	+	1,5	0,005
83	1430149_at	Ndufa3	NADH dehydrogenase (ubiquinone) 1 alpha subcomplex, 3	-	1,6	0,005
84	1423506_a_at	Nnat	neuronatin	-	1,7	0,007
85	1432517_a_at	Nnmt	nicotinamide N-methyltransferase	-	1,6	0,008
86	1421686_at	Npvf	neuropeptide VF precursor	-	1,7	0,002
87	1429572_at	Nsun7	NOL1/NOP2/Sun domain family, member 7	-	1,6	0,002
88	1454098_at	Olfr112	olfactory receptor 112	+	1,6	0,006
89	1427956_at	Pcgf1	polycomb group ring finger 1	-	1,6	0,001
90	1453144_at	Pisd-ps3	phosphatidylserine decarboxylase, pseudogene 3	-	4,5	0,001
91	1429452_x_at	Pisd-ps3	phosphatidylserine decarboxylase, pseudogene 3	-	4,1	0,002
92	1453145_at	Pisd-ps3	phosphatidylserine decarboxylase, pseudogene 3	-	3,9	0,002
93	1439069_a_at	Pisd-ps3	phosphatidylserine decarboxylase, pseudogene 3	-	2,2	0,003
94	1434975_x_at	Pisd-ps3	phosphatidylserine decarboxylase, pseudogene 3	-	1,9	0,004
95	1429361_at	Pmch	pro-melanin-concentrating hormone	+	9,4	0,001
96	1432129_a_at	Prrx1	paired related homeobox 1	+	1,6	0,001
97	1446560_at	Prss23	protease, serine, 23	-	1,5	0,004
98	1449798_at	Rab3c	RAB3C, member RAS oncogene family	+	1,6	0,007
99	1456674_at	Rad54b	RAD54 homolog B (S. cerevisiae)	-	2,1	0,007
100	1422268_a_at	Rps6kb2	ribosomal protein S6 kinase, polypeptide 2	-	1,5	0,006
101	1417643_at	Rsph1	radial spoke head 1 homolog (Chlamydomonas)	-	1,6	0,005
102	1451603_at	Rtbdn	retbindin	-	1,5	0,007
103	1434908_at	Scaf1	SR-related CTD-associated factor 1	-	1,6	0,001
104	1428695_at	Sdr39u1	short chain dehydrogenase/reductase family 39U, member 1	-	1,6	0,002
105	1424923_at	Serpina3g	serine (or cysteine) peptidase inhibitor, clade A, member 3G	-	1,7	0,004
106	1416625_at	Serping1	serine (or cysteine) peptidase inhibitor, clade G, member 1	-	1,6	0,003
107	1436989_s_at	Slc12a6	solute carrier family 12, member 6	+	1,5	0,008
108	1416966_at	Slc22a8	solute carrier family 22 (organic anion transporter), member 8	-	1,8	0,005
109	1425883_at	Smg6	Smg-6 homolog, nonsense mediated mRNA decay factor (C. elegans)	+	1,7	0,003
110	1443727_x_at	Smyd1	SET and MYND domain containing 1	-	1,5	0,004
111	1422960_at	Srd5a2	steroid 5 alpha-reductase 2	-	1,7	0,001
112	1422979_at	Suv39h2	suppressor of variegation 3-9 homolog 2 (Drosophila)	+	1,6	0,001
113	1422531_at	Syt5	synaptotagmin V	-	1,6	0,004
114	1443123_at	Tanc2	tetratricopeptide repeat, ankyrin repeat and coiled-coil containing 2	+	1,7	0,004
115	1442312_at	Tbl1xr1	transducin (beta)-like 1X-linked receptor 1	+	1,7	0,001
116	1425028_a_at	Tpm2	tropomyosin 2, beta	-	1,5	0,009
117	1439043_at	Tra2a	transformer 2 alpha homolog (Drosophila)	+	2,5	0,009
118	1440938_at	Treml2	triggering receptor expressed on myeloid cells-like 2	+	1,6	0,007
119	1450041_a_at	Tub	tubby candidate gene	-	1,7	0,000
120	1421766_at	Uchl4	ubiquitin carboxyl-terminal esterase L4	+	1,6	0,002
121	1444534_at	Uhrf1bp1	UHRF1 (ICBP90) binding protein 1	-	1,5	0,004
122	1435386_at	Vwf	Von Willebrand factor homolog	-	1,6	0,002
123	1453426_a_at	Wdfy1	WD repeat and FYVE domain containing 1	-	1,9	0,000
124	1439005_x_at	Ywhaz	tyrosine 3-monooxygenase/tryptophan 5-monooxygenase activation protein, zeta polypeptide	+	1,7	0,009
125	1436981_a_at	Ywhaz	tyrosine 3-monooxygenase/tryptophan 5-monooxygenase activation protein, zeta polypeptide	+	1,7	0,005
126	1449691_at	Zfp644	zinc finger protein 644	+	1,7	0,002

5.2 DNA methylation patterns of various Bdnf promoters in PS mice

5.2.1 Introduction

Chronic and/or excessive stress during pregnancy is known to enhance the release of stress hormones like cortisol and corticotrophin-releasing hormone (CRH) into the maternal and fetal bloodstream, thereby impacting upon early brain development. As such, prenatal stress (PS) is suggested to increase the risk of developing depression and anxiety disorders in the offspring later in life (for review see e.g. Weinstock 2008). Whereas emotional disorders are among the leading causes of disability worldwide, their underlying molecular mechanisms are still poorly understood. There is growing evidence that brain-derived neurotrophic factor (BDNF), which is known for regulating neurogenesis as well as synaptic plasticity (McAllister *et al.* 1999) and its associate involvement in learning and memory (Poo 2001; Lu 2003; Lu and Chang 2004), plays an important role in this respect (Pezet and Malcangio 2004). For example, chronic administration of antidepressants results in an increase in rodent hippocampal and cortical BDNF levels (Nibuya *et al.* 1995; Nibuya *et al.* 1996). In addition, individuals, who were treated with antidepressants at the time of suicidal death, display enhanced BDNF levels in the hippocampus and prefrontal cortex (Chen *et al.* 2001; Dwivedi *et al.* 2003; Karege *et al.* 2005). Next to this, effects of antidepressants can be imitated by infusions of BDNF protein into the hippocampus of rodents (Siuciak *et al.* 1997; Shirayama *et al.* 2002), supporting the so-called 'neurotrophin hypothesis of depression', which postulates that decreased BDNF levels in the hippocampus and prefrontal cortex may contribute to atrophy and cell loss in the respective brain area, as observed in some depressed subjects (Duman and Monteggia 2006). In line with this hypothesis, stress, be it acute or chronic, is able to downregulate BDNF expression (Nibuya *et al.* 1995; Smith *et al.* 1995; Schaaf *et al.* 1998; Pizarro *et al.* 2004), whereas chronic, but not acute administration of antidepressants is able to reverse the effects of stress on BDNF (Nibuya *et al.* 1995; Russo-Neustadt *et al.* 1999). Recently, it has been shown that epigenetic modifications may play an important role in this context (for overview, see Boulle *et al.* 2012). For example, social defeat stress was shown to enhance the repressive histone methylation on the Bdnf promoters of transcript III and IV, whereas chronic administration of imipramine reversed this effect by inducing permissive histone acetylation at the same promoter regions (Tsankova *et al.* 2006). However, less is known about the role of DNA methylation patterns of the *Bdnf* gene in this respect.

In the present study we used bisulfite treatment of DNA followed by matrix-assisted laser desorption/ionization time-of-flight mass spectrometry (MALDI-TOF MS) analyzed by the sequenom-

EpiTYPER platform in order to examine the effects of prenatal maternal stress exposure on the degree of methylation at various *Bdnf* promoters (I,IV and IX).

5.2.2 Materials and methods

Animals for the EpiTYPER MALDI-TOF mass spectrometry study

DNA of murine hippocampus and cortex was provided by Daniel van den Hove and his group (Behan *et al.* 2011). The mice were treated as already described elsewere (Behan *et al.* 2011). Briefly, the pregnant dams (C57BL/6) were exposed to PS by restraining them in 250 ml glass cylinders, filled with 5 mm water, whilst being exposed to bright light. This procedure was applied during the last week of pregnancy 3 times daily for 45 min. Control mice were left undisturbed in their home cages. After behavioral tests for cognition (ORT), anxiety (EZM) and depressive-related behavior (Sucrose intake and FST) the mice were killed and brains collected. DNA was extracted by the help of QIAamp® DNA Mini kit (Qiagen, Hilden, Germany) following the manufactor´s instructions.

Animals for the pyrosequencing study

See 2.1.1

EpiTYPER MALDI-TOF mass spectrometry

EpiTYPER is a bisulfite-treatment-based method for the detection and quantitation of DNA methylation. Non-methylated cytosine (C) is converted to uracil (U), while methylated Cs remain unchanged by bisulfite treatment of genomic DNA. The differences in methylation can be detected by the mass spectrometer because C and U bases differ in their weights.

The bisulfite treatment was followed by a modified protocol from Zymo Research EZ DNA Methylation Kit. First, the CT-conversion reagent was prepared. To the CT-conversion reagent, 750 µl ddH$_2$O (or DEPC-H$_2$O) and 210 µl M-Dilution Buffer were added. This was mixed by vortexing for 10 min. Afterwards, to 500 – 1000 ng of total DNA, 5 µl M-dilution buffer and ddH_20 to a total volume of 50 µl were added, well mixed and incubated at 37°C for 15 min. After incubation, 100 µl of the prepared CT-conversion reagent was added to each sample and lightly vortexed. The reaction mix was then incubated in the dark with the following protocol: 21 cycles (95°C, 30 sec; 50°C, 15 min). Subsequently, the samples were incubated on ice for 10 min. 400 µl M-binding buffer was added to the samples and mixed by pipetting up and down. After that, the samples were loaded into a Zymo-Spin I Column, which was placed in a 2 ml collection tube. Afterwards, it was centrifuged at 11200 rpm for 30 sec and the flow through was discarded. M-wash buffer was then added to the column and spinned for 30 sec at full speed. Subsequently, 200 µl of M-desulphonation buffer was added to the column and incubated at room temperature for 15 min. After that, it was centrifuged for 30 sec at full speed. Afterwards, it was washed with M-wash buffer for 2 times. At the end, 100 µl ddH_2O was added directly to the column matrix and briefly spinned at 3000 rpm to elute the DNA. The bisulfited DNA (Bi-DNA) was aliquoted and stored at -20°C if not directly used.

Following the bisulfite treatment, a PCR was performed. 2.22 µl ddH_2O, 0.5µl 10x Hot Start buffer (Qiagen), 0.04 µl dNTP Mix (25mM each), 1 µl forward + reverse primer with a T7 promoter (1 µM each), 0.2 µl $MgCl_2$ and 1 µl Bi-DNA were mixed and incubated: 94°C for 15 min; 45 cycles (94°C, 20 sec; 62°C (variable), 30 sec; 72°C, 1 min); 72°C, 1 min; 4°C, 5 min. During PCR amplification, a T7 promoter for *in vitro* transcription was introduced to the 5' end of one strand of each amplicon. After the PCR, the shrimp alkaline phosphatase (SAP) enzyme solution (1.7 µl RNase free water, 0.3 µl SAP) was added to each reaction to degrade any unincorporated nucleotides and incubated at 37°C for 20 min and then for 5 min at 85°C. Subsequently, the cleavage transcription/RNase A cocktail (3.21 µl RNase free water, 5xT7 polymerase buffer, 0.22 µl T-cleavage mix, 0.22 µl DTT (10 mM), 0.4 µl T7 R&DNA polymerase (50 U/µl) and 0.06 µl RNase A) was added to 2 µl of PCR/SAP solution and incubated for 3 hours at 37°C. In this step, RNase A cleaves specifically at every C. For cleaning up the reaction products, 20 µl ddH2O and 6 mg resin were added to each reaction and rotated for 10 min. Afterwards it was centrifuged at 3000 rpm. Then, using the MassArray® Nanodispenser S, 20 nl of the samples was transferred onto a 384 SpectroCHIP® and calibrant was transferred from the calibrant well (70 µl) onto the calibrant patches of the 384 SpectroCHIP®. Subsequently, the MALDI-TOF MS was run.

To validate the results, we aimed at replicating some of the differentially methylated CpG sites in a second experiment.

Pyrosequencing

For validation of the DNA methylation microarray, we established the pyrosequencing method by using a candidate gene which we did not pick from the microarray (Bdnf).

For pyrosequencing, the DNA methylation Gold kit and its protocol from Zymo Research (Irvine, USA) were used in a slightly modified manner. The input amount of DNA was 800 ng and the conversion took place at following conditions: 98°C for 10 minutes, 53°C for 4 hours.

The PCR protocol (with biotinylated primers), was as follows: 94°C, 5 min; 41 cycles (94°C, 20 sec; 54°C, 30 sec; 72°C, 1 min); 72°C, 3 min. To 10 µl of the PCR product, 2 µl of streptavidin sepharose HP beads, 40 µl of binding buffer and 28 µl of high purity water were added. After shaking the plate for 5 min at 1400 rpm, a vacuum head isolated the template. Then, templates were washed with 70% ethanol, denaturized with basic solution and washed with water. The template was added to 11.5 µl of annealing buffer and 0.5 µl pyroprimer (10mM), which was incubated for 2 minutes at 80°C.

Statistical analysis

As we expected differences between females and males in the PS paradigm, we stratified for sex. Stress effects in males or in females were calculated by the help of non-parametric Mann-Whitney-U test. The significance level was set at $P < 0.05$ for every test. P-values between 0.05 and 0.1 were referred to as a trend. Differences in methylation of the Bdnf promoter IV assessed by pyrosequencing were analyzed by the help of two-way ANONVA. All analyses were carried out by the help of the SPSS software Version 20.0.

5.2.3 Results

The percentage of DNA methylation within the promoter I of the Bdnf gene was very low in the hippocampus and in the cortex (see Figure 5-1A, 5-1D). In the hippocampus, we could detect significant differences between PS and control males at CpG site 6 (P=0.008) and between PS and control females at CpG site 28 and 39-40 (P=0.025, respectively). In the cortex, there were significant changes between PS and control females at CpG sites 28 (P=0.003), 37 (P=0.050) and 39-40

(P=0.003). At promoter IV, a descending pattern towards the transcription start side (between CpG site 15 and 19-20) could be measured in the hippocampus and in the cortex. In the hippocampus, several significant changes could be detected: At CpG sites 19-20 between control and PS males (P=0.004) and at CpG site 11 (P=0.026), 12 (P=0.049) and 19-20 (P=0.018) between control females and PS females. At promoter IX, in comparison to promoter IV and I, a high mehylation level was observed. In the hippocampus, we found a significant difference at CpG site 6 (P=0.028) between PS and control females. In the cortex, we detected significant differences between control males and PS males at CpG sites 6 (P=0.033), 7 (P=0.033), 9 (P=0.04), 10 (P=0.035) and 13 (P=0.04).

In a second control experiment we tried to replicate some of these significant changes. Although the overall degrees of methylation were similar at the various CpG sites, the specific effects did not reach significance anymore (data not shown).

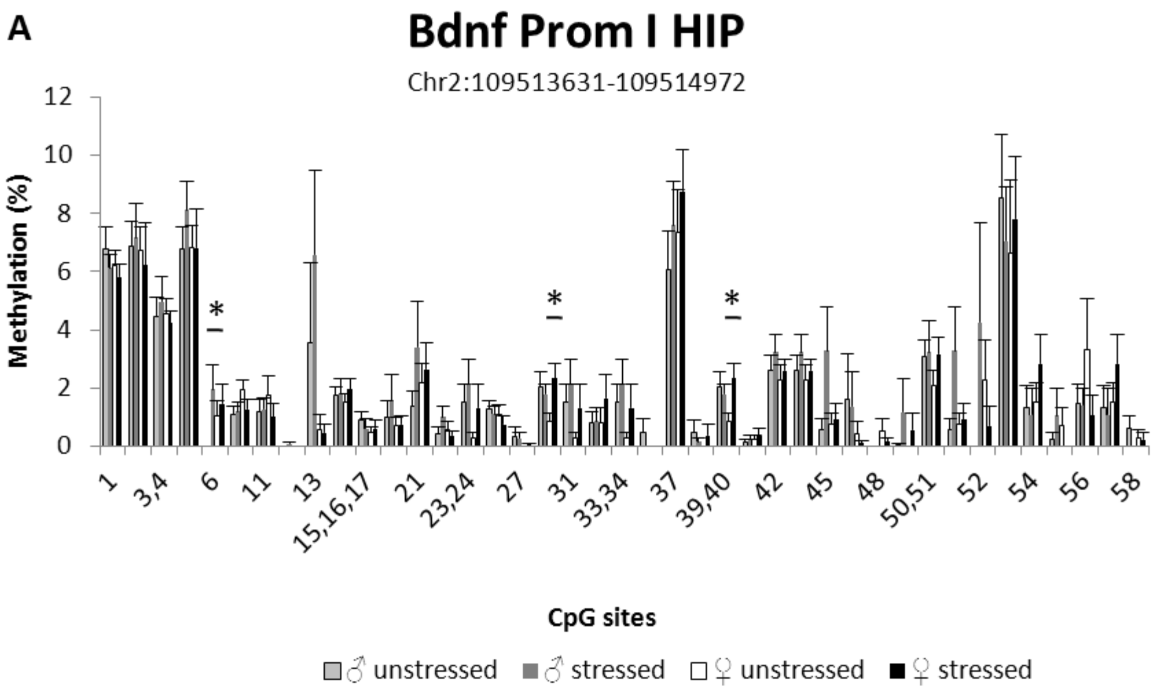

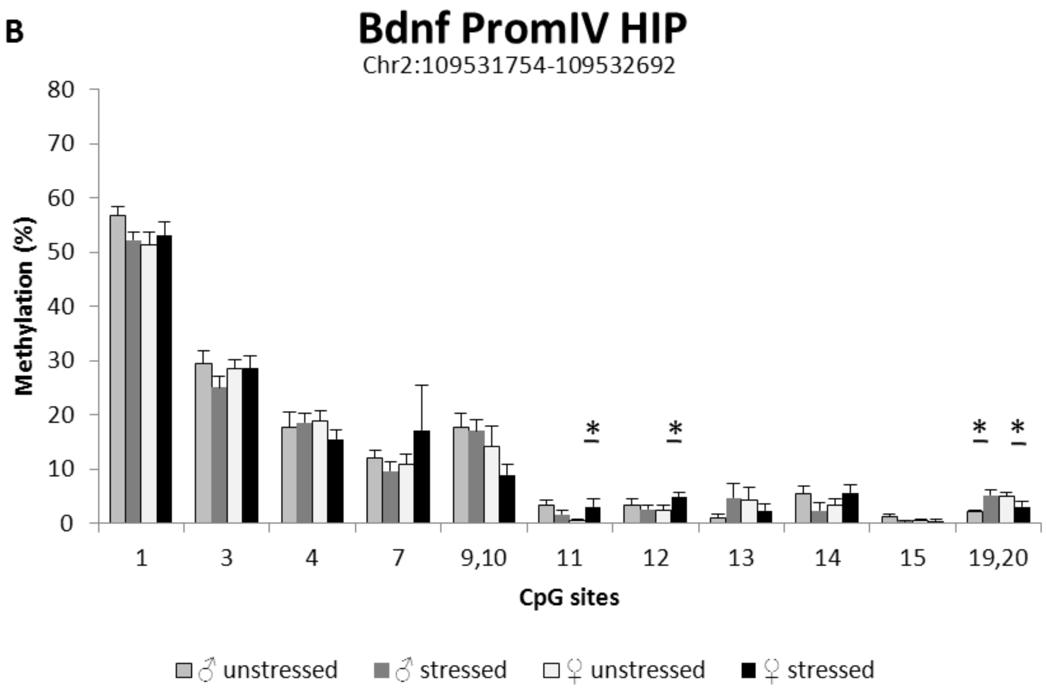
B
Bdnf PromIV HIP
Chr2:109531754-109532692
Methylation (%)
80
70
60
50
40
30
20
10
0
*
*
*
*
1
3
4
7
9,10
11
12
13
14
15
19,20
CpG sites
▨ ♂ unstressed
▨ ♂ stressed
☐ ♀ unstressed
■ ♀ stressed

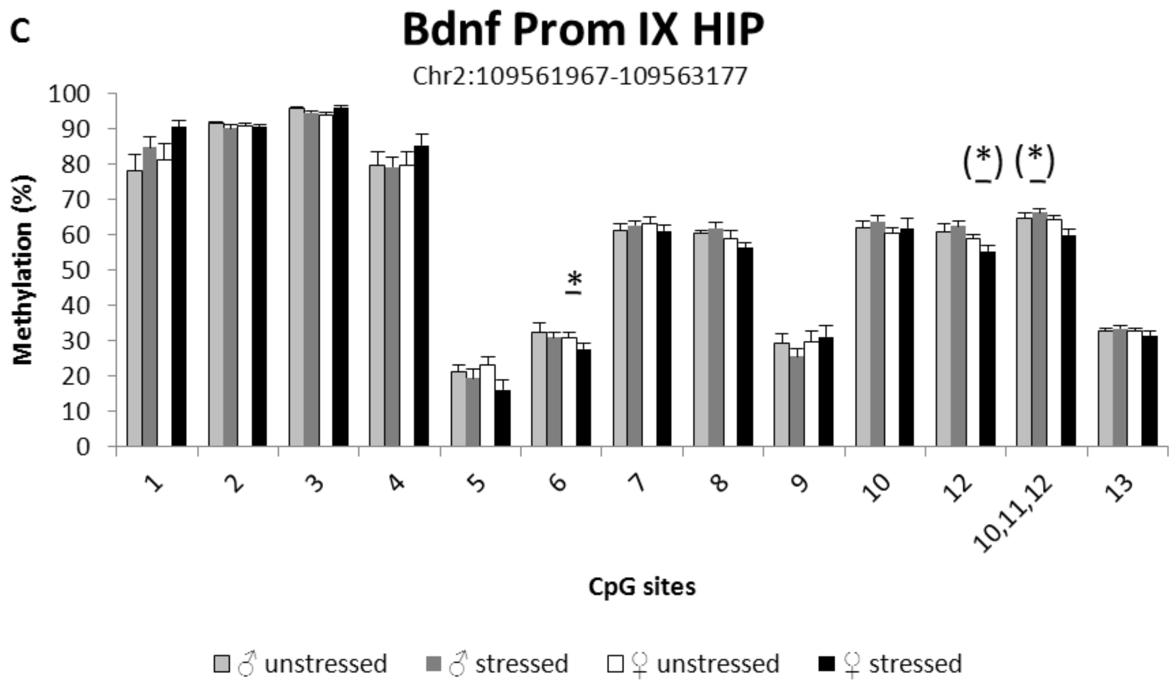
C
Bdnf Prom IX HIP
Chr2:109561967-109563177
Methylation (%)
100
90
80
70
60
50
40
30
20
10
0
*
(*)
(*)
1
2
3
4
5
6
7
8
9
10
12
10,11,12
13
CpG sites
▨ ♂ unstressed
▨ ♂ stressed
☐ ♀ unstressed
■ ♀ stressed

D

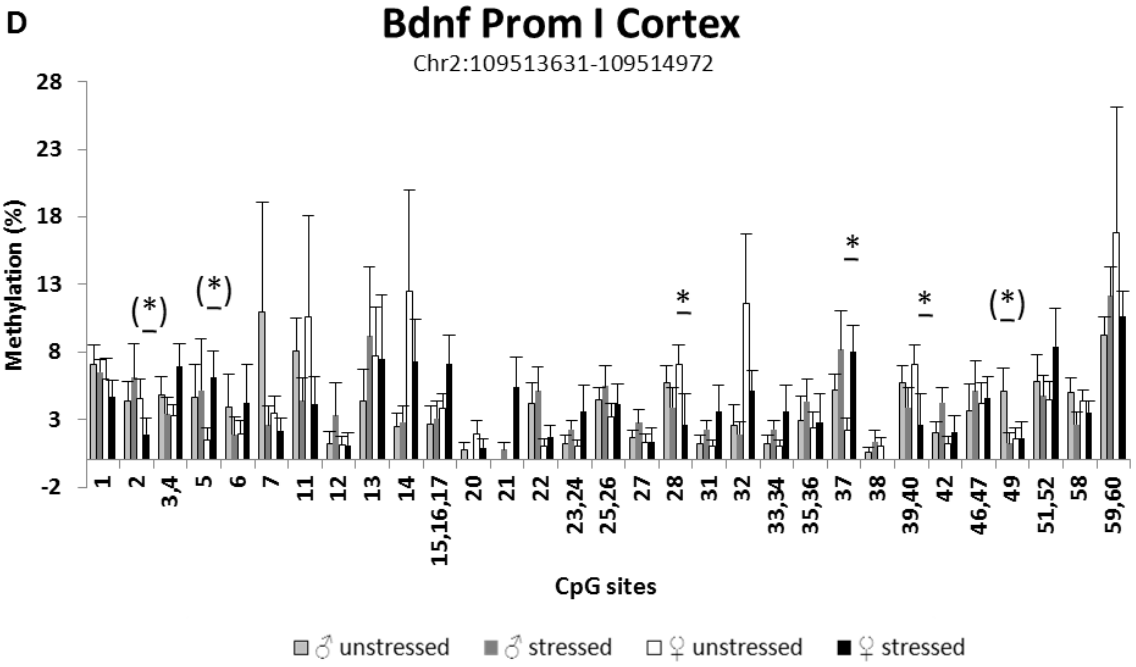
Bdnf Prom I Cortex
Chr2:109513631-109514972
Methylation (%)
28
23
18
13
8
3
-2
1
2
3,4
5
6
7
11
12
13
14
15,16,17
20
21
22
23,24
25,26
27
28
31
32
33,34
35,36
37
38
39,40
42
46,47
49
51,52
58
59,60
(*)
(*)
*
*
*
(*)
CpG sites
♂ unstressed
♂ stressed
♀ unstressed
♀ stressed

E

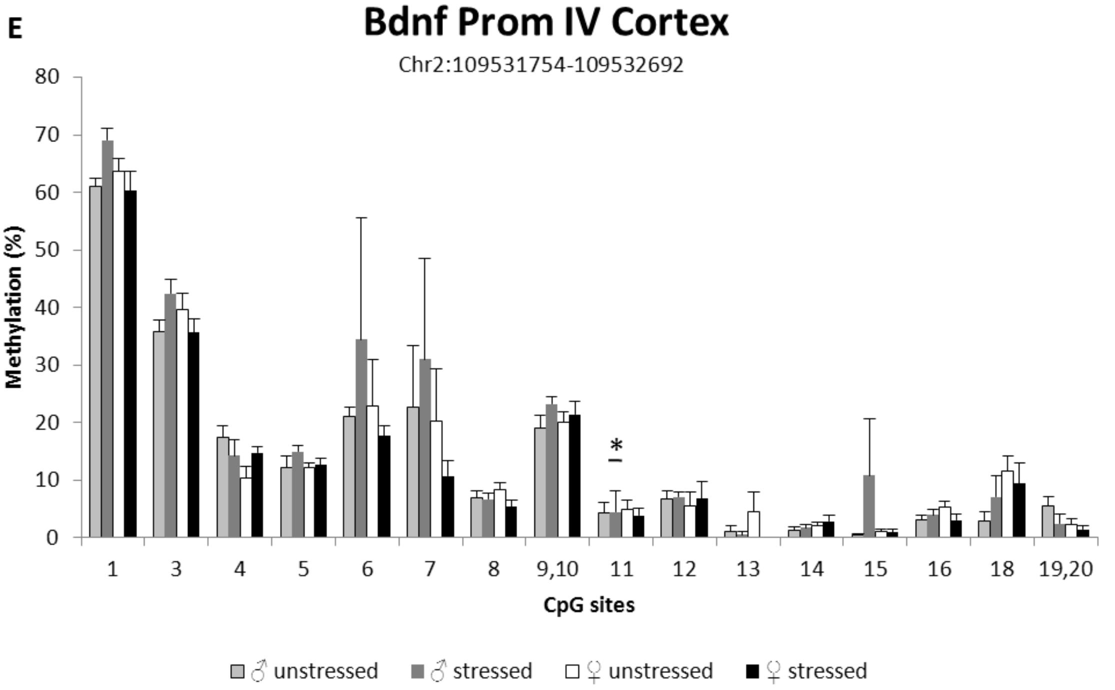
Bdnf Prom IV Cortex
Chr2:109531754-109532692
Methylation (%)
80
70
60
50
40
30
20
10
0
1
3
4
5
6
7
8
9,10
11
12
13
14
15
16
18
19,20
*
CpG sites
♂ unstressed
♂ stressed
♀ unstressed
♀ stressed

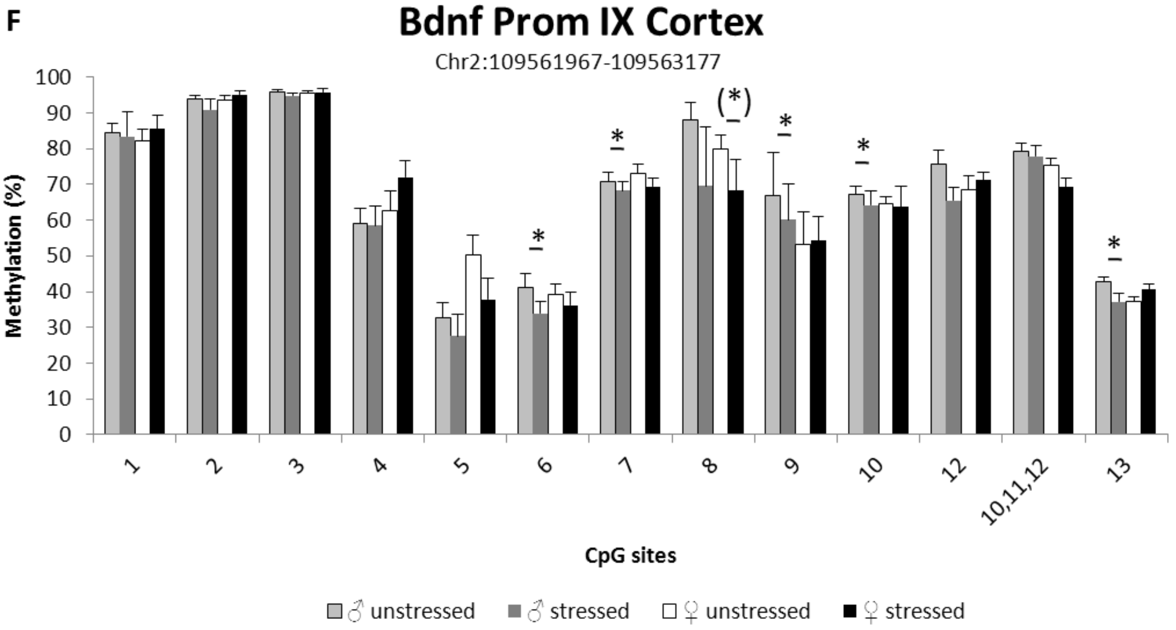

Figure 5-1 A-F. DNA Methylation patterns of various brain-derived neurotrophic factor (Bdnf) promoters (Prom) in the hippocampus (HIP) and cortex. At Prom I (A, D), the average degree of methylation was relatively low in the cortex and in hippocampus. At Prom IV (B, E), a decrease towards the transcription start side (between 15 and 19,20) was observed. Prom IX (C, F) was relatively highly methylated in comparison to Prom I and IV. Data represent mean + SEM.

The methylation status of three CpG sites of the Bdnf promoter IV (CpG 1,2,3; see Figure 5-2) was assessed by the use of pyrosequencing. At these distinct CpG sites no differences between control and PS mice or 5-Htt+/- and WT mice could be detected.

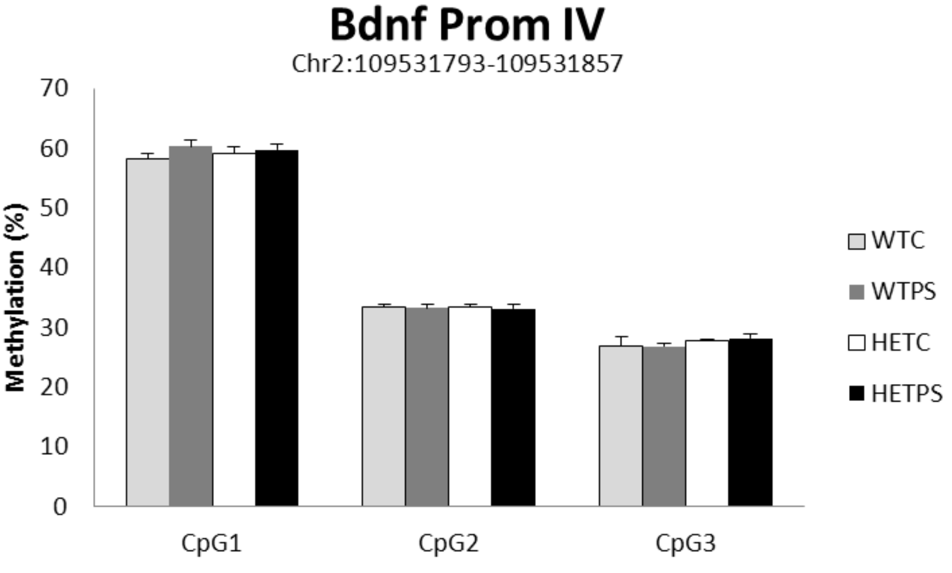

Figure 5-2. Methylation status of Bdnf Promoter IV. Three CpG sites of the Bdnf Promoter IV were measured but no signififcant differences between prenatal stress (PS) and control (C) or 5-Htt deficient (HET) mice and wildtype (WT) mice could be detected. Data represent mean + S.E.M. N=7-10 mice/group.

5.2.4 Discussion

Although the results at single CpG sites (indicating various sex-dependent effects of prenatal stress) could not be replicated, the overall methylation patterns of the various CpG sites at the different promoters were confirmed. The low methylation state at promoter I points to an increase of Bdnf exon I expression in the hippocampus and cortex. Overall, information about the methylation state at promoter I in the brain is poor. Interestingly, Munoz and coworkers revealed a correlation between performance in the novel object recognition task and Bdnf promoter I methylation (Munoz *et al.* 2010). Further, Bredy and colleagues report an upregulation of Bdnf exon I expression after extinction of conditioned fear in the prefrontal cortex, which came in parallele with a trend of histone (H) 4 acetylation around the respective promoter I (Bredy *et al.* 2007). Another study on bipolar disorder (BD) I and II demonstrated a downregulation of BDNF expression in BD II patients but not in BD I patients in comparison to control individuals (D'Addario *et al.* 2012). Accordingly, the BDNF promoter I was hypermethylated in BD II patients. Interestingly, BDNF promoter I was specifically hypermethylated in BD patients who took mood stabilizers plus antidepressants when compared to those who only took mood stabilizers. Furthermore, lithium and valproate, the latter of which is known to inhibit HDAC, were linked with a decreased promoter I methylation in comparison to other drugs.

Our data suggest that there is a decline in methylation of promoter IV towards the transcription start site. Furthermore, the binding site for calcium/cyclic adenosine monophosphate (cAMP)–responsive element binding protein (CREB) at CpG 13 is only minimally methylated in all four groups indicating a binding oportunity for CREB. This pattern is similar when examining promoter IV (former promoter III) methylation in murine E18 + 5 days *in vitro* neuronal cells cultured with 10 % calf serum (amongst other cultures) (see supplements of Chen *et al.* 2003). Additionaly, a study by Mueller and colleagues revealed a relatively low degree of promoter IV methylation state near the CREB binding site, whereas the CpG site before the CREB binding site (CpG 14) showed an equal percentage of methylation like in our study (Mueller et al 2008). Interestingly, Mueller and coworkers, who investigated the effects of PS exposure during the first week of pregnancy, could not detect any differences at the examined CpG sites between stressed and control mice, as well.

Using pyrosequencing, we assessed the methylation status of 3 CpG sites of the Bdnf Promoter IV and could not detect any significant differences. As already stated above, this is in line with another study by Müller and coworkers which revealed no significant changes in the Bdnf Promoter IV methylation between PS and control animals (Mueller and Bale 2008). Interestingly, Tsankova and her colleagues found that defeat stress was able to increase histone methylation near promoter IV, an epigenetic modification which is thought to repress gene expression (Tsankova *et al.* 2006). Chronic treatment with imipramine could reverse this effect by inducing permissive histone acetylation. Further studies have to investigate if histone modifications also play a role in PS exposure on a 5-Htt deficient background.

In contrast to promoter I and IV, we found very high degrees of methylation at promoter IX, which is in line with another study by Zajac and coworkers, which also revealed high methylation at promoter IX (Zajac *et al.* 2010).

Limitations

The Sequenom EpiTYPER Mass Array MALDI-TOF analysis has a sensitivity of 5 %. That possibly could be the reason for the non-replication as we detected only small differences. Another drawback of this method is that it cannot distinguish between fragments of the same mass which leads to overlapping fragments. Furthermore, if two or more CpG sites are located on one fragment, the software is not able to calculate different rates for each CpG site. In general, bisulfite treatment causes a loss of 95% of DNA material and might therefore lead to variability of the results (Grunau *et al.* 2001).

Conclusions

In conclusion, the EpiTYPER Mass Array MALDI-TOF technique is not very sensitive and has further drawbacks. In general, the bisulfite-treated DNA should be aliquoted and frozen at -20°C and a thaw and freezing cycle should be avoided.

5.3 DNA methylation analysis of Arfgef1 in a maternal care paradigm

This study was performed at the European Molecular Biology Laboratory (EMBL) in Monterotondo (Italy) in colaboration with Dr. Cornelius Gross and his colleagues.

5.3.1 Introduction

Early-life adversity can have severe consequences for adult psychopathology. One of such an adverse situation is bad parenting. As far as humans are concerned, studies on the influence of early family experiences are primarily based on cases of severe adversity like childhood maltreatment or parental loss, which have been associated with enhanced ACTH (for review see (Tarullo and Gunnar 2006)) or cortisol responses (Luecken 1998; Luecken and Appelhans 2006) after psychosocial stress. However, even milder variations in parenting behavior have shown to be relevant. For example, Engert as well as Pruessner and colleagues reported that young adults and elderly who experienced low parental care display enhanced cortisol responses (Engert *et al.* 2010) and dopamine release in the ventral striatum (Pruessner *et al.* 2004) in reaction to psychosocial stress. Furthermore, a parenting style with low levels of structure (i.e. organization and consistency) in middle childhood predicts awakening cortisol responses as well as cortisol responses to the “Trier Social Stress Test” in the offspring at around 16 years of age (Ellenbogen and Hodgins 2009).

Animal studies indicate that in rodents, maternal behavior has longlasting consequences on anxiety-like behavior of the offspring. For example, maternal separation for several hours a day during the early postnatal period leads to enhanced anxiety-like behaviors and enhanced hormonal reactivity to stress (Kalinichev *et al.* 2002).Similarly, pups raised by low licking-and-grooming mothers show increased levels of anxiety compared to pups raised by mothers that display high licking-and-grooming (Caldji *et al.* 1998). Cross-fostering studies revealed that these influences are primarily environmental and cross-fostering offspring of low licking-and-grooming mothers to high licking-and-grooming mothers is able to convey low anxiety to the offspring (Liu *et al.* 2000). These findings indicate that variations in maternal behavior serve as a mechanism for the nongenomic transmission of individual differences in stress reactivity across generations. There are several indications of the underlying molecular mechanisms in adult animals exposed to different rearing environments pointing to persistent changes in gene expression. For example, decreased expression and function of the glucocorticoid receptor (GR) has been linked to low maternal care (for review see (Seckl and Meaney 2004)). Additionally, the DNA degree of methylation at the promoter region of the GR gene was increased whereas histone H3-K9 acetylation was decreased in the hippocampus of these animals (Weaver *et al.* 2004). Treatment of these rats in adulthood with the histone deacetylase (HDAC) inhibitor tricostatin A reversed the effects of low licking-and-grooming on GR expression. McGowan and colleagues were able to translate these findings to the human by a study in which they examined the hippocampus of suicide victims with a history of childhood abuse and found a decreased GR expression combined with an increased GR promoter methylation in suicide victims compared to controls (McGowan *et al.* 2009).

5.3.2 Materials and methods

Animals

The hippocampal material for this study was provided by Dr. Cornelius Cross and his colleagues. Briefly, for this study, BALB/cByJIco (later called BC) and C57BL/ 6JIco (later called B6) strains were used to bred for two different F1 hybrids, B6xBC (B6 mother, BC father) and BCxB6 (C mother and B6 father). These two groups of offspring were genetically identical except for the sex chromosomes of the male mice. Further, they differ in the rearing environment during the first weeks of life as BC mothers display lower maternal care when compared to B6 mothers. At 2 months of age the right hippocampus from 6-8 male F1 hybrid mice was collected.

DNA extraction

For the actual probes, the DNA was extracted by Dr. Enrica Audero according to the following protocol: 200 µl lysis buffer and 10µl proteinkinase (20mg/ml) was added to the brain tissue, which was then incubated at 56°C over night. Afterwards it was centrifuged for 5 min at room temperature and the supernatant was kept. 250 µl (1 Vol) phenol-chloroform-isoamylalcohol (PCI; 25:24:1) was added. Then, it was again centrifuged at 4000 rpm at 4°C and the upper layer was kept. To that, 200 µl (1 Vol) PCI was added. After that, it was centrifuged at 14.000 rpm at 4°C for 5 min. To the upper phase was then added 2.5 Vol ethanol (100%) and 0.1 Vol 3M NaOH. It was again centrifuged for 5 min at 14.000 rpm (4°C). Afterwards the pellet was washed (2 times) with 70% cold ethanol, air-dried for one hour and solved in 100 µl TE (1x).

Genome-wide methylation profiling with SOLiD^{TM} System Mate-Paired Libraries

To examine the genome-wide methylation in F1 BCxB6 and B6xBC mice, Dr. Enrica Audero prepared Mate-Paired Libraries in collaboration with Timothy Bestor. Briefly, each DNA sample was split into two compartments. To isolate unmethylated DNA, the DNA was digested with a methylation-specific restriction enzyme (McrBC; leading to the M-signal). This enzyme is an endonuclease which cleaves DNA containing methylcytosine on one or both strands. To isolate methylated domains, the DNA was digested with methylation-sensitive restriction enzymes (AciI, BstUI, HhaI, HpaLL, HpyCH4IV; leading to the R-signal). These enzymes are endonucleases whose activity is blocked by cytosine methylation. Afterwards the DNA ends were repaired to blunt-ended DNA. Then, the genomic DNA was methylated by EcoP15I, which is a restriction enzyme that is able to methylate the 5th base in its binding site CAGCAG in the presence of a methyl-group donor and the absence of ATP. Afterwards, the methylated DNA is ligated with EcoP15I CAP (CA-overhang; unmethylated binding site of EcoP15I). Next, DNA fragments were separated according to their size by the use of gel fractionation, because small fragments are preferred to circulate in the next step. The fragments were then circulated by ligating them with a biotin-dT oligo (TG/GT-overhang). Afterwards the circulated DNA fragment was cleaved again by digestion with EcoP15I, which cleaves at two unmethylated, inversely oriented recognition sides which results in 90 bp Mate-paired genomic DNA fragments. To amplify all fragments with the same primers, the fragments are ligated with 2 primer adaptors at their ends, resulting in 156 Mate-paired genomic DNA fragments. To purify the library from side products, streptavidin beads were added, which bind specifically to biotin labeled internal adaptors in the library molecules. After that, the library was amplified and in the last step the libraries were purified by PAGE electrophoresis of the PCR products and excision of the 156 bp library band. The resulting DNA was measured by a Bioanalyzer. The actual genome-wide methylation profiling by Methyl-MAPS (methylation mapping analysis by paired-end sequencing) was performed by Bestor and colleagues (see (Rollins *et al.* 2006))

Bisulfite sequencing

To analyze the methylation pattern of the genome-wide screening resulted candidate genes, I established the bisulfite sequencing method: First, bisulfite conversion was performed according to the protocol of the EpiTect bisulfite kit from Qiagen (Cat. no.: 59104). Afterwards a PCR was performed: 45 µl Platinum PCR SuperMix (High fidelity), Invitrogen, 0.125 µl forward + 0.125 reverse primer (100 µM), 0.75 µl H_2O and 4 µl bisulfited DNA. The PCR protocol was as follows: 1 cycle 5 min, 94°C; 40 cycles (1 min, 94°C; 30 sec, 52°C [individual for each primer]; 45 sec, 72°C); 1 cycle 7 min, 72°C. The PCR product was then purified by a gel extraction according to QIAquick gel extraction kit, Qiagen. Next, A-overhangs were added to the PCR product for ligation afterwards: 26 µl PCR product, 1 µl dATP (10 mM), 5 µl 10x PCR-Buffer II (Applied Biosystems) and 1.2 µl ampliTaq DNA Polymerase (5 U/µl) (Applied Biosystems). Then, this was incubated for 30 min at 72°C. For ligation 4 µl PCR product, 1 µl salt solution and 1 µl TOPO vector were incubated for 5 min at room temperature. Transformation and cloning was performed according to the TOPO TA cloning kit dual promoter, (with Top10F cells; Invitrogen). For minipreparation, the picked clones were incubated in 3 ml LB-medium (+ampicilline) over night at 37°C. Plasmid purification was performed according to the QIAprep Spin Miniprep kit protocol, Qiagen. For sequencing the probes were prepared as follows: A sequencing PCR was performed with 10 ng for 1000 bp DNA, 1.3 µl (of 2.5 µM) M13-F Primer, 8 µl Big Dye and to the final volume of 20 µl water was added. The PCR protocol was as follows: 95°C, 5 min; 25 cycles (95°C, 15 sec; 52°C, 15 sec; 60°C, 3 min). Afterwards a precipitation followed. To the PCR product 64 µl ethanol (100%) and 16 µl water was added. Then, it was centrifuged at 14.000 rpm for 20 min at room temperature. The supernatant was removed and the pellet was washed with 50 µl ethanol (70%). It was again centrifuged for 5 min at room temperature (14.000 rpm). The supernatant was removed completely and the pellet was air-dried. Afterwards the pellet was dissolved in 10 µl water. To 3 µl of this solution 12 µl of formamide was added and boiled at 95°C for 2 min. At the end, the solution was put on ice for 2 min. The actual sequencing was performed by the sequencing service at the EMBL in Monterotondo. BiQ Analyzer was used to analyze the data (Bock *et al.* 2005).

5.3.3 Results

Genome-wide methylation profiling revealed that *ADP-ribosylation factor guanine nucleotide-exchange factor (Arfgef) 1* may be differentially methylated in BC versus B6 mice as indicated in the unmethylated-signal (M) at the BC section where there are no signals at the B6 and BC (R) sections (see Fig. 5-2). To further evaluate the meaning of the signals, bisulfite sequencing was performed. When applying this method for one sample of the BC group, we found that most of the CpG sites were unmethylated. CpG sites 4, 8 and 9 showed a methylation status of 25% (see Fig. 5-3).

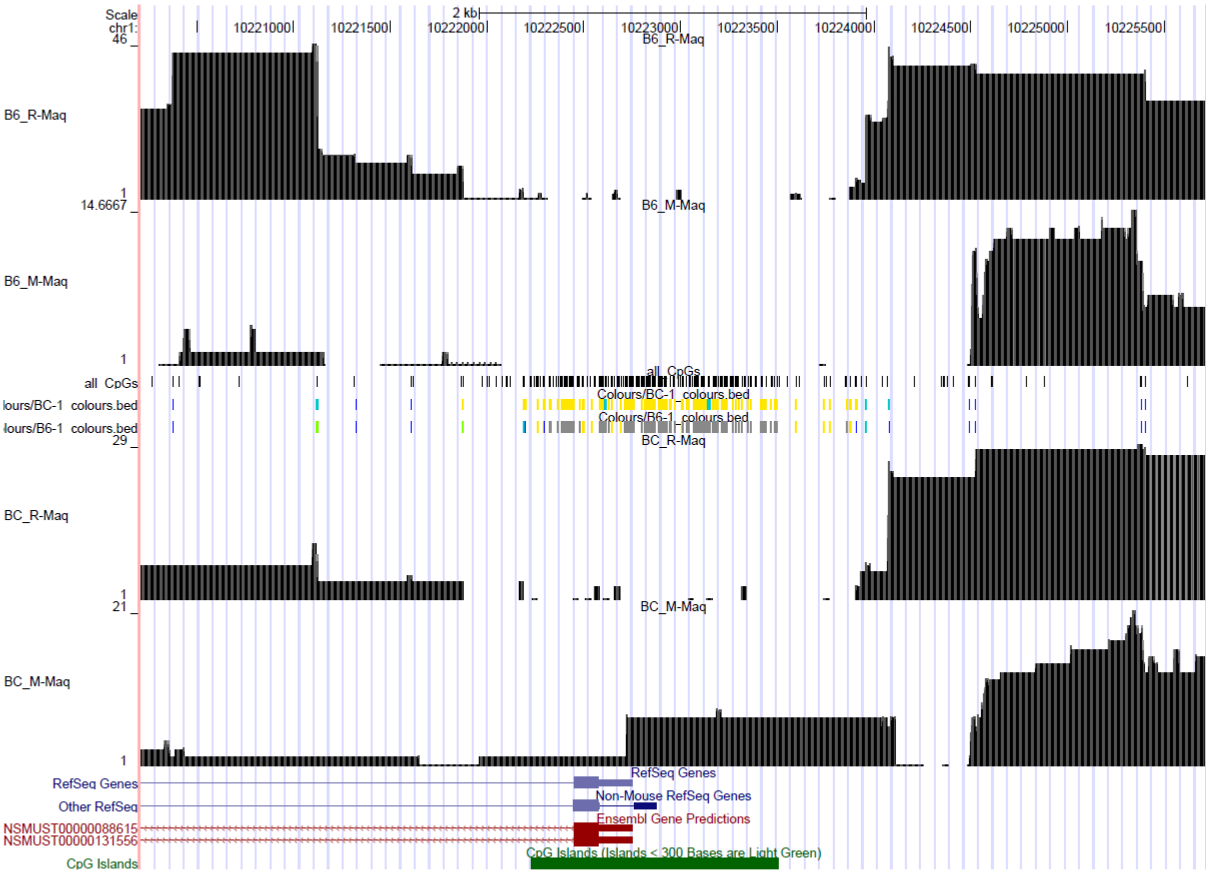

Figure 5-2. Methylation signals for ADP-ribosylation factor guanine nucleotide-exchange factor (Arfgef) 1. The M-signal (unmethylated) at the Balb/C (BC) section where there are no signals at the other sections might indicate a different methylation status between BC and C54BL/6 (B6) mice.

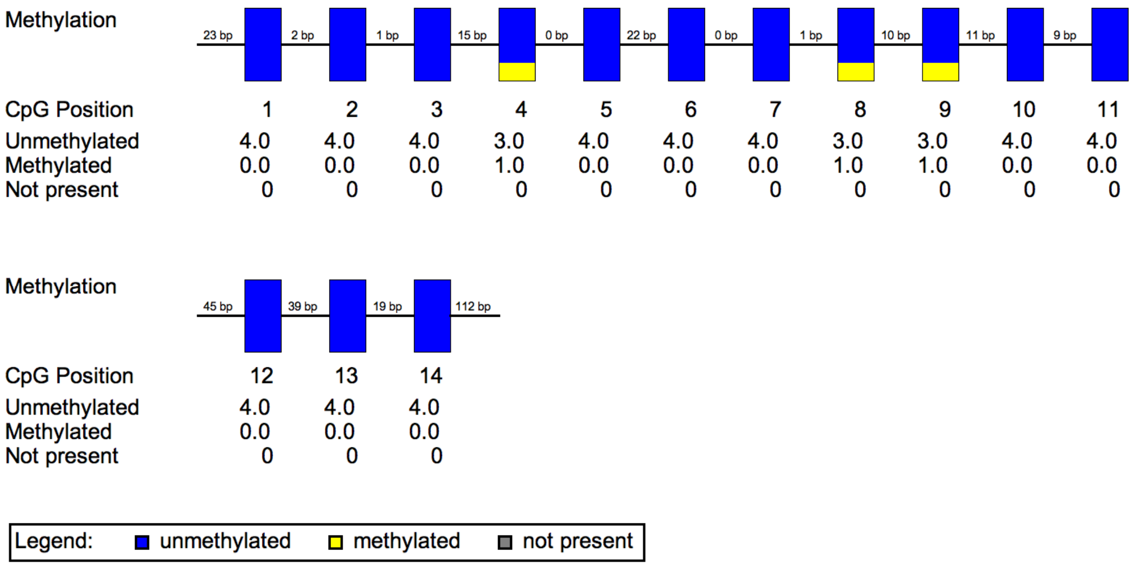

CpG Position	1	2	3	4	5	6	7	8	9	10	11	12	13	14
Unmethylated	4.0	4.0	4.0	3.0	4.0	4.0	4.0	3.0	3.0	4.0	4.0	4.0	4.0	4.0
Methylated	0.0	0.0	0.0	1.0	0.0	0.0	0.0	1.0	1.0	0.0	0.0	0.0	0.0	0.0
Not present	0	0	0	0	0	0	0	0	0	0	0	0	0	0

Legend: 🟦 unmethylated 🟨 methylated ⬛ not present

Figure 5-3 Methylation profile of some CpG sites in the Arfgef1 promoter (Chr1: 10222025-10223730). Most of the CpG sites were unmethylated whereas CpG site 4, 8 and 9 were 25 % methylated.

5.3.4 Discussion

Genome-wide methylation profiling revealed that Arfgef1 may be differentially methylated in BC versus B6 mice. Bisulfite sequencing revealed that the M-signal of the BC mice is really an unmethylated signal. Arfgef (also called BIG1) is a brefeldin A-inhibited guanine nucleotide-exchange protein, which activates class I ADP-ribosylation factors (ARF1-3) by catalyzing the replacement of bound GDP with GTP, an action critical for the regulation of protein transport in eukaryotic cells (Padilla *et al.* 2008). Additionally, Arfgef1 is known to scaffold and interact with proteins in other cellular compartments. In mammalian cells, its dysregulation may affect the structure and function of the Golgi apparatus (Pfeffer 1992). Recently, it was reported that Arfgef1 promoter is hypermethylated in breast cancer cells (Kim *et al.* 2011). Furthermore, it is known to be important in the glycosylation of beta1 integrin by Golgi enzymes which shows its important role in development and other vital processes. Therefore, a different regulation of Arfgef1 expression by DNA methylation through developmental stress might account for the differences in anxiety behavior seen when there are variations in maternal care (Calatayud and Belzung 2001). These data suggest that Arfgef1 may play an important biological role which, however, needs further validation.

5.4 References

Achen, M. G., M. Jeltsch*, et al.* (1998). "Vascular endothelial growth factor D (VEGF-D) is a ligand for the tyrosine kinases VEGF receptor 2 (Flk1) and VEGF receptor 3 (Flt4)." Proc Natl Acad Sci U S A **95**(2): 548-553.

Aerts, S., G. Thijs*, et al.* (2004). "Comprehensive analysis of the base composition around the transcription start site in Metazoa." BMC Genomics **5**(1): 34.

Akiyama, K., S. Ichinose*, et al.* (2002). "Study of expression of myelin basic proteins (MBPs) in developing rat brain using a novel antibody reacting with four major isoforms of MBP." J Neurosci Res **68**(1): 19-28.

Andrews, M. H. and S. G. Matthews (2004). "Programming of the hypothalamo-pituitary-adrenal axis: serotonergic involvement." Stress **7**(1): 15-27.

Arora, V., H. H. Cheung*, et al.* (2007). "Degradation of survivin by the X-linked inhibitor of apoptosis (XIAP)-XAF1 complex." J Biol Chem **282**(36): 26202-26209.

Asaoka, Y. and H. Nishina (2010). "Diverse physiological functions of MKK4 and MKK7 during early embryogenesis." J Biochem **148**(4): 393-401.

Backdahl, L., M. Herberth*, et al.* (2009). "Gene body methylation of the dimethylarginine dimethylamino-hydrolase 2 (Ddah2) gene is an epigenetic biomarker for neural stem cell differentiation." Epigenetics **4**(4): 248-254.

Barco, A., J. M. Alarcon*, et al.* (2002). "Expression of constitutively active CREB protein facilitates the late phase of long-term potentiation by enhancing synaptic capture." Cell **108**(5): 689-703.

Barr, C. S., T. K. Newman*, et al.* (2004). "Sexual dichotomy of an interaction between early adversity and the serotonin transporter gene promoter variant in rhesus macaques." Proc Natl Acad Sci U S A **101**(33): 12358-12363.

Bartke, A., P. C. Doherty*, et al.* (1984). "Effects of estrogen-induced hyperprolactinemia on endocrine and sexual functions in adult male rats." Neuroendocrinology **39**(2): 126-135.

Bartolomucci, A., V. Carola*, et al.* (2010). "Increased vulnerability to psychosocial stress in heterozygous serotonin transporter knockout mice." Dis Model Mech **3**(7-8): 459-470.

Behan, A. T., D. L. van den Hove*, et al.* (2011). "Evidence of female-specific glial deficits in the hippocampus in a mouse model of prenatal stress." Eur Neuropsychopharmacol **21**(1): 71-79.

Ben-Jonathan, N., J. L. Mershon*, et al.* (1996). "Extrapituitary prolactin: distribution, regulation, functions, and clinical aspects." Endocr Rev **17**(6): 639-669.

Benediktsson, R., A. A. Calder*, et al.* (1997). "Placental 11 beta-hydroxysteroid dehydrogenase: a key regulator of fetal glucocorticoid exposure." Clin Endocrinol (Oxf) **46**(2): 161-166.

Bengel, D., A. Heils*, et al.* (1997). "Gene structure and 5'-flanking regulatory region of the murine serotonin transporter." Brain Res Mol Brain Res **44**(2): 286-292.

Bengel, D., D. L. Murphy*, et al.* (1998). "Altered brain serotonin homeostasis and locomotor insensitivity to 3, 4-methylenedioxymethamphetamine ("Ecstasy") in serotonin transporter-deficient mice." Mol Pharmacol **53**(4): 649-655.

Bennett, A. J., K. P. Lesch*, et al.* (2002). "Early experience and serotonin transporter gene variation interact to influence primate CNS function." Mol Psychiatry **7**(1): 118-122.

Bet, P. M., B. W. Penninx*, et al.* (2009). "Glucocorticoid receptor gene polymorphisms and childhood adversity are associated with depression: New evidence for a gene-environment interaction." Am J Med Genet B Neuropsychiatr Genet **150B**(5): 660-669.

Bing, O., C. Moller*, et al.* (1993). "Anxiolytic-like action of centrally administered galanin." Neurosci Lett **164**(1-2): 17-20.

Blakely, R. D., L. J. De Felice*, et al.* (1994). "Molecular physiology of norepinephrine and serotonin transporters." J Exp Biol **196**: 263-281.

Bock, C., S. Reither*, et al.* (2005). "BiQ Analyzer: visualization and quality control for DNA methylation data from bisulfite sequencing." Bioinformatics **21**(21): 4067-4068.

Bole-Feysot, C., V. Goffin*, et al.* (1998). "Prolactin (PRL) and its receptor: actions, signal transduction pathways and phenotypes observed in PRL receptor knockout mice." Endocr Rev **19**(3): 225-268.

Bonaguidi, M. A., T. McGuire*, et al.* (2005). "LIF and BMP signaling generate separate and discrete types of GFAP-expressing cells." Development **132**(24): 5503-5514.

Borsini, F. and A. Meli (1988). "Is the forced swimming test a suitable model for revealing antidepressant activity?" Psychopharmacology (Berl) **94**(2): 147-160.

Boulle, F., D. L. van den Hove*, et al.* (2012). "Epigenetic regulation of the BDNF gene: implications for psychiatric disorders." Mol Psychiatry **17**(6): 584-596.

Bradley, R. G., E. B. Binder*, et al.* (2008). "Influence of child abuse on adult depression: moderation by the corticotropin-releasing hormone receptor gene." Arch Gen Psychiatry **65**(2): 190-200.

Bredy, T. W., H. Wu*, et al.* (2007). "Histone modifications around individual BDNF gene promoters in prefrontal cortex are associated with extinction of conditioned fear." Learn Mem **14**(4): 268-276.

Burgdorf, J., R. A. Kroes*, et al.* (2010). "Uncovering the molecular basis of positive affect using rough-and-tumble play in rats: a role for insulin-like growth factor I." Neuroscience **168**(3): 769-777.

Cabrera, R. J., E. L. Rodriguez-Echandia*, et al.* (1999). "Effects of prenatal exposure to a mild chronic variable stress on body weight, preweaning mortality and rat behavior." Braz J Med Biol Res **32**(10): 1229-1237.

Cadet, R., P. Pradier*, et al.* (1986). "Effects of prenatal maternal stress on the pituitary adrenocortical reactivity in guinea-pig pups." J Dev Physiol **8**(6): 467-475.

Calatayud, F. and C. Belzung (2001). "Emotional reactivity in mice, a case of nongenetic heredity?" Physiol Behav **74**(3): 355-362.

Caldji, C., B. Tannenbaum*, et al.* (1998). "Maternal care during infancy regulates the development of neural systems mediating the expression of fearfulness in the rat." Proc Natl Acad Sci U S A **95**(9): 5335-5340.

Canli, T., E. Congdon*, et al.* (2008). "Additive effects of serotonin transporter and tryptophan hydroxylase-2 gene variation on neural correlates of affective processing." Biol Psychol **79**(1): 118-125.

Canli, T. and K. P. Lesch (2007). "Long story short: the serotonin transporter in emotion regulation and social cognition." Nat Neurosci **10**(9): 1103-1109.

Canli, T., K. Omura*, et al.* (2005). "Beyond affect: a role for genetic variation of the serotonin transporter in neural activation during a cognitive attention task." Proc Natl Acad Sci U S A **102**(34): 12224-12229.

Canli, T., M. Qiu*, et al.* (2006). "Neural correlates of epigenesis." Proc Natl Acad Sci U S A **103**(43): 16033-16038.

Cantor-Graae, E., T. F. McNeil*, et al.* (1994). "Are neurological abnormalities in well discordant monozygotic co-twins of schizophrenic subjects the result of perinatal trauma?" Am J Psychiatry **151**(8): 1194-1199.

Capuron, L., J. F. Gumnick*, et al.* (2002). "Neurobehavioral effects of interferon-alpha in cancer patients: phenomenology and paroxetine responsiveness of symptom dimensions." Neuropsychopharmacology **26**(5): 643-652.

Capuron, L., A. Ravaud*, et al.* (2000). "Early depressive symptoms in cancer patients receiving interleukin 2 and/or interferon alfa-2b therapy." J Clin Oncol **18**(10): 2143-2151.

Capuron, L., S. Su*, et al.* (2008). "Depressive symptoms and metabolic syndrome: is inflammation the underlying link?" Biol Psychiatry **64**(10): 896-900.

Carola, V., G. Frazzetto*, et al.* (2008). "Identifying molecular substrates in a mouse model of the serotonin transporter x environment risk factor for anxiety and depression." Biol Psychiatry **63**(9): 840-846.

Caronia, G., J. Wilcoxon*, et al.* (2010). "Bone morphogenetic protein signaling in the developing telencephalon controls formation of the hippocampal dentate gyrus and modifies fear-related behavior." J Neurosci **30**(18): 6291-6301.

Carroll, J. C., J. M. Boyce-Rustay*, et al.* (2007). "Effects of mild early life stress on abnormal emotion-related behaviors in 5-HTT knockout mice." Behav Genet **37**(1): 214-222.

Carroll, J. E., C. P. Campanile*, et al.* (1982). "The effect of prolactin on human aldosterone-producing adenomas in vitro." J Clin Endocrinol Metab **54**(4): 689-692.

Caspi, A., A. R. Hariri*, et al.* (2010). "Genetic sensitivity to the environment: the case of the serotonin transporter gene and its implications for studying complex diseases and traits." Am J Psychiatry **167**(5): 509-527.

Caspi, A. and T. E. Moffitt (2006). "Gene-environment interactions in psychiatry: joining forces with neuroscience." Nat Rev Neurosci **7**(7): 583-590.

Caspi, A., K. Sugden*, et al.* (2003). "Influence of life stress on depression: moderation by a polymorphism in the 5-HTT gene." Science **301**(5631): 386-389.

Champoux, M., A. Bennett*, et al.* (2002). "Serotonin transporter gene polymorphism, differential early rearing, and behavior in rhesus monkey neonates." Mol Psychiatry **7**(10): 1058-1063.

Chapman, R. H. and J. M. Stern (1979). "Failure of severe maternal stress or ACTH during pregnancy to affect emotionality of male rat offspring: implications of litter effects for prenatal studies." Dev Psychobiol **12**(3): 255-267.

Charney, D. S. (2004). "Psychobiological mechanisms of resilience and vulnerability: implications for successful adaptation to extreme stress." Am J Psychiatry **161**(2): 195-216.

Chen, A. C., Y. Shirayama*, et al.* (2001). "Expression of the cAMP response element binding protein (CREB) in hippocampus produces an antidepressant effect." Biol Psychiatry **49**(9): 753-762.

Chen, J. C., J. Tonkiss*, et al.* (1992). "Prenatal protein malnutrition in rats enhances serotonin release from hippocampus." J Nutr **122**(11): 2138-2143.

Chen, Q. and D. Schubert (2002). "Presenilin-interacting proteins." Expert Rev Mol Med **4**(19): 1-18.

Chen, W. G., Q. Chang*, et al.* (2003). "Derepression of BDNF transcription involves calcium-dependent phosphorylation of MeCP2." Science **302**(5646): 885-889.

Cheng, M. Y., E. L. Bittman*, et al.* (2005). "Regulation of prokineticin 2 expression by light and the circadian clock." BMC Neurosci **6**: 17.

Cheng, M. Y., C. M. Bullock*, et al.* (2002). "Prokineticin 2 transmits the behavioural circadian rhythm of the suprachiasmatic nucleus." Nature **417**(6887): 405-410.

Cizza, G., A. H. Marques*, et al.* (2008). "Elevated neuroimmune biomarkers in sweat patches and plasma of premenopausal women with major depressive disorder in remission: the POWER study." Biol Psychiatry **64**(10): 907-911.

Clapp, C., L. Torner*, et al.* (1994). "The prolactin gene is expressed in the hypothalamic-neurohypophyseal system and the protein is processed into a 14-kDa fragment with activity like 16-kDa prolactin." Proc Natl Acad Sci U S A **91**(22): 10384-10388.

Clements, A. D. (1992). "The incidence of attention deficit–hyperactivity disorder in children whose mothers experienced extreme psychological stress." Ga Educ Res **91**: 1-14.

Coe, C. L. and G. R. Lubach (2005). "Prenatal origins of individual variation in behavior and immunity." Neurosci Biobehav Rev **29**(1): 39-49.

Collier, D. A., G. Stober*, et al.* (1996). "A novel functional polymorphism within the promoter of the serotonin transporter gene: possible role in susceptibility to affective disorders." Mol Psychiatry **1**(6): 453-460.

Coppen, A. (1967). "The biochemistry of affective disorders." Br J Psychiatry **113**(504): 1237-1264.

Coppen, A., D. M. Shaw*, et al.* (1967). "Tryptophan in the treatment of depression." Lancet **2**(7527): 1178-1180.

Copper, R. L., R. L. Goldenberg*, et al.* (1996). "The preterm prediction study: maternal stress is associated with spontaneous preterm birth at less than thirty-five weeks' gestation. National Institute of Child Health and Human Development Maternal-Fetal Medicine Units Network." Am J Obstet Gynecol **175**(5): 1286-1292.

Coussons-Read, M. E., M. Lobel*, et al.* (2012). "The occurrence of preterm delivery is linked to pregnancy-specific distress and elevated inflammatory markers across gestation." Brain Behav Immun **26**(4): 650-659.

Crawley, J. N. (1996). "Minireview. Galanin-acetylcholine interactions: relevance to memory and Alzheimer's disease." Life Sci **58**(24): 2185-2199.

D'Addario, C., B. Dell'Osso*, et al.* (2012). "Selective DNA methylation of BDNF promoter in bipolar disorder: differences among patients with BDI and BDII." Neuropsychopharmacology **37**(7): 1647-1655.

Dantzer, R., J. C. O'Connor*, et al.* (2008). "From inflammation to sickness and depression: when the immune system subjugates the brain." Nat Rev Neurosci **9**(1): 46-56.

Dauprat, P., G. Monin*, et al.* (1984). "The effects of psychosomatic stress at the end of pregnancy on maternal and fetal plasma cortisol levels and liver glycogen in guinea-pigs." Reprod Nutr Dev **24**(1): 45-51.

de Kloet, E. R., R. H. Derijk*, et al.* (2007). "Therapy Insight: is there an imbalanced response of mineralocorticoid and glucocorticoid receptors in depression?" Nat Clin Pract Endocrinol Metab **3**(2): 168-179.

de Kloet, E. R., M. Joels*, et al.* (2005). "Stress and the brain: from adaptation to disease." Nat Rev Neurosci **6**(6): 463-475.

De Kloet, E. R., E. Vreugdenhil*, et al.* (1998). "Brain corticosteroid receptor balance in health and disease." Endocr Rev **19**(3): 269-301.

de Weerth, C. and J. K. Buitelaar (2005). "Physiological stress reactivity in human pregnancy--a review." Neurosci Biobehav Rev **29**(2): 295-312.

Dennis, G., Jr., B. T. Sherman*, et al.* (2003). "DAVID: Database for Annotation, Visualization, and Integrated Discovery." Genome Biol **4**(5): P3.

Dickerson, P. A., B. E. Lally*, et al.* (2005). "Early emergence of increased fearful behavior in prenatally stressed rats." Physiol Behav **86**(4): 586-593.

DiPietro, J., Novak MF, Costigan KA, Atella LD, Reusing SP (2006). "Maternal psychological distress during pregnancy in relation to child development at age two." Child Dev **77**: 573–587.

Donahue, C. P., R. V. Jensen*, et al.* (2002). "Transcriptional profiling reveals regulated genes in the hippocampus during memory formation." Hippocampus **12**(6): 821-833.

Donahue, C. P., K. S. Kosik*, et al.* (2006). "Growth hormone is produced within the hippocampus where it responds to age, sex, and stress." Proc Natl Acad Sci U S A **103**(15): 6031-6036.

Dudley, K. J., X. Li*, et al.* (2011). "Epigenetic mechanisms mediating vulnerability and resilience to psychiatric disorders." Neurosci Biobehav Rev **35**(7): 1544-1551.

Duman, R. S., J. Malberg*, et al.* (2000). "Neuronal plasticity and survival in mood disorders." Biol Psychiatry **48**(8): 732-739.

Duman, R. S. and L. M. Monteggia (2006). "A neurotrophic model for stress-related mood disorders." Biol Psychiatry **59**(12): 1116-1127.

Dunning, B. E. and G. J. Taborsky, Jr. (1988). "Galanin--sympathetic neurotransmitter in endocrine pancreas?" Diabetes **37**(9): 1157-1162.

Dwivedi, Y., H. S. Rizavi*, et al.* (2003). "Altered gene expression of brain-derived neurotrophic factor and receptor tyrosine kinase B in postmortem brain of suicide subjects." Arch Gen Psychiatry **60**(8): 804-815.

Ellenbogen, M. A. and S. Hodgins (2009). "Structure provided by parents in middle childhood predicts cortisol reactivity in adolescence among the offspring of parents with bipolar disorder and controls." Psychoneuroendocrinology **34**(5): 773-785.

Emamian, E. S., D. Hall*, et al.* (2004). "Convergent evidence for impaired AKT1-GSK3beta signaling in schizophrenia." Nat Genet **36**(2): 131-137.

Engert, V., C. Buss*, et al.* (2010). "Investigating the association between early life parental care and stress responsivity in adulthood." Dev Neuropsychol **35**(5): 570-581.

Estanislau, C. and S. Morato (2005). "Prenatal stress produces more behavioral alterations than maternal separation in the elevated plus-maze and in the elevated T-maze." Behav Brain Res **163**(1): 70-77.

Fabre, V., C. Beaufour*, et al.* (2000). "Altered expression and functions of serotonin 5-HT1A and 5-HT1B receptors in knock-out mice lacking the 5-HT transporter." Eur J Neurosci **12**(7): 2299-2310.

Fang, V. S., S. Refetoff*, et al.* (1974). "Hypogonadism induced by a transplantable, prolactin-producing tumor in male rats: hormonal and morphological studies." Endocrinology **95**(4): 991-998.

Fanselow, M. S. and H. W. Dong (2010). "Are the dorsal and ventral hippocampus functionally distinct structures?" Neuron **65**(1): 7-19.

Föcking, M., *et al.* (2012). "Proteomic investigations of the hippocampus in prenatally stressed mice." in preparation.

Fortier, E., A. Noreau*, et al.* (2010). "Early impact of 5-HTTLPR polymorphism on the neural correlates of sadness." Neurosci Lett **485**(3): 261-265.

Fredericks, C. A., E. M. Drabant*, et al.* (2010). "Healthy young women with serotonin transporter SS polymorphism show a pro-inflammatory bias under resting and stress conditions." Brain Behav Immun **24**(3): 350-357.

Fredrickson, B. L. (2001). "The role of positive emotions in positive psychology. The broaden-and-build theory of positive emotions." Am Psychol **56**(3): 218-226.

Fuxe, K., A. Jansson*, et al.* (1998). "Galanin modulates 5-hydroxytryptamine functions. Focus on galanin and galanin fragment/5-hydroxytryptamine1A receptor interactions in the brain." Ann N Y Acad Sci **863**: 274-290.

Gatt, J. M., C. B. Nemeroff*, et al.* (2010). "Early life stress combined with serotonin 3A receptor and brain-derived neurotrophic factor valine 66 to methionine genotypes impacts emotional brain and arousal correlates of risk for depression." Biol Psychiatry **68**(9): 818-824.

Gaughran, F., J. Payne*, et al.* (2006). "Hippocampal FGF-2 and FGFR1 mRNA expression in major depression, schizophrenia and bipolar disorder." Brain Res Bull **70**(3): 221-227.

Gillman, M. W. (2005). "Developmental origins of health and disease." N Engl J Med **353**(17): 1848-1850.

Gitau, R., A. Cameron*, et al.* (1998). "Fetal exposure to maternal cortisol." Lancet **352**(9129): 707-708.

Gluckman, P. D. and M. A. Hanson (2004). "Living with the past: evolution, development, and patterns of disease." Science **305**(5691): 1733-1736.

Gould, T. D., K. C. O'Donnell*, et al.* (2008). "Generation and behavioral characterization of beta-catenin forebrain-specific conditional knock-out mice." Behav Brain Res **189**(1): 117-125.

Gould, T. D., C. A. Zarate*, et al.* (2004). "Glycogen synthase kinase-3: a target for novel bipolar disorder treatments." J Clin Psychiatry **65**(1): 10-21.

Grammatopoulos, D. K. (2008). "Placental corticotrophin-releasing hormone and its receptors in human pregnancy and labour: still a scientific enigma." J Neuroendocrinol **20**(4): 432-438.

Griffin, W. C., 3rd, H. D. Skinner*, et al.* (2003). "Mild prenatal stress in rats is associated with enhanced conditioned fear." Physiol Behav **79**(2): 209-215.

Gross, R. E., M. F. Mehler*, et al.* (1996). "Bone morphogenetic proteins promote astroglial lineage commitment by mammalian subventricular zone progenitor cells." Neuron **17**(4): 595-606.

Grunau, C., S. J. Clark*, et al.* (2001). "Bisulfite genomic sequencing: systematic investigation of critical experimental parameters." Nucleic Acids Res **29**(13): E65-65.

Gue, M., A. Bravard*, et al.* (2004). "Sex differences in learning deficits induced by prenatal stress in juvenile rats." Behav Brain Res **150**(1-2): 149-157.

Gutknecht, L., C. Kriegebaum*, et al.* (2009). "Spatio-temporal expression of tryptophan hydroxylase isoforms in murine and human brain: convergent data from Tph2 knockout mice." Eur Neuropsychopharmacol **19**(4): 266-282.

Habib, K. E., P. W. Gold*, et al.* (2001). "Neuroendocrinology of stress." Endocrinol Metab Clin North Am **30**(3): 695-728; vii-viii.

Hakak, Y., J. R. Walker*, et al.* (2001). "Genome-wide expression analysis reveals dysregulation of myelination-related genes in chronic schizophrenia." Proc Natl Acad Sci U S A **98**(8): 4746-4751.

Hansen, D., H. C. Lou*, et al.* (2000). "Serious life events and congenital malformations: a national study with complete follow-up." Lancet **356**(9233): 875-880.

Hariri, A. R., V. S. Mattay*, et al.* (2002). "Serotonin transporter genetic variation and the response of the human amygdala." Science **297**(5580): 400-403.

Harkin, A. J., K. H. Bruce*, et al.* (1999). "Nitric oxide synthase inhibitors have antidepressant-like properties in mice. 1. Acute treatments are active in the forced swim test." Eur J Pharmacol **372**(3): 207-213.

Hayashi, A., M. Nagaoka*, et al.* (1998). "Maternal stress induces synaptic loss and developmental disabilities of offspring." Int J Dev Neurosci **16**(3-4): 209-216.

Hayden, E. P., D. N. Klein*, et al.* (2010). "The dopamine D2 receptor gene and depressive and anxious symptoms in childhood: associations and evidence for gene-environment correlation and gene-environment interaction." Psychiatr Genet **20**(6): 304-310.

Hedegaard, M., T. B. Henriksen*, et al.* (1993). "Psychological distress in pregnancy and preterm delivery." BMJ **307**(6898): 234-239.

Hedegaard, M., T. B. Henriksen*, et al.* (1996). "Do stressful life events affect duration of gestation and risk of preterm delivery?" Epidemiology **7**(4): 339-345.

Heiming, R. S., F. Jansen*, et al.* (2009). "Living in a dangerous world: the shaping of behavioral profile by early environment and 5-HTT genotype." Front Behav Neurosci **3**: 26.

Heinz, A., D. F. Braus*, et al.* (2005). "Amygdala-prefrontal coupling depends on a genetic variation of the serotonin transporter." Nat Neurosci **8**(1): 20-21.

Hellman, A. and A. Chess (2007). "Gene body-specific methylation on the active X chromosome." Science **315**(5815): 1141-1143.

Herman, J. P., C. M. Prewitt*, et al.* (1996). "Neuronal circuit regulation of the hypothalamo-pituitary-adrenocortical stress axis." Crit Rev Neurobiol **10**(3-4): 371-394.

Heron, J., T. G. O'Connor*, et al.* (2004). "The course of anxiety and depression through pregnancy and the postpartum in a community sample." J Affect Disord **80**(1): 65-73.

Hof, P. R., V. Haroutunian*, et al.* (2003). "Loss and altered spatial distribution of oligodendrocytes in the superior frontal gyrus in schizophrenia." Biol Psychiatry **53**(12): 1075-1085.

Holderbach, R., K. Clark*, et al.* (2007). "Enhanced long-term synaptic depression in an animal model of depression." Biol Psychiatry **62**(1): 92-100.

Holmes, A., D. L. Murphy*, et al.* (2002). "Reduced aggression in mice lacking the serotonin transporter." Psychopharmacology (Berl) **161**(2): 160-167.

Holmes, A., R. J. Yang*, et al.* (2003). "Mice lacking the serotonin transporter exhibit 5-HT(1A) receptor-mediated abnormalities in tests for anxiety-like behavior." Neuropsychopharmacology **28**(12): 2077-2088.

Holmes, A., R. J. Yang*, et al.* (2002). "Evaluation of antidepressant-related behavioral responses in mice lacking the serotonin transporter." Neuropsychopharmacology **27**(6): 914-923.

Homberg, J. R. and K. P. Lesch (2011). "Looking on the bright side of serotonin transporter gene variation." Biol Psychiatry **69**(6): 513-519.

Homberg, J. R., Van den Hove D.L.A (2012). "The Serotonin Transporter Gene and Functional and Pathological Adaptation to Environmental Variation Across the Life Span. ." Progress in Neurobiology **in press**.

Hu, X. Z., R. H. Lipsky*, et al.* (2006). "Serotonin transporter promoter gain-of-function genotypes are linked to obsessive-compulsive disorder." Am J Hum Genet **78**(5): 815-826.

Huang da, W., B. T. Sherman*, et al.* (2009). "Systematic and integrative analysis of large gene lists using DAVID bioinformatics resources." Nat Protoc **4**(1): 44-57.

Huber, W., A. von Heydebreck*, et al.* (2002). "Variance stabilization applied to microarray data calibration and to the quantification of differential expression." Bioinformatics **18 Suppl 1**: S96-104.

Huizink, A. C., E. J. Mulder*, et al.* (2004). "Prenatal stress and risk for psychopathology: specific effects or induction of general susceptibility?" Psychol Bull **130**(1): 115-142.

Huttunen, M. O. and P. Niskanen (1978). "Prenatal loss of father and psychiatric disorders." Arch Gen Psychiatry **35**(4): 429-431.

Illingworth, R., A. Kerr*, et al.* (2008). "A novel CpG island set identifies tissue-specific methylation at developmental gene loci." PLoS Biol **6**(1): e22.

Ioshikhes, I. P. and M. Q. Zhang (2000). "Large-scale human promoter mapping using CpG islands." Nat Genet **26**(1): 61-63.

Jackson, S., S. Hodgkinson*, et al.* (1991). "IGF1 and 2 in two models of adrenal growth." J Steroid Biochem Mol Biol **40**(1-3): 399-404.

Jacobs, B. L., H. van Praag*, et al.* (2000). "Adult brain neurogenesis and psychiatry: a novel theory of depression." Mol Psychiatry **5**(3): 262-269.

Jaenisch, R. and A. Bird (2003). "Epigenetic regulation of gene expression: how the genome integrates intrinsic and environmental signals." Nat Genet **33 Suppl**: 245-254.

Jansen, F., R. S. Heiming*, et al.* (2010). "Modulation of behavioural profile and stress response by 5-HTT genotype and social experience in adulthood." Behav Brain Res **207**(1): 21-29.

Jones, K. L., R. M. Smith*, et al.* (2010). "Combined effect of maternal serotonin transporter genotype and prenatal stress in modulating offspring social interaction in mice." Int J Dev Neurosci **28**(6): 529-536.

Joukov, V., K. Pajusola*, et al.* (1996). "A novel vascular endothelial growth factor, VEGF-C, is a ligand for the Flt4 (VEGFR-3) and KDR (VEGFR-2) receptor tyrosine kinases." EMBO J **15**(2): 290-298.

Kairisalo, M., L. Korhonen*, et al.* (2009). "NF-kappaB-dependent regulation of brain-derived neurotrophic factor in hippocampal neurons by X-linked inhibitor of apoptosis protein." Eur J Neurosci **30**(6): 958-966.

Kalinichev, M., K. W. Easterling*, et al.* (2002). "Long-lasting changes in stress-induced corticosterone response and anxiety-like behaviors as a consequence of neonatal maternal separation in Long-Evans rats." Pharmacol Biochem Behav **73**(1): 131-140.

Karege, F., G. Vaudan*, et al.* (2005). "Neurotrophin levels in postmortem brains of suicide victims and the effects of antemortem diagnosis and psychotropic drugs." Brain Res Mol Brain Res **136**(1-2): 29-37.

Karg, K., M. Burmeister*, et al.* (2011). "The serotonin transporter promoter variant (5-HTTLPR), stress, and depression meta-analysis revisited: evidence of genetic moderation." Arch Gen Psychiatry **68**(5): 444-454.

Kask, K., M. Berthold*, et al.* (1997). "Galanin receptors: involvement in feeding, pain, depression and Alzheimer's disease." Life Sci **60**(18): 1523-1533.

Kenis, G. and M. Maes (2002). "Effects of antidepressants on the production of cytokines." Int J Neuropsychopharmacol **5**(4): 401-412.

Kenis, G., J. Prickaerts*, et al.* (2011). "Depressive symptoms following interferon-alpha therapy: mediated by immune-induced reductions in brain-derived neurotrophic factor?" Int J Neuropsychopharmacol **14**(2): 247-253.

Keshet, Y. and R. Seger (2010). "The MAP kinase signaling cascades: a system of hundreds of components regulates a diverse array of physiological functions." Methods Mol Biol **661**: 3-38.

Kessler, R. C., P. Berglund*, et al.* (2005). "Lifetime prevalence and age-of-onset distributions of DSM-IV disorders in the National Comorbidity Survey Replication." Arch Gen Psychiatry **62**(6): 593-602.

Khoshbouei, H., M. Cecchi*, et al.* (2002). "Behavioral reactivity to stress: amplification of stress-induced noradrenergic activation elicits a galanin-mediated anxiolytic effect in central amygdala." Pharmacol Biochem Behav **71**(3): 407-417.

Kikusui, T., Y. Kiyokawa*, et al.* (2007). "Deprivation of mother-pup interaction by early weaning alters myelin formation in male, but not female, ICR mice." Brain Res **1133**(1): 115-122.

Kikusui, T., Y. Takeuchi*, et al.* (2004). "Early weaning induces anxiety and aggression in adult mice." Physiol Behav **81**(1): 37-42.

Kilic, F., D. L. Murphy*, et al.* (2003). "A human serotonin transporter mutation causes constitutive activation of transport activity." Mol Pharmacol **64**(2): 440-446.

Kim, J. H., T. W. Kim*, et al.* (2011). "Downregulation of ARFGEF1 and CAMK2B by promoter hypermethylation in breast cancer cells." BMB Rep **44**(8): 523-528.

Kobayashi, T., K. Washiyama*, et al.* (2011). "Inhibition of G protein-activated inwardly rectifying K+ channels by different classes of antidepressants." PLoS One **6**(12): e28208.

Kopchick, J. J. and J. M. Andry (2000). "Growth hormone (GH), GH receptor, and signal transduction." Mol Genet Metab **71**(1-2): 293-314.

Korte, S. M., J. M. Koolhaas*, et al.* (2005). "The Darwinian concept of stress: benefits of allostasis and costs of allostatic load and the trade-offs in health and disease." Neurosci Biobehav Rev **29**(1): 3-38.

Kranich, S., K. Hattermann*, et al.* (2009). "VEGFR-3/Flt-4 mediates proliferation and chemotaxis in glial precursor cells." Neurochem Int **55**(8): 747-753.

Krishnan, V., M. H. Han*, et al.* (2007). "Molecular adaptations underlying susceptibility and resistance to social defeat in brain reward regions." Cell **131**(2): 391-404.

Kuan, P. F., H. Chun*, et al.* (2008). "CMARRT: a tool for the analysis of ChIP-chip data from tiling arrays by incorporating the correlation structure." Pac Symp Biocomput: 515-526.

Kunjara, S., A. L. Greenbaum*, et al.* (2012). "Effects of long-term experimental diabetes on adrenal gland growth and phosphoribosyl pyrophosphate formation in growth hormone-deficient dwarf rats." Int J Exp Pathol **93**(3): 196-201.

Laloux, C., J. Mairesse*, et al.* (2012). "Anxiety-like behaviour and associated neurochemical and endocrinological alterations in male pups exposed to prenatal stress." Psychoneuroendocrinology.

Leibowitz, S. F. (1995). "Brain peptides and obesity: pharmacologic treatment." Obes Res **3 Suppl 4**: 573S-589S.

Leonard, B. E. and A. Myint (2009). "The psychoneuroimmunology of depression." Hum Psychopharmacol **24**(3): 165-175.

Lesage, J., F. Del-Favero*, et al.* (2004). "Prenatal stress induces intrauterine growth restriction and programmes glucose intolerance and feeding behaviour disturbances in the aged rat." J Endocrinol **181**(2): 291-296.

Lesch, K. P. (2011). "When the serotonin transporter gene meets adversity: the contribution of animal models to understanding epigenetic mechanisms in affective disorders and resilience." Curr Top Behav Neurosci **7**: 251-280.

Lesch, K. P., U. Balling*, et al.* (1994). "Organization of the human serotonin transporter gene." J Neural Transm Gen Sect **95**(2): 157-162.

Lesch, K. P., D. Bengel*, et al.* (1996). "Association of anxiety-related traits with a polymorphism in the serotonin transporter gene regulatory region." Science **274**(5292): 1527-1531.

Lesch, K. P. and A. Heils (2000). "Serotonergic gene transcriptional control regions: targets for antidepressant drug development?" Int J Neuropsychopharmacol **3**(1): 67-79.

Lesch, K. P., J. Meyer*, et al.* (1997). "The 5-HT transporter gene-linked polymorphic region (5-HTTLPR) in evolutionary perspective: alternative biallelic variation in rhesus monkeys. Rapid communication." J Neural Transm **104**(11-12): 1259-1266.

Lewejohann, L., V. Kloke*, et al.* (2010). "Social status and day-to-day behaviour of male serotonin transporter knockout mice." Behav Brain Res **211**(2): 220-228.

Li, H., L. Zhang*, et al.* (2009). "Differential expression of mitogen-activated protein kinase signaling pathway in the hippocampus of rats exposed to chronic unpredictable stress." Behav Brain Res **205**(1): 32-37.

Li, J. D., W. P. Hu*, et al.* (2009). "Disruption of the circadian output molecule prokineticin 2 results in anxiolytic and antidepressant-like effects in mice." Neuropsychopharmacology **34**(2): 367-373.

Li, Q., C. Wichems*, et al.* (2000). "Reduction in the density and expression, but not G-protein coupling, of serotonin receptors (5-HT1A) in 5-HT transporter knock-out mice: gender and brain region differences." J Neurosci **20**(21): 7888-7895.

Li, W., C. A. Cogswell*, et al.* (1998). "Neuronal differentiation of precursors in the neocortical ventricular zone is triggered by BMP." J Neurosci **18**(21): 8853-8862.

Lim, D. A., A. D. Tramontin*, et al.* (2000). "Noggin antagonizes BMP signaling to create a niche for adult neurogenesis." Neuron **28**(3): 713-726.

Lister, R., M. Pelizzola*, et al.* (2009). "Human DNA methylomes at base resolution show widespread epigenomic differences." Nature **462**(7271): 315-322.

Liu, D., J. Diorio*, et al.* (2000). "Maternal care, hippocampal synaptogenesis and cognitive development in rats." Nat Neurosci **3**(8): 799-806.

Liu, L., A. Li*, et al.* (2001). "Maternal glucocorticoid treatment programs HPA regulation in adult offspring: sex-specific effects." Am J Physiol Endocrinol Metab **280**(5): E729-739.

Liu, Y. F., K. Bertram*, et al.* (2004). "Stress induces activation of stress-activated kinases in the mouse brain." J Neurochem **89**(4): 1034-1043.

Lotrich, F. E., R. E. Ferrell*, et al.* (2009). "Risk for depression during interferon-alpha treatment is affected by the serotonin transporter polymorphism." Biol Psychiatry **65**(4): 344-348.

Lou, H. C., D. Hansen*, et al.* (1994). "Prenatal stressors of human life affect fetal brain development." Dev Med Child Neurol **36**(9): 826-832.

Lu, B. (2003). "BDNF and activity-dependent synaptic modulation." Learn Mem **10**(2): 86-98.

Lu, B. and J. H. Chang (2004). "Regulation of neurogenesis by neurotrophins: implications in hippocampus-dependent memory." Neuron Glia Biol **1**(4): 377-384.

Lu, B., P. T. Pang*, et al.* (2005). "The yin and yang of neurotrophin action." Nat Rev Neurosci **6**(8): 603-614.

Lu, X., A. M. Barr*, et al.* (2005). "A role for galanin in antidepressant actions with a focus on the dorsal raphe nucleus." Proc Natl Acad Sci U S A **102**(3): 874-879.

Luecken, L. J. (1998). "Childhood attachment and loss experiences affect adult cardiovascular and cortisol function." Psychosom Med **60**(6): 765-772.

Luecken, L. J. and B. M. Appelhans (2006). "Early parental loss and salivary cortisol in young adulthood: the moderating role of family environment." Dev Psychopathol **18**(1): 295-308.

Luijk, M. P., F. P. Velders*, et al.* (2010). "FKBP5 and resistant attachment predict cortisol reactivity in infants: gene-environment interaction." Psychoneuroendocrinology **35**(10): 1454-1461.

Lundberg, J., J. Borg*, et al.* (2007). "A PET study on regional coexpression of 5-HT1A receptors and 5-HTT in the human brain." Psychopharmacology (Berl) **195**(3): 425-433.

Lupien, S. J., B. S. McEwen*, et al.* (2009). "Effects of stress throughout the lifespan on the brain, behaviour and cognition." Nat Rev Neurosci **10**(6): 434-445.

Mabie, P. C., M. F. Mehler*, et al.* (1999). "Multiple roles of bone morphogenetic protein signaling in the regulation of cortical cell number and phenotype." J Neurosci **19**(16): 7077-7088.

Majzoub, J. A. and K. P. Karalis (1999). "Placental corticotropin-releasing hormone: function and regulation." Am J Obstet Gynecol **180**(1 Pt 3): S242-246.

Mannie, Z. N., J. Barnes*, et al.* (2009). "Memory impairment in young women at increased risk of depression: influence of cortisol and 5-HTT genotype." Psychol Med **39**(5): 757-762.

Marcus, S. M. (2009). "Depression during pregnancy: rates, risks and consequences--Motherisk Update 2008." Can J Clin Pharmacol **16**(1): e15-22.

Martinowich, K., D. Hattori*, et al.* (2003). "DNA methylation-related chromatin remodeling in activity-dependent BDNF gene regulation." Science **302**(5646): 890-893.

Martinowich, K., H. Manji*, et al.* (2007). "New insights into BDNF function in depression and anxiety." Nat Neurosci **10**(9): 1089-1093.

Martins-de-Souza, D., G. Maccarrone*, et al.* (2010). "Proteome analysis of the thalamus and cerebrospinal fluid reveals glycolysis dysfunction and potential biomarkers candidates for schizophrenia." J Psychiatr Res **44**(16): 1176-1189.

Mathews, T. A., D. E. Fedele*, et al.* (2004). "Gene dose-dependent alterations in extraneuronal serotonin but not dopamine in mice with reduced serotonin transporter expression." J Neurosci Methods **140**(1-2): 169-181.

McAllister, A. K., L. C. Katz*, et al.* (1999). "Neurotrophins and synaptic plasticity." Annu Rev Neurosci **22**: 295-318.

McClung, C. A. (2007). "Circadian genes, rhythms and the biology of mood disorders." Pharmacol Ther **114**(2): 222-232.

McDonald, M. P. and J. N. Crawley (1997). "Galanin-acetylcholine interactions in rodent memory tasks and Alzheimer's disease." J Psychiatry Neurosci **22**(5): 303-317.

McEwen, B. S. (1999). "Stress and hippocampal plasticity." Annu Rev Neurosci **22**: 105-122.

McEwen, B. S. (2003). "Mood disorders and allostatic load." Biol Psychiatry **54**(3): 200-207.

McGowan, P. O., A. Sasaki*, et al.* (2009). "Epigenetic regulation of the glucocorticoid receptor in human brain associates with childhood abuse." Nat Neurosci **12**(3): 342-348.

McLean, M., A. Bisits*, et al.* (1995). "A placental clock controlling the length of human pregnancy." Nat Med **1**(5): 460-463.

McLean, M. and R. Smith (1999). "Corticotropin-releasing Hormone in Human Pregnancy and Parturition." Trends Endocrinol Metab **10**(5): 174-178.

Meaney, M. J. and M. Szyf (2005). "Environmental programming of stress responses through DNA methylation: life at the interface between a dynamic environment and a fixed genome." Dialogues Clin Neurosci **7**(2): 103-123.

Meijer, A. (1985). "Child psychiatric sequelae of maternal war stress." Acta Psychiatr Scand **72**(6): 505-511.

Melcangi, R. C., V. Magnaghi*, et al.* (1997). "Corticosteroid effects on gene expression of myelin basic protein in oligodendrocytes and of glial fibrillary acidic protein in type 1 astrocytes." J Neuroendocrinol **9**(10): 729-733.

Meller, E., C. Shen*, et al.* (2003). "Region-specific effects of acute and repeated restraint stress on the phosphorylation of mitogen-activated protein kinases." Brain Res **979**(1-2): 57-64.

Mennicken, F., C. Hoffert*, et al.* (2002). "Restricted distribution of galanin receptor 3 (GalR3) mRNA in the adult rat central nervous system." J Chem Neuroanat **24**(4): 257-268.

Miller, A. H., V. Maletic*, et al.* (2009). "Inflammation and its discontents: the role of cytokines in the pathophysiology of major depression." Biol Psychiatry **65**(9): 732-741.

Moller, C., W. Sommer*, et al.* (1999). "Anxiogenic-like action of galanin after intra-amygdala administration in the rat." Neuropsychopharmacology **21**(4): 507-512.

Moore, R. Y. (1997). "Circadian rhythms: basic neurobiology and clinical applications." Annu Rev Med **48**: 253-266.

Morgan, C. A., 3rd, S. Southwick*, et al.* (2004). "Relationships among plasma dehydroepiandrosterone sulfate and cortisol levels, symptoms of dissociation, and objective performance in humans exposed to acute stress." Arch Gen Psychiatry **61**(8): 819-825.

Morgan, C. A., 3rd, S. Wang*, et al.* (2000). "Plasma neuropeptide-Y concentrations in humans exposed to military survival training." Biol Psychiatry **47**(10): 902-909.

Morley-Fletcher, S., M. Darnaudery*, et al.* (2003). "Prenatal stress in rats predicts immobility behavior in the forced swim test. Effects of a chronic treatment with tianeptine." Brain Res **989**(2): 246-251.

Morley-Fletcher, S., M. Rea*, et al.* (2003). "Environmental enrichment during adolescence reverses the effects of prenatal stress on play behaviour and HPA axis reactivity in rats." Eur J Neurosci **18**(12): 3367-3374.

Mueller, B. R. and T. L. Bale (2008). "Sex-specific programming of offspring emotionality after stress early in pregnancy." J Neurosci **28**(36): 9055-9065.

Munafo, M. R., S. M. Brown*, et al.* (2008). "Serotonin transporter (5-HTTLPR) genotype and amygdala activation: a meta-analysis." Biol Psychiatry **63**(9): 852-857.

Munafo, M. R., C. Durrant*, et al.* (2009). "Gene X environment interactions at the serotonin transporter locus." Biol Psychiatry **65**(3): 211-219.

Munck, A., P. M. Guyre*, et al.* (1984). "Physiological functions of glucocorticoids in stress and their relation to pharmacological actions." Endocr Rev **5**(1): 25-44.

Munoz, P. C., M. A. Aspe*, et al.* (2010). "Correlations of recognition memory performance with expression and methylation of brain-derived neurotrophic factor in rats." Biol Res **43**(2): 251-258.

Murgatroyd, C., A. V. Patchev*, et al.* (2009). "Dynamic DNA methylation programs persistent adverse effects of early-life stress." Nat Neurosci **12**(12): 1559-1566.

Murphy, D. L. and K. P. Lesch (2008). "Targeting the murine serotonin transporter: insights into human neurobiology." Nat Rev Neurosci **9**(2): 85-96.

Nibuya, M., S. Morinobu*, et al.* (1995). "Regulation of BDNF and trkB mRNA in rat brain by chronic electroconvulsive seizure and antidepressant drug treatments." J Neurosci **15**(11): 7539-7547.

Nibuya, M., E. J. Nestler*, et al.* (1996). "Chronic antidepressant administration increases the expression of cAMP response element binding protein (CREB) in rat hippocampus." J Neurosci **16**(7): 2365-2372.

Nietzer, S. L., M. Bonn*, et al.* (2011). "Serotonin transporter knockout and repeated social defeat stress: impact on neuronal morphology and plasticity in limbic brain areas." Behav Brain Res **220**(1): 42-54.

Nogami, H., R. Hoshino*, et al.* (2007). "Region-specific expression and hormonal regulation of the first exon variants of rat prolactin receptor mRNA in rat brain and anterior pituitary gland." J Neuroendocrinol **19**(8): 583-593.

O'Connor, T. G., Y. Ben-Shlomo*, et al.* (2005). "Prenatal anxiety predicts individual differences in cortisol in pre-adolescent children." Biol Psychiatry **58**(3): 211-217.

O'Donnell, K. J., A. Bugge Jensen*, et al.* (2012). "Maternal prenatal anxiety and downregulation of placental 11beta-HSD2." Psychoneuroendocrinology **37**(6): 818-826.

O'Hara, R., C. M. Schroder*, et al.* (2007). "Serotonin transporter polymorphism, memory and hippocampal volume in the elderly: association and interaction with cortisol." Mol Psychiatry **12**(6): 544-555.

Ogle, T. F. and J. I. Kitay (1979). "Interactions of prolactin and adrenocorticotropin in the regulation of adrenocortical secretions in female rats." Endocrinology **104**(1): 40-44.

Olivier, J. D., L. A. Jans*, et al.* (2008). "Acute tryptophan depletion dose dependently impairs object memory in serotonin transporter knockout rats." Psychopharmacology (Berl) **200**(2): 243-254.

Ong, A. D., C. S. Bergeman*, et al.* (2006). "Psychological resilience, positive emotions, and successful adaptation to stress in later life." J Pers Soc Psychol **91**(4): 730-749.

Ongur, D., W. C. Drevets*, et al.* (1998). "Glial reduction in the subgenual prefrontal cortex in mood disorders." Proc Natl Acad Sci U S A **95**(22): 13290-13295.

Padilla, P. I., M. Uhart*, et al.* (2008). "Association of guanine nucleotide-exchange protein BIG1 in HepG2 cell nuclei with nucleolin, U3 snoRNA, and fibrillarin." Proc Natl Acad Sci U S A **105**(9): 3357-3361.

Pagel, M. D., G. Smilkstein*, et al.* (1990). "Psychosocial influences on new born outcomes: a controlled prospective study." Soc Sci Med **30**(5): 597-604.

Pallares, M. E., P. A. Scacchi Bernasconi*, et al.* (2007). "Effects of prenatal stress on motor performance and anxiety behavior in Swiss mice." Physiol Behav **92**(5): 951-956.

Pasamanick, B. and A. Kawi (1956). "A study of the association of prenatal and paranatal factors with the development of tics in children; a preliminary investigation." J Pediatr **48**(5): 596-601.

Patin, V., B. Lordi*, et al.* (2002). "Effects of prenatal stress on maternal behavior in the rat." Brain Res Dev Brain Res **139**(1): 1-8.

Pearson, G., F. Robinson*, et al.* (2001). "Mitogen-activated protein (MAP) kinase pathways: regulation and physiological functions." Endocr Rev **22**(2): 153-183.

Perkins, A. V., E. A. Linton*, et al.* (1995). "Corticotrophin-releasing hormone and corticotrophin-releasing hormone binding protein in normal and pre-eclamptic human pregnancies." Br J Obstet Gynaecol **102**(2): 118-122.

Persico, A. M., A. Baldi*, et al.* (2003). "Reduced programmed cell death in brains of serotonin transporter knockout mice." Neuroreport **14**(3): 341-344.

Petraglia, F., P. Florio*, et al.* (1996). "Peptide signaling in human placenta and membranes: autocrine, paracrine, and endocrine mechanisms." Endocr Rev **17**(2): 156-186.

Pezawas, L., A. Meyer-Lindenberg*, et al.* (2005). "5-HTTLPR polymorphism impacts human cingulate-amygdala interactions: a genetic susceptibility mechanism for depression." Nat Neurosci **8**(6): 828-834.

Pezet, S. and M. Malcangio (2004). "Brain-derived neurotrophic factor as a drug target for CNS disorders." Expert Opin Ther Targets **8**(5): 391-399.

Pfeffer, S. R. (1992). "GTP-binding proteins in intracellular transport." Trends Cell Biol **2**(2): 41-46.

Phelps, C. J., T. J. Collier*, et al.* (1987). "Effect of chronic hyperprolactinemia on tuberoinfundibular dopaminergic neurons: histofluorescence in aged and in diethylstilbestrol-treated male rats." Brain Res **411**(1): 108-119.

Pi, X. J. and D. R. Grattan (1998). "Distribution of prolactin receptor immunoreactivity in the brain of estrogen-treated, ovariectomized rats." J Comp Neurol **394**(4): 462-474.

Pizarro, J. M., L. A. Lumley*, et al.* (2004). "Acute social defeat reduces neurotrophin expression in brain cortical and subcortical areas in mice." Brain Res **1025**(1-2): 10-20.

Poo, M. M. (2001). "Neurotrophins as synaptic modulators." Nat Rev Neurosci **2**(1): 24-32.

Prasad, H. C., C. B. Zhu*, et al.* (2005). "Human serotonin transporter variants display altered sensitivity to protein kinase G and p38 mitogen-activated protein kinase." Proc Natl Acad Sci U S A **102**(32): 11545-11550.

Prickaerts, J., Steckler, T. (2005). "Effects of glucocorticoids on emotion and cognitive processes in animals." Handbook of Stress and the Brain, Part 1: The Neurobiology of Stress **15**: 359–386.

Pruessner, J. C., F. Champagne*, et al.* (2004). "Dopamine release in response to a psychological stress in humans and its relationship to early life maternal care: a positron emission tomography study using [11C]raclopride." J Neurosci **24**(11): 2825-2831.

Raison, C. L., A. S. Borisov*, et al.* (2009). "Activation of central nervous system inflammatory pathways by interferon-alpha: relationship to monoamines and depression." Biol Psychiatry **65**(4): 296-303.

Rassnick, S., A. F. Sved*, et al.* (1994). "Locus coeruleus stimulation by corticotropin-releasing hormone suppresses in vitro cellular immune responses." J Neurosci **14**(10): 6033-6040.

Ravary, A., A. Muzerelle*, et al.* (2001). "Abnormal trafficking and subcellular localization of an N-terminally truncated serotonin transporter protein." Eur J Neurosci **13**(7): 1349-1362.

Reichardt, L. F. (2006). "Neurotrophin-regulated signalling pathways." Philos Trans R Soc Lond B Biol Sci **361**(1473): 1545-1564.

Reichenberg, A., R. Yirmiya*, et al.* (2001). "Cytokine-associated emotional and cognitive disturbances in humans." Arch Gen Psychiatry **58**(5): 445-452.

Reul, J. M. and E. R. de Kloet (1985). "Two receptor systems for corticosterone in rat brain: microdistribution and differential occupation." Endocrinology **117**(6): 2505-2511.

Risch, N., R. Herrell*, et al.* (2009). "Interaction between the serotonin transporter gene (5-HTTLPR), stressful life events, and risk of depression: a meta-analysis." JAMA **301**(23): 2462-2471.

Robinson, B. G., R. L. Emanuel*, et al.* (1988). "Glucocorticoid stimulates expression of corticotropin-releasing hormone gene in human placenta." Proc Natl Acad Sci U S A **85**(14): 5244-5248.

Robinson, C. M., P. T. Hale*, et al.* (2005). "The role of IFN-gamma and TNF-alpha-responsive regulatory elements in the synergistic induction of indoleamine dioxygenase." J Interferon Cytokine Res **25**(1): 20-30.

Roiser, J. P., U. Muller*, et al.* (2007). "The effects of acute tryptophan depletion and serotonin transporter polymorphism on emotional processing in memory and attention." Int J Neuropsychopharmacol **10**(4): 449-461.

Rollins, R. A., F. Haghighi*, et al.* (2006). "Large-scale structure of genomic methylation patterns." Genome Res **16**(2): 157-163.

Rondo, P. H., R. F. Ferreira*, et al.* (2003). "Maternal psychological stress and distress as predictors of low birth weight, prematurity and intrauterine growth retardation." Eur J Clin Nutr **57**(2): 266-272.

Roy, A., E. Gorodetsky*, et al.* (2010). "Interaction of FKBP5, a stress-related gene, with childhood trauma increases the risk for attempting suicide." Neuropsychopharmacology **35**(8): 1674-1683.

Ruijter, J. M., C. Ramakers*, et al.* (2009). "Amplification efficiency: linking baseline and bias in the analysis of quantitative PCR data." Nucleic Acids Res **37**(6): e45.

Ruiz, R. J., J. Fullerton*, et al.* (2002). "Predicting risk of preterm birth: the roles of stress, clinical risk factors, and corticotropin-releasing hormone." Biol Res Nurs **4**(1): 54-64.

Russo-Neustadt, A., R. C. Beard*, et al.* (1999). "Exercise, antidepressant medications, and enhanced brain derived neurotrophic factor expression." Neuropsychopharmacology **21**(5): 679-682.

Sajdyk, T. J., A. Shekhar*, et al.* (2004). "Interactions between NPY and CRF in the amygdala to regulate emotionality." Neuropeptides **38**(4): 225-234.

Sapolsky, R. M., L. C. Krey*, et al.* (1986). "The neuroendocrinology of stress and aging: the glucocorticoid cascade hypothesis." Endocr Rev **7**(3): 284-301.

Sapolsky, R. M. and M. J. Meaney (1986). "Maturation of the adrenocortical stress response: neuroendocrine control mechanisms and the stress hyporesponsive period." Brain Res **396**(1): 64-76.

Sargent, P. A., K. H. Kjaer*, et al.* (2000). "Brain serotonin1A receptor binding measured by positron emission tomography with [11C]WAY-100635: effects of depression and antidepressant treatment." Arch Gen Psychiatry **57**(2): 174-180.

Schaaf, M. J., J. de Jong*, et al.* (1998). "Downregulation of BDNF mRNA and protein in the rat hippocampus by corticosterone." Brain Res **813**(1): 112-120.

Schiepers, O. J., M. C. Wichers*, et al.* (2005). "Cytokines and major depression." Prog Neuropsychopharmacol Biol Psychiatry **29**(2): 201-217.

Schildkraut, J. J. and S. S. Kety (1967). "Biogenic amines and emotion." Science **156**(3771): 21-37.

Schmidt, M. V., D. Trumbach*, et al.* (2010). "Individual stress vulnerability is predicted by short-term memory and AMPA receptor subunit ratio in the hippocampus." J Neurosci **30**(50): 16949-16958.

Schmitt, A., R. Mossner*, et al.* (2003). "Organic cation transporter capable of transporting serotonin is up-regulated in serotonin transporter-deficient mice." J Neurosci Res **71**(5): 701-709.

Schneider-Rivas, S., C. Paredes-Carbajal*, et al.* (2007). "Effects of testosterone and growth hormone on long-term retention and extinction of a passive avoidance response in young and aged rats." Int J Neurosci **117**(10): 1443-1456.

Schneiderman, N., G. Ironson*, et al.* (2005). "Stress and health: psychological, behavioral, and biological determinants." Annu Rev Clin Psychol **1**: 607-628.

Seckl, J. R. and M. J. Meaney (2004). "Glucocorticoid programming." Ann N Y Acad Sci **1032**: 63-84.

Secoli, S. R. and N. A. Teixeira (1998). "Chronic prenatal stress affects development and behavioral depression in rats." Stress **2**(4): 273-280.

Shaked, M., K. Weissmuller*, et al.* (2008). "Histone deacetylases control neurogenesis in embryonic brain by inhibition of BMP2/4 signaling." PLoS One **3**(7): e2668.

Shen, H. W., Y. Hagino*, et al.* (2004). "Regional differences in extracellular dopamine and serotonin assessed by in vivo microdialysis in mice lacking dopamine and/or serotonin transporters." Neuropsychopharmacology **29**(10): 1790-1799.

Shepherd, J. K., S. S. Grewal*, et al.* (1994). "Behavioural and pharmacological characterisation of the elevated "zero-maze" as an animal model of anxiety." Psychopharmacology (Berl) **116**(1): 56-64.

Shirayama, Y., A. C. Chen*, et al.* (2002). "Brain-derived neurotrophic factor produces antidepressant effects in behavioral models of depression." J Neurosci **22**(8): 3251-3261.

Shishkina, G. T., T. S. Kalinina*, et al.* (2010). "Resistance to the development of stress-induced behavioral despair in the forced swim test associated with elevated hippocampal Bcl-xl expression." Behav Brain Res **213**(2): 218-224.

Sik, A., P. van Nieuwehuyzen*, et al.* (2003). "Performance of different mouse strains in an object recognition task." Behav Brain Res **147**(1-2): 49-54.

Silva, E. J., L. F. Felicio*, et al.* (2004). "Prolactin induces adrenal hypertrophy." Braz J Med Biol Res **37**(2): 193-199.

Siuciak, J. A., D. R. Lewis*, et al.* (1997). "Antidepressant-like effect of brain-derived neurotrophic factor (BDNF)." Pharmacol Biochem Behav **56**(1): 131-137.

Smith, M. A., S. Makino*, et al.* (1995). "Stress and glucocorticoids affect the expression of brain-derived neurotrophic factor and neurotrophin-3 mRNAs in the hippocampus." J Neurosci **15**(3 Pt 1): 1768-1777.

Smyth, G. K., J. Michaud*, et al.* (2005). "Use of within-array replicate spots for assessing differential expression in microarray experiments." Bioinformatics **21**(9): 2067-2075.

Smyth, G. K., J. Michaud*, et al.* (2005). "Use of within-array replicate spots for assessing differential expression in microarray experiments." Bioinformatics **21**(9): 2067-2075.

Smyth, G. K. and T. Speed (2003). "Normalization of cDNA microarray data." Methods **31**(4): 265-273.

Smyth, G. K. and T. Speed (2003). "Normalization of cDNA microarray data." Methods **31**(4): 265-273.

Sonntag, W. E., M. Ramsey*, et al.* (2005). "Growth hormone and insulin-like growth factor-1 (IGF-1) and their influence on cognitive aging." Ageing Res Rev **4**(2): 195-212.

Southwick, S. M., M. Vythilingam*, et al.* (2005). "The psychobiology of depression and resilience to stress: implications for prevention and treatment." Annu Rev Clin Psychol **1**: 255-291.

Staal, F. J., T. C. Luis*, et al.* (2008). "WNT signalling in the immune system: WNT is spreading its wings." Nat Rev Immunol **8**(8): 581-593.

Stein, A., E. A. Campbell*, et al.* (1987). "Social adversity, low birth weight, and preterm delivery." Br Med J (Clin Res Ed) **295**(6593): 291-293.

Stott, D. H. (1973). "Follow-up study from birth of the effects of prenatal stresses." Dev Med Child Neurol **15**(6): 770-787.

Sullivan, P. F., M. C. Neale*, et al.* (2000). "Genetic epidemiology of major depression: review and meta-analysis." Am J Psychiatry **157**(10): 1552-1562.

Sun, L. Y., K. Al-Regaiey*, et al.* (2005). "Local expression of GH and IGF-1 in the hippocampus of GH-deficient long-lived mice." Neurobiol Aging **26**(6): 929-937.

Sutcliffe, J. S., R. J. Delahanty*, et al.* (2005). "Allelic heterogeneity at the serotonin transporter locus (SLC6A4) confers susceptibility to autism and rigid-compulsive behaviors." Am J Hum Genet **77**(2): 265-279.

Suzuki, M. M. and A. Bird (2008). "DNA methylation landscapes: provocative insights from epigenomics." Nat Rev Genet **9**(6): 465-476.

Swanson, C. J., T. P. Blackburn*, et al.* (2005). "Anxiolytic- and antidepressant-like profiles of the galanin-3 receptor (Gal3) antagonists SNAP 37889 and SNAP 398299." Proc Natl Acad Sci U S A **102**(48): 17489-17494.

Talge, N. M., C. Neal*, et al.* (2007). "Antenatal maternal stress and long-term effects on child neurodevelopment: how and why?" J Child Psychol Psychiatry **48**(3-4): 245-261.

Taliaz, D., N. Stall*, et al.* (2010). "Knockdown of brain-derived neurotrophic factor in specific brain sites precipitates behaviors associated with depression and reduces neurogenesis." Mol Psychiatry **15**(1): 80-92.

Tarullo, A. R. and M. R. Gunnar (2006). "Child maltreatment and the developing HPA axis." Horm Behav **50**(4): 632-639.

Tempel, D. L. and S. F. Leibowitz (1990). "Galanin inhibits insulin and corticosterone release after injection into the PVN." Brain Res **536**(1-2): 353-357.

Thompson, R. J., K. J. Parker*, et al.* (2011). "Oxytocin receptor gene polymorphism (rs2254298) interacts with familial risk for psychopathology to predict symptoms of depression and anxiety in adolescent girls." Psychoneuroendocrinology **36**(1): 144-147.

Torche, F. (2011). "The effect of maternal stress on birth outcomes: exploiting a natural experiment." Demography **48**(4): 1473-1491.

Torner, L., N. Toschi*, et al.* (2001). "Anxiolytic and anti-stress effects of brain prolactin: improved efficacy of antisense targeting of the prolactin receptor by molecular modeling." J Neurosci **21**(9): 3207-3214.

Torres, G. E., R. R. Gainetdinov*, et al.* (2003). "Plasma membrane monoamine transporters: structure, regulation and function." Nat Rev Neurosci **4**(1): 13-25.

Tsankova, N., W. Renthal*, et al.* (2007). "Epigenetic regulation in psychiatric disorders." Nat Rev Neurosci **8**(5): 355-367.

Tsankova, N. M., O. Berton*, et al.* (2006). "Sustained hippocampal chromatin regulation in a mouse model of depression and antidepressant action." Nat Neurosci **9**(4): 519-525.

Tsao, C. W., Y. S. Lin*, et al.* (2006). "Cytokines and serotonin transporter in patients with major depression." Prog Neuropsychopharmacol Biol Psychiatry **30**(5): 899-905.

Tugade, M. M. and B. L. Fredrickson (2004). "Resilient individuals use positive emotions to bounce back from negative emotional experiences." J Pers Soc Psychol **86**(2): 320-333.

Turek, F. W. (2007). "From circadian rhythms to clock genes in depression." Int Clin Psychopharmacol **22 Suppl 2**: S1-8.

Turner, C. A., H. Akil*, et al.* (2006). "The fibroblast growth factor system and mood disorders." Biol Psychiatry **59**(12): 1128-1135.

Uher, R., A. Caspi*, et al.* (2011). "Serotonin transporter gene moderates childhood maltreatment's effects on persistent but not single-episode depression: replications and implications for resolving inconsistent results." J Affect Disord **135**(1-3): 56-65.

Valentino, R. J., S. L. Foote*, et al.* (1983). "Corticotropin-releasing factor activates noradrenergic neurons of the locus coeruleus." Brain Res **270**(2): 363-367.

van Dam, P. S. and A. Aleman (2004). "Insulin-like growth factor-I, cognition and brain aging." Eur J Pharmacol **490**(1-3): 87-95.

van den Hove, D. L., S. B. Jakob*, et al.* (2011). "Differential effects of prenatal stress in 5-Htt deficient mice: towards molecular mechanisms of gene x environment interactions." PLoS One **6**(8): e22715.

van den Hove, D. L., G. Kenis*, et al.* (2010). "Maternal stress-induced reduction in birth weight as a marker for adult affective state." Front Biosci (Elite Ed) **2**: 43-46.

Van den Hove, D. L., H. W. Steinbusch*, et al.* (2006). "Prenatal stress and neonatal rat brain development." Neuroscience **137**(1): 145-155.

van Donkelaar, A., R. V. Martin*, et al.* (2010). "Global estimates of ambient fine particulate matter concentrations from satellite-based aerosol optical depth: development and application." Environ Health Perspect **118**(6): 847-855.

van Os, J. and J. P. Selten (1998). "Prenatal exposure to maternal stress and subsequent schizophrenia. The May 1940 invasion of The Netherlands." Br J Psychiatry **172**: 324-326.

Vandesompele, J., K. De Preter*, et al.* (2002). "Accurate normalization of real-time quantitative RT-PCR data by geometric averaging of multiple internal control genes." Genome Biol **3**(7): RESEARCH0034.

Vanmierlo, T., K. Rutten*, et al.* (2011). "Liver X receptor activation restores memory in aged AD mice without reducing amyloid." Neurobiol Aging **32**(7): 1262-1272.

Vialou, V., A. J. Robison*, et al.* (2010). "DeltaFosB in brain reward circuits mediates resilience to stress and antidepressant responses." Nat Neurosci **13**(6): 745-752.

Volke, V., G. Wegener*, et al.* (2003). "Antidepressant- and anxiolytic-like effects of selective neuronal NOS inhibitor 1-(2-trifluoromethylphenyl)-imidazole in mice." Behav Brain Res **140**(1-2): 141-147.

Wada, A. (2009). "Lithium and neuropsychiatric therapeutics: neuroplasticity via glycogen synthase kinase-3beta, beta-catenin, and neurotrophin cascades." J Pharmacol Sci **110**(1): 14-28.

Wadhwa, P. D., C. Dunkel-Schetter*, et al.* (1996). "Prenatal psychosocial factors and the neuroendocrine axis in human pregnancy." Psychosom Med **58**(5): 432-446.

Wadhwa, P. D., C. A. Sandman*, et al.* (1993). "The association between prenatal stress and infant birth weight and gestational age at birth: a prospective investigation." Am J Obstet Gynecol **169**(4): 858-865.

Ward, A. J. (1991). "Prenatal stress and childhood psychopathology." Child Psychiatry Hum Dev **22**(2): 97-110.

Watson, J. B., S. A. Mednick*, et al.* (1999). "Prenatal teratogens and the development of adult mental illness." Dev Psychopathol **11**(3): 457-466.

Weaver, I. C., N. Cervoni*, et al.* (2004). "Epigenetic programming by maternal behavior." Nat Neurosci **7**(8): 847-854.

Weaver, I. C., A. C. D'Alessio*, et al.* (2007). "The transcription factor nerve growth factor-inducible protein a mediates epigenetic programming: altering epigenetic marks by immediate-early genes." J Neurosci **27**(7): 1756-1768.

Weinstock, M. (1997). "Does prenatal stress impair coping and regulation of hypothalamic-pituitary-adrenal axis?" Neurosci Biobehav Rev **21**(1): 1-10.

Weinstock, M. (2001). "Alterations induced by gestational stress in brain morphology and behaviour of the offspring." Progress in Neurobiology **65**(5): 427-451.

Weinstock, M. (2005). "The potential influence of maternal stress hormones on development and mental health of the offspring." Brain Behav Immun **19**(4): 296-308.

Weinstock, M. (2008). "The long-term behavioural consequences of prenatal stress." Neurosci Biobehav Rev **32**(6): 1073-1086.

Weiss, J. M., R. W. Bonsall*, et al.* (1998). "Galanin: a significant role in depression?" Ann N Y Acad Sci **863**: 364-382.

Welberg, L. A., J. R. Seckl*, et al.* (2000). "Inhibition of 11beta-hydroxysteroid dehydrogenase, the foeto-placental barrier to maternal glucocorticoids, permanently programs amygdala GR mRNA expression and anxiety-like behaviour in the offspring." Eur J Neurosci **12**(3): 1047-1054.

Wellman, C. L., A. Izquierdo*, et al.* (2007). "Impaired stress-coping and fear extinction and abnormal corticolimbic morphology in serotonin transporter knock-out mice." J Neurosci **27**(3): 684-691.

White, P. C., T. Mune*, et al.* (1997). "11 beta-Hydroxysteroid dehydrogenase and the syndrome of apparent mineralocorticoid excess." Endocr Rev **18**(1): 135-156.

Whitnall, M. H. (1989). "Stress selectively activates the vasopressin-containing subset of corticotropin-releasing hormone neurons." Neuroendocrinology **50**(6): 702-707.

Wiley, J. L., A. F. Cristello*, et al.* (1995). "Effects of site-selective NMDA receptor antagonists in an elevated plus-maze model of anxiety in mice." Eur J Pharmacol **294**(1): 101-107.

Woo, N. H., H. K. Teng*, et al.* (2005). "Activation of p75NTR by proBDNF facilitates hippocampal long-term depression." Nat Neurosci **8**(8): 1069-1077.

Wu, X., Y. He*, et al.* (2010). "Essential role of interleukin-15 receptor in normal anxiety behavior." Brain Behav Immun **24**(8): 1340-1346.

Wu, X., H. Hsuchou*, et al.* (2011). "Interleukin-15 affects serotonin system and exerts antidepressive effects through IL15Ralpha receptor." Psychoneuroendocrinology **36**(2): 266-278.

Wultsch, T., S. Chourbaji*, et al.* (2007). "Behavioural and expressional phenotyping of nitric oxide synthase-I knockdown animals." J Neural Transm Suppl(72): 69-85.

Wust, S., R. Kumsta*, et al.* (2009). "Sex-specific association between the 5-HTT gene-linked polymorphic region and basal cortisol secretion." Psychoneuroendocrinology **34**(7): 972-982.

Xu, L., R. Anwyl*, et al.* (1997). "Behavioural stress facilitates the induction of long-term depression in the hippocampus." Nature **387**(6632): 497-500.

Yano, A., Y. Fujii*, et al.* (2006). "Glucocorticoids suppress tumor angiogenesis and in vivo growth of prostate cancer cells." Clin Cancer Res **12**(10): 3003-3009.

Yehuda, R., S. Brand*, et al.* (2006). "Plasma neuropeptide Y concentrations in combat exposed veterans: relationship to trauma exposure, recovery from PTSD, and coping." Biol Psychiatry **59**(7): 660-663.

Yehuda, R., S. R. Brand*, et al.* (2006). "Clinical correlates of DHEA associated with post-traumatic stress disorder." Acta Psychiatr Scand **114**(3): 187-193.

Yoder, J. A., N. S. Soman*, et al.* (1997). "DNA (cytosine-5)-methyltransferases in mouse cells and tissues. Studies with a mechanism-based probe." J Mol Biol **270**(3): 385-395.

Zacher, B., P. F. Kuan*, et al.* (2010). "Starr: Simple Tiling ARRay analysis of Affymetrix ChIP-chip data." BMC Bioinformatics **11**: 194.

Zajac, M. S., T. Y. Pang*, et al.* (2010). "Wheel running and environmental enrichment differentially modify exon-specific BDNF expression in the hippocampus of wild-type and pre-motor symptomatic male and female Huntington's disease mice." Hippocampus **20**(5): 621-636.

Zearfoss, N. R., J. M. Alarcon*, et al.* (2008). "A molecular circuit composed of CPEB-1 and c-Jun controls growth hormone-mediated synaptic plasticity in the mouse hippocampus." J Neurosci **28**(34): 8502-8509.

Zemojtel, T., S. M. Kielbasa*, et al.* (2011). "CpG deamination creates transcription factor-binding sites with high efficiency." Genome Biol Evol **3**: 1304-1311.

Zeng, H., B. A. Schimpf*, et al.* (2007). "Thyrotropin-releasing hormone receptor 1-deficient mice display increased depression and anxiety-like behavior." Mol Endocrinol **21**(11): 2795-2804.

Zhu, L. J., C. Gazin*, et al.* (2010). "ChIPpeakAnno: a Bioconductor package to annotate ChIP-seq and ChIP-chip data." BMC Bioinformatics **11**: 237.

Zuena, A. R., J. Mairesse*, et al.* (2008). "Prenatal restraint stress generates two distinct behavioral and neurochemical profiles in male and female rats." PLoS One **3**(5): e2170.

5.5 Abbreviations

5-HT	Serotonin
5-HTT	Serotonin transporter
5-Htt+/-	heterozygous for the serotonin transporter
5-HTTLPR	5-HTT linked polymorphic region
ACTH	Adrenocorticotrophic hormone
Arfgef1	ADP-ribosylation factor guanine nucleotide-axchange factor 1
AVP	Vasopressin
B6	C57BL/6
BC	Balb/C
Bdnf	Brain derived neurotrophic factor
Bmpr1b	bone morphogenetic protein receptor type 1B
bp	base pairs
C	Cytosine
C	Control
Cacna1d	calcium channel voltage dependent, L type, alpha 1D subunit
Cacng3	calcium channel, voltage dependent, gamma subunit 3
Cacng3	calcium channel, voltage-dependent, gamma subunit 3
Camk2a	calcium/calmodulin-dependent protein kinase II alpha
Camk2d	calcium/calmodulin-dependent protein kinase II, delta
CNS	Central nervous system
CORT	Corticosterone
Crh	Corticotrophin releasing hormone
Crk	v-crk sarcoma virus CT10 oncogen homolog
Ctcf	CCCTC-binding factor
DAVID	Database for Annotation, Visualization and Integrated Discovery
Dnmt1	DNA methyltransferase
DRN	Dorsal raphe nucleus
EZM	Elevated zero maze
Fgf1	fibroblast growth factor 1
Fgfr1	Fibroblast growth factro receptor 1
Figf	Fos-induced growth factor
Fos	FBJ osteosarcoma oncogene
FST	Forced swim test
Fzd3	frizzled homolog 3
G	Guanine
Gal	Galanin
Galr3	galanin receptor 3
Gdi2	dissociation inhibitor 2

GDP	guanosine diphosphate
Gh	Growth hormone
Gja	gap junction protein, alpha 1
GPC	glial precursor cell
GR	Glucocorticoid receptor
HDAC	Histone-deacetylase
HET	5-Htt+/-
HPA	Hypothalamus-pituitary-adrenal
Il12a	interleukin 12a
Il1r1	interleukin 1 receptor, type 1
Il4	interleukin4
Jun	jun oncogen
Kcnip2	Kv channel-interacting protein 2
Kcnj5	potassium inwardly-rectifying channel, subfamiliy j, member 5
kDa	kilo Dalton
KEGG	Kyoto Encyclopedia of Genes and Genomes
LIMMA	Linera models for Microarray analysis
l	long
LSD	Least significant difference
MALDI-TOF	Matrix assisted laser disorption ionisation time of flight
Map2k7	mitogen-activated protein kinase kinase 7
Map3k12	mitogen-activated protein kinase kinase kinase 12
Mapk8ip3	mitogen-activated protein kinase 8 interacting protein
Mbp	Myelin based protein
MDD	major depression disorder
min	Minute
NGF	nerve growth factor
Nos1	nitrit oxide synthase 1, neuronal
NT	Neurotrophin
Ntrk2	neurotrophic tyrosine kinase, receptor type 2
ORT	Object regocnition task
PeS	Perinatal stress
Phox2a	paired-like homeobox 2a
Pla2g5	Phospholipase As, group 5
Ppp1r1b	protein phosphatase 1, regulatory (inhibitor) subunit 1B
Prkar2b	protein kinase, cAMP dependent regulatory, type II beta
Prkcc	protein kinase C, gamma

Prl	Prolactin
Prok2	prokineticin
PS	Prenatal stress
Psen1	Presenilin 1
qRT-PCR	quantitative real-time polymerase chain reaction
Rac2	RAS-related C3 botulinum substrate 2
RDI	relative discrimination index
Rock1	Rho-associated coiled-coil containing protein kinase 1
s	short
sec	second
Slc6a4	solute carrier family 6, member 4
Smad7	MAD homolog 7
Syt5	synaptotagmin V
Tnfrsf1a	tumor necrosis factor receptor subfamily, member 1a
Trhr	thyrotropin releasing hormone receptor
Trp53	transformation related protein 53
Ttn	Titin
Vegf	vascular endothelial growth factor
Xaf1	XIAP associated factor 1
Zzef1	zinc finger, ZZ-type with EF hand domain 1

5.6 Publications

- Van den Hove DLA* and **Jakob SB***, Schraut KG, Kenis G, Schmitt AG, Kneitz S, Scholz CJ, Wiescholleck V, Ortega G, Prickaerts J, Steinbusch H, Lesch KP. Differential effects of prenatal stress in 5-Htt deficient mice: towards molecular mechanisms of gene x environment interactions. Plos one, 2011, 6(8):e22715. Epub 2011 Aug 12.

  * Equal contribution

- Boulle F, Van den Hove DLA, **Jakob SB**, Rutten BP, Hamon M, VAN OS J, Lesch KP, Lanfumey L, Steinbusch HW, Kenis G. Epigenetic regulation of the BDNF gene: implications for psychiatric disorders. Mol Psychiatry, 2012, Jun;17(6):584-96.

5.7 Acknowledgements

Prof. Dr. Klaus-Peter Lesch danke ich für die Möglichkeit meine Doktorarbeit in seinem Labor anzufertigen und die sehr gute Betreuung hierbei. Weiterhin bedanke ich mich für die Finanzierung nachdem mein Stipendium ausgelaufen war. Ich möchte mich auch für die zahlreichen Ausflüge, Grillabende und Abendessen, die jedes Mal viel Spaß gemacht und lecker geschmeckt haben, bei ihm und seiner Frau **Silke Groß-Lesch** bedanken. Außerdem bedanke ich mich für die Geduld und die Unterstützung die er mir entgegengebracht hat.

Prof. Dr. Thomas Dandekar danke ich für die Erstellung des Zweitgutachtens und die immer sehr stressfreien und hilfreichen Progress Reports mit ihm.

Dr. Daniel van den Hove danke ich vielmals für die Unterstützung und Korrekturen diverser Arbeiten inklusive diser hier. Außerdem bedanke ich mich für die leider seltenen aber immer lustigen Treffen, die sehr effektiv waren. Bedanken möchte ich mich auch für die unzähligen, hilfreichen Diskussionen über die Arbeit und das Leben im Allgemeinen. Vielen Dank auch für die Geduld und die psychologischen Tips, die mich z.T. zum Weinen gerührt aber meistens zum Lachen animiert haben. Ich war bestimmt nicht einfach und bei der ein oder anderen statistischen analYsis musste ich widersprechen, aber ABdrÜcken wollte er mich nie. Die Betreuung war SOZUSAGEN WONDERBRA. Dank je wel!

I thank **Dr. Cornelius Gross** for the opportunity to work in his lab at the EMBL in Monterotondo. Furthermore I would like to thank **Dr. Enrica Audero** and **Dr. Elena Amendola**, who supervised me during my stay at the EMBL. Moreover I say thank you to **Dr. Apar Jain, Laura Dumas** and **Bianca Silva** for showing and visiting Rome together with me.

Vielen Dank auch an **Prof. Norbert Sachser** und **Dr. Rebecca Heiming** für die gute Zusammenarbeit und die zur Verfügungstellung der perinatalen Stress-Mäusegehirne.

Bedanken möchte ich mich auch bei **Dr. Susanne Kneitz** und **Dr. Claus-Jürgen Scholz** für die biostatistische Analyze und für die Beantwortung vieler Fragen.

Ich bedanke mich auch bei **Prof. Dr. Martin Heisenberg** und dem **GK 1156**, durch den ich die ersten 2 Jahre meiner Promotion finanziert wurde. Weiterhin bedanke ich mich bei der **Graduate School of Life Science (GSLS)** und ihren Mitarbeitern, da ich dadurch viele interessante Workshops und Seminare besuchen konnte, die mich weitergebracht haben.

Vielen, vielen Dank auch an das komplette Labor. Die Stimmung war immer 1A und es hat immer Spaß gemacht zur Arbeit zu gehen. Wir sind zusammen durch Dick und Dünn gegangen, wie in einer

großen Familie. Ganz besonders bedanke ich mich bei **Gabi Ortega** ohne die ich wahrscheinlich nie eine Doktorarbeit angefangen hätte. Außerdem bedanke ich mich bei ihr, dass sie mir immer mit Rat und Tat beigestanden hat. Es macht einfach Spaß mit ihr über Probleme bezüglich der Arbeit aber auch sonstige Probleme zu sprechen, da sie sich sehr gut auskennt. Weiterhin bedanke ich mich sehr herzlich bei **Karla Schraut**, die durch ihre liebenswerte und intelligente Art unser kleines Team sehr bereichert hat. Bedanken möchte ich mich auch bei **Dr. Angelika Schmitt**, die mir in meiner Diplomarbeit das wissenschaftliche Arbeiten beigebracht hat und die auch während meiner Doktorarbeit immer ein offenes Ohr für mich hatte. Außerdem bedanke ich mich bei **Elisabeth Findeiss**, **Linda Schmitt** und **Mareen Engel**, die mir während ihrer Praktika bei meiner Doktorarbeit geholfen haben. Weiterhin bedanke ich mich bei **Prof. Dr. Andreas Reif**, der an mich geglaubt hat als ich nicht mehr an mich geglaubt hatte.

Von ganzem Herzen bedanke ich mich auch bei meinen Freunden, die immer zu mir gehalten haben und ohne die die Welt nicht so schön wäre und mir damit die doch etwas anstrengende Zeit der Doktorarbeit versüßt haben. Ganz besonders bedanke ich mich bei **Beatrice Brems**, die mir schon seit 28 Jahren treu zur Seite steht und immer für mich da ist auch wenn wir uns schon länger nicht gesehen und gesprochen haben. Bedanken will ich mich auch bei **Dr. Michaela Eckert**, meine Studienliebe, die mich während des kompletten Studiums begleitet und mit der ich immer viel Spaß hatte. Sie hat mich immer aufgemuntert, auch wenn es mir mal nicht so gut ging. Außerdem bedanke ich mich bei **Hannah Müller-Pein**, die liebe Mitbewohnerseele, die mir wieder die Lust auf Pfannkuchen und auf andere diverse Sachen beigebracht hat. Herzlichen Dank auch an **Katharina Försch**, mit der ich viele schöne Dinge erlebt habe besonders in den vielen VIP-Bereichen bei diversen Veranstaltungen aber auch in Rom, Amsterdam, Berlin und natürlich in Würzburg. Ich bedanke mich auch bei **Dr. Michael Zirbs**, der über viele Jahre hinweg meine Launen ausgehalten hat.

Mein ganz besonderer Dank geht an meine Eltern, **Carmen und Karl-Dieter Jakob**, die immer an mich geglaubt haben und mich finanziell aber auch mit hilfreichen Tips versorgt haben. Herzlich bedanken möchte ich mich auch bei meinem Bruder, **Manuel Jakob**, der immer ein offenes Ohr für mich hat und für mich da ist, wenn ich ihn brauche.

Last but not least bedanke ich mich bei meinem Freund, **Nico Falgner**, der darauf geachtet hat, dass ich nicht zuviel arbeite und stattdessen (mit ihm zusammen) das Leben genieße.

Affidavit

I hereby declare that my thesis entitled "Molecular mechanisms of early-life stress in 5-Htt deficient mice: Gene x environment interactions and epigenetic programming" is the result of my own work. I did not receive any help or support from commercial consultants. All sources and / or materials applied are listed and specified in the thesis.

Furthermore, I verify that this thesis has not yet been submitted as part of another examination process neither in identical nor in similar form.

Würzburg……………………………………………………………………………………………

Date Signature

Eidesstattliche Erklärung

Hiermit erkläre ich an Eides statt, die Dissertation „Molekulare Mechanismen von Entwicklungsstress bei 5-Htt defizienten Mäusen: Gen x Umweltinteraktionen und epigenetische Programmierung" eigenständig, d.h. insbesondere selbstständig und ohne Hilfe eines kommerziellen Promotionsberaters, angefertigt und keine anderen als die von mir angegebenen Quellen und Hilfsmittel verwendet zu haben.

Ich erkläre außerdem, dass die Dissertation weder in gleicher noch in ähnlicher Form bereits in einem anderen Prüfungsverfahren vorgelegen hat.

Würzburg……………………………………………………………………………………

Datum Unterschrift